INTEGRATING RAINFALL RUNOFF AND EVAPORATION MODELS FOR ESTIMATING SOIL WATER STORAGE DURING FALLOW UNDER IN-FIELD RAINWATER HARVESTING

By

Mussie Ghebrebrhan Zerizghy

A dissertation submitted in accordance with the requirements for the Philosophiae Doctor degree in the Faculty of Natural and Agricultural Sciences, Department of Soil, Crop and Climate Sciences at the University of the Free State, Bloemfontein, South Africa.

Promoter: Prof. LD van Rensburg

Co-promoter: Dr. J.J. Anderson

January 2012

Contents

DECLARATION

I declare that the thesis hereby submitted by me for the Philosophiae Doctor in Soil Science degree at the University of the Free State is my own independent work and has not previously submitted by me to another University/Faculty. I further cede copyright of the thesis in favour of the University of the Free State.

Mussie Ghebrebrhan Zerizghy

Signature_____

Date: January, 2012

Place: Bloemfontein, South Africa

ACKNOWLEDGEMENT

- "*They are new every morning: great is thy faithfulness*" Lam 3:23, my utmost gratitude to You my God, the Author of my life.

- Heartfelt gratitude to my promoter Prof L.D. van Rensburg for the always-open office, invaluable inputs, patient guidance and continued encouragement throughout the study.

- My co-promoter, Dr. Kobus Anderson, your readiness to help and valuable inputs is greatly appreciated.

- Special thanks to Mr. S.S. Mavimbela for your invaluable support during the field data collection period.

- Unreserved gratitude to Mr. B. Keotshabe and Mr. B. Schoonwinkel for generously sharing your research information.

- My sincere gratitude to Mr. Elias Jokwane - very handy and reliable person, Mr. G. Madito, Mr. R. Snetler, Mr. M. Heine, and Mr. J.W. Hoffmann - the field work would not have been possible without your support.

- I am very grateful to the research cluster, water management in water-scarce areas, of the University of the Free State for the bursary I received.

- Special thanks to the Agricultural Research Council - Institute of Soil, Climate and Water (ARC – ISCW) for access to weather data.

- Special thanks to these colleagues who made profound inputs in me: Dr T.B. Zere, Mr. W.A. Tesfuhuney, Mr. D.K. Chemei, Mr. G.L. Yada, Mr. Z.A. Bello, Dr. I.B.U. Haka, Mr. B.T. Kuenene, Mr. C.M. Tfwala, Mr. G. Hatutale, and Mr. B.B. Mabuza.

- My family and friends, your best wishes for me, continued love and prayers, they were my propellers. I am greatly indebted to you.

LIST OF TABLES

LIST OF FIGURES

LIST OF APPENDICES

ABSTRACT

In-field rainwater harvesting (IRWH) is a beneficial water conservation practice. Fallowing is an important strategy to enhance water conservation. Fallowing consists of a period where no crops are grown (bare) and the field is kept free from weeds to stop unproductive transpiration losses. In such a system, to determine the rainwater storage under the profile of the basin the processes of in-field runoff and evaporation are very important. Until the storage capacity for the soil is exceeded these two processes are the sole determinants of the rainwater received. In this study, it was hypothesized that it will be possible to characterize the water balance for an IRWH system by integrating rainfall-runoff and evaporation models and estimate water storage during fallow period. The field, prepared for IRWH, was kept fallow and soil water evaporation and in-field runoff observation experiments were conducted. The IRWH plots were prepared in three basin to runoff strip length (RSL) ratios: 1:1, 1:2 and 1:3. The study was conducted on the Kenilworth/Bainsvlei and Paradys/Tukulu ecotopes. These ecotopes share the same climate and topography, but have different soil types.

Rainfall characterization was done by using long-term rainfall data. Rainfall event amount, duration and intensity classification with corresponding percentages of representation were obtained. This classification is important in producing relevant rainfall simulations. Rainfall simulations to observe the effect of rainfall intensity pattern on runoff amount and infiltration progress were conducted. The results showed that the rainfall intensity pattern had a significant effect on the runoff amount for the Paradys/Tukulu ecotope, but not for the Kenilworth/Bainsvlei ecotope. The advance of the infiltration front, despite the clay content difference of the top horizon of the two ecotopes, revealed that it only affected the top 200 mm. Having observed that the amount of simulated rain tops the majority of rain events received in these ecotopes, this shows that rainwater infiltration and runoff are mainly affected by the top horizon of the soil. Thus, the infiltration progress during rainfall event, for an IRWH system, can be grossly categorized according the top horizon considered.

Soil water evaporation is an important parameter that decides the fate of the received rainwater. Hence, accurate quantification of this parameter is of paramount significance. The neutron water meter and DFM capacitance probe were compared to measure soil water evaporation from the top 300 mm. It was found that the capacitance probes performed better. Thus capacitance probes were used to measure soil water evaporation across different sections of the micro-landscape created by the IRWH system. These measurements were used to compare evaporation across different sections of the micro-landscape and among different basin to RSL ratios. There were significant differences in the evaporation observed across the sections of the micro-landscape. The plot level evaporation comparison between the different basin to RSL ratios, however, did not show significant differences.

Modelling of in-field runoff and soil water evaporation was done by selecting two models each research field. For the runoff modelling, an empirical runoff model was developed and compared to the Morin & Cluff (1980) (MC) runoff model. The models were calibrated for each basin to RSL ratio. Both models showed good prediction performance on validation data. The RMSE values for the empirical runoff model were 5.9, 4.2 and 7.1; 4.0, 3.8 and 5.5 mm for the 1:1, 1:2 and 1:3 basin to RSL ratios of Kenilworth/Bainsvlei and Paradys/Tukulu ecotopes, respectively. These values for the MC model were 6.9, 5.1 and 8.5; 6.4, 7.8 and 9.2 mm, respectively. It was concluded that the empirical runoff model performed better than MC model on both ecotopes.

Similarly, an empirically developed evaporation model and Ritchie (1972) evaporation prediction (REP) model were calibrated for both ecotopes and different basin to RSL ratios. The empirical model related cumulative evaporation to the square root of days after rain and square root of cumulative reference evaporation. The validation of the empirical evaporation model showed that the RMSE values for the 1:1, 1:2 and 1:3 basin to RSL ratios were 0.74, 2.7 and 3.5; 1.0, 1.8 and 4.3 mm on the Kenilworth/Bainsvlei and Paradys/Tukulu ecotopes, respectively. These values for the REP model were 1.1, 2.5 and 3.2; 1.2, 1.6 and 3.2 mm, respectively. The model performance varied on the two ecotopes. Overall, the empirical evaporation model performed better on the

Kenilworth/Bainsvlei ecotope, while the REP model performed better on the Paradys/Tukulu ecotope.

The best performing runoff and evaporation models were integrated in a soil water balance exercise during a fallow period. The water balance was conducted for long (18 months) and short (6 months) fallow periods. The plot level RSE values ranged from 8 to 33% and 29 to 58% for the long and short fallows, respectively. These ranges for the Paradys/Tukulu were 7 to 24% and 23 to 56% for the long and short fallows, respectively. For long fallow the storage gains achieved were not different among the different basin to RSL ratios. For the short fallow, however, the storage gains increased with increasing RSL.

Key-words: rainwater harvesting, rainfall characterization, rainfall simulation, in-field runoff, evaporation, modelling, fallow, soil water storage, soil water balance

1. Introduction

1.1. Motivation

Fresh water is one of the world's most precious commodities which is progressively getting more scarce (Rijsberman, 2006). Since the distribution of water is very uneven, this progressive change might not be perceptible in some areas of the world. However, in arid and semi-arid regions, where the annual evaporative demand of the atmosphere is much higher than the annual intercepted rainfall, the growing scarcity and the demand thereof for water is obvious. This scarcity greatly impinges on the agricultural sector which accounts on average for about 70% of fresh water use globally (Sepaskhah & Ahmadi, 2010). The scarcity of water is magnified on the face of the growing population and the concurrent growing demand from other sectors of the economy. This condition demands for efficient use of the available water resources. Rainwater is one such resource that requires improved use efficiency. Rainwater is the cheapest water that can be used for agriculture. Efficient utilization of this resource can thus help mitigate the demand pressure.

One way of maximizing efficiency of rainwater use is employing *in-situ* rainwater harvesting practices (Ngigi *et al.*, 2006; Ren *et al*., 2010). Up until the end of the previous millennium, such practices as a way of improving agricultural system, did not receive much attention in the sub-Saharan Africa (Rockström, 2000). In South Africa, a practice known as in-field rainwater harvesting (IRWH) was introduced by Hensley *et al.* (2000). Subsequently, many studies have been conducted on the IRWH system dealing with the effect of runoff and crop yield modelling, mulching and assessing its potential on different ecotopes (Botha *et al.*, 2003; Zere *et al.*, 2005; Botha, 2006; Welderufael, 2006; Anderson, 2007). These studies mainly focused on the phenomena of IRWH during the growing period. Hensley *et al.* (2000) and Botha *et al*. (2003) indicated that fallowing contributed to better yields during the following season. Anderson (2007) also emphasised that the water stored during the fallow period ensured better plant establishment. Furthermore, Botha (2006) and Anderson (2007) used crop growth models to simulate yields for longer periods which included the fallow seasons. They indicated

that the drawback of the models was the lack of water balance simulation during the fallow period. Thus modelling the principal components of the water balance during the fallow period is imperative.

Fallowing is another way to improve the rainwater productivity. It helps to store water over a period when no crop is grown and the field is kept free from weeds (Lampurlanes *et al*., 2002). The length of the fallow period can vary depending on the desired outcome and viability of the practice. In South Africa, the fallow period can be as short as 8 months (Botha, 2006) or longer which skips one or more growing seasons (Hensley *et al*., 2000). In the case of the short fallow, the practice is aimed at conserving the out of season rain. The long fallow on the other hand can store water both during the main rainy season and out of season rains.

1.2. Hypothesis

It was hypothesized that it will be possible to characterize the water balance for the IRWH crop production technique by integrating rainfall-runoff and evaporation models and estimate water storage during the fallow period which will be available for the next crop.

1.3. Objectives

The general objective of the study was to select and evaluate different rainfall-runoff and evaporation models with respect to IRWH during a fallow period. In order to obtain the general objective, the following specific objectives were formulated:

i. To characterize rainfall characteristics of the Bloemfontein area
ii. To determine the influence of rainfall intensity patterns on infiltration and runoff
iii. To compare capacitance probes and neutron water meter for soil water evaporation measurement
iv. To evaluate the influence of the micro-landscape created by the IRWH on the soil water evaporation
v. To model evaporation and runoff on two different ecotopes in Bloemfontein

vi. To integrate, both the runoff and evaporation model to predict water storage under IRWH during the fallow period.

1.4. Description of IRWH and the study areas

IRWH as *in-situ* rainwater harvesting practice has a simple, but sound surface configuration as shown in the diagrammatic representation of IRWH in Figure 1.1. This water management practice involves tilling of the land following a zero-level slope to form a basin of 1 m wide. The basin is the runoff-collection part of the rainwater harvesting setup. With the original design, as proposed by Hensley *et al*. (2000), runoff is induced from a 2 m wide crusted runoff strip that serves as a mini-catchment area. The harvested water is stored in the profile below the basins providing a means of reducing direct evaporation from the soil surface. The effectiveness of the IRWH practice in increasing yield and risk reduction against crop failure resulting from the erratic nature of rainfall was reported (Hensley *et al.*, 2000; Botha *et al.*, 2003; Kundhlande *et al.*, 2004).

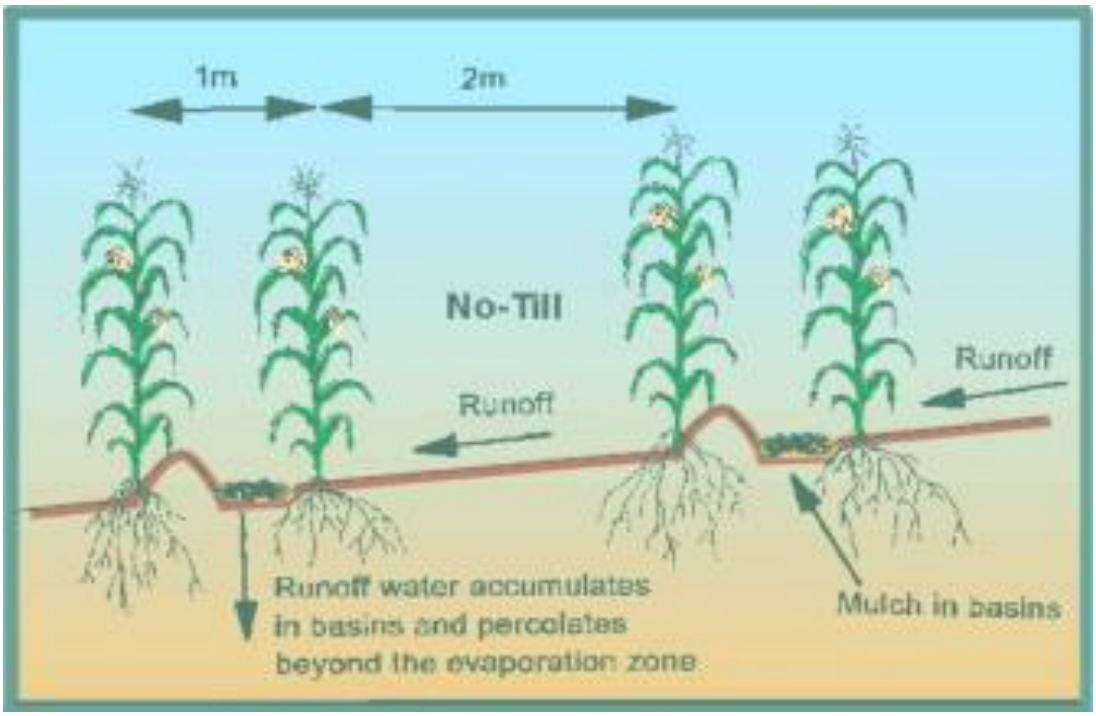

Figure 1.1 Schematic diagram of the in-field rainwater harvesting technique (after Botha *et al*., 2003).

The study was conducted on two sites on the outskirts of Bloemfontein, South Africa. These sites were on the experimental farms of the Natural Science and Agricultural Faculty of the University of Free State. The study sites provided two ecotopes. An ecotope is defined as a land with homogenous climate, topography and soil resources (MacVicar *et al.*, 1974). The climate and topography of these two sites were similar but the soils varied. The study areas were located on the highveld with semi-arid climatic conditions. The long-term climatic data, which is representative of both ecotopes, is shown in Table 1.1. This data was obtained for the Glen Agricultural institute situated not more than 25 kilometres from the two sites.

1.4.1. Paradys/Tukulu ecotope

The first study ecotope is located at Paradys experimental farm. It is located 29º 13’ 23” S and 26º 12’ 41” E. The IRWH plots were prepared during 2008 by hand. The basins were constructed using spades and rakes and by raking the soil to form the ridge on the lower part of the slope. These plots had a width of 5 m, while the length varied according to the basin to runoff strip length (RSL) ratio. Thus the plot dimensions were 5 x 6, 5 x 9 and 5 x 12 m for the 1:1, 1:2 and 1:3 basin to RSL ratios. These plots have been maintained during the fallow period. The plots on which measurements were done were placed in a middle of other two IRWH plots which were not used for measurement of soil water content. This provided a buffer from the surrounding conventional system. The runoff measurements were done in one of the peripheral plots as shown in Figure 1.2. The soil form for these plots was Tukulu. Detailed information for physical properties of the soil (Table 1.2) and the soil profile (Table 1.3) are provided below.

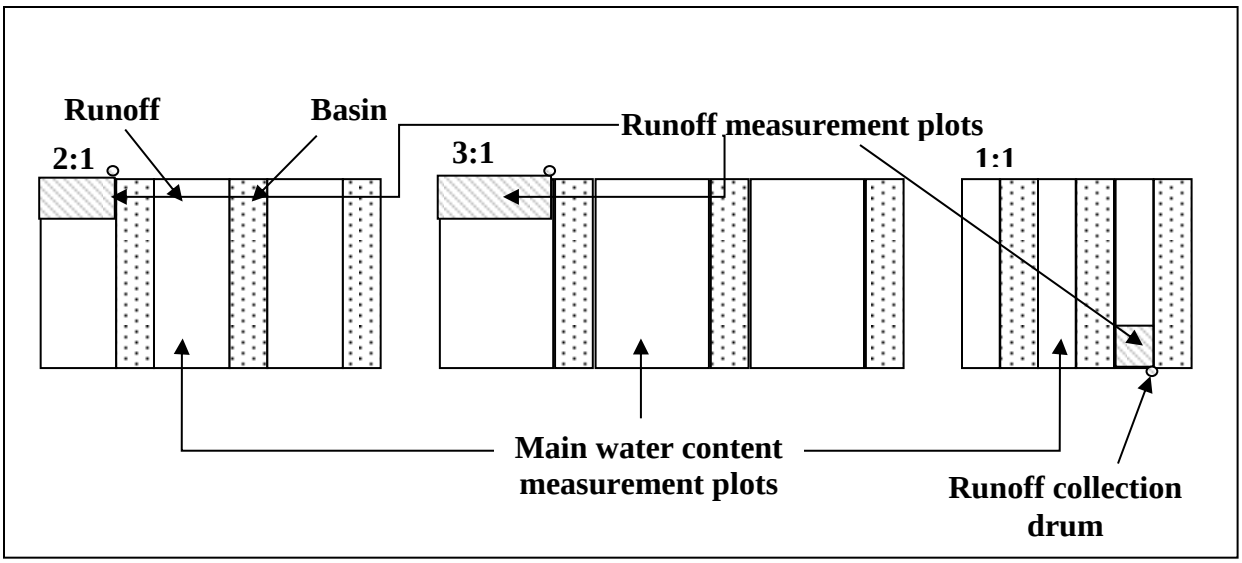

Figure 1.2: Sketch of the experimental set up of the IRWH plots at the Paradys/Tukulu ecotope.

1.4.2. Kenilworth/Bainsvlei ecotope

The second site was the Kenilworth experimental farm. It is located 29º 1' 16" S and 26º 8' 48" E. The field (Figure 1.3) on which the experiment was conducted has been under IRWH since the 2007/2008 planting season. Since this IRWH practice was done on a field of about 1 ha (100 by 92 m) mechanized tillage was employed. The plots were prepared by using a mouldboard plough and disking in autumn 2007 in an East-West direction. The runoff strips in the plots were racked with a laser machine to even-out the surface roughness, and obtain a runoff slope that would direct flow towards the basins. On the subsequent rainfall events the soil surface had created a crust which was paramount in runoff inducement.

This field was planted with maize for two seasons under IRWH practice. In the 2009/2010 season it was fallowed and the IRWH micro-landscape was maintained. The experimental plots were selected within this field. The field contained three runoff strip size variations. The size variations were basin to runoff ratios of 1:1, 1:2 and 1:3. Similar to the Paradys/Tukulu ecotope, runoff measurement plots were constructed within the field. The soil type of this field was of the Bainsvlei soil form. The physical soil properties information (Table 1.2) and profile description (Table 1.4) are provided below.

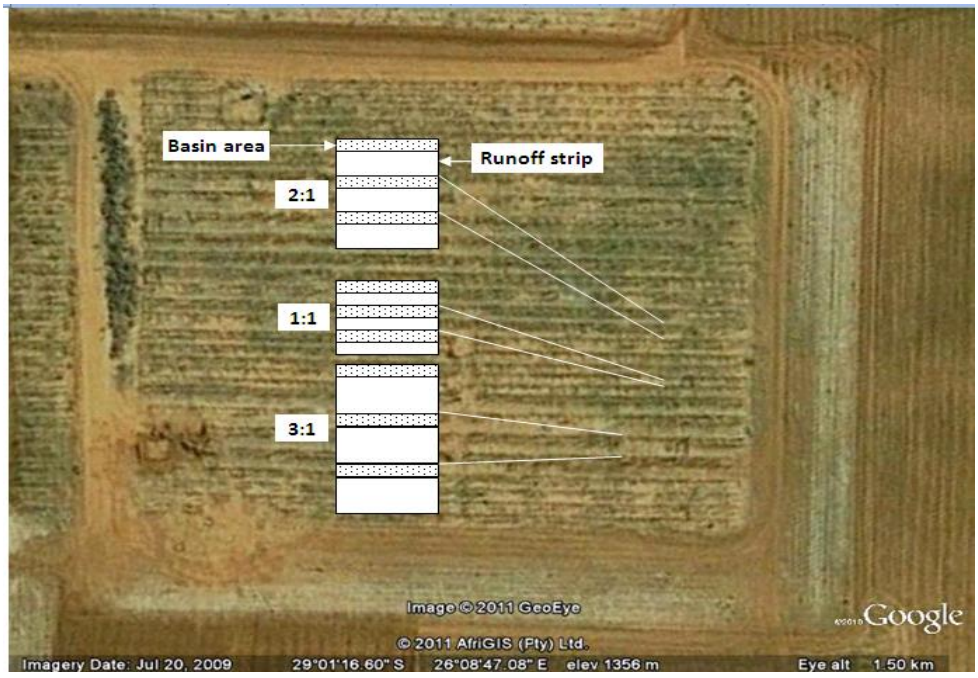

Figure 1.3: Sketch of the experimental set up of the IRWH plots at the Kenilworth/Bainsvlei ecotope.

Table 1.1 Long term climate data for the Glen Agricultural Institute (After Botha, 2006).

Item	Jul	Aug	Sep	Oct	Nov	Dec	Jan	Feb	Mar	Apr	May	Jun	Long term mean
Rain (mm)	8.1	11.6	19.3	49.0	68.2	66.6	83.4	77.6	80.7	49.3	19.9	9.0	542.7
Evaporation[1]	93.5	141	198	239	256	292	277	208	177	126	111	82	2198
MaxT (°C)[2]	17.8	20.6	24.4	25.4	28.3	30.2	30.8	29.5	27.4	23.9	20.5	17.9	24.8
Min T (°C)	-1.6	0.9	5.2	9.2	12.0	14.0	15.3	14.8	12.6	7.8	2.8	-1.1	7.5
Ave. T (°C)	8.1	10.7	14.8	17.5	20.1	22.0	23.0	22.1	19.9	15.8	11.6	8.2	16.2
Aridity index[3]	0.09	0.08	0.10	0.21	0.27	0.23	0.30	0.37	0.46	0.39	0.18	0.11	0.23

[1] Class A pan.
[2] T = temperature in °C; mean values for the month.
[3] Aridity index = rain/evaporation.

Table 1.2 Physical properties of the Bainsvlei and Tukulu soils (After Chimungu, 2009).

Ecotope	Physical characteristics	Soil horizons					
		A	B1	B2	B3	B4	B5
Kenilworth/Bainsvlei	Coarse sand (2 - 0.5 mm) (%)	0.4	0.3	0.3	0.3	0.3	0.6
	Medium sand (0.5 - 0.25) (%)	7.1	5.2	5.4	4.1	3.3	6.0
	Fine sand (0.25 - 0.106 mm) (%	61.4	55.1	53.8	44.9	64.3	48.3
	Very fine sand (0.106 - 0.53mm) (%)	16.8	15.1	15.5	18.0	17.3	17.0
	Silt (%)	4.0	4.0	6.0	8.0	4.0	6.0
	Clay (%)	8.0	18.1	18.0	22.1	8.1	20.1
	Bulk density (Mg m^{-3})	1.66	1.68	1.66	1.67	1.68	1.67
Paradys/Tukulu	Coarse sand (2-0.5 mm) (%)	3.1	1.6	1.3			
	Medium sand (0.5-0.25) (%)	2.8	2.7	1.6			
	Fine sand (0.25-0.106 mm) (%)	42.4	42.2	23.2			
	Very fine sand (0.106-0.53mm) (%)	25.6	19.6	9.9			
	Silt (%)	6.0	3.0	8.0			
	Clay (%)	18.6	28.9	54.8			
	Bulk density (Mg m^{-3})	1.67	1.68	1.71			

1.5. The scope and limitation of the study

The study deals with the modelling of the IRWH. The study has assayed the modelling of IRWH system by addressing the objectives outlined above. The modelling focused on the two major forms of soil water loss, runoff and soil water evaporation, among the components of the soil water balance. Besides the runoff and soil water evaporation, the rainfall events prevailing in the ecotopes are characterized. When conducting water balance by integrating the components, drainage simulations are conducted by using existing drainage curve data (Chimungu, 2009). The modelling process involves use of empirical methods which restricts the application to the same ecotope.

Table 1.3 Profile description of the Tukulu soil form (After Chimungu, 2009).

Map/photo:	2926 Bloemfontein	Soil form and family:	Tukulu *Dikeni*
Latitude +Longitude	29° 13' 25"/26° 12' 08"	Surface rockiness:	None
Altitude:	1417 m	Occurrence of flooding:	None
Terrain unit:	Midslope	Wind erosion:	Slight wind
Slope:	1%	Water erosion:	None
Slope shape:	Straight	Vegetation/Land use:	Agronomic field crops
Aspect:	South	Water table:	None
Microrelief:	None	Described by:	M. Hensley & J. Chimungu
Parent Material Solum:	Origin single, Aeolian, solid rock	Date described:	12/06/09
Underlying Material	Sandstone (Feldspathic)	Weathering of underlying material:	Weak physical, moderate chemical
		Alteration of underlying material:	Ferruginised

Horizon	Depth (mm)	Description	Diagnostic horizon
A	0-270	Moist state; dry colour: reddish brown (2.5YR5/4); moist colour: reddish brown 2.5YR4/4; texture: fine sandy loam; structure: apedal massive: consistence: friable; few fine pores; common roots; gradual transition.	Orthic
B1	270-500	Moist state; dry colour: reddish brown (2.5YR5/4); moist colour: reddish brown (2.5YR4/4); texture: fine sandy clay loam; structure: apedal massive becoming weak subangular blocky towards transition: consistence: friable; few fine pores; few clay cutans; very few fine pore; common roots; clear, tonguing transition.	Neocutanic
C1	500-800	Moist state; dry colour. Dark greyish brown 2.5YR4/2; moist colour. grey 2.5Y5/0; texture: clay; common distinct grey and yellow reduced iron oxide mottles: few prominent black oxidised iron oxide mottles; structure: prismatic; consistence: firm; few slickensides; common clay cutans; very few roots; gradual transition.	Unconsolidated material, with signs of wetness
C2	800-±1350	Allows water to enter, hence the presence of roots. It chops out of the profile relatively easily up to ±1350 mm, getting harder towards the bottom and probably very impermeable slightly deeper.	

Table 1.4 Profile description of the Bainsvlei soil form (After Chimungu, 2009).

Map/photo:	2926 Bloemfontein	Soil form and family:	Bainsvlei Amalia
Latitude +Longitude	29˚ 1’ 00”/26˚ 08’ 00”	Surface rockiness:	None
Altitude:	1354	Occurrence of flooding:	None
Terrain unit:	Lower foot slope	Wind erosion:	Slight wind
Slope:	1%	Water erosion:	None
Slope shape:	Straight	Vegetation/Land use:	Agronomic field crops
Aspect:	North-west	Water table:	None
Microrelief:	None	Described by:	M. Hensley & J. Chimungu
Parent Material Solum:	Origin single, Aeolian	Date described:	14/06/09
Underlying Material	Sandstone (Feldspathic)	Weathering of underlying material:	Weak physical to moderate chemical
		Alteration of underlying material:	Ferruginised

Horizon	Depth (mm)	Description	Diagnostic horizon
A	0 -250	Moist state; dry colour: yellowish red (5YR5/6); moist colour: reddish brown (5YR4/4); texture: fine loamy sand; structure: apedal massive; consistence: friable; few fine normal pores; water absorption: 1 second; few roots; gradual smooth transition.	Orthic
B1	250-420	Moist state; dry colour: red (2.5YR4/8); moist colour: red (2.5YR4/6); texture: fine sandy loam; structure: apedal massive; Consistence: friable; few fine normal pores; water absorption: 1 second; few roots; gradual smooth transition.	Red apedal
B2	420-700	Moist state; dry colour: yellowish red (5YR5/8); moist colour: red (2.5YR4/6); texture: fine sandy loam; few fine faint black illuvial humus mottles; structure: apedal massive; consistence: friable; common fine normal pores; water absorption: 1 second; few roots; gradual wavy transition.	Red apedal
B3	700-1200	Moist state; dry colour: yellowish red (5YR4/6); moist colour: reddish brown (5YR4/4); texture: fine sandy clay loam; common fine faint black illuvial humus mottles; structure: apedal massive; consistence: slightly firm; common fine normal pores; water absorption: 1 second; clear wavy transition.	Red apedal
B4	1200-1450	Moist state; dry colour: strong brown (7.5YR5/8); moist colour: strong brown (7.5YR5/6); texture; fine sand; few fine faint black illuvial humus mottles; structure: apedal massive; consistence: friable; water absorption: 1 second; few roots; clear wavy transition.	Non diagnostic; yellow brown Aeolian sand
B5	1450-1850	Moist state; moist colour: strong brown (7.5YR4/6); texture: fine sandy loam; many medium distinct grey and yellow reduced iron oxide mottles; many medium distinct red and black oxidised iron oxide mottles; structure: apedal massive; consistence: friable; water absorption: 1 second(s); few roots; gradual smooth transition.	Soft plinthic
C	1850-2220	Similar to B5 with patches of weathered feldspathic sandstone; colour of mottles similar to B5 but more prominent.	

References

Anderson, J.J., 2007. Rainfall-runoff relationships and yield responses of maize and dry beans on the Glen/Bonheim ecotope using conventional tillage and in-field rainwater harvesting. Ph.D. thesis University of the Free State, Bloemfontein.

Botha, J.J., van Rensburg, L.D., Anderson, J.J., Hensley, M., Macheli, M.S., van Staden, P.P., Kundhlande, G., Groenewald, D.C. & Baiphethi, M.N., 2003. Water conservation techniques on small plots in semi-arid areas to enhance rainfall use efficiency, food security, and sustainable crop production. Water Research Commission report No. 1176/1/03, Pretoria, South Africa.

Botha, J.J., 2006. Evaluation of maize and sunflower production in semi-arid area using in-field rainwater harvesting. Ph.D. thesis University of the Free State, Bloemfontein, South Africa.

Chimungu, J.G., 2009. Comparison of field and laboratory measured hydraulic properties of selected diagnostic soil horizons. M.Sc. thesis University of the Free State, Bloemfontein, South Africa.

Hensley, M., Botha, J.J., Anderson, J.J., van Staden, P.P. & du Toit, A., 2000. Optimizing rainfall use efficiency for developing farmers with limited access to irrigation water. Water Research Commission report No. 878/1/00, Pretoria, South Africa.

Kundhlande, G., Groenewald, D.C., Baiphethi, M.N., Viljoen, M.F., Botha, J.J., van Rensburg, L.D. & Anderson, J.J., 2004. Socio-Economic Study on water conservation techniques in semi-arid areas. Water Research Commission report No. 1267/1/04. Pretoria, South Africa.

Lampurlanes, J., Angas, P. & Martinez, C.C., 2002. Tillage effects on water storage during fallow and on barley root growth and yield in two contrasting soils of the semi-arid Segarra region in Spain. *Soil & Tillage Research* **65**:207-220.

Macvicar, C.N., Scotney, D.M., Skinner, T.E., Niehaus, H.S. & Loubser, J.H., 1974. A classification of land (climate, terrain form, soil) primarily for rainfed agriculture. *S. Afr. J. Agric. Ext.* **3**:21-24.

Ngigi, S.N., Rockström, J. & Savenije, H.H.G., 2006. Assessment of rainwater retention in agricultural land and crop yield increase due to conservation tillage in Ewaso Ng'iro river basin, Kenya. *Phys. Chem. Earth* **31**:910–918.

Ren, X., Chen, X. & Jia, Z., 2010. Effect of rainfall collecting with ridge and furrow on soil moisture and root growth of corn in semiarid Northwest China. *J. Agron. Crop Sci.* **196**:109–122.

Rijsberman, F.R., 2006. Water scarcity: fact or fiction*? Agric. Water Manage.* **80**:5–22.

Rockström, J., 2000. Water resources management in smallholder farms in Eastern and Southern Africa: an overview. *Phys. Chem. Earth* **25**:275-283.

Sepaskhah, A.R. & Ahmadi, S.H., 2010. A review on partial root-zone drying irrigation. *Int. J. Plant Prod.* **4**(4):241-258.

Welderufael, W.A., 2006. Quantifying rainfall-runoff relationships on selected benchmark ecotopes in Ethiopia: a primary step in water harvesting research. Ph.D. thesis University of the Free State, Bloemfontein, South Africa.

Zere, T.B., van Huyssteen, C.W. & Hensley, M., 2005. Estimation of runoff at Glen in the Free State province of South Africa. *Water SA* **31**(1):17-22.

2. Characterization of rainfall in the Central South African Highveld for application in rainwater harvesting

Abstract

In-field rainwater harvesting (IRWH), a runoff farming system, is a beneficial water management technique for crop production in arid and semiarid areas. In-field rainwater harvesting is influenced by rainfall characteristics, and hence this study aimed to identify and characterize rainfall events, and determine rainfall parameters that were of significance in in-field runoff. Two algorithms of event identification were developed. The algorithm that identified events spanning over a 24-hour day limit as a single event, gave better identification results which were characterized. This enabled systematic grouping of rainfall parameters. About 33% of the total rainfall amount received had zero potential to be harvested as runoff in the IRWH system. Therefore, a runoff harvesting practice needs to use the remaining 67%. Rainfall events that lasted half an hour or longer were of rainwater harvesting importance. This could be the minimum duration guideline when simulating rainfall for rainwater harvesting studies. Rainfall event amount and intensity were of significant importance for IRWH runoff determination**.**

Keywords: rainwater harvesting, rainfall characteristics, runoff, rainfall event identification

2.1. Introduction

Dryland cropping in arid and semi-arid regions has climatic limitations, particularly that of rainfall (Rockström, 2000; Thomas, 2008). The limitation of rainfall demands that great care be given to understanding rainfall behaviour and to devise means to make best use of it (Batisani & Yarnal, 2010). To address the challenge of the erratic nature of rainfall, rainwater harvesting has become a common practice. In-field rainwater harvesting (IRWH) is one form of rainwater harvesting, which maximizes effectiveness of rainwater by reducing the ex-field runoff to zero (Hensley *et al.*, 2000). The in-field rainwater harvesting technique has a no-till runoff strip surface that directs runoff into the basins from where the runoff water infiltrate deeper into the soil profile and stored for later use by the planted crops. Crops are planted on the edges of these basins, thereby ensuring a better use of the rainwater (Hensley *et al.*, 2000; Botha *et al.*, 2003). To determine the proportion of rainwater reaching the basins, three aspects are of importance; (i) rainfall interception by the canopy of the crops, (ii) surface properties of the soil and (iii) rainfall characteristics such as amount, duration and intensity. This research focussed on the third aspect as it is fundamental for the application of research designed to measure rainfall-runoff relationships on IRWH.

Characterization of rainfall is very important for the planning and implementation of rainwater harvesting systems (Rappold, 2005). Rawitz & Hillel (1971) characterized rainfall events for the purpose of developing a method of determining rainwater harvesting potential. Morin *et al.* (1984) develop a method of runoff prediction based on known soil properties and the analysis of historical rainfall data. They identify important indices of rainfall characteristics but the scale is coarse. Ngigi (1999) proposed the incorporation of rainfall distribution in the designing of rainwater catchment systems. More valuable inputs from characterization of rainfall can be drawn if it would be done by identifying individual rainfall events (Dunkerley, 2008a). Dunkerley (2008b) provides good description of such identification of rainfall events and challenges associated with it. Such characterization of historical rainfall data could contribute in designing IRWH systems.

Various studies on rainfall characterization have been carried out in South Africa. These studies however focused on the prediction of extreme storms (Nel, 2007; Dyson, 2009), seasonal rainfall characteristics with regard to predictability (Tennant & Hewitson, 2002) and the recurrence of storms of interest (Smithers & Schulze, 2000; Nel, 2007). There is little work done with regard to identifying individual rainstorms and analysing the properties of individual rain events. Nel (2008) describes rainfall events prevailing in the KwaZulu-Natal Drakensberg, South Africa, by analysing 5-minute rainfall data. Walker & Tsubo (2003) made a statistical study of rainfall characteristics in Bloemfontein, Glen and Pretoria, South Africa. Dimensionless hyetographs, which do not depend on the amount and duration of a rainfall event, were used to analyse rainfall intensity data from Bloemfontein and Pretoria. The dimensionless hyetographs for these areas, which predominantly experience a convective storm type, are not different when compared in seasonal and geographic terms (Tsubo *et al.*, 2005).

The need for rainfall event property analyses becomes important when designing the simulation of rainstorms. A review done by Dunkerley (2008a) shows that many rainfall simulation studies are biased towards higher rainfall intensity and lack correlation with the natural rainfall. For instance, studies with rainfall intensities as high as 30 times the average rainfall intensity of ordinary (non-exceptional) events are presented as acceptable simulations (Dunkerley, 2008a). Hence, undertaking the task of ordinary rainfall property analysis can form a basis for the useful exercise of average rainfall simulation in a way that can yield relevant results.

In this study it was hypothesised that despite the erratic nature of rainfall, it would be possible to analyze historical rainfall data and classify the rainfall patterns. The application of the research will improve the scientific basis for selecting representative rainfall events as treatments in rainfall simulation studies. Thus, the objectives of this study were:

i. to develop an acceptable systematic way of identifying individual rainfall events from pluviographic data,

ii. to statistically characterize rainfall events according to amount, duration and intensity , and

iii. to identify rainfall parameters of significance with regard to runoff generation and rainwater harvesting.

2.2. Methodology

2.2.1. Description of the study area

The data were obtained from the Glen Agricultural Institute located in the central South African highveld. The highveld consists of the high-plateaus of South Africa, covering about 30% of the country's land area (Wikipedia, 2010). The study-area has a semi-arid climate, with a long-term annual average rainfall of 540 mm and a high annual evaporative demand that can be four times more than received rainfall (Anderson, 2007). This is reflected in a low aridity index (UNEP, 1992) of 0.24 of the area (Anderson, 2007). The rainy season is from October to April.

2.2.2. *Representativeness of the data*

For the purpose of aiding comprehension, the years for which the data are analysed are categorised with regard to wetness. The wetness categories are decided by taking the long-term (1922 -2006) annual average rainfall (μ) and the standard deviation (σ). The years receiving annual rainfall amount below $\mu - \sigma$ were categorized as dry. The years that received annual rainfall amount between $\mu - \sigma$ and $\mu + \sigma$ (boundary values included) were categorized as average (intermediate). Those years that received annual rainfall amount greater than $\mu + \sigma$ were categorized as wet.

The analysis of long-term annual rainfall data for the same locality showed that 70% of the years received average rainfall, while the dry and wet years accounted for 15% each. The 15 years considered in this study corresponded well with the long-term values. The years that received average annual rainfall were 67%, while the dry and wet years accounted 20% and 13%, respectively. This shows that the 15 year data used in this study represents the three categories comparably as the long-term would.

2.2.3. Rainfall event identification

The analyses were done on pluviographic data collected from 1992 to 2007. Data records contained a 1-minute resolution of rainfall amounts collected by a tipping-bucket pluviograph equipped with a data logger. The instruments used over the years differed; those used from 1992 to 1999 had a bucket of 0.2 mm, while the ones from 2000 to 2004 and 2005 to 2007 had 0.1 and 0.254 mm buckets, respectively.

Rainfall was recorded in a format that showed the amount of rainfall received at a certain time, with the day, hour and minute marked for each entry. The data record did not show individual events and a method of identifying individual events was devised with an assumed minimum inter-event time (MIT). Walker & Tsubo (2003) used an MIT of 3 hours, which was also used in this study. The MIT was used when developing algorithms (Figures 2.1 and 2.2) that included consecutive records to determine if they belonged in a same rainfall event, thereby enabling identification of individual events. The algorithms were implemented on Excel® software by using a simple program of a series of 'If statements' validating the decision given at the algorithms.

Each algorithm was tested for its capability of identifying events happening in a day, given that the MIT was observed. The first algorithm (Figure 2.1) assumed that individual events were contained within a 24-hour day, starting 0:00 AM and ending same hour next day. However, if an event started in a given day and continued to the next day, it was split to make two separate events. This assumption to some extent contradicted the idea of having a specific MIT, because the duration between such events was smaller than the MIT. To address this issue, a second algorithm (Figure 2.2) was used that could combine events stretching beyond the 24-hour limit, as far as MIT was observed.

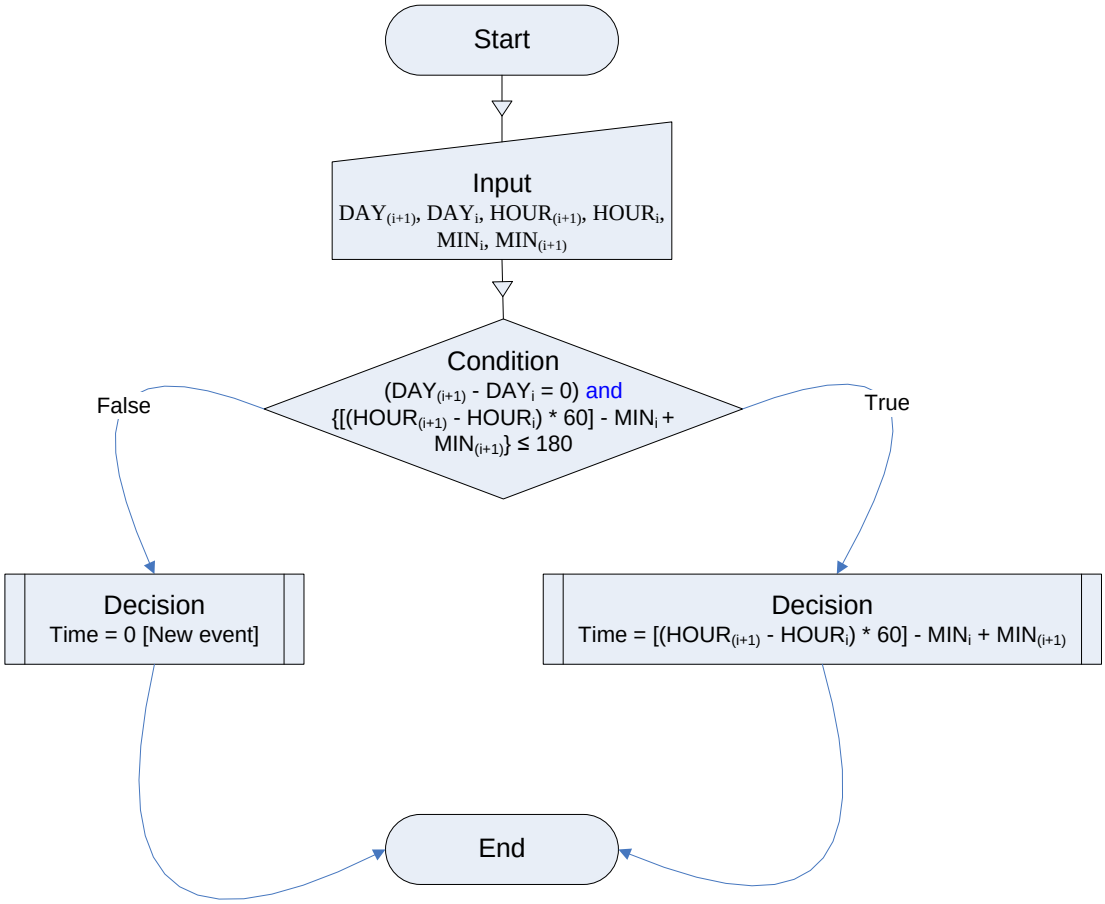

Figure 2.1 An algorithm for determining duration from consecutive records and identifying individual events within a 24-hour day limit.

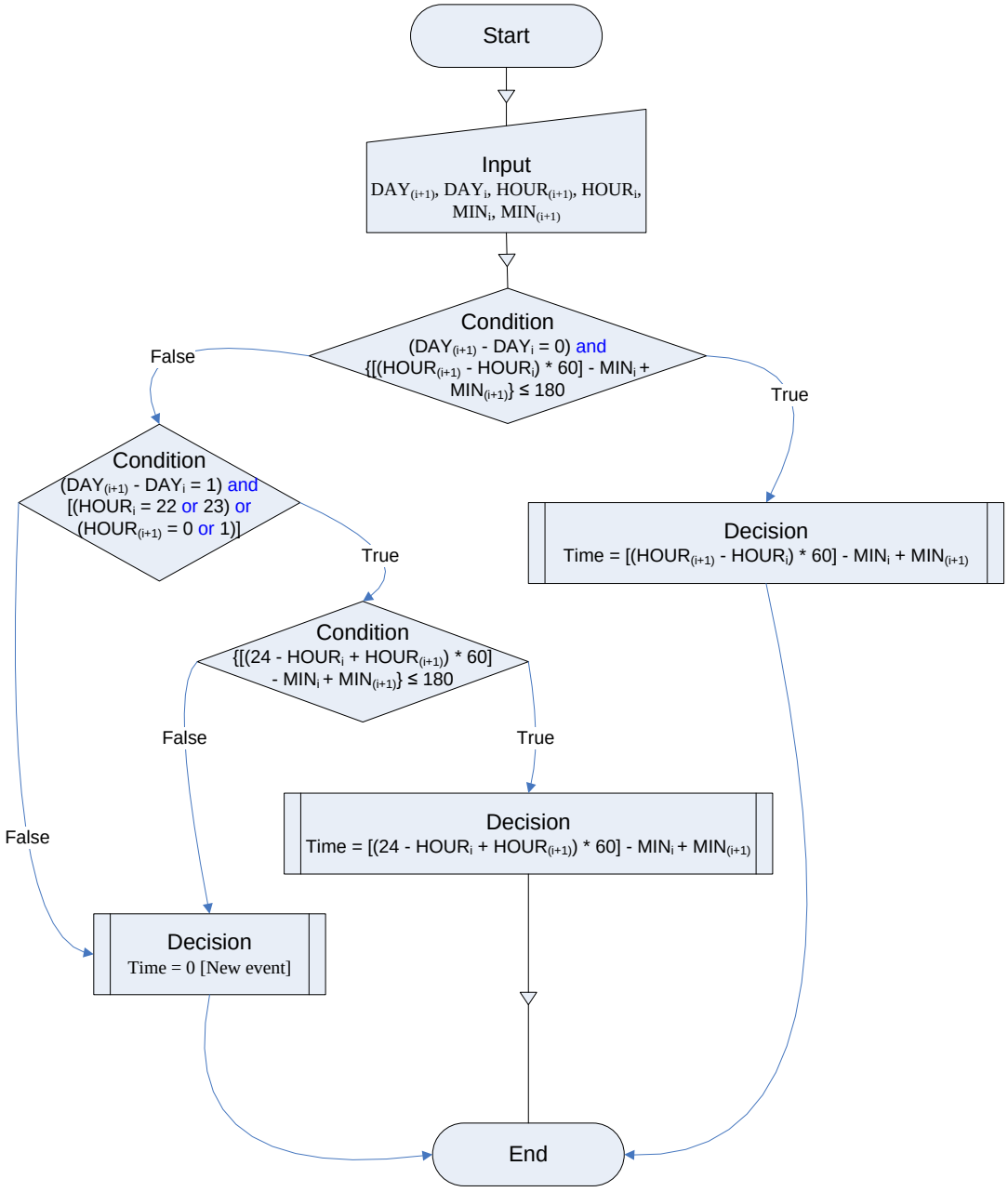

Figure 2.2 An algorithm for determining duration from consecutive records and identifying individual events with no day limit.

The algorithms given in Figures 2.1 and 2.2 determined whether the time elapsed between two consecutive entries in the pluviograph record belonged to the same event or not. If the consecutive entries belonged to the same event, the time elapsed was given as the output. If the time elapsed was longer than the MIT, zero was given as output marking the start of a new event.

2.2.4. Statistical characterization of rainfall events

SAS® software (SAS Institute Inc., 2006) and Excel® software were used for the statistical analyses of the properties of identified rainfall events. The rainfall properties considered for analyses were: duration, peak intensity and time of peak intensity, mean event rainfall amounts, mean event rate (intensity) and frequencies of different rainfall amounts. Input data were used to calculate the averages, sums, and standard deviations. Amount and duration of all events were analysed. Additionally events, which were capable of causing runoff (rainfall events > 8 mm) were analysed separately. From local agricultural field experience an event amount of 8 mm was adopted as threshold value for inducing runoff (Hensley *et al.*, 2000; Walker & Tsubo, 2003). Narrow range groupings of rainfall amounts were constructed for which the rainfall events falling within these ranges were counted and the corresponding amounts and percentages determined. The frequency count for classes of event duration and the corresponding amount of rain contributed was also calculated.

For the purpose of using a shape parameter to determine time of peak intensity, the measure of skewness was used. In measuring the skewness, event duration was plotted with the intensities recorded as a frequency. The frequency distribution plotted this way depicted the shape of the hyetograph. Skewness was a measure of symmetry of a given distribution and thus gave good information about the shape of the hyetograph. Only the shape of hyetograph and intensity analyses of rainfall events causing runoff (> 8 mm) were considered, because the study focussed on application of outcomes for IRWH. The shape analysis was calculated for events throughout the year and for events during the rainy season. The shape evaluation focussed on identifying events with peak intensities early, in the middle or late during a rainfall event. Skewness results were categorized as right-skewed, left-skewed, and symmetric for positive, negative and zero values, respectively. Bulmer (1979) provides a guide to the measure of skewness, which was applied in this study: skewness values greater than 1 in absolute value was considered highly skewed, values between 0.5 and 1 in absolute values were slightly skewed and values between 0 and 0.5 in absolute values were considered reasonably symmetrical.

2.2.5. Selection of rainfall parameters

Correlation tests were done to identify the contribution of rainfall parameters to runoff generation. By taking rainfall event characteristics and runoff data collected for a Glen/Bonheim ecotope (Hensley *et al.* 2000), a canonical correlation analysis (SAS Institute Inc., 2006) was used to measure significance of the rainfall characteristics considered in runoff generation. These data were collected from experimental plots under IRWH for three seasons from 1996 to 1999 (Hensley *et al.* 2000). The rainfall characteristics were the parameters generally available from weather stations equipped for measuring rainfall intensity, rainfall amount, event duration, peak-intensity, overall-average intensity, and average recorded intensity. Three parameters of intensity were considered, namely peak intensity, overall-average intensity and average recorded intensity. Overall-average intensity was computed by duration-weighted averaging of the recorded intensities. Average recorded intensity, on the other hand, was the average computed by adding the intensity values recorded and then dividing it by the number of records. The canonical correlation provided the correlation between all the variables. Furthermore, it provided a canonical variate, which was made of all the variables and had best correlation with the measured runoff. Regression coefficients of the variables making up the variate are provided, which reflect the contribution each variable makes. T-test results are also given showing the significance of the contribution.

2.3. Results and discussion

2.3.1. Algorithms of rainfall event identification

The two algorithms identified all rainfall events including single-tip events. This enabled the computation of time elapsed from the start of the rainfall event and intensities as the ratio of the recorded amount to time elapsed between records. The only exceptions were single tip events and the first record of an event, which had no time lapses. The two algorithms differed in identifying the number and duration of rainfall events (Table 2.1). The first algorithm identified 92 more events (all rainfall events) than the second algorithm. This was mainly because a 24-hour limit was set for the first algorithm, which could split one event spanning over two days to be considered as two events. The second

algorithm combined such events and thus fewer events were identified. A different scenario was observed for rainfall events > 8 mm. The first algorithm identified 4 events less than the second algorithm. When the details of the data were considered, those instances where differences occurred for events spanning two days were the same as in the above explanation. However, the second filter of "> 8 mm" disqualified some events from the first algorithm after being split into two (i.e. split resulting in one or two events having less than 8 mm).

The comparison between event duration was consistently more in the second algorithm for all rainfall events and rainfall events > 8 mm. In this instance, the time between two records on either side of the hour 24:00 were excluded in the first algorithm, but included in the second algorithm.

Table 2.1 Total count, amount and duration of rainfall events identified with the first and second algorithms.

Rainfall parameters	1st Algorithm (24-hour day limit)		2nd Algorithm (no limit)	
	All	> 8 mm	All	> 8 mm
Number of events	1138	176	1046	180
Total amount (mm)	4713	3015	4713	3160
Total duration (days)	91.4	38.1	94.3	45.6

The second algorithm's event identification was not compromised by having an MIT and did not split an event into two (Table 2.1). This was an improvement on the first algorithm, the assumption of which was employed by Nel (2008) and Dyson (2009) in South Africa. Thus, the following results discussed in this study used only the second algorithm. Nevertheless, the first algorithm is useful in comparing other studies, which make the same assumptions (Nel, 2008). The first algorithm may be used to compare data with other stations that do not have detailed minute-by-minute recordings but only daily values. However, care must be exercised because the starting time of a 24-hour day of different stations can vary.

2.3.2. Event amount

Narrow range groupings of rainfall amounts are given in Table 2.2. A very important characteristic of the rainfall was derived from Table 2.2, namely 83% of the rainfall events were less than 8 mm. These events amounted to 33% of the total rainfall received. When considering events capable of inducing runoff (events of > 8 mm) the bulk of events (~76%) ranged from 8 to 20 mm. These events are of great importance to rainwater harvesting because they account for 53% of the total rainfall.

Table 2.2 Classes of rain event amount with corresponding frequency, amount and percentages.

Rainfall amount range (x) (mm)	Events > 8 mm				All events			
	Count	Percentage of total	Rain amount (mm)	Percentage of total	Count	Percentage of total	Rain amount (mm)	Percentage of total
$x \leq 1$	0	0	0	0.0	442*	42.3	146	3.1
$1 < x \leq 8$	0	0	0	0.0	424	40.5	1407	29.9
$8 < x \leq 15$	108	60	1178	37.3	108	10.3	1178	25.0
$15 < x \leq 20$	29	16.1	495	15.7	29	2.8	495	10.5
$20 < x \leq 25$	14	7.8	312	9.9	14	1.3	312	6.6
$25 < x \leq 30$	5	2.8	132	4.2	5	0.5	132	2.8
$30 < x \leq 40$	15	8.3	500	15.8	15	1.4	500	10.6
$40 < x \leq 50$	4	2.2	181	5.7	4	0.4	181	3.8
$x > 50$	5	2.8	362	11.5	5	0.5	362	7.7
Total	180	100	3160	100	1046	100	4713	100

* This number includes 239 single-tip events

The maximum rainfall amount recorded was 85 mm, while the average event amount over the entire measuring period was very low, at 4.1 - 4.5 mm. The average event amount increased to 17.1 - 17.6 mm when only events of more than 8 mm were considered. A standard deviation of 7.6 mm (variance of 57.8 mm) indicated a large variation in the amounts recorded. The minimum event amount recorded was 0.1 mm, which was a single-tip event. The single-tip events (because of different instruments used, they ranged between 0.1 - 0.254 mm) made up about 23% of all identified events. Dunkerley (2008b) found a comparable percentage (19.5%) of single-tip events in one instance of his varying MIT experiment, but this is incidental because his MIT was 8 times the one used in this study. The single-tip events did not provide adequate

information about the nature of the event except for the amount, because there is no indication at what time the rain started.

2.3.3. Event duration

The classes of event duration, frequency and amount of rain are given in Table 2.3. The average event duration was 130 minutes. This value was 21% lower compared to that of Walker & Tsubo (2003) for the same area. The difference was attributed to Walker & Tsubo (2003) excluding single tip events that were included in this analysis. The average event duration became more than double when events of > 8 mm were considered. Another parameter worth reporting was the very high standard deviation (200 minutes), which was indicative of how variable the event duration could be.

Table 2.3 Classes of rain event duration with corresponding frequency, amount and percentages.

Rainfall duration range (x) (min)	Events > 8 mm				All events			
	Count	Percentage of total	Rain amount (mm)	Percentage of total	Count	Percentage of total	Rain amount (mm)	Percentage of total
$x \leq 1$*	0	0	0	0.0	239	22.9	50	1.1
$1 < x \leq 5$	0	0	0	0.0	51	4.9	20	0.4
$5 < x \leq 10$	0	0	0	0.0	49	4.7	52	1.1
$10 < x \leq 15$	0	0	0	0.0	33	3.2	63	1.3
$15 < x \leq 20$	0	0	0	0.0	29	2.8	34	0.7
$20 < x \leq 25$	0	0	0	0.0	31	3	66	1.4
$25 < x \leq 30$	3	1.7	22	0.7	23	2.2	62	1.3
$30 < x \leq 60$	12	6.7	160	5.1	100	9.6	350	7.4
$60 < x \leq 90$	9	5	105	3.3	76	7.3	312	6.6
$90 < x \leq 120$	14	7.8	195	6.2	67	6.4	330	7.0
$120 < x \leq 150$	17	9.4	227	7.2	49	4.7	309	6.5
$150 < x \leq 180$	5	2.8	90	2.9	36	3.4	184	3.9
$180 < x \leq 240$	24	13.3	348	11.0	78	7.5	498	10.6
$240 < x \leq 300$	15	8.3	307	9.7	51	4.9	436	9.2
$300 < x \leq 360$	10	5.6	122	3.8	32	3.1	223	4.7
$360 < x \leq 480$	19	10.6	302	9.5	38	3.6	374	7.9
$480 < x \leq 600$	20	11.1	392	12.4	27	2.6	433	9.2
$x > 600$	32	17.8	892	28.2	37	3.5	917	19.5
Total	180	100	3160	100	1046	100	4713	100

*single-tip rain events [not reflective of duration taken]

The duration of all events fell within each rainfall duration range whereas events of > 8 mm had a threshold range of $25 < x \leq 30$ minutes (Table 2.3). The rainfall events of > 8 mm, the group of rainwater harvesting importance, took at least 25 minutes and as long as 31 hours. In this group 46% of the events were 4 hours or shorter. When all events were considered, the percentage of events lasting 4 hours or less increased to 82.6% and the frequency count did not reflect the amount of rain received. Inversely, the frequency count of the > 8 mm group was proportional to the amount of rain received.

2.3.4. Shape of hyetograph

Skewness values that were used to evaluate the shapes of the hyetographs are given in Table 2.4. Events with amounts of > 8 mm in a year and in the rainy season are summarised.

Table 2.4 Skewness values and the corresponding percentage for rainfall events of > 8 mm.

Skewness value range (x)	All events		Rainy season	
	Frequency	Percentage of the total	Frequency	Percentage of the total
$x \leq -0.5$	39	21.7	35	21.7
$-0.5 < x \leq 0.5$	61	33.9	51	31.7
$x > 0.5$	80	44.4	75	46.6
Total	180	100	161	100.0

Using the guideline of Bulmer (1979) and considering all rain events the hyetographs presented as follows: a third were symmetrical, 22% were left skewed and 44% were right skewed. The hyetographs for events during the rainy season deviated slightly from all events. Generally, a high number of the events presented with early peak intensity. This finding corresponds well with the finding of Walker & Tsubo (2003) in that 49% of the events recorded for the Bloemfontein area had peak intensities in the first quartile of an event.

2.3.5. Rainfall rate (intensity) values

Investigating the actual ranges of intensities is also imperative and Dunkerley (2008a) separates the terms “instantaneous rainfall rate” and “mean rainfall rate”. The latter is generally referred to in the literature as “rainfall intensity”. For this study the latter term was used because the values were calculated by dividing the rainfall amount received with the elapsed time (1 minute). Table 2.5 shows the summary collated by considering intensity values calculated for rainfall events with amounts > 8 mm.

Table 2.5 Frequency count for mean event and peak rainfall intensity for rainfall events of > 8 mm.

Range for mean event intensity (x) (mm hr^{-1})	Frequency	Percentage of total	Range for peak intensity recorded (x) (mm hr^{-1})	Frequency	Percentage (%)
$x \leq 5$	121	67.2	$x \leq 10$	8	4.4
$5 < x \leq 10$	35	19.4	$10 < x \leq 25$	52	28.9
$10 < x \leq 20$	20	11.1	$25 < x \leq 50$	59	32.8
$20 < x \leq 30$	3	1.7	$50 < x \leq 75$	30	16.7
$30 < x \leq 40$	1	0.6	$75 < x \leq 100$	22	12.2
$x > 40$	0	0.0	$x > 100$	9	5.0
Total	180	100.0		180	100.0

Table 2.5 provides the distribution of mean and peak intensity values. Accordingly, 67% of the rainfall events recorded had mean event intensity ≤ 5 mm hr^{-1}. This apparently low value of mean event intensity, compared to instantaneous intensity, should not be interpreted as displaying a generally low rainfall intensity in the area under study. The value was low mainly because the rainfall duration could include any dry interval that was less than the MIT of 3 hours because the intensity was averaged over the entire duration. According to Laakso *et al.* (2003) and Tokay & Short (1996) rainfall rates below 5 mm hr^{-1} may be classed into events with mean intensity of < 1 mm hr^{-1} are considered very light; those between 1 and 2 mm hr^{-1} are light; between 2 and 5 mm hr^{-1} are classified as moderate; > 5 mm hr^{-1} are heavy. For instance there was only 1 event recorded in which the mean event intensity was greater than 30 mm hr^{-1}. This event occurred on the 50th day of 2006, without any interruption and amounted to 22.8 mm over a period of 40 minutes. The intensity varied during the storm and reached a peak intensity of 91 mm hr^{-1}. Contrary to this, an event recorded on the 59th day of 2002 scored 2.5 mm hr^{-1} for the mean event intensity, but the peak intensity was the highest of the entire data recorded, i.e. 468 mm hr^{-1}. Fortunately the peak intensity only lasted for 1 minute. Further investigation on the data of this event revealed two 1-hour and another 2-hour interruption, which lowered the mean intensity event.

The frequency of peak intensities (Table 2.5) provides a good understanding of how high intensities can get. The range ≤ 10 mm hr^{-1} scored only 4% of all events. The majority of events (33%) had peak intensities on the range of $25 < x \leq 50$ mm hr^{-1}. Considerable

numbers of events were found in the ranges of $10 < x \leq 25$ and $50 < x \leq 75$ mm hr^{-1}, with 29% and 17%, respectively. Seventeen percent of the events also scored peak intensity of more than 75 mm hr^{-1}.

2.3.6. Short f*allow rainfall characterization*

The rainfall events that were received during the 6-month short fallow were analysed separately. The short fallow refers to the period that elapses between the harvest time of a summer crop (June 1) and planting of another summer crop (November 30). The results of these analyses are presented in Appendix A.1-4. Generally, the patterns observed for the fallow are similar to that of year-round events were considered. The similarity could be from the fact that the short fallow data is subset of the year-round data, nevertheless some differences in the percentage scores were observed.

Similar to that of year-round events around 83% of the events had amount of less 8 mm. These events amounted to 27%. For events of > 8 mm the bulk of events came as events 8 – 20 mm. These represent 42% of the events in the > 8 mm group. The shift observed for the 6 month fallow rain events was that events of more than 30 mm accounted for 50% of the > 8 mm rain events. This provides good indication of the potential for runoff generation and better water storage into the basins during the fallow period.

The duration of fallow rainfall events had the same pattern with that of the year round events. The average duration per event was 127 minutes and this had a standard deviation of 213 minutes. This shows that the average duration would not be good indicator of the duration because it was highly variable.

The shape of hyetograph analysis showed that the proportion (21%) of left skewed events were comparable to that of year-round events. The proportion of events with early peak intensity decreased and that of events having their peak intensity in the middle of the event increased to 49%. Although the effect of shape of hyetograph in runoff generation is soil dependent, less proportion of events with early peak intensity corresponds with higher runoff potential. The logic behind this assumption is that the synchronization of

early peak intensity with the relatively higher infiltration rate of dry soil leads to less runoff.

The peak intensities recorded for the rainfall events of the fallow period had comparable trend with that of the year-round events. The percentages for the mean event intensity, however, were higher for the fallow period rainfall events. As indicated with the other rainfall parameters above, although the runoff generation is dependent on the specific condition happening during an event, the higher mean rainfall intensity indicates relatively higher potential for rainwater harvesting.

2.3.7. Application in rainfall simulation and in-field rainwater harvesting

If correctly designed and applied, rainfall simulation enables the creation of rainfall properties as comparable as possible with actual events, thereby providing a controlled environment for conducting rainfall-runoff experiments. With the results provided above, systematically summarizing the characteristics of rainfall events prevailing in the study area, it became much easier to design a typical rainfall event that was representative of natural rainfall. Depending on the desired target or objective, any rainfall type of interest can be designed and a corresponding percentage of representation given.

Such useful application was one of the objectives of this study with regards to simulation of rainfall for IRWH. Rainfall simulation for IRWH helps to quantify the runoff that can be generated from the runoff strips and ultimately the water that would be available for crops planted on either side of the basins. For instance, more than 80% (Table 2.1) of rainfall events had amounts less than 8 mm. Since the objective of simulation is the study of runoff generation, the designed rainfall events should not focus on this category, but on the remaining less than 20% of the events. This focus can further be justified using the proportion of the contribution of this category to the total amount received, in this case 65%. The simulation results supported by such information would give a clear picture when dealing with the result. The same value can be given to event duration and intensity values, thereby increasing the credibility of the results. This addresses the criticism Dunkerley (2008a) identified in many research results using rainfall simulation. He

concluded that many simulation experiments had rainfall rates typical of those that can be categorized as extreme or exceptional.

The result from the canonical correlation analysis had two parts. The first part was the correlation of rainfall characteristics with runoff amount. As reported in Table 2.6, all the rainfall characteristics had positive correlation although to a varying degree. The event amount and peak intensity had strong positive correlation, while average recorded intensity was ranked lower. Event duration and overall average intensity had comparable correlation with runoff. This similarity came from using duration in computing overall average intensity. The second part of the analysis gave regression results between canonical variables (variates). The canonical variables considered were the rainfall characteristic placed in one group and the runoff variable in another. The regression between these groups provided an R^2 of 0.95, leaving very little unexplained pattern. It should be noted that the rainfall characteristics cannot fully explain runoff generation. This exercise was only meant to identify rainfall parameters of significance with regard to runoff generation. To obtain such good R^2, the contribution each variable made towards the canonical variable is provided as the standardized coefficient in Table 2.6. These coefficients were the weights associated with each variable towards predicting the runoff amount. Assisting with the separation of significance of the contribution, t-test results are also provided in Table 2.6. According to the level of significance, three rainfall characteristics were identified as making major contribution in runoff generation, namely: event amount, average recorded intensity and peak intensity. Thus, the inclusion of only these three rainfall parameters could give comparable R^2 as to when all the variables are included. A large amount of information with regard to runoff generation can be deduced from rainfall amount and intensity of the rain.

Table 2.6 Result from canonical correlation analysis between rainfall parameters and runoff.

Rainfall variables	Correlation with Runoff amount	Regression results		
		Standardized coefficients	t-value for coefficients	Prob>/t/
Overall average intensity	0.3113	0.0212	0.3572	0.7232
Peak intensity	0.7693	0.1822	1.9803	0.0561*
Average recorded intensity	0.552	0.2263	2.2959	0.0282**
Event duration	0.374	0.0437	0.5388	0.5937
Event amount	0.9116	0.7307	11.9481	<.0001**

** Significant at 95% * Significant at 90%

The results of this study corresponded well with findings of Abu Hammad *et al.* (2006) in that rainfall amount had higher correlation with runoff. However, in the stepwise regression Abu Hammad *et al.* (2006) found that the rainfall erosivity index (EI_{30}), storm duration and 30-minute maximum intensity (I_{30}) were the significant parameters. This study differs because event duration was not a significant finding (Table 2.6). The I_{30} intensity parameter can correspond with the two intensity parameters used in this study. This finding attests to the importance intensity has on runoff generation. When comparing the two parameters, overall and recorded average intensities, the latter gave better information on how rainfall varied during an event. The information given by overall average intensity is evened out by the time factor (Van Dijk *et al.*, 2005). To avoid that the overall is evened out by time, sub-event intensity characteristics like the one used by Abu Hammad *et al.* (2006) or the ones used in this study would be more meaningful.

2.4. Conclusions and recommendations

In this study a systematic method of identifying individual rainfall events was developed. By comparing the two algorithms, the one that did not have time limit provided a better representation of rainfall events. This identification of individual rainfall events enabled the statistical characterization of rainfall events. The categorization of events into classes according to their properties, with the corresponding proportion of representation

provided information to design more realistic and representative events in rainfall simulation.

About 33% of the total rainfall amount received had zero potential to be harvested as runoff in the IRWH system. This means a runoff harvesting practice needs to appropriate the use of the remaining 67%. The duration of rainfall events of rainwater harvesting importance lasted half an hour or longer. This can serve as the minimum duration guideline when simulating rainfall for rainwater harvesting studies. Among the rainfall characteristics considered, rainfall amount and rainfall intensity were of most significant importance for runoff determination for IRWH. Thus, special attention needs to be given to the amount and intensity of rainfall events.

References

Abu Hammad, A.H., Børresen, T. & Haugen, L.E., 2006. Effects of rain characteristics and terracing on runoff and erosion under the Mediterranean. *Soil & Tillage Research* **87**(1):39-47.

Anderson, J.J., 2007. Rainfall-runoff relationships and yield responses of maize and dry beans on the Glen/Bonheim ecotope using conventional tillage and in-field rainwater harvesting. Ph.D. thesis University of the Free State, Bloemfontein, South Africa.

Batisani, N. & Yarnal, B., 2010. Rainfall variability and trends in semi-arid Botswana: implications for climate change adaptation policy. *Appl. Geogr.* **30**(4):483-489.

Botha, J.J., van Rensburg, L.D., Anderson, J.J., Hensley, M., Macheli, M.S., van Staden, P.P., Kundhlande, G., Groenewald, D.C. & Baiphethi, M.N., 2003. Water conservation techniques on small plots in semi-arid areas to enhance rainfall use efficiency, food security, and sustainable crop production. Water Research Commission Report No. 1176/1/03, Pretoria, South Africa.

Bulmer, M.G., 1979. *Principles of statistics.* Dover Publications, New York.

Dunkerley, D., 2008a. Rain event properties in nature and in rainfall simulation experiments: a comparative review with recommendations for increasingly systematic study and reporting. *Hydrol. Processes* **22**:4415-4435.

Dunkerley, D., 2008b. Identifying individual rain events from pluviograph records: a review with analysis of data from an Australian dryland site. *Hydrol. Processes* **22**:5024-5036.

Dyson, L.L., 2009. Heavy daily-rainfall characteristics over the Gauteng Province. *Water SA* **35**(5):627-638.

Hensley, M., Botha, J.J., Anderson, J.J., van Standen, P.P. & du Toit, A., 2000. Optimizing rainfall efficiency for developing farmers with limited access to irrigation water. Water Research Commission Report No. 878/1/00, Pretoria, South Africa.

Laakso, L., Grönholm, T., Rannik, Ü., Kosmale, M., Fiedler, V., Vehkamäki, H. & Kulmala, M., 2003. Ultrafine particle scavenging coefficients calculated from 6 years field measurements. *Atmos. Environ.* **37**:3605-3613.

Morin, J., Rawitz, E., Hoogmoed, W.B. & Benyamini, Y., 1984. Tillage practices for soil and water conservation in the semi-arid zone III. Runoff modeling as a tool for conservation tillage design. *Soil & Tillage Research* **4**:215-224.

Nel, W., 2007. Intra-storm attributes of extreme storm events in the Drakensberg, *Phys. Geogr.* **28**(2):158-169.

Nel, W., 2008. Observations on daily rainfall events in the KwaZulu-Natal Drakensberg. *Water SA* **34**(2):271-274.

Ngigi, S., 1999. Optimization of rainwater catchment systems design parameters in the arid and semi-arid lands of Kenya. Proceedings of the 9th international rainwater catchment systems conference. Petrolina, Brazil - July 6-9, 1999.

Rappold, G.D., 2005. Precipitation analysis and agricultural water availability in the Southern highlands of Yemen. *Hydrol. Process*. **19**:2437–2449.

Rawitz, E. & Hillel, D., 1971. A method for characterizing the runoff potential rainfall in water harvesting schemes. *Water Resour. Res*. **7**(2):401-405.

Rockström, J., 2000. Water resources management in smallholder farms in Eastern and Southern Africa: an overview. *Phys. Chem. Earth Pt. B* **25**(3):275-283.

SAS Institute Inc., 2006. *Administering SAS® Enterprise Guide® 4.1*. Cary, NC: SAS Institute Inc.

Smithers, J.C. & Schulze, R.E., 2000. Development and evaluation of techniques for estimating short duration design rainfall in South Africa. Water Research Commission Report No. 681/1/00, Pretoria, South Africa.

Soil Classification Working Group, 1991. *Soil classification: a taxonomic system for South Africa.* Department of Agricultural Development, Pretoria.

Tennant, W.J. & Hewitson, B., 2002. Intra-seasonal rainfall characteristics and their importance to the seasonal prediction problem. *Int. J. Climatol.* **22**(9):1033-1048.

Thomas, R.J., 2008. Opportunities to reduce the vulnerability of dryland farmers in Central and West Asia and North Africa to climate change. *Agriculture, Ecosystems & Environment* **126**(1-2):36-45.

Tokay, A. & Short, D.A., 1996. Evidence from tropical raindrop spectra of the origin of rain from stratiform versus convective clouds. *J. Appl. Meteorol.* **35**:355-371.

Tsubo, M., Walker, S. & Hensley, M., 2005. Quantifying risk for water harvesting under semi-arid conditions: Part I. Rainfall intensity generation. *Agric. Water Manage*. **76**(2):77-93.

UNEP, 1992. *World atlas of desertification*. 1st edition. Edward Arnold, London.

Van Dijk, A.I.J.M., Meesters, A.G.C.A., Schellekens, J. & Bruijnzeel, L.A., 2005. A two-parameter exponential rainfall depth-intensity distribution applied to runoff and erosion modelling. *J. Hydrol.* **300**:155-171.

Walker, S. & Tsubo, M., 2003. Estimation of rainfall intensity for potential crop production on clay soil with in-field water harvesting practices in a semi-arid area. Water Research Commission Report No. 1049/1/02. Pretoria, South Africa.

Wikipedia, 2010. Highveld (September 2008). In *Wikipedia: The Free Encyclopedia*. Wikimedia Foundation Inc. Encyclopedia on-line. Available from http://en.wikipedia.org/wiki/Highveld. Internet. Retrieved 10 April 2010.

3. Influence of rainfall intensity patterns on infiltration-runoff under in-field rainwater harvesting

Abstract

In determining the potential of rainwater harvesting systems, calculating the amount of rainwater harvested is a formidable challenge. This challenge is further magnified by the erratic rainfall prevailing in arid and semi-arid areas. A mobile rainfall simulator was used to overcome this challenge and simulate rain events of variable intensity patterns. The aim of this study was to investigate how well natural rainfall can be simulated, to explore the penetration depth of infiltrating water and to investigate the effect of rainfall intensity pattern on infiltration-runoff amounts. The study was conducted on Kenilworth/Bainsvlei and Paradys/Tukulu ecotopes with soil surfaces prepared for in-field rainwater harvesting. Three different rainfall intensity patterns were used as treatments, viz. normal shaped, right-skewed, and constant application. The result showed that the mobile rainfall simulator provided storm events representative of natural storms. On both soils with 8 and 18% clay content of the top horizon, the infiltration front affected only the top 200 mm. This finding indicated that, given the kind of rainfall that is common in these ecotopes, infiltration will vary only if the top horizons vary and hence soils can be grouped accordingly. Intensity patterns can play a role in the amount of runoff on the Paradys/Tukulu ecotope whereas on the Kenilworth/Bainsvlei ecotope the role played was not significant. Thus a parameter representative of the intensity patterns needs to be included when predicting the runoff potential on Paradys/Tukulu ecotope and similar ecotopes.

Key words: rainwater harvesting, rainfall intensity, runoff, infiltration, soil water

3.1. Introduction

Partitioning rainfall into infiltration and runoff has always been a concern for any rainwater harvesting practice (Rawitz & Hillel, 1971; Tauer *et al*., 1991; Boers, 1994; Young *et al.,* 2002) and particularly in-field rainwater harvesting (IRWH), a tillage practice which was recently introduced by Hensley *et al.* (2000). The IRWH tillage practice makes two major partitions in the field: the runoff generating part – *the runoff strip,* and the runoff receiving part – *the basin*. Runoff is encouraged in the former, while in the latter infiltration is the preferred process. This unique setting of inducing runoff for the purpose of concentrating and storing it on the basins, demands a better understanding on the partitioning of infiltration and runoff. This is basically the quantification of the extra runoff water being harvested when juxtaposed with a conventional practice. With this in mind, Hensley *et al.* (2000) and Botha *et al.* (2003) reported a regression model predicting the amount of runoff that can be generated on ecotopes they studied. Zere *et al.* (2005) also simulated runoff generation on a Glen/Tukulu ecotope by emphasizing its application on IRWH. Welderufael *et al.* (2008) simulated runoff generation for the purpose of investigating a scenario of IRWH application as compared to a conventional system. Hence, works that have been done show that infiltration/runoff partitioning of rainfall is central in IRWH practice.

The erratic nature of rainfall in arid and semi-arid areas makes it difficult to get the desired pre-designed rainfall intensity patterns for a specific experiment. This difficulty is compounded by the scarcity of rainfall/runoff data collected for IRWH. Thus the use of mobile rainfall simulator becomes an attractive option in generating a pre-designed rainfall event. Flanagan *et al*. (1987) and Frauenfeld & Truman (2004) used simulated rainfall to study the effect of rainfall intensity pattern on infiltration, runoff and soil loss.

Whether from simulated or natural rainfalls, as rainwater falls on a soil surface, the progress of infiltration and runoff generation can be categorized as subsurface controlled or surface controlled (Smith *et al*., 2002). The subsurface controlled scenario portrays a situation in which saturation is built up from the subsurface of the soil. As the soil becomes saturated, the water that is applied cannot be accommodated and runoff occurs.

This means runoff generation is not dependent on the rate of application. In the surface controlled scenario, on the other hand, runoff is a function of infiltrability. The runoff generated is infiltration excess and is a function of surface conditions and rainfall characteristics. After recognition of the decay of infiltration rate with time by Horton (1936), others (Philip, 1957; Mein and Larson, 1973; Morin & Benyamini, 1977) have tried to capture the significance of different factors that affect the process. The work by Morin & Benyamini (1977), for instance, builds on Horton's finding and incorporates two factors that play a major role: the surface particle strength and intensity. Similar work by Xue & Gavin (2008) incorporated rainfall intensity into the Horton's equation as a major factor influencing infiltration.

Under situations where surface conditions are homogenous, the rainfall characteristics become the main factor that can bring about a difference. Rainfall can be characterized by the parameters duration, amount and intensity (Walker & Tsubo, 2003). When a single rainfall event is considered, the variable parameter of the three is rainfall intensity. When duration and amount are kept constant, infinite variation of intensity is possible. This variation can have an influence on infiltration response of the soil. Mein & Larson (1973) provide different scenarios showing infiltration behaviour under different rainfall intensities. For instance, under situations where application rate happens to be lower than initial infiltration rate of the soil, the observed infiltration will be determined by application rate. As the infiltration process progresses the water entering the soil reduces the suction in the soil and thus reduce the infiltration rate to the final infiltration rate, which is theoretically equated to saturated hydraulic conductivity (K_s). The perceptions held about the rate of decrease in infiltration rate has been revealed in the models (equations) developed to represent the infiltration process (Horton, 1936; Philip, 1957; Mein & Larson, 1973; Morin & Benyamini, 1977; Xue & Gavin, 2008).

The objective of this study was to investigate the effect of rainfall intensity patterns on infiltration/runoff response Bainsvlei/Kenilworth and Paradys/Tukulu ecotopes under IRWH. Additionally the penetration of infiltrating water by instantaneous measurement of soil water content and how well natural rainfall could be simulated was explored. The experiments mimicked natural rainfall patterns to a practicable extent. The distribution of

intensity values during a rainfall event determined the pattern of the rainfall event. Rainfall events starting with high intensity and decreasing at a later stage of an event and intensities following a normal distribution were considered. To enable comparison with previous conventional studies, rainfall event of constant intensity was also included.

3.2. Materials and methods

3.2.1. Description of the experimental site

The experiments were done on plots under in-field rainwater harvesting (IRWH) on the Kenilworth/Bainsvlei and Paradys/Tukulu ecotopes. The Kenilworth/Bainsvlei ecotope has an orthic, sandy loam A-horizon of 250 mm overlying a thick red apedal B-horizon which goes down to 1850 mm. The A-horizon despite great proportion (84%) of the particles being sand still formed crust on the surface, enabling runoff inducement for application of IRWH. The B-horizon was fairly homogenous with massive structure with clay content ranging from 8 – 20%. The B-horizon although fairly homogenous sub-horizons (B_1 – B_5) differing in colour and particle size distribution can be identified. This sandy loam B-horizon was underlain by a C-horizon which goes to the depth of 2200 mm.

The Paradys/Tukulu ecotope was characterized with soil displaying clearly differentiated horizons. The soil had an apedal orthic A-horizon with a sandy clay loam texture. This horizon overlay a weakly developed blocky sandy clay B-horizon. The top horizon has a thickness of 200 mm while the neocutanic B-horizon varies between 200 – 400 mm in thickness. The C-horizon is composed of unconsolidated material varying in thickness from 200 – 500 mm. The clay content of the soil increased down the profile, starting with 18% for the top horizon and reached up to 50% for the C-horizon.

3.2.2. Rainfall simulation

The experimental setup made use of artificial rainfall simulation, which was able to produce variable rainfall intensities. This feature of producing variable rainfall intensities enabled the intention of mimicking natural rainfall events practically possible. The rainfall simulator used was the HoFrey (Figure 3.1), which is described in detail by

Bennie *et al.* (1994) and has also been used by Bothma (2009). The Hofrey simulator had a closed compartment (Figure 3.1(a)) with adjustable height of oscillating sprinkler nozzle. This simulator is equipped with pressure gauges and timer control for the oscillation of the sprinkler. In the closed compartment, a metal frame (Figure 3.1(b)) of 1m by 1m was inserted 10 cm into the soil, forming the boundary of the plot under study. On the down slope side of this frame, it had a gutter into which a pipe was connected for the purpose of runoff collection (Figure 3.1(c)).

3.2.3. Calibration of the rainfall simulator

The calibration of the rainfall simulator was done by running it on a surface covered with plastic and collecting the water coming as runoff (Figure 3.1). A plastic mesh was laid over the surface of the plastic to dissipate the energy of water drops and reduce splash loss. Intensity manipulation was done by altering the oscillation timer. First calibration for different timer settings was done by running the simulator for 5 minutes. In this simulation every 5-minute run was discrete, which makes it different from a continuous simulation. A regression equation was derived from the result. Based on this equation, simulation of two natural rain storms which occurred in 1996 (DOY 35 and 44) were done by taking average of 5-minute intensity. Simulation of DOY 35 and 44 storms which lasted for 80 and 65 minutes respectively were done with a 5-minute alteration of timer setting to achieve the required intensity. From the result of these runs the calibration of storms under un-interrupted runs and timed-alteration of intensity was obtained. The intended rainfall pattern and the resulting rainfall pattern were compared. From this second round of calibration the setup for the treatments of different rainfall intensity patterns were prepared.

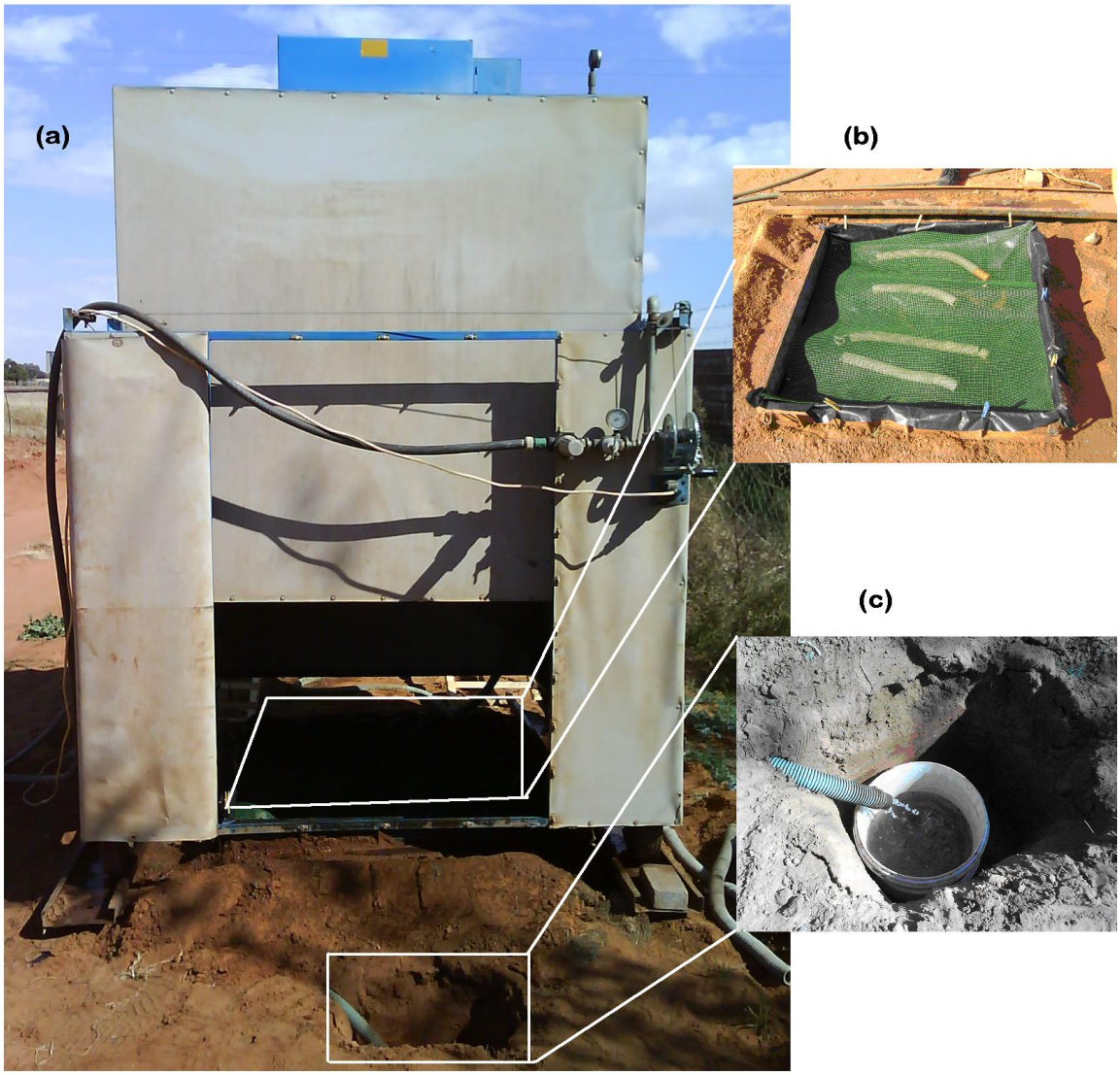

Figure 3.1 Hofrey rainfall simulator setup during calibration of the simulator.

3.2.4. Experimental design

Three treatments that emulated rainfall intensity variation were setup. For the purpose of objective comparison, each treatment duration and rainfall amount was the same. Each simulation lasted for 70 minutes and rainfall amount of 30.8 mm was received within the frame of 1 m by 1 m. The first treatment was composed of five minute rainfall intensity variation during the simulation-event and the pattern of variation was made to follow a normal distribution shape. The second treatment also had 5-minute alteration of intensity with a skewed variation pattern, i.e. the higher intensities coming earlier during

simulation-event and decreasing towards the end. The third treatment had no intensity alteration. A rainfall intensity of 26.5 mm hr^{-1} was applied throughout the simulation time.

3.2.5. Measurement of progress of infiltration

During the simulation, time taken to runoff was recorded. A regular five minute measurement of runoff was also observed. The infiltration rate was calculated from the difference of runoff rate and rainfall intensity. Two DFM capacitance probes were installed on every trial and provided another option for measuring the amount of infiltration and enabled instantaneous measurement of soil water content. The probes recorded the temperature and percentage of soil water content every 5 minute at four depths. Soil samples before and after the trials were taken for gravimetric soil water measurement, which were used to calibrate the DFM probe measurements.

3.2.6. Statistical analysis

Statistical comparison of the results collected for each treatment was done using SAS software (SAS Institute Inc., 2006). Analysis of variance for the three treatments of rainfall intensity patterns was done in terms of runoff amount generated and time taken to runoff commencement. The analysis of variation for amount generated was done both for every measurement of 5 minute and for the whole event.

3.3. Results and discussion

3.3.1. Rainfall simulation

From the Hofrey calibration results shown in Figure 3.2, it could be seen that the timer control setting of the simulator followed a definite pattern fitting well on a power regression line. The coefficient of determination obtained (R^2 = 0.98) attested to the visual goodness of fit observed in Figure 3.2.

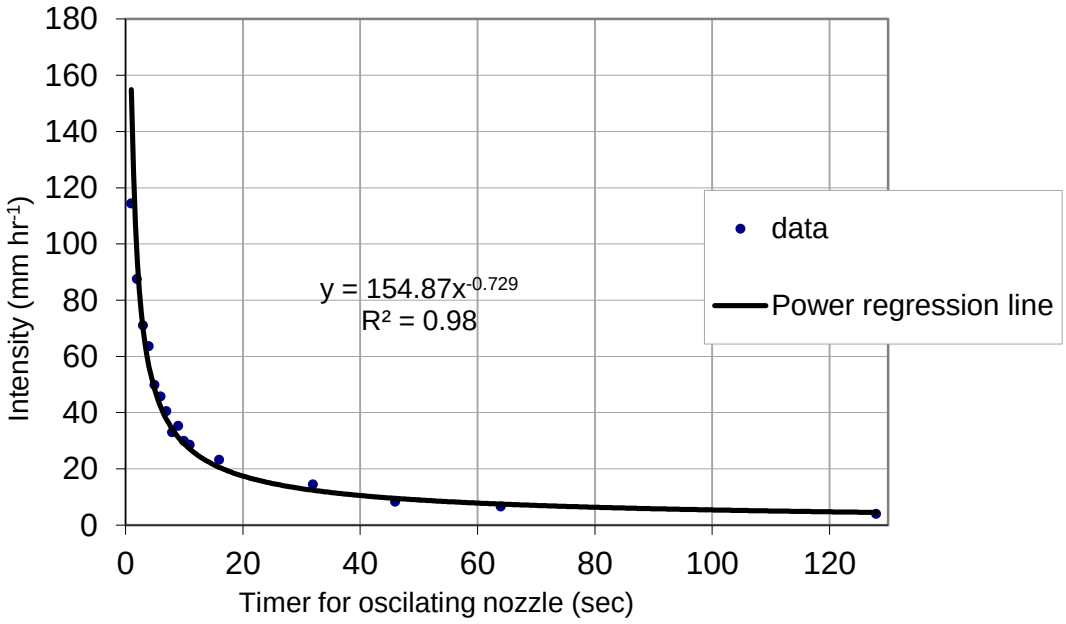

Figure 3.2 Timer settings for generating different intensities (first calibration).

Comparison of intended and measured intensities was done for the calibration storms. The intended intensities were predicted by the equation given in Figure 3.2. Figure 3.3 shows the intended versus measured intensities, with the fitted line deviating slightly from the 1:1 line. The accuracy of the calibration equation was tested statistically and is shown in Table 3.1. The results showed that it had excellent coefficient of determination (R^2) and index of agreement (D-index) of 0.99. A slope value close to one (0.87) and a y-intercept of close to zero (-0.4) showed that correspondence between the intended and measured intensities was good. As reflected in Table 3.1 the simulation done had an acceptable agreement with a root mean square error (RMSE) of 5.9 mm hr^{-1} and mean absolute error (MAE) of 4.4 mm hr^{-1}. The mean absolute error gives the average error that would be introduced by using the calibration equation. This value was only 4.4 mm hr^{-1} which translated into only 0.37 mm for every 5 minute manipulation of intensities. Nevertheless, to further improve on the simulation, the actual measured values from simulated storms were used instead of values obtained from the regression equation given in Figure 3.2. This corrected the deviation observed on bigger values of intensities.

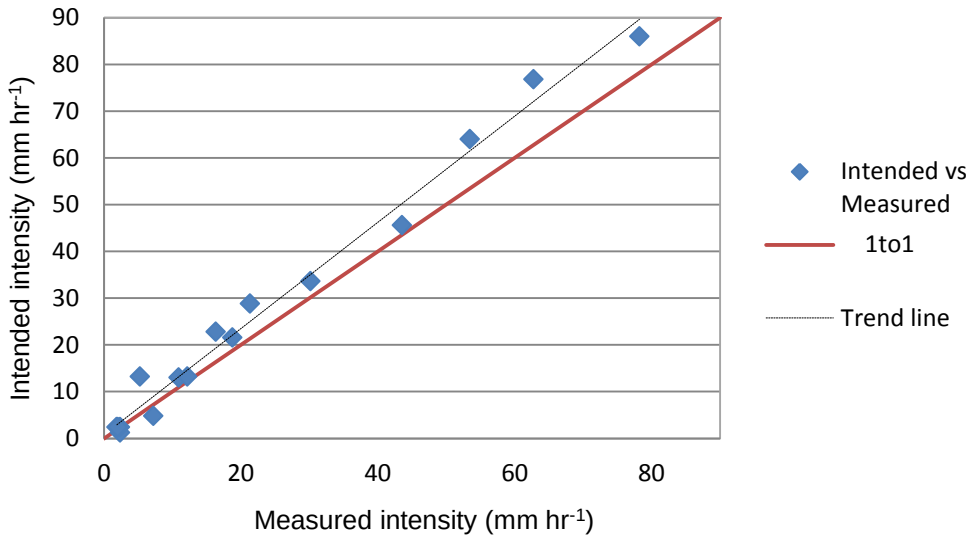

Figure 3.3 Measured and intended intensities plotted in reference to the 1:1 line.

Table 3.1 Statistical evaluation of the comparison between the intended versus measured intensities (mm hr^{-1}) of the Hofrey.

Statistical parameters	values
RMSE	5.94
RMSEs	5.26
RMSEu	2.76
MAE	4.38
R^2	0.97
D-index	0.97
slope (b)	0.87
intercept (a)	-0.40
RMSEs/RMSE	0.89

3.3.2. Infiltration-runoff

Figures 3.4 and 3.5 show the observed infiltration-runoff results of the three rainfall intensity patterns for the two ecotopes considered. The lines on the graphs represent application rate and the infiltration response of the soil. As observed in Figures 3.4 and 3.5, as long as the application rate does not exceed the infiltration rate there is no runoff

generated. The shaded areas under the graphs indicate the cumulative amount of runoff up to the time considered. As indicated on the graphs the runoff amount was the difference between the area under application and the area under infiltration rate. The amount of total runoff values (Table 3.2) observed on the Paradys/Tukulu ecotope were 19.4, 17.9 and 15.0 mm for constant, normal and skewed, respectively, whereas on the Kenilworth/Bainsvlei ecotope, the total runoff amounts were 17.0, 16.7 and 14.8 mm for skewed, constant and normal rainfall patterns, respectively. The variation in total runoff amount observed for different treatments were discernible from the area coverage of shades labelled as "runoff" on the legends of Figures 3.4 and 3.5.

Another parameter considered for comparison of the treatments was time to runoff (Table 3.2). Time to runoff showed consistency in both ecotopes although the values were not comparable. It was found that the runoff response came quicker for skewed, followed by constant and normal rainfall patterns respectively. This response corresponded well with the expected results. This was mainly because the treatments were time dependent.

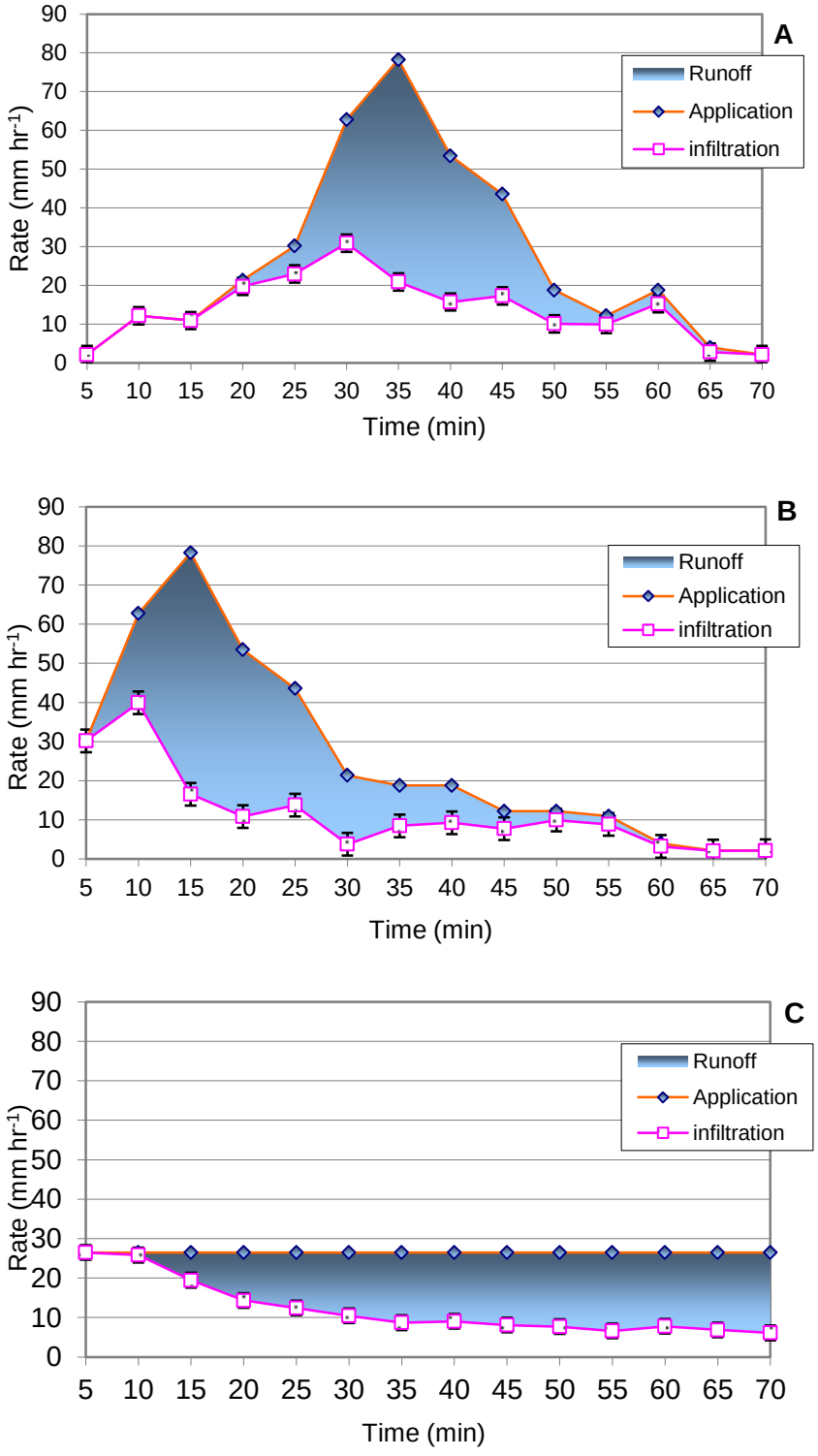

Figure 3.4 Application and infiltration rates with the resulting runoff for three treatments: (a) Normal, (b) Skewed, and (c) Constant applications on Kenilworth/Bainsvlei ecotope.

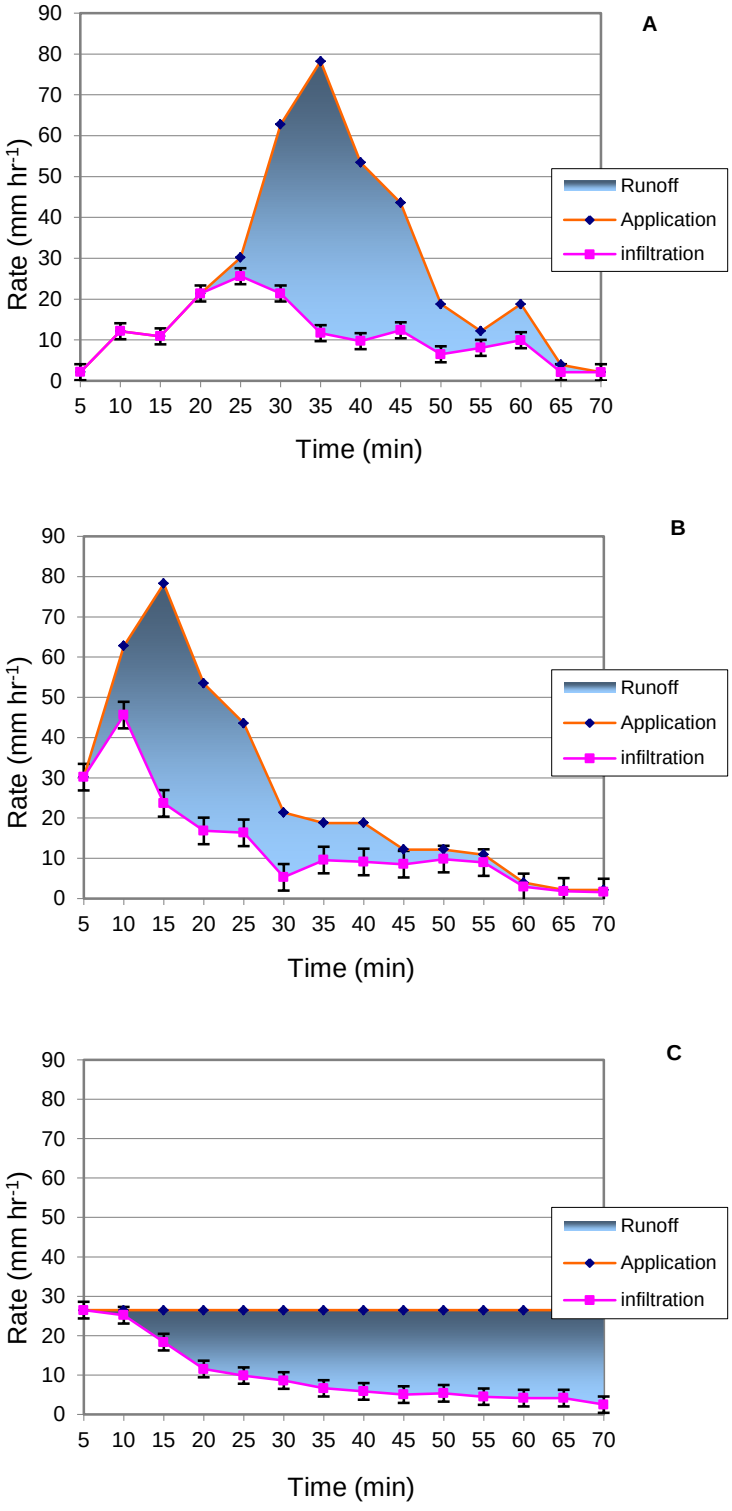

Figure 3.5 Application and infiltration rates with the resulting runoff for three treatments: (a) Normal, (b) Skewed, and (c) Constant applications on Paradys/Tukulu ecotope.

Table 3.2 Total runoff and time to runoff for various treatments on the Paradys/Tukulu and Kenilworth/Bainsvlei ecotopes.

Parameter	Replication	Kenilworth/Bainsvlei ecotope			Paradys/Tukulu ecotope		
		Normal	Skewed	Constant	Normal	Skewed	Constant
Total runoff (mm)	**1**	10.05	15.90	14.31	19.42	14.74	21.62
	2	14.51	18.65	20.38	16.80	15.40	16.81
	3	19.83	16.51	15.55	17.42	14.96	19.66
Average		14.80	17.02	16.74	17.88	15.03	19.36
Time to runoff (minutes)	**1**	25.33	7.48	9.01	21.00	5.00	7.66
	2	21.38	6.58	8.56	24.00	5.50	15.00
	3	17.16	7.61	7.71	22.50	7.67	5.50
Average		21.29	7.22	8.43	22.50	6.06	9.39

Statistical analysis was done on the observed infiltration-runoff parameters shown in Table 3.2. The analysis of variance done on the total amount of runoff (Table 3.3) revealed that there was significant difference between the treatments on the Paradys/Tukulu ecotope with an $LSD_{0.05}$ of 3.2 mm. The total amount of runoff from the constant rainfall pattern was markedly different from the other two treatments. This finding was in line with results obtained by Flanagan *et al*. (1987). They showed there was significant difference in runoff resulting from storm patterns. On the other hand, no significant difference was found for total amount of runoff on the Kenilworth/Bainsvlei ecotope (Table 3.3). The Kenilworth/Bainsvlei result supported the findings of Frauenfeld & Truman (2004) who showed that intensity pattern did not have a significant difference on total runoff or infiltration but affected time to runoff and soil loss. Parson & Stone (2006) having experimented with 5 different patterns and 3 different soil types concluded that no consistent difference was found on runoff amounts. In screening the effect of rainfall pattern, what Parson & Stone (2006) had done was that they observed if there was consistent effect on all soils by doing two-way analysis of variance. They did not test the treatment variation separately on the different soils, which was the case with this study. These mixed results indicated that to some extent, rainfall intensity patterns played a role, but was not consistent on all soils. The result from the

Kenilworth/Bainsvlei ecotope gave good indication that even if the influence of intensity on runoff amount was significant, the influence of the soil could offset the effect. The ANOVA done for the effect of intensity pattern on time to runoff (Table 3.3) showed significant difference on both soils. This was in keeping with the findings of Frauenfeld & Truman (2004). The results showed that the normal rainfall pattern took longer to start runoff followed by constant and skewed rainfall patterns and there was no significant difference between the two ecotopes. Table 3.3 also show the probability values for obtaining the F-values calculated for the treatment and blocking (replicas). The P-values obtained for the blocks consistently showed that there was no significant difference on the blocks used to replicate the treatments. Table 3.3 also compares the cumulative runoff starting from the 20^{th} minute. Treatments showed significant difference to start with and the difference continued well up to the 50^{th} minute for the Paradys/Tukulu ecotope and up to the 45^{th} minute for the Kenilworth/Bainsvlei ecotope. After 50 minutes the cumulative runoff became comparable for all treatments, but at the end of the storm it became again significantly different for the Paradys/Tukulu ecotope.

The logic behind the treatment differences was the matching of application rate and soil infiltration response. In other words, higher application rate matched by higher infiltration rate would yield little or no runoff. Early during a storm, infiltration into a dry soil progresses faster owing to the higher sorptivity and matric suction values of a dry soil. The measure of these parameters decreases as water enters into the soil. Higher intensity rate coming early during a storm can result in higher infiltration as compared to higher intensities coming late during a storm. This condition was clearly observed on the runoff results from the Paradys/Tukulu ecotope. The skewed rainfall pattern owing to the early arrival of the higher intensities yielded the least runoff, followed by the normally distributed. Under the constant application on the other hand, runoff continuously increased, which resulted in higher cumulative runoff.

Table 3.3 ANOVA results for the three treatments on the Kenilworth/Bainsvlei and Paradys/Tukulu ecotopes.

Time (min)	Kenilworth/Bainsvlei ecotope						Paradys/Tukulu ecotope					
	Average Treatment Runoff (mm)			LSD (0.05)	P-Values		Average Treatment Runoff (mm)			LSD (0.05)	P-Values	
	Normal	Skewed	Constant		Treatment	Block	Normal	Skewed	Constant		Treatment	Block
20	0.1 ^{A}	10.6 ^{B}	1.7 ^{C}	1.2	<.001	0.202	0.0^{A}	9.0^{B}	2.0^{C}	1.9	<.001	0.586
25	0.7 ^{B}	13.1 ^{A}	2.8 ^{B}	2.1	<.001	0.374	0.4 ^{A}	11.3 ^{B}	3.4 ^{C}	2.1	<.001	0.480
30	3.4 ^{B}	14.6 ^{A}	4.2 ^{B}	3.5	0.002	0.331	3.8 ^{B}	12.6 ^{A}	4.9 ^{B}	2.0	<.001	0.312
35	8.2 ^{B}	15.4 ^{A}	5.6 ^{B}	4.7	0.010	0.344	9.4 ^{A}	13.4 ^{B}	6.6 ^{C}	2.2	0.002	0.263
40	11.3^{AB}	16.2^{A}	7.1^{B}	5.4	0.023	0.328	13.0 ^{A}	14.2 ^{A}	8.3 ^{B}	2.3	0.004	0.242
45	13.5 ^{AB}	16.6 ^{A}	8.6 ^{B}	5.9	0.048	0.324	15.6 ^{A}	14.5 ^{A}	10.1 ^{B}	2.4	0.007	0.239
50	14.2 ^{AB}	16.8 ^{A}	10.2 ^{B}	6.2	0.099	0.312	16.6 ^{A}	14.7 ^{A}	11.8 ^{B}	2.7	0.018	0.247
55	14.4 ^{A}	16.9 ^{A}	11.9 ^{A}	6.5	0.207	0.295	17.0 ^{A}	14.9 ^{AB}	13.6 ^{B}	2.8	0.071	0.257
60	14.7 ^{A}	17.0 ^{A}	13.4 ^{A}	6.7	0.406	0.286	17.7 ^{A}	15.0 ^{A}	15.5 ^{A}	3.0	0.122	0.255
65	14.8 ^{A}	17.0 ^{A}	15.0 ^{A}	6.9	0.649	0.277	17.9^{A}	15.0 ^{A}	17.4^{A}	3.2	0.125	0.260
70	14.8^{A}	17.0^{A}	16.7^{A}	7.0	0.658	0.270	17.9 ^{AB}	15.0 ^{A}	19.4 ^{B}	3.2	0.047	0.260
Time to runoff	21.3 ^{A}	7.2 ^{B}	8.4^{B}	5.1	0.003	0.337	22.5 ^{A}	6.1 ^{B}	9.4 ^{B}	6.8	0.005	0.383

- Means followed by the same letter are not significantly different.

The runoff observed on the Kenilworth/Bainsvlei ecotope depicted a different story. The order of cumulative runoff amount was skewed, constant and normal rainfall distributions. This order reversed the logic given above. One possible explanation could be the effect of raindrop energy on crust formation. The study done by Roth & Helming (2007) showed that the dispersion of the crust lead to increased runoff amounts. The crusts formed on the Kenilworth/Bainsvlei ecotope were weaker as compared to the Paradys/Tukulu and this might have led to dispersion of the crust and hence more runoff.

Figure 3.6 shows the progress of infiltration process at different times through the course of simulated rain showers. This was a novel practice enabled with the use of DFM probes which continually log the water content as water infiltration progressed. From Figure 3.6, progress of water entrance to the soil, which is depicted by the line shifting to the right, could be clearly seen. These general patterns were the same for the corresponding treatments on the two ecotopes. For instance, the water content for the top 50 mm was observed to range between 5 to 17%, but only the normal distribution captured the intermediate values. For the other two treatments, the value of water content reached the highest within the first 20 minutes and it acts as a transmission zone to the lower part of the horizon. This corresponded well with the ANOVA results for the time to runoff (Table 3.3) which showed that the normal pattern showed significant difference compared to the other two. This further attests to the fact that runoff occurs only after the surface soil is brought to the maximum possible water content.

The difference in pattern observed could be explained more around the soil type than the treatments which were variation in intensity pattern. The marked difference in clay content between the top horizons of the two soils explained the reading taken at 150 mm. The difference between the initial and the final water content ranged between 1.4 and 2% for the Tukulu soil whereas that of the Bainsvlei ranged between 4.3 and 5.3%. This meant relatively more water had reached the 150 mm depth on the Bainsvlei soil than the Tukulu soil. From the depiction of Figure 3.6 it is observed that infiltration progress was restricted within the top horizon. In both ecotopes, 200 mm was the approximate depth to which the wetting front could reach. The rainfall amount used for simulation, topping the major proportion of the rainfall events prevailing in study area (Table 2.2), similar

infiltration response is expected during rain events. This finding can shed light into the study of infiltration with regard to different soil types. In studying infiltration (not redistribution) into a given soil, the physical properties of the top horizon only need to be considered. This reasoning can yield a very useful generalization, especially in the South African Soil Classification System. This system provides 5 possible diagnostic top horizons and the infiltration behaviours can thus be classified accordingly. Despite this useful generalization caution needs to be applied especially when dealing with the orthic A-horizon, which can display a wide range of physical properties.

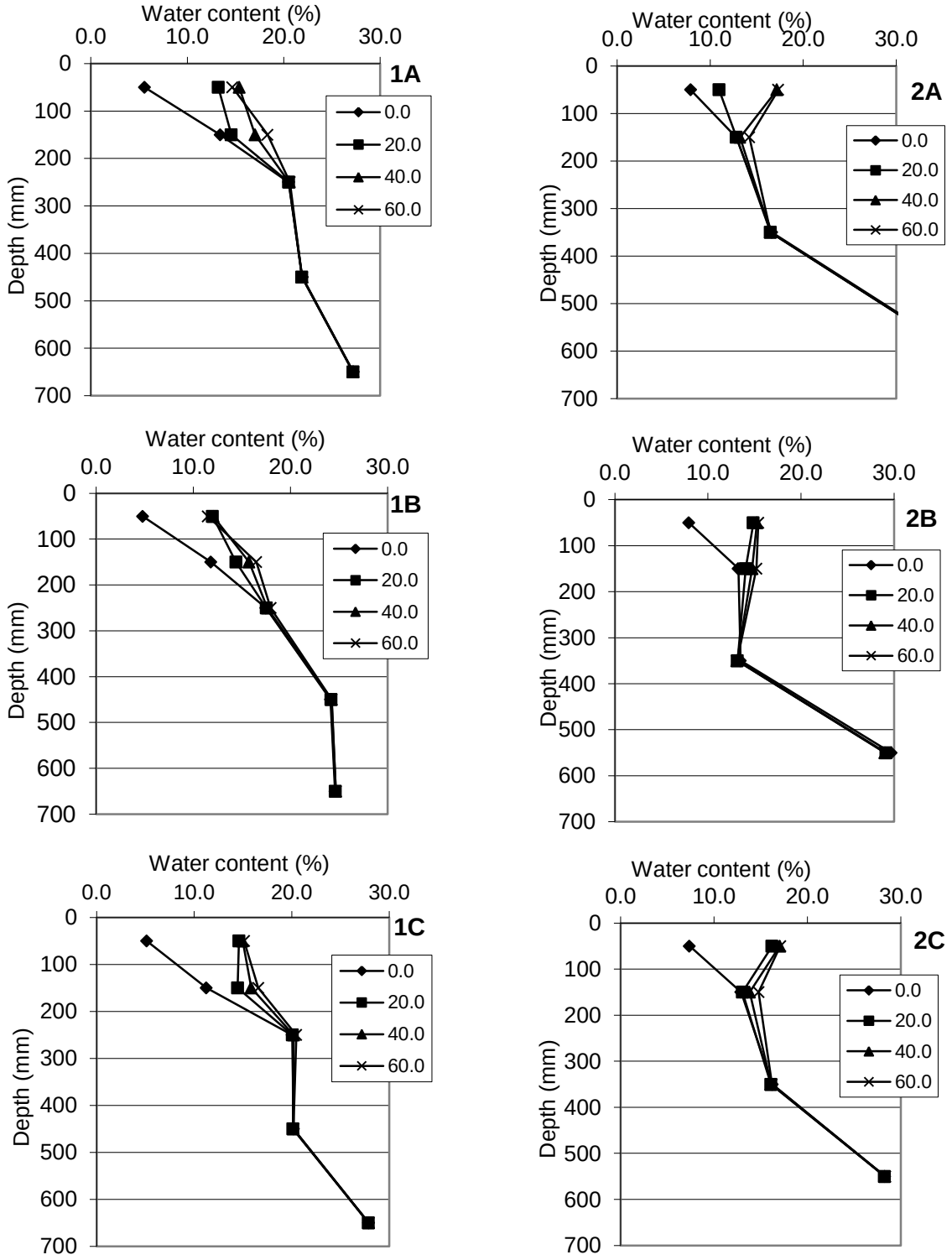

Figure 3.6 Water content versus depth at different times (0, 20, 40 and 60 min) for Kenilworth/Bainsvlei (1) and Paradys/Tukulu ecotopes (2) under different intensity patterns (A, Normal; B, Skewed; C, Constant).

3.4. Conclusions and recommendations

The Hofrey rainfall simulator is adequate to provide variable intensities that can mimic the natural rainfall with practically short periods of variation. Such portable rainfall simulator would be beneficial in studying further the rainfall-runoff relationship under IRWH. The Hofrey setup did not only provide rainfall simulation but also enabled measurement of infiltration from application side. The introduction of DFM probes on the other hand enabled instantaneous measurement of change in soil water content and thereby providing good record of amount of water entering and leaving the rooting zone. In using the DFM probes the *in situ* calibration must be done to obtain good results.

From the findings of this study, useful lessons were extracted on the application of IRWH in identifying important factors determining the amount of rainwater harvested as affected by the processes of infiltration and runoff. The mixed results found with regard to the effect of rainfall intensity pattern on runoff amounts did not enable generalization with regard to its effect on different soils. Nevertheless, the significant difference between the treatments observed on the Paradys/Tukulu ecotope indicated that there is a need to include patterns of intensity as a role player when predicting infiltration or runoff. The result obtained from the Kenilworth/Bainsvlei ecotope, on the other hand, emphasized that there are cases in which soil properties could have dominant roles in controlling infiltration and runoff. Thus specifically on this soil, special focus need to be bestowed on the soil than the intensity pattern variation. With the finding of such mixed results, it is recommended that further studies need to be done to investigate other factors which might vary with change of intensity pattern. For instance, in the above discussion crust strength was speculated to have played a role in changing amount runoff, and is a candidate for further study.

References

Bennie, A.T.P., Hoffman, J.E., Coetzee, M.J. & Vrey, H.S., 1994. Storage and utilization of rainwater in soils for the stabilization of crop production in semi-arid zones [Afr.]. Water Research Commission report No. 227/1/94, Pretoria, South Africa.

Boers, T.M., 1994. *Rainwater harvesting in arid and semi-arid zones*. International Land Reclamation and Improvement Intstitute (ILRI). Wageningen, Netherlands.

Botha, J.J., van Rensburg, L.D., Anderson, J.J., Hensley, M., Macheli, M.S., van Staden, P.P., Kundhlande, G., Groenewald, D.C. & Baiphethi, M,N., 2003. Water conservation techniques on small plots in semi-arid areas to enhance rainfall use efficiency, food security, and sustainable crop production. Water Research Commission report No. 1176/1/03, Pretoria, South Africa.

Bothma, C.B., 2009. In-field runoff and soil water storage on duplex soils at Paradys Experimental Farm. M.Sc. thesis University of the Free State, Bloemfontein, South Africa.

Flanagan, D.C., Foster, G.R. & Moldenhauer, W.C., 1987. Storm pattern effect on infiltration, runoff, and erosion. *Trans. ASAE* **31**(2):414-420.

Frauenfeld, B. & Truman, C., 2004. Variable rainfall intensity effects on runoff and interrill erosion from two coastal plain Ultisols in Georgia. *Soil Sci*. 169(2):143-154.

Hensley, M., Botha, J.J., Anderson, J.J., van Staden, P.P. & du Toit, A., 2000. Optimizing rainfall use efficiency for developing farmers with limited access to irrigation water. Water Research Commission report No. 878/1/00, Pretoria, South Africa.

Horton, R.A., 1936. Hydrologic interrelations of water and soils. *Soil Sci. Soc. Am. Proc.* **1**:401–429.

Mein, R.G. & Larson, C.L., 1973. Modelling infiltration during a steady rain. *Water Resour. Res.* **9**(2):384–394.

Morin, J. & Benyamini, Y., 1977. Rainfall infiltration into bare soils. *Water Resour. Res.* **3**(5):813-817.

Parson, A.J. & Stone, P.M., 2006. Effects of intra-storm variations in rainfall intensity on inter-rill runoff and erosion. *Catena* **67**:68-78.

Philip, J.R., 1957. The theory of infiltration: 4. Sorptivity and algebraic infiltration equations. *Soil Sci*. **84**:257-264.

Rawitz, E. & Hillel, D., 1971. A Method for characterizing the runoff potential rainfall in water harvesting schemes. *Water Resour. Res*. **7**(2):401-405.

Roth, C.H. & Helming, K., 2007. Dynamics of surface sealing, runoff formation and inter-rill soil loss as related to rainfall intensity, micro-relief and slope. *J. Plant Nutr. Soil Sci.* **155**(3):209-216.

SAS Institute Inc., 2006. *Administering SAS® Enterprise Guide® 4.1*. Cary, NC: SAS Institute Inc.

Smith, R.E., Smettem, K.R.J., Broadbridge, P. & Woolhiser, D.A., 2002. *Infiltration theory for hydrologic applications*. American Geophysical Union (AGU), Washington DC.

Tauer, W., Prinz, D. & Vögtle, T., 1991. The potential of runoff-farming in the Sahel region: developing a methodology to identify suitable areas. *Water Resources Management* **5**:281-287.

Walker, S. & Tsubo, M., 2003. Estimation of rainfall intensity for potential crop production on clay soil with in-field water harvesting practices in a semi-arid area. Water Research Commission report No. 1049/ 1/02, Pretoria, South Africa.

Welderufael, W.A., Le Roux, P.A.L. & Hensley, M., 2008. Quantifying rainfall-runoff relationships on the Dera Calcic Fluvic Regosol ecotope in Ethiopia. *Agric. Water Manage.* **95**:1223-1232.

Xue, J. & Gavin, K., 2007. Effect of rainfall intensity on infiltration into partly saturated slopes. *Geotech Geol Eng*. **26**(2):199-209.

Young, M.D.B., Gowing, J.W., Wyseure, G.C.L. & Hatibu, N., 2002. Parched-Thirst: development and validation of a process-based model of rainwater harvesting. *Agric. Water Manage.* **55**:121-140.

Zere, T.B., van Huyssteen, C.W. & Hensley, M., 2005. Estimation of runoff at Glen in the Free State province of South Africa. *Water SA* **31**(1):17-22.

4. Comparison of the DFM capacitance probe and neutron water meter to measure soil water evaporation

Abstract

Accurate measurement of soil water evaporation is an important parameter that needs to be taken into consideration in the design of water efficient agricultural systems. With this study the DFM capacitance probes and neutron water meter were compared to measure evaporation from the soil surface. The measured evaporation values were compared to the control values measured with mini-lysimeters. Calibration of the DFM capacitance probes and neutron water meter was done in the laboratory using the top soil of a Bainsvlei soil form. Field measurements of soil water content were done on the same Bainsvlei soil. The calibration results indicated a good correspondence (R^2 = 0.99) between the measured values and known volumetric soil water contents. There was no significant difference (p = 95%) between the DFM evaporation measurements and the control, whereas the neutron water meter and control differed significantly. It was concluded that the DFM capacitance probe is a better tool than the neutron water meter in measuring evaporation from the top soil.

Keywords: Neutron water meter, DFM capacitance probe, evaporation

4.1. Introduction

In order to use the scarce water resource for agricultural production as effectively as possible it is important that soil water can be measured as accurate as possible. The amount of water in the soil determines how strongly the water molecules are being retained in the soil matrix. The soil water can range from thin hygroscopic films tightly held around soil particles to saturation where all the soil macro pores are filled with water. The amount of soil water determines the forces that control its movement. These forces determine the availability of soil water for plant use and processes of water movement like evaporation and drainage. Thus accurate measurement of soil water determines how accurately these components of water balance will be quantified.

The conventional method of determining soil water content is described by Gardner (1986). With this method a soil sample is taken and kept in an air-tight container until it is weighed, where after it is oven dried at 105ºC for 24 hours and weighed again. The difference between the wet and dry weight expressed as a percentage of the dry weight provided the gravimetric soil water content. This method of measurement, although very accurate, is time consuming and costly. Furthermore, since the measurement employs destructive-sampling, repeated measurements on the same spot are not possible. To overcome this constraint indirect methods of soil water content measurement have been developed. One such method is the neutron water meter (NWM). This method was proposed in the 1940s and has been in use with continual improvement being incorporated (Bell, 1987). Despite the improvement, the NWM still has some drawbacks. The major concern is the health hazard of exposure to the radioactive radiation that is needed for neutron scattering. Besides this, although measurements could be done repeatedly, continuous logging of soil water contents has not been possible. These drawbacks have been addressed with the introduction of the capacitance based soil water content measurements. The advancement of electronics has enabled capacitance based soil water content measurement probes to record continuous measurements of soil water contents. The ease of use and the relatively cheaper availability of such probes make them candidate for use.

Measuring the changes in soil water contents to quantify evaporation from the soil surface soil water has been done with various instruments. The NWM has been used to measure soil water contents at different points in time and if all the other components of the soil water balance equation were measured it is possible to calculate the loss of soil water through evaporation from the soil surface (McGowan & Williams, 1980; Bennie *et al.*, 1994; 1998). With the application of the same principle of monitoring change, some studies quantifying evaporation using capacitance probes have also been done (Verhoef *et al*., 2006; Mounzer *et al*., 2008). Comparison between the NWM and capacitance probes with regard to measuring soil water accurately has been done (Evett *et al.*, 2002; Heng *et al.*, 2002; Hossain, 2008). Botha *et al*. (2001) compared the performance of NWM and frequency domain reflectometry (FDR) probes in monitoring soil water change. They found that the FDR performed better and that NWM is not suited to measuring small changes in water content and the water content of the top horizon. This result was also confirmed by van Rensburg et al. (2003). Nevertheless, the NWM continued to be used in monitoring soil water change and conducting water balance (Botha et al., 2003; Van Huyssteen, 2009). From such water balance exercises the evaporation component is determined, which to a great extent happens from the top horizon. One possible explanation for its continued use could be that the alternative considered (FDR) was relatively expensive (Botha et al., 2001). Other cheaper capacitance probes with improved ease of use are being produced. DFM probes are such alternative which have multi-depth sensors that can measure soil water content and temperature.

The DFM capacitance probes are relatively new probes which are being introduced to monitor soil water change mainly under irrigated systems. The objective of this study was to establish the suitability of the DFM probes for use in measuring soil water evaporation from the soil surface by comparing it to the instrument which is in still in wide use, the NWM.

4.2. Materials and methods

4.2.1. Description of the experiment

The field experiment was conducted on the Kenilworth/Bainsvlei ecotope. Soil water measurements were taken on rain-free days. Evaporation was taken as the change in soil water content between consecutive measurements. The micro-lysimeter, DFM capacitance probes and NWM were used to measure the soil water contents. For most evaporation studies the micro-lysimeter has been used (Boast & Robertson, 1982; Wythers *et al.*, 1999; Bremer, 2003) and served as a control when comparing the evaporation measured by the DFM capacitance probe and NWM (Paruelo *et al.*, 1991).

The comparison of the DFM probe and NWM was done within a bigger experiment where evaporation from eleven different sections of the micro-landscape of the in-field rainwater harvesting *(IRWH*) system was monitored. The experiment was repeated in five different drying cycles.

4.2.2. Soil water measurement

4.2.2.1. DFM capacitance probes

DFM capacitance probes were used as one of the methods to measure the soil water content. The capacitance based probes measure soil water by measuring the dielectric constant of the soil (Hossain, 2008). The dielectric constants of various materials differ and specifically that of water is much higher than that of soil. Thus, depending on the amount of water in the soil the dielectric value changes and this is quantified by capacitance sensors. The DFM probes (Figure 4.1) are multilevel soil water and temperature measuring probes. The probes had a length of 1200 mm and had six sensors placed at 200, 400, 600, 800, 1000 and 1200 mm. The probes can take measurement at intervals set by the user.

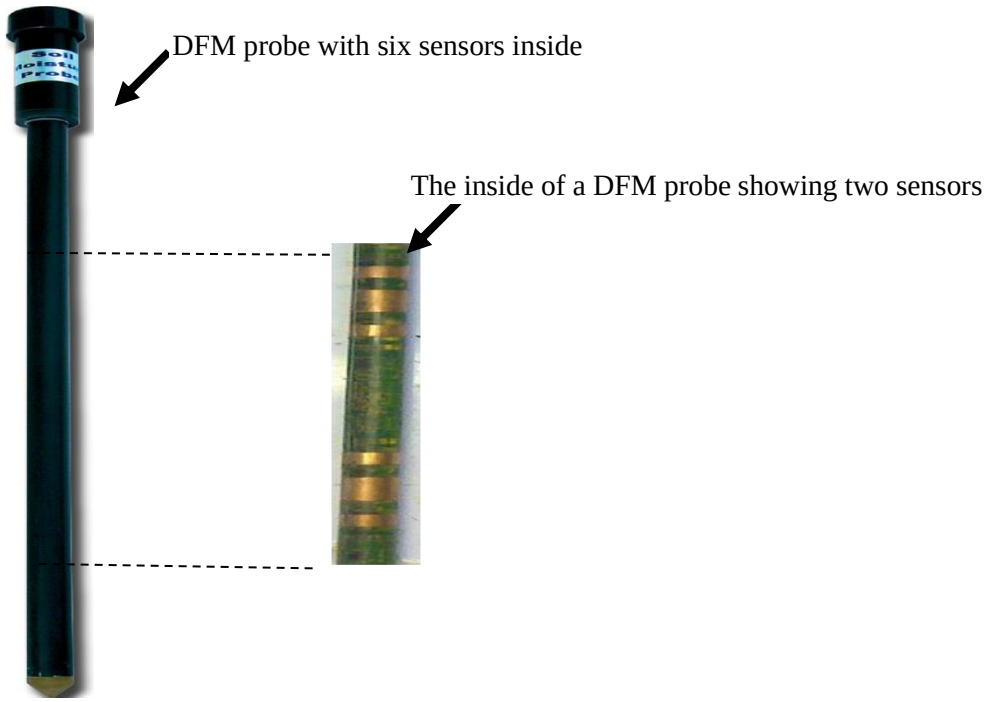

Figure 4.1 The multi-level water content measuring DFM capacitance probe.

4.2.2.2. Neutron water meter (NWM)

The NWM (Figure 4.2) is a reliable method of measuring soil water content. This instrument uses fast neutron scattering to detect the amount of water in the soil. The hydrogen molecule in water slows down the scattering neutrons and results in thermalized neutrons, which are counted by the instrument and related to the water content. To use this instrument at different soil depths, an access tube is inserted into the soil (Figure 4.2). A probe which has a source of neutrons and a counter that measures the thermalized neutrons is inserted through this access tube to a pre-determined depth. For this experiment a "WaterMan" NWM (Serial No: D366NJ1099) was used. The cable clamps of this machine were set to take measurements at soil depths of 150, 450, 750, 1050, 1350 and 1650 mm.

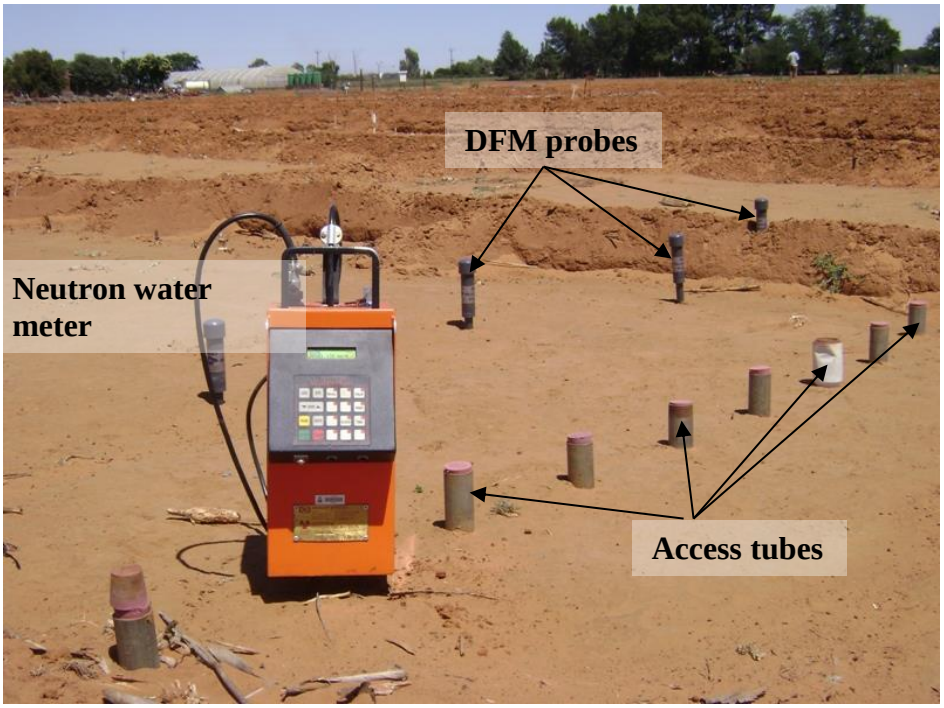

Figure 4.2 Neutron water meter, access tubes and DFM probes on the experiment field.

4.2.2.3. Micro-lysimeters

The micro-lysimeters (Figure 4.3) used were cylinders with a diameter of 70 mm and 300 mm long. Hoffman (1997) and Bennie *et al.* (1998) have used the same micro-lysimeters to measure evaporation. The soil cores in the lysimeters were prepared by pressing the micro-lysimeters into the soil surface. This was done to produce undisturbed soil columns which were representative of the natural packing. The lysimeters were fitted with stoppers to hold the soil column in place. For easy insertion and removal of the micro-lysimeter in the ground hole, a lining tube was put in place (Sharratt & McWilliams, 2005). This lining tube preserved the hole intact by protecting the soil wall from falling in. The evaporative loss was determined by weighing the lysimeters and computing the difference between consecutive weighing. This gravimetrically determined change in soil water was converted to depth units by dividing it with the surface area of the micro-lysimeters.

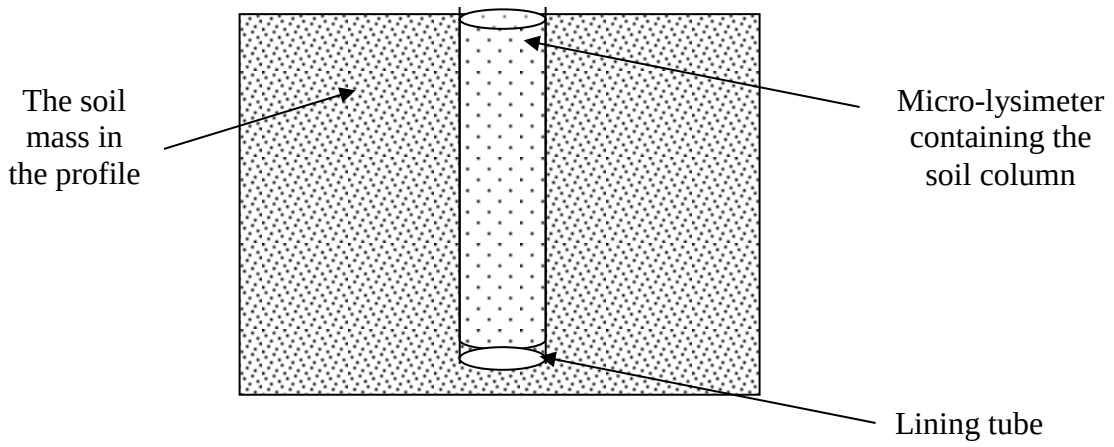

Figure 4.3 Schematic description of micro-lysimeter installation in the soil profile.

4.2.3. Measurement of soil water evaporation

Evaporation of soil water was measured as the difference between measurement days for the three soil water measuring methods. Unrealistic values were removed from the data set and values corresponding to the missing values were not used during comparison of the means and hence the effect was not reflected in the statistical results.

4.2.4. Calibration of the soil water measuring instruments

A laboratory calibration of the DFM probes and NWM was done. For this purpose top-soil was collected from a field on Kenilworth/Bainsvlei ecotope. The soil was air dried and five samples were taken for determination of the gravimetric soil water content. To prepare soil columns of known water content and bulk density the soil was packed into 210 *l* plastic drums with a diameter of 270 mm and height of 920 mm. These drums were air-tight containers (Figure 4.4) with only two small openings on the top through which the soil was packed. An access tube was installed in the middle of the drum (Figure 4.4) and the opening properly sealed. To provide the dry-end and wet-end of the soil two sets of drums were used. The drums representing the dry-end were filled with a known mass of air-dried soil. Drums were well shaken to imitate the natural packing of the soil. The bulk density was determined by taking the mass of soil filled into the drum and the volume contained by the soil. The drums representing the wet-end were prepared in the same way except that water was added to bring the known soil mass to saturation. The mass of the water added to saturate the soil column was recorded. The volumetric water

content of the soils in the drums was calculated by determining the gravimetric water content from the weight of soil fitted into the drums and multiplying it with the bulk density.

Figure 4.4 Two 1200 mm DFM probes inserted into a soil filled drum for calibration.

4.2.4.1. Calibration of DFM capacitance probes

For the calibration of the DFM capacitance probes the probes were installed into the drums by pushing them into the soil column and were set to stay in the soil for at least 6 hours. Two probes were installed per drum through the openings on top of the drum (Figure 4.4). After the probes were inserted, the holes were sealed using plastic tape to protect water loss through evaporation. The installed probes measured the soil water content of the drums every 30 minutes. To provide acceptable replication 31 probes were used for calibration. There were 16 measuring sessions on each drum (two probes being installed at a time). Due to the limited height of the drums only three sensors on each probe recorded the water content. Since the water content of the soil column was

homogenous each sensor on a probe was considered individually without any reference to depth. A DFM reading which did not indicate good contact between probe and the soil was discarded and 84 sensor readings from a total of 93 was provided. These readings were randomly divided into two data sets. Half of the data was used for calibration and the remaining half was used to validate the calibration equation.

4.2.4.1.1. Temperature correction for the sensors

It had been observed that readings of capacitance sensors were affected by temperature. Thus correcting for temperature was essential. For this purpose, monitoring of the DFM readings was conducted in a temperature-controlled room. A PVC cylinder filled with de-ionized water provided a homogenous medium into which the DFM probes were immersed. DFM readings were recorded at 5, 15, 25 and 35°C. Each temperature was maintained for a period of 48 hours. The slope of the regression between temperature and the DFM readings provided the rate of change (slope). The slope was then used to derive a linear correction equation (Equation 4.1) similar to the one reported by Fares *et al.* (2009). The equation was designed to bring the readings taken at different temperature to the same temperature of 25°C. The equation is given below:

$$\mathbf{DFM_{NT} = (25 - DFM_T)* S + DFM_R} \quad (4.1)$$

Where:

DFM_{NT} = new transformed DFM reading (%)

DFM_T = temperature reading from DFM probe (%)

DFM_R = water content reading from DFM probe (%)

S = Slope determined from the relationship between temperature and DFM reading

The DFM readings recorded for the soil columns prepared in the drums were temperature corrected by using Equation 4.1. A linear regression equation between the DFM readings and known volumetric soil water content was developed.

4.2.4.2. Calibration of NWM

The same drums that were used for the calibration of the DFM probes were also used to calibrate the NWM. Measurements were taken twice daily at a depth of 300 and 600 mm. Since the water content was homogenous within each drum, no attempt was made to separate the readings by depth during the analysis. Four randomly selected readings were used for calibration. The calibration was done by linearly relating the NWM readings with the volumetric soil water content. The resulting linear equation was then tested (validated) on the remaining four readings.

4.2.5. Statistical analysis

SAS software (SAS Institute Inc., 2006) was used to perform the regression for both DFM readings and NWM readings against the measured volumetric soil water content values. Validation of the calibration equation was done by using the model performance parameters suggested by Willmott (1982). These parameters include the index of agreement (D-index), mean absolute error (MAE), root mean square error (RMSE) with its systematic ($RMSE_s$) and unsystematic ($RMSE_u$) components, and the coefficient of determination (R^2). Willmott (1982) points out that in a "good" model the RMSEs should approach zero; a large RMSEs indicates bias. The D-index should approach one and the RMSEu should be as close as possible to the RMSE, indicating that the deviations of simulated from measured values are random. SAS software was also used for t-test comparison between evaporation values of the micro-lysimeter and DFM as well as the micro-lysimeter and NWM.

4.3. Results and discussion

4.3.1. Calibration results of DFM probes and NWM

A summary of the soil water content measurements using the capacitance probes and NWM probe of the known soil water content values is given in Table 4.1. For a given soil water, the average reading by the DFM probes and the NWM with the observed variation are shown in Table 4.1. The coefficient of variation (CV) indicated there was much more variation on the readings taken for the dry soil compared to the wet soil. This trend was

observed for both the DFM and NWM probes. The CV observed for the NWM readings of the dry top soil was exceptionally high. There was also a variation on the readings taken at the two depths.

Table 4.1 Water content and bulk density values of soil in the drum and the corresponding average DFM and neutron water meter (NWM) readings.

Soil column	Bulk density (kg m^{-3})	Clay percentage	Volumetric water content (%)	DFM reading (n = 84)		NWM reading (n = 8)	
				Average (%)	CV	Average (Count ratio)	CV
Air-dried	1340	7.5	2.2	12.5	10.1	13.1	56.2
Saturated	1340		40.5	67.0	3.4	166.9	1.95

CV = coefficient of variation

The linear regression lines indicating the correspondence between DFM reading and the volumetric soil water contents are presented in Figure 4.5. The DFM readings and the volumetric values are expressed as percentages. The regression line and calibration equation are presented on the same figure. The resulting R^2 (0.99) indicated that the DFM probe readings strongly correlated with the volumetric soil water content. The linear regression had a prediction interval of 95% which is indicated by the dotted lines on both sides of the regression line. Most of the measured data points as well as points predicted by the regression line fall within this interval.

The linear regression between NWM readings and the volumetric soil water content is presented in Figure 4.6. An R^2 of 0.99 indicated there is a good correlation between the NWM readings and volumetric soil water contents. Figure 4.6 also indicate the good performance of the linear regression fit.

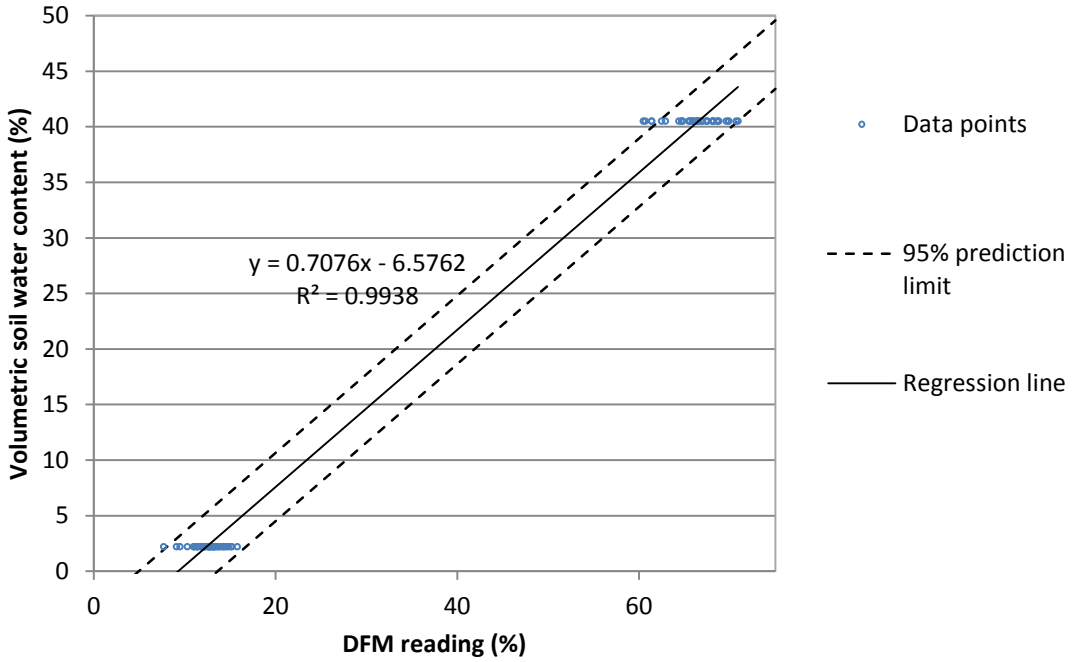

Figure 4.5 Regression line between DFM readings and volumetric soil water contents for the top soil of the Kenilworth/Bainsvlei ecotope [n = 84 from 42 sensors].

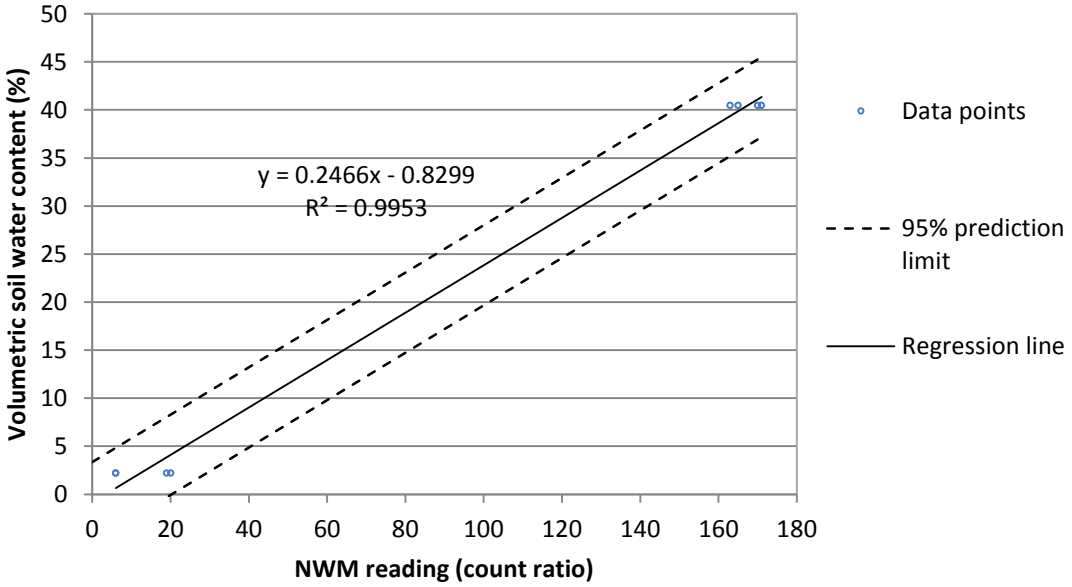

Figure 4.6 Regression line between neutron water meter (NWM) reading and volumetric soil water content for the top soil of the Kenilworth/Bainsvlei ecotope [n = 8].

4.3.2. Validation of the calibration equation of the DFM probes and NWM

The calibration equation for converting the DFM and NWM readings into volumetric soil water content were validated on separate data sets from which they were developed. The summary of the statistical performance of the calibration equations is presented in Table 4.2. The observed RMSE values were very small for both probes and ranged between 1 – 1.35%. Excellent values of R^2 and D-index showed that there was good agreement between the measured and computed values of volumetric soil water contents. This was further confirmed by close to 1 values of slope for the regression line between measured and computed volumetric soil water contents. The y-intercept values were small values close to zero indicating good correspondence even with smaller values of soil water contents. The ratio of the RMSEs/RMSE for both instruments was not more than 0.36. This indicates that the errors involved in the prediction of the water contents were random.

Table 4.2 Statistical validation results of the calibration equation of the DFM capacitance probe and neutron water meter.

Statistical parameter	Top soil of the Kenilworth/Bainsvlei ecotope	
	DFM	NWM
RMSE	1.077	1.348
RMSEs	0.389	0.328
RMSEu	1.004	1.308
MAE	0.766	1.171
R^2	0.998	0.995
D-index	0.999	0.999
slope (b)	1.019	0.983
Y-intercept (a)	-0.113	0.305
RMSEs/RMSE	0.361	0.243

4.3.3. Comparison of DFM probes and NWM for measuring evaporation

The evaporation values computed from observations during rain-free days are presented in Tables 4.3 to 4.5. From the 21 measurement days, 5 rain-free drying cycles were identified. The drying cycles contained eight daily evaporation values and four 3-day cumulative evaporation values.

Table 4.3 Evaporation (mm) values measured with the micro-lysimeter technique on a bare in-field rainwater harvesting plot on the Kenilworth/Bainsvlei ecotope.

Drying cycles	Number of evaporation days	Lysimeters											
		1	2	3	4	5	6	7	8	9	10	11	12
1	1	1.03	- *	2.70	1.14	3.52	2.52	0.98	0.73	2.61	2.31	1.29	1.36
	1	2.09	4.42	2.43	1.14	2.90	1.95	1.72	1.18	1.82	2.34	2.09	1.79
	1	1.65	2.18	1.47	0.85	1.22	1.64	0.76	0.88	1.06	1.86	1.60	1.19
2	1	2.15	- *	2.00	1.53	3.08	1.72	1.69	1.30	1.32	2.40	1.85	1.78
	1	- *	1.76	1.92	1.14	1.98	1.14	0.65	1.39	1.32	1.83	2.62	1.72
	1	1.38	2.81	1.79	0.91	1.41	0.89	0.89	1.07	1.29	1.35	2.52	1.38
3	3	3.16	3.66	4.01	3.77	4.71	4.18	3.76	3.03	4.12	2.82	7.63	3.88
	3	2.55	2.98	2.99	4.46	3.33	3.08	2.55	2.45	5.42	0.80	3.05	2.06
4	1	2.69	4.57	3.48	2.33	- *	4.02	3.94	1.90	- *	- *	3.11	3.41
	3	- *	2.98	2.89	1.68	7.39	4.24	2.90	1.86	8.43	5.54	3.91	2.70
5	3	7.35	- *	6.38	3.94	- *	4.42	4.75	7.48	6.90	- *	6.91	5.47
	1	0.91	0.98	1.08	0.73	2.26	1.11	0.59	1.08	0.71	1.09	1.39	0.75

* Unrealistic values removed from dataset

Table 4.4 Evaporation (mm) values measured with DFM probes at the in-field rainwater harvesting field of Kenilworth/Bainsvlei ecotope.

Drying cycles	Number of evaporation days	DFM probes											
		1	2	3	4	5	6	7	8	9	10	11	12
1	1	1.24	1.52	0.00	2.62	8.87	1.57	0.00	2.71	- *	0.02	1.50	1.90
	1	0.71	1.04	0.00	1.71	1.24	0.00	0.00	1.54	0.00	0.00	0.37	0.00
	1	0.56	0.18	0.00	1.27	1.45	0.32	0.64	1.22	0.00	0.00	0.08	0.00
2	1	3.31	4.84	0.52	3.29	1.50	1.07	1.71	0.00	1.94	0.14	1.54	0.69
	1	0.00	7.55	0.00	0.00	0.13	0.20	0.28	0.00	1.01	0.00	0.00	0.23
	1	1.21	- *	0.45	1.36	0.69	0.45	0.80	0.28	1.36	0.17	0.00	0.41
3	3	0.00	0.27	0.00	0.89	1.41	0.02	1.10	0.00	1.97	0.00	0.61	1.08
	3	0.25	2.31	0.00	- *	0.33	0.85	0.66	1.45	2.69	0.00	1.50	1.49
4	1	0.19	5.92	0.00	2.79	2.60	0.00	0.00	1.27	4.03	0.00	0.00	0.00
	3	8.24	10.67	7.54	10.66	3.70	4.48	4.36	3.02	5.46	2.11	7.68	6.95
5	3	- *	7.15	4.75	8.80	5.03	6.36	5.95	3.31	6.95	3.57	8.36	3.25
	1	6.64	2.15	6.34	8.20	1.99	3.69	4.46	1.98	2.00	2.11	6.38	1.73

* Data removed due to unrealistic response

Table 4.5 Evaporation (mm) values measured with NWM at the in-field rainwater harvesting field of Kenilworth/Bainsvlei ecotope.

Drying cycles	DOY and Number of evaporation days	NWM access tubes											
		1	2	3	4	5	6	7	8	9	10	11	12
1	315 (1)	0.22	0.16	0.25	0.00	1.13	0.00	0.00	0.18	0.22	0.19	7.36	0.00
	316 (1)	0.06	0.82	0.49	5.86	0.54	0.00	0.00	0.35	0.42	0.09	0.09	0.00
	317 (1)	0.00	0.22	0.24	0.02	0.00	0.00	0.00	0.63	0.59	0.00	0.00	0.00
2	328 (1)	0.00	0.00	0.00	0.21	0.55	0.00	0.05	0.48	0.00	0.00	0.00	0.68
	329 (1)	0.83	0.00	0.97	0.60	0.50	0.00	0.00	0.69	0.00	0.05	0.06	0.44
	330 (1)	0.00	0.00	0.23	0.00	0.30	0.22	0.05	0.44	0.00	0.10	0.00	0.38
3	334 (3)	0.10	0.15	0.43	1.12	0.98	0.00	0.08	1.37	0.00	0.01	0.00	1.14
	338 (3)	0.19	0.00	1.16	0.94	0.31	0.00	0.00	0.50	0.00	0.00	0.00	0.09
4	345 (1)	2.17	0.00	2.63	2.04	0.00	0.00	0.00	2.79	0.00	0.07	0.00	1.45
	348 (3)	0.63	0.00	0.42	0.94	3.64	0.00	0.00	1.13	0.00	0.02	0.00	1.23
5	60* (3)	-	-	-	-	-	-	-	-	-	-	-	-
	61* (1)	-	-	-	-	-	-	-	-	-	-	-	-

* Not measured due to technical problems

The paired t-test comparisons done on the evaporation values measured by DFM probes and NWM versus the control (micro-lysimeter) are presented in Table 4.6. The results showed that the DFM evaporation values were not significantly different at 95% probability. Contrary to the DFM results, all the comparisons between NWM evaporation and control, except two, were significantly different.

Table 4.6 T-test results for paired comparison of DFM vs. lysimeter and neutron water meter (NWM) vs. lysimeter evaporation values.

Difference	Mean	DF	t-value	Pr > |t|	Difference	Mean	DF	t-value	Pr > |t|
DFM1 - Lys1	-0.39	8	-0.44	0.67	NWM1 - Lys1	-1.75	7	-5.91	< 0.001**
DFM2 - Lys2	0.82	7	0.57	0.59	NWM2 - Lys2	-3.02	7	-9.46	< 0.001**
DFM3 - Lys3	-1.13	11	-1.32	0.21	NWM3 - Lys3	-1.89	9	-7.29	< 0.001**
DFM4 - Lys4	2.04	10	1.88	0.09	NWM4 - Lys4	-0.72	9	-1.06	0.19
DFM5 - Lys5	-1.05	9	-1.28	0.23	NWM5 - Lys5	-2.40	8	-7.24	< 0.001**
DFM6 - Lys6	-0.99	11	-1.70	0.12	NWM6 - Lys6	-2.52	9	-6.10	< 0.001**
DFM7 - Lys7	-0.43	11	-0.73	0.48	NWM7 - Lys7	-1.97	9	-5.06	< 0.001**
DFM8 - Lys8	-0.63	11	-1.24	0.24	NWM8 - Lys8	-0.72	9	-2.97	0.02**
DFM9 - Lys9	-0.90	9	-1.94	0.08	NWM9 - Lys9	-2.91	8	-3.4	0.01**
DFM11 - Lys11	-0.27	10	-0.33	0.75	NWM11 - Lys11	-1.62	8	-1.63	0.14
DFM12 - Lys12	-0.81	11	-1.39	0.19	NWM12 - Lys12	-1.59	9	-9.42	< 0.001**

** Statistically significant at 95% probability DF – degrees of freedom (n-1)

The results confirmed that there was good correspondence between the changes in soil water content measured by the micro-lysimeter and the DFM. Since the DFM probes are relatively new products in the market the thorough evaluation of DFM probes with regard to its precision, accuracy and reliability of its measurements over a wide range of soils is needed. Nevertheless, the performance of other capacitance probes can be related to it in measuring evaporation. ECH_2O probes were used to measure soil water content of drying

coir by van der Westhuizen (2009) and drying soil cores by Nhtlabatsi (2010). Both reported an accuracy of less than 0.005 mm mm^{-1}. Such good performance in measuring soil water content can explain the sensitivity of the DFM probes in sensing the small values of daily soil water evaporation.

The results indicated that there was significant difference between the soil water evaporation measured by micro-lysimeters and the NWM. This does not disprove the reliability of NWM in measuring soil water content, over the entire rootzone. The reliability of the NWM to measure soil water content is undisputed (Evett *et al*., 2002; Heng *et al*., 2002; Mounzer *et al*., 2008). Nevertheless, the use of the NWM to monitor the rather small water content changes in the top soil seems not to be suitable for measuring soil water evaporation. This supports the finding by Botha *et al*. (2001) which compared the NWM and FDR. This can be due to one of two reasons. Firstly, the instrument carries about 2% error arising from random counting error (Bell, 1987). The random counting error is an unavoidable error for the NWM, the best practice is to keep it as small as possible. This can hamper the NWM from sensing small changes in soil water contents brought about by evaporation from the soil surface. Secondly, the NWM reading errors mostly occur in the top horizon of the soil profile where there is a possibility of radiation escaping through the surface and hence not giving a fully representative reading of the water content (McGowan & Williams, 1980). This failure of the NWM to observe daily change in water content, caused by evaporation from bare soil, is also validated by other data collected by the authors (not reported here). Daily NWM water content measurements done on Glen/Bonheim, Glen/Swartland and Paradys/Tukulu ecotopes in 2008 showed that no reliable daily-evaporation measurements could be done using this method. Hensley *et al.* (2000) and Botha (2006) have reported evaporation values from the water content monitoring conducted by NWM. However, with their studies they have calculated the evaporation values from the water balance equation where all the other variables were known or measured. Their measurements were also done over longer periods and not based on daily water losses due to evaporation.

Various other studies comparing capacitance probes and NWM had been done previously (Evett *et al*., 2002; Heng *et al*., 2002; Mwale *et al*., 2005; Mounzer *et al*., 2008; Vera *et*

al., 2009). These studies confirmed the observation that the capacitance probes are sensitive enough to measure small changes in the soil water contents due to water losses through evaporation from the soil surface. However, the presence of air-pockets could result in wrong readings (Mwale *et al*., 2005). Thus, to increase the reliability of the capacitance probes, there is a need to ensure proper installation of the probes. On the other hand, the above mentioned studies confirmed that the NWM gave consistent readings over a wide range of soil textures and soil water contents. This was attributed to the ability of the NWM to measure bigger volumes of soil and relatively less sensitivity to soil heterogeneity (Heng *et al*., 2002; Vera *et al*., 2009). These studies have also confirmed the accuracy of the NWM to measure the soil water contents of the whole rootzone, but the evaporation sensitive zone usually forms only a small fraction of the total rootzone. Hoffman (1997) generally computed the zone to be the top 300 mm. As discussed above, for NWM sensing the soil water content change in the evaporation sensitive zone of the sol profile can be less accurate. Mounzer *et al*. (2008) reported that both capacitance probes and NWM performed well in measuring the evaporation from a cropped field and that the capacitance probe correlated well with the values predicted by the FAO methodology.

4.4. Conclusions and recommendations

The DFM capacitance probes and NWM were used to compare the measurement of soil water evaporation. Measurements with the DFM probes and NWM provided good agreement with the gravimetrically determined soil water contents. Both instruments can be used to monitor the change in soil water contents and the multi-depth measuring capabilities provide a good tool to measure the soil water content of a soil profile. However, from the results it can be concluded that DFM probes provide more accurate measurements of evaporation from the top soil than the NWM. Based on the observation made during the experiment it is recommended that proper care be taken when installing the DFM probes to provide good contact between the probe and the soil.

References

Bell, J.P., 1987. Neutron probe practice (Third Edition). Report 19. Institute of Hydrology. Wallingford, UK.

Bennie, A.T.P., Hoffman, J.E., Coetzee, M.J. & Vrey, H.S., 1994. Storage and utilization of rainwater in soils for the stabilization of crop production in semi-arid zones [Afr.]. Water Research Commission report No. 227/1/94, Pretoria, South Africa.

Bennie, A.T.P., Strydom, M.G. & Vrey, H.S., 1998. The application of computer models for agricultural water management on ecotope level [Afr.]. Water Research Commission report No. 625/1/98, Pretoria, South Africa.

Boast, C.W. & Robertson, T.M., 1982. A "micro-lysimeter" method for determining evaporation from bare-soil: description and laboratory evaluation. *Soil Sci. Soc. Am. J.* **46**:689-696.

Botha, J.J., 2006. Evaluation of maize and sunflower production in semi-arid area using in-field rainwater harvesting. Ph.D. thesis University of the Free State, Bloemfontein, South Africa.

Bremer, D.J., 2003. Evaluation of micro-lysimeters used in turfgrass evapotranspiration studies using the dual-probe heat-pulse technique. *Agron. J.* **95**:1625-1632.

Evett, S.R., Laurent, J.P., Cepuder, P. & Hignett, C., 2002. Neutron scattering, capacitance and TDR soil water content measurements compared on four continents. Paper presented at the 17th World Congress of Soil Science, 14 – 21, August 2002. Thailand. Paper No. 1021.

Fares, A., Safeeq, M. & Jenkins, D.M., 2009. Adjusting temperature and salinity effects on single capacitance sensors. *Pedosphere* **19**(5):588-596.

Gardner, W.H., 1986. Water content. In: Klute, A., (ed.) Methods of soil analysis: Part I Physical and mineralogical properties. American Society of Agronomy and Soil Science Society of America, Madison, Wisconsin, USA. pp. 493-544.

Heng, L.K., Cayci, G., Kutuk, C., Arrillaga, J.L. & Moutonnet, P., 2002. Comparison of soil moisture sensors between neutron probe, Diviner 2000 and TDR under tomato crops. Paper presented at the 17th World Congress of Soil Science, 14 - 21, August 2002. Thailand. Paper No. 1532.

Hensley, M., Botha, J.J., Anderson, J.J., van Staden, P.P. & du Toit, A., 2000. Optimizing rainfall efficiency for developing farmers with limited access to irrigation water. Water Research Commission report No. 878/1/00, Pretoria, South Africa.

Hoffman, J.E., 1997. Quantifying and prediction of evaporation from the soil surface under dryland crop production [Afr.]. Ph.D. thesis University of the Free State, Bloemfontein, South Africa.

Hossain, M.D.B., 2008. EM38 for measuring and mapping soil moisture in a cracking clay soil. Ph.D. thesis University of New England, Armidale New South Wales, Australia.

McGowan, M. & Williams, J.B., 1980. The water balance of an agricultural catchment. 1. Estimation of evaporation from soil water records. *J. Soil Sci.* **31**:217-230.

Mounzer, O.H., Hernández, R.M., Villena, I.A., Muñoz, J.V., Ruiz-Sánchez, M.C., Vargas, L.M.T., Arnaldos, V.P. & García, J.M.A., 2008. Estimating evapotranspiration by capacitance and neutron probes in a drip-irrigated apricot orchard. *Interciencia* **33**(8):586-590.

Mwale, S.S., Azam-Ali, S.N. & Sparkes, D.L., 2005. Can the PR1 capacitance probe replace the neutron probe for routine soil-water measurement? *Soil Use Manage.* **21**:340-347.

Nhtlabatsi, N.N., 2010. Soil surface evaporation studies on the Glen/Bonheim ecotope. Ph.D. thesis University of the Free State, Bloemfontein, South Africa.

Paruelo, J.M., Aguiar, M.R. & Golluscio, R.A., 1991. Evaporation estimates in arid environments: an evaluation of some methods for the Patagonian steppe. *Agric. For. Meteorol.* **55**:127-132.

SAS Institute Inc., 2006. *Administering SAS® Enterprise Guide® 4.1*. Cary, NC: SAS Institute Inc.

Sharratt, B.S. & McWilliams, D.A., 2005. Microclimatic and rooting characteristics of narrow-row versus conventional-row corn. *Agron. J.* **97**:1129-1135.

Van der Westhuizen, R.J., 2009. Laboratory procedure to calibrate EC-10 and EC-20 capacitance sensors in coir. Ph.D. thesis University of Stellenbosch, Stellenbosch, South Africa.

Vera, J., Mounzer, O., Ruiz-Sánchez, M.C., Abrisqueta, I., Tapia, L.M. & Abrisqueta, J.M., 2009. Soil water balance trial involving capacitance and neutron probe measurements. *Agric. Water Manage.* **96**:905-911.

Verhoef, A., Fernández-Gálvez, J., Diaz-Espejo, A., Main, B.E. & El-Bishti, M., 2006. The diurnal course of soil moisture as measured by various dielectric sensors: effects of soil temperature and the implications for evaporation estimates. *J. Hydrol.* **321**:147–162.

Willmott, C.J., 1982. Some comments on the evaluation of model performance. *Bull. Amer. Meteor. Soc.* **63**:1309-1313.

Wythers, K.R., Lauenroth, W.K. & Paruelo, J.M., 1999. Bare-soil evaporation under semi-arid field conditions. *Soil Sci. Soc. Am. J.* **63**:1341–1349.

5. The influence of the micro-landscape of the in-field rainwater harvesting system on evaporation

Abstract

In-field rainwater harvesting (IRWH) has a unique micro-landscape composed of ridge and furrow on the basin strip and flat crusted runoff strip. The length of the runoff strip can vary depending on the basin to runoff strip ratio. This micro-landscape determines how rainwater moves in the system and subsequently the amount of the evaporation from the soil surface (Es). The aims of this study were to compare water loss through Es on the micro-landscape sections (ridge, furrow and runoff strip) of the standard IRWH technique and to evaluate the effect of different basin-runoff ratios of IRWH on Es. DFM capacitance probes were used to measure Es on different sections of the micro-landscape. Slope comparison of the linear relationship between cumulative Es plotted and square root of time (Ritchie's α-value) for each section of the micro-landscape was used to evaluate Es difference. The result revealed that Es varied among the different sections of the micro-landscape. The spatially averaged Es, however, representing the whole plot did not show significant variation with varying runoff strip length. The observed Es variation can have an implication in modelling Es in the IRWH system. The whole IRWH plot can not be treated as homogenous surface and separate model parameters need to be used for each section.

Key words: micro-landscape, evaporation, IRWH

5.1. Introduction

IRWH, being an *in situ* rainwater harvesting technique, was designed with a unique soil surface shape (micro-landscape) to enhance crop yields in semi-arid zones. The design of the micro-landscape comprised of a 2 m runoff strip with a slight slope (< 4%) towards the 1 m basin strip (Figure 1.1). The purpose of the runoff strip is to serve as a catchment for harvesting rainwater. As a result tillage operations on this strip are restricted to methods that will ensure a smooth surface that will enhance runoff or reduce infiltration. For example, weed control is preferably done by spraying of herbicides instead of conventional tillage (disc or chisel ploughs) methods. Conventional tillage methods tend to disturb the soil of the runoff strip which improves infiltration instead of inducing in-field runoff. The purpose of the basin strip is to store the run-on from the runoff strips. Consequently the surface storage capacity of the basin strips is of utmost importance to prevent over-spilling of the basins. Hensley *et al*. (2000) estimated that small basins of 700 mm wide x 1300 mm long x 100 mm deep will be sufficient to store a 75 mm rainstorm and its run-on component within the IRWH system employed near Bloemfontein (semi-arid climate). In practice, the basin strip is made manually using spades and rakes. It comprises of a main ridge with a height that varies between 250 – 300 mm and a width of about 250 - 300 mm. Lateral movement along the ridge is controlled with cross ridges every 1500 mm. The micro landscape structure of the basin and runoff strips has been proven to be very effective in impeding ex-field runoff losses (Hensley *et al.*, 2000; Mzezewa & van Rensburg, 2011).

Detailed soil water balance (SWB) studies over a period of three years by Hensley *et al*. (2000) revealed new insight on the soil water-crop relations induced by the IRWH system. Firstly, they observed that maize and sunflower yields were about 50% higher in IRWH than conventional prepared (mouldboard plough) plots on mainly clay and duplex soils at Glen and Thaba Nchu, South Africa. Secondly, the research indicated that water conserved through in-field runoff (IR_{off}) could only partially explain the increase in the observed yields of IRWH. Accordingly annual IR_{off} varied between 13.7 and 31.2% under rainfall conditions that varied between 452 and 589 mm. The harvested water was taken as transpiration which could be converted to biomass using transpiration efficiency

coefficients of the crops (Bennie *et al*., 1998). Thirdly, the researchers observed that the *in situ* rainwater harvesting technique also conserves significant amounts of water by reducing evaporation of soil water (Es) compared to the conventional plots. The Es varied 230 and 280 mm over the growing season in the IRWH plots. However, despite the significant amount of water conserved in IRWH compared to the conventional tillage plots Es remained the main mechanism of water loss, irrespective of tillage technique. Against this background, Botha *et al.* (2003) evaluated the effect of mulch types and surface coverage to reduce Es under IRWH. A conclusion was drawn that mulches contributed to reduce Es and hence increased yields up to 15 and 21% for maize and sunflower, respectively, depending on the percentage coverage of the runoff strips. This work was exclusively conducted on IRWH with a 1 m basin strip and 2 m runoff strip, i.e 1:2 basin to runoff ratio.

Recent advances in IRWH technology enable farmers to make use of basin: runoff ratios of their choice. One of the advances is the development of tractor drawn implements by van Rensburg *et al.* (2012). These implements comprised of a ridge plough and a puddle plough. The ridge plough was designed for constructing the wall of the basin by drawing the implement along the slope of the field. In the process, the implement leaves a furrow along the ridge. These furrows are modified with a puddle plough that creates cross ridges within basin strips. Thus, from the description above it is clear that IRWH system has a characteristic micro-landscape, i.e. a ridge, a furrow and a smooth runoff strip (Figure 1.1). The runoff strip length (RSL) will change depending on the basin to runoff ratio preference. Smaller RSLs will probably be used in ecotopes with high IR_{off} potential and wider RSLs for lower IR_{off} potentials (Bothma, 2009). With such envisaged changes, it was hypothesized that the basin to runoff ratios will affect Es. Botha *et al*. (2003) also recommended further studies on Es as it seems to be the main mechanism of water loss under the standard (1:2 basin to RSL ratio) IRWH layout. Thus, the aims of this chapter were: Firstly, to compare water loss through Es on the micro-landscape sections (ridge, furrow and runoff strip) of the standard IRWH technique. Secondly, to evaluate the effect of different basin-runoff ratios of IRWH on Es.

5.2. Materials and methods

5.2.1. Description of the experimental sites

The Es experiment was conducted on two ecotopes: Kenilworth/Bainsvlei and Paradys/Tukulu. The two ecotopes have a similar climate and topography, but differs with respect to their soils. The relevant soil properties for the two soils are summarised in Tables 1.2 – 1.4. The rainy season for the two ecotopes is during summer (October to April). The evaporation demand is also higher during this period. The monthly climatic information is given in Table 1.1.

5.2.2. Experimental design and layout

The experimental design for determining Es on the two ecotopes comprised of three basin to runoff ratios of IRWH, *viz.* the standard 1:2, 1:1 and 1:3 ratios. The main treatments are the different sections of the micro landscapes created by IRWH, namely the ridge and furrow and the runoff strip (Figure 5.1). The runoff strip was further divided into 1 m sections depending on the basin to RSL ratio. Hence, the treatments were:

1:1 – Ridge, furrow and runoff-strip 1 m

1:2 – Ridge, furrow, runoff-strip 1 m and runoff-strip 2 m

1:3 – Ridge, furrow, runoff-strip 1 m, runoff-strip 2 m and runoff-strip 3 m

Both experiments were not replicated because there was constraint of not having enough soil water measuring probes. The measurement of Es was repeated over different periods to accommodate varying atmospheric conditions. These repeated measurement provided 3 drying cycles for both ecotopes.

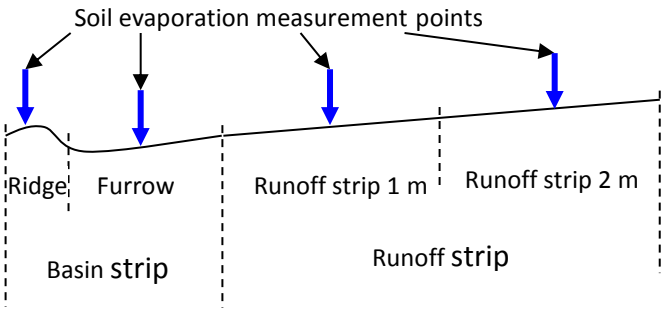

Figure 5.1 Schematic diagram of the cross-sectional view of micro-landscape formed by the 1:2 basin to RSL ratio of IRWH and the soil water measurement points (indicated by arrows).

5.2.3. Measurement of soil water content, soil temperature and Es

In this experiment calibrated DFM capacitance probes were used to measure the soil water content. Soil specific calibration was done according to the method explained in section 4.3.4. These probes were of two lengths; 800 mm and 1200 mm. The 800 mm long probes were used in the shallower soil of the Paradys/Tukulu ecotope. The soil water and temperature sensors are positioned at 100, 200, 300, 400, 600 and 800 mm depths. The longer probes were installed in the Kenilworth/Bainsvlei ecotope. The six sensors are positioned at 200, 400, 600, 800, 1000 and 1200 mm depths. The probes installed in the field were placed as shown in Figures 5.1 and 5.2. The first probe installed on the ridge, the second installed in the furrow 500 mm away from the ridge and the third probe installed on the runoff strip, a 1000 mm away from the second probe. Probes were installed in the middle of the one meter extended RSL sections. The probes were programmed to take measurement at an interval of one hour. When computing daily change in soil water content, the measurements at a specific hour of the day (6:00 AM) were considered.

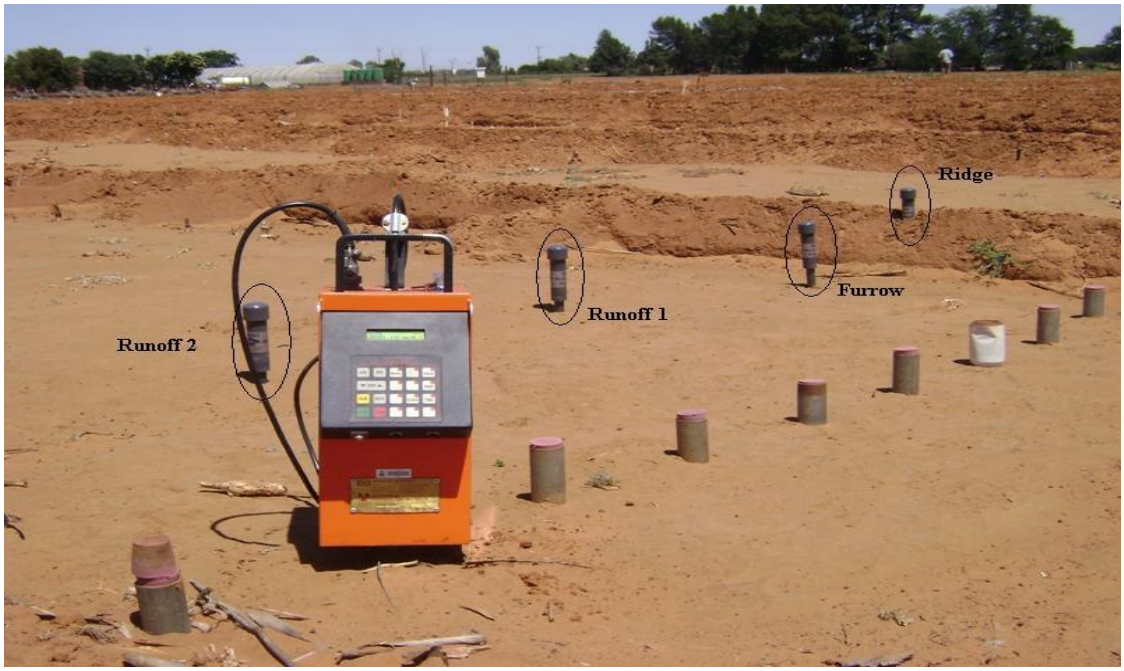

Figure 5.2 DFM probes installed at different sections of the micro-landscape created by IRWH.

The soil water content was monitored from 08 November 2009 up to 27 May 2010 and 05 November 2009 up to 08 June 2010, for Paradys/Tukulu and Kenilworth/Bainsvlei ecotopes, respectively. Distinct drying cycles were identified for each ecotope. These drying cycles were rain free days following a rainy day. The choice of the rain free days simplifies the computation of soil water evaporation as the change in soil water content between consecutive days. Three drying cycles were identified for the Kenilworth/Bainsvlei ecotope; viz. 17 to 23 February, 25 February to 2 March and 6 to 17 April 2010. For the Paradys/Tukulu ecotope the following three drying cycles were identified: 19 November to 27, 2009; April 06 to 14, 2010 and May 16 to 26, 2010.

The Es for each section of the micro-landscape was determined from the measured soil water change. The cumulative Es obtained for each micro-landscape section was plotted against the square root of time. A linear function was fitted to the data. The slope of this line represents the α-value of Ritchie (1972).

5.2.4. Statistical analysis and tools employed

5.2.4.1. Comparison of micro-landscape sections

5.2.4.1.1. Es on the micro landscape sections of the standard basin to RSL ratio

The cumulative Es values for the days of the drying cycles were plotted against the square root of time to show the linear relationship they depict. To obtain Ritchie's α-value this linear relationship was forced to have a zero intercept. This was done for the four sections of the micro-landscape. Graphpad's Prism 5 (GraphPad Software Inc., 2007) linear regression was used to evaluate this relationship between the cumulative evaporation and the square root of time. The same statistical package was used to assess slope homogeneity, which is equivalent to analysis of covariance (ANCOVA), between the regression lines (Zar, 1984).

5.2.4.1.2. Soil water and temperature comparison

The soil water content and temperature for the top horizon over different section of the micro-landscape were compared by employing ANOVA. Two -factor ANOVA without replication was used (Zar, 1984). For the soil water comparison a 5-day drying cycle (April 6 – 10, 2010) was selected. The two factors used in ANOVA were measurement days and the different sections of the micro-landscape. In the case of soil temperature comparison, the two factors were drying cycle and the different sections of the micro-landscape. These analyses were conducted by employing the data analysis tool pack in Excel.

5.2.4.1.3. Factors influencing Es

The different sections of the micro-landscape induced by IRWH were used as the units for the linear modelling in influencing the slope of the relationship of cumulative evaporation versus time. The slopes (α-values) for each unit were then related to different parameters that can influence soil water evaporation. The parameters considered were soil water content at the start of the drying cycle, average reference evaporation, RSL and average soil temperature. Stepwise regression was conducted to determine the importance of these factors in influencing the α-values. The stepwise regression takes one parameter

at a time and include it on the model, only if it is significant at 85% probability (α = 0.15). Thus, the summary of this exercise shows only the parameters that were significant at this level. The stepwise regression was conducted on SAS software (SAS Institute Inc., 2006).

5.2.4.1.4. Sensitivity analysis for slope variation

To observe the impact of using one slope value or different slope value for the sections of the micro-landscape, sensitivity analysis of predicted Es was conducted. This analysis was conducted by gauging the percentage difference of the Es predicted by a common slope for the whole plot from the scenarios in which separate slope was used for each section. This percentage comparison was done in Excel.

5.2.4.2. Es on the different basin to runoff ratios

A basin to RSL ratio of 1:2 has been used as the standard IRWH practice. Studies are underway to quantify the optimum ratio for dryland (Tesfuhuney, 2012) and irrigation-supplemented (Mavimbela, 2012) IRWH system in the Central part of South Africa. RSLs of 1 and 3 m are proposed as possible alternatives. To investigate the effect of adopting this change on the evaporation observed from the IRWH field, the spatially averaged evaporation of the three ratios were compared. To spatially average the cumulative evaporation, the evaporation measured for each section of the micro landscape was first converted into per unit of length they represent. Then evaporation for every unit length was added and divided by the total length to get the average. Statistical comparison was conducted by employing analysis of variance (ANOVA). Since the experiment was not replicated, two-factor ANOVA without replication was used (Zar, 1984). The two factors were: the drying cycle and the basin to RSL ratio. Excel's data analysis tool pack was used for the statistical analysis.

5.3. Results and discussion

5.3.1. Comparison of micro-landscape sections (standard IRWH)

5.3.1.1. Cumulative Es process

The process of cumulative evaporation *versus* time (days$^{-0.5}$) for the different sections of the micro-landscape of the standard IRWH (1:2 ratio) system for both ecotopes during the three drying cycles is depicted in Figure 5.3. From the line-graphs it is clear that the furrow section consistently lost more water through Es than the other sections, irrespective of the ecotope. On the Kenilworth/Bainsvlei ecotope, the ridge section constantly follows the furrow section in the rank of losing water to Es. Water loss in both the first and second one-meter runoff strip sections follow interchangeably after the ridge section. On the Paradys/Tukulu ecotope the ridge section and the first one-meter runoff strip section follow second in rank to the furrow section, interchangeably. The second one-meter runoff strip consistently showed the lowest Es of all sections. From the above depictions of the cumulative evaporation versus time (Figure 5.3), general observation can be taken, but more tangible inferences can be drawn from the comparison of the slopes of the fitted regression lines as will be seen in the next section.

5.3.1.2. Ritchie's α-values

The α-values of Ritchie (1972) for the different sections of the micro-landscape for the two ecotopes are summarised in Table 5.1 (given in the pair-wise comparison). Considering the results of the Kenilworth/Bainsvlei ecotope reveal that α-values varied over the sections and for different drying cycles. The α-values ranged between 0.5 and 2.8 mm day$^{-0.5}$ over the three drying cycles. The ratios of the highest to the lowest α-values were 4.8, 1.9 and 2.6 for the first, second and third drying cycles, respectively. The statistical comparison as indicated by the P-values, which show that there was significant difference between the different sections of the micro-landscape (see comparison of all sections). The pair wise comparison indicated significant difference amongst micro-landscape sections; there were only two cases of none significance. Furthermore, the similarities observed on the pair-wise comparison were positional. This

means the similarities observed were sections of the micro-landscape positioned next to each other.

The result for the Paradys/Tukulu ecotope depicts the same trend of α-values variation. The α-values observed ranged between 1.6 and 7.0 mm $day^{-0.5}$ over the drying cycles. The values observed for this ecotope were higher compared to Kenilworth/Bainsvlei ecotope. The ratios of the highest to the lowest α-values were 2.4, 1.9 and 2.9 for the first, second and third drying cycles, respectively. The slope homogeneity comparison also showed that there was significant difference between the different sections of the micro-landscape. To further observe the difference among the different sections, pair-wise comparison was done (Table 5.1). This pair-wise comparison revealed that there was significant difference except in 7 cases. In those cases the similarity observed, as explained above, was positional.

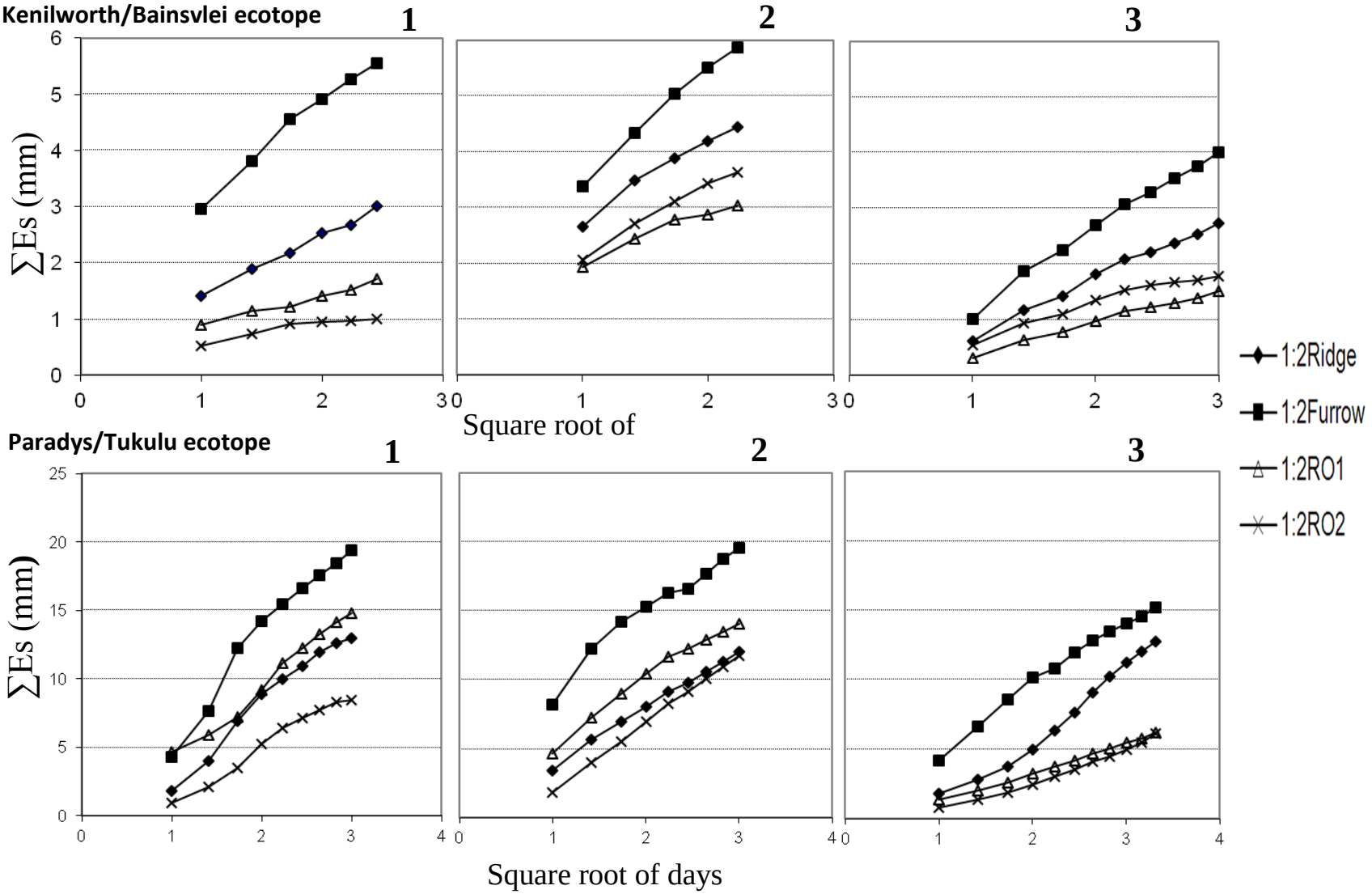

Figure 5.3 Cumulative evaporation (∑Es) observed (top 300 mm) in the different landscape sections of the standard IRWH during the three drying cycles for Kenilworth/Bainsvlei and Paradys/Tukulu ecotopes.

Table 5.1 Detail statistics on Ritchie's α-values for the different micro-landscape sections of the standard IRWH system for Kenilworth/Bainsvlei and Paradys/Tukulu ecotopes.

Ecotope	Comparison of micro-landscape sections	First drying cycle			Second drying cycle			Third drying cycle		
		Ritchie's α-values	F-value	P-value	Ritchie's α-values	F-value	P-value	Ritchie's α-values	F-value	P-value
Kenilworth/Bainsvlei	All		104.6	<0.001		23.3	<0.001		139.2	<0.001
	Ridge vs. Furrow	1.3 – 2.4	44.4	<0.001	2.2 – 2.8	15.7	0.007	0.9 – 1.3	56.7	<0.001
	Ridge vs. RO1	1.3 – 0.7	93.2	<0.001	2.2 – 1.5	12.2	0.013	0.9 – 0.5	131.8	<0.001
	Ridge vs. RO2	1.3 – 0.5	127.9	<0.001	2.2 – 1.8	1.0	0.347	0.9 – 0.6	76.1	<0.001
	Furrow vs. RO1	2.4 – 0.7	131.3	<0.001	2.4 – 1.5	66.9	<0.001	1.3 – 0.5	325.0	<0.001
	Furrow vs. RO2	2.4 – 0.5	161.5	<0.001	2.4 – 1.8	37.0	0.001	1.3 – 0.6	218.5	<0.001
	RO1 vs. RO2	0.7 – 0.5	9.5	0.015	1.5 – 1.8	10.3	0.018	0.5 – 0.6	0.0	0.933
Paradys/Tukulu	All		14.6	<0.001		3.2	0.038		90.1	<0.001
	Ridge vs. Furrow	4.3 – 6.6	7.0	0.020	4.0 – 7.0	6.1	0.027	3.4 – 4.7	2.2	0.1577
	Ridge vs. RO1	4.3 – 4.8	0.4	0.514	4.0 – 4.9	2.9	0.113	3.4 – 1.8	138.7	<0.001
	Ridge vs. RO2	4.3 – 2.7	17.8	<0.001	4.0 – 3.6	43.0	<0.001	3.4 – 1.6	108.0	<0.001
	Furrow vs. RO1	6.6 – 4.8	10.6	0.006	7.0 – 4.9	1.3	0.271	4.7 – 1.8	187.9	<0.001
	Furrow vs. RO2	6.6 – 2.7	32.5	<0.001	7.0 – 3.6	0.3	0.575	4.7 – 1.6	129.0	<0.001
	RO1 vs. RO2	4.8 – 2.7	17.5	<0.001	4.9 – 3.6	1.4	0.256	1.8 – 1.6	2.5	0.130

5.3.1.3. Factors influencing Es

5.3.1.3.1. Soil temperature comparison

The above statistical results showed that there was difference in the cumulative evaporation observed over different micro-landscape sections of IRWH. The difference in Es can be explained by the basic drivers of evaporation, i.e. the supply of heat, vapour pressure gradient, and supply of water (Hillel, 1982). Generally no major difference in the intercepted radiation as well as vapour pressure gradient is expected between the runoff, furrow and ridge areas. The average soil temperatures during the three drying cycles across the different sections were plotted in Figure 5.4. The statistical comparison to check if there was any difference in thermal conditions of the surfaces of these sections showed there was significant difference at P-value of 0.05 (Table 5.2). The result indicates the temperature differences observed both for different sections and different drying cycles were significant. Nevertheless, there was no consistent relationship between observed surface temperature and evaporation. In other words, the surface temperature ranking for the sections does not match that of evaporation. Hanks *et al*. (1961) are of the opinion that if all other environmental conditions are the same, evaporation is directly proportional to soil temperature. Nevertheless, they assert that under field conditions where there is much variation with other concurrent factors and other factors are limiting the process the relationship is not direct. This means the limiting factors can mask the direct effect temperature has on evaporation. This point can be clearly observed in that although there is consistency in the temperature levels between the drying cycles, the response for the different section are not the same for the two soils. From Figure 5.4 it can be seen that it is runoff-1m that had highest temperature for the Kenilworth/Bainsvlei ecotope, while for the Paradys/Tukulu ecotope it was the furrow.

Table 5.2 Summary of statistical comparison of surface temperature over different sections and drying cycles.

Factors	Kenilworth/Bainsvlei ecotope		Paradys/Tukulu ecotope	
	F-value	P-value	F-value	P-value
Drying cycles	1059.3	<0.001	650.6	<0.001
Micro-landscape sections	26.8	<0.001	23.1	0.001

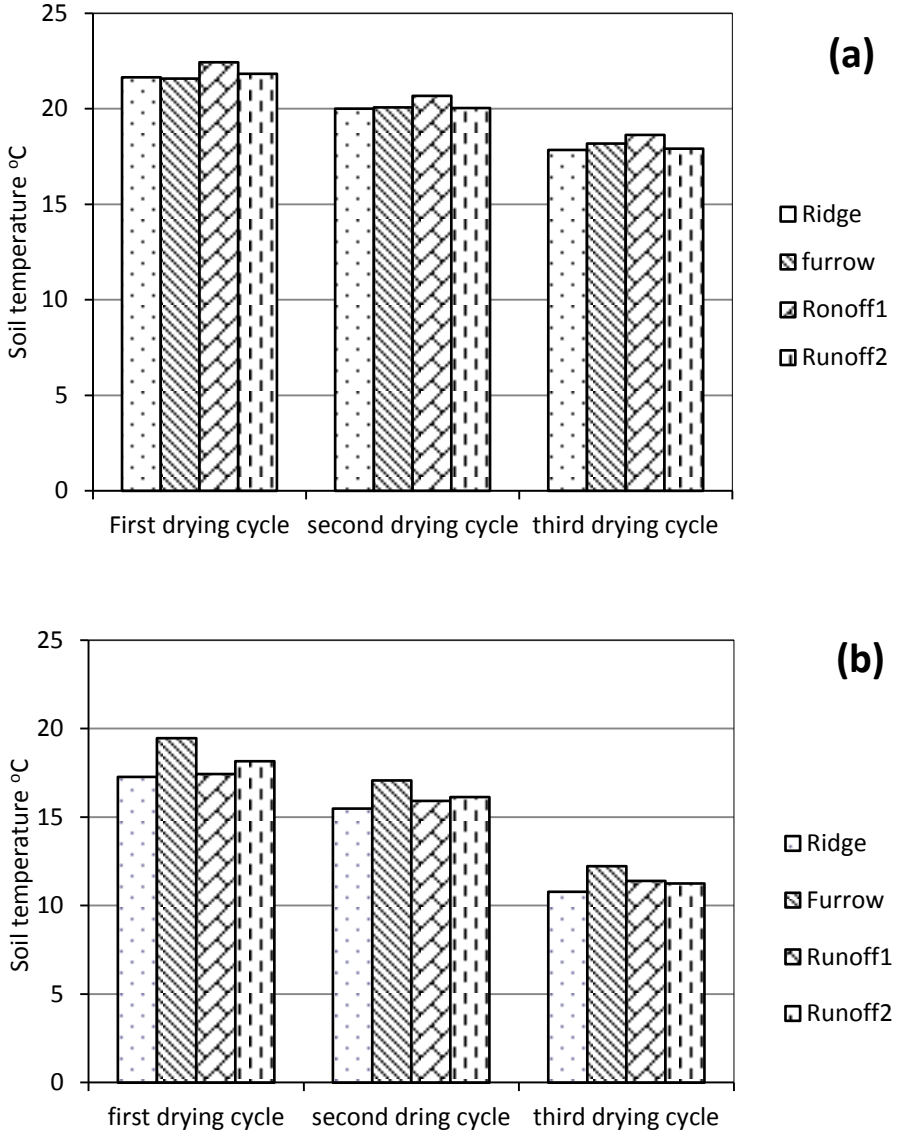

Figure 5.4 Average soil surface temperature during the drying cycles on the (a) Kenilworth/Bainsvlei ecotope and the (b) Paradys/Tukulu ecotope.

The above assumption, no significant atmospheric influence, is further strengthened by the fact that the first stage of evaporation spans only for a very short period in semi-arid climates (Daamen *et al*., 1995; Hoffman, 1997; Suleiman & Ritchie, 2003). It is only in the first stage of evaporation that the atmospheric factors exhibit a controlling role (this can be different during winter season) (Daamen *et al*., 1995). This disqualifies the deterministic role of vapour gradient and supply of heat. Thus the difference will be mainly coming from the supply of water. Kerridge *et al*. (2008) describe evaporation

from soil surface as being affected by canopy shading and availability of water. In the case of this experiment canopy shading is absent and shading that can be generated by the IRWH tillage structures is insignificant given the height and the east-west orientation of the structures. As a result, water available for evaporation greatly determined the amount of evaporation from a given soil. This contention is strengthened by the observed fact that in many instances the evaporation was higher on the furrow and sections bordering the furrow. For objective comparison of the factors influencing evaporation from different sections of the micro-landscape, Section 5.3.1.3.3 deals with weighting the effect of the factors.

5.3.1.3.2. Soil water comparison

The inference given above relating soil water evaporation and soil water content is based on the design of the IRWH system. The system is designed to concentrate runoff into the furrows which is a sink as far as runoff is concerned and this yields a variation in soil water content across the micro-landscape. The statistical comparison of water content across the different sections of the micro-landscape showed that there was significant difference (Table 5.3). The result also showed that the water content was significantly different with the consecutive days of the drying cycle. The result was consistent for both ecotopes.

Table 5.3 Summary of statistical comparison of soil water content over different sections and days after rain.

Factors	Kenilworth/Bainsvlei ecotope		Paradys/Tukulu ecotope	
	F-value	P-value	F-value	P-value
Days after rain	19.9	<0.001	3.7	0.03
micro-landscape sections	29.2	<0.001	3.6	0.04

The water content comparison revealed that dynamics of water is not one dimensional. The spatial variation of soil water content across the different sections implies that there was matric potential gradient. This matric gradient drives the movement of water in the soil, which is known as redistribution. This indicates that the soil water change observed in the top horizon of the furrows was not only through evaporation but also through

redistribution to the adjacent sections having lower water potential. This means the furrow which was a sink for IR_{off} also acted as a source for evaporation and redistribution. Such observation highlights the complexity of water dynamics during evaporation with regard to the route followed. Thus, there is a need for further study to investigate the rout and significance of such water movement either by intensive measurement or using 2-dimensional hydraulic model. Nevertheless, it must be stressed that the effect of such redistribution is significant only at higher soil water potential. Bresler *et al*. (1969) found that allowing time for redistribution resulted in lower evaporation compared to evaporation and redistribution happening together. However, under field conditions both are bound to happen together.

5.3.1.3.3. Weighting the factors that influence evaporation amount

The results on the step wise regression of parameters that might influence soil water evaporation (RSL, initial soil water content, average soil temperature and average reference evaporation) are summarized in Table 5.4. As indicated in the material and methods section, only the parameters that were significant at P-value of 0.15 were included into the model. Based on the R^2 results it is clear that soil water content has a bigger weight in determining Ritchie's α-values. The average reference evaporation had achieved the required level of significance for the Paradys/Tukulu ecotope, but not for the Kenilworth/Bainsvlei ecotope. This difference can be explained by the wider difference in average reference evaporation observed for the different drying cycles at the Paradys/Tukulu ecotope. This is mainly because the first drying cycle was in November (summer) and the last one in May (end of summer). The observations for the Kenilworth/Bainsvlei ecotope were taken between February and April, when no wide difference in evaporative demand occurred. The RSL and average soil temperature variables did not achieve the required level of significance to be included into the regression model.

Table 5.4 Summary of stepwise regression analysis for alpha-value determination.

Step	Kenilworth/Bainsvlei ecotope				Paradys/Tukulu ecotope			
	Variable Entered	Partial R^2	Model R^2	Pr > F	Variable Entered	Partial R^2	Model R^2	Pr > F
1	Water content	0.36	0.36	0.001	Water content	0.40	0.40	0.008
2					Average reference evaporation	0.16	0.56	0.046

The coefficient of determination values obtained for the models in both ecotopes were not high enough that a model based on the considered parameters could be proposed for predicting Ritchie's α-values. Nevertheless, the weights assigned to each variable considered reveal the importance of each factor in influencing Ritchie's α-value obtained on different sections of the micro-landscape of IRWH. The finding that soil water content had a larger influence in determining the α-value strengthens the deductions made in the previous section based on the requirement of soil water evaporation described by Hillel (1982). This agrees with findings of Bonsu (1997). He found that α-value showed positive and significant ($p = 0.001$) correlation with soil water content. The other significant factor observed was the influence of the atmospheric demand. This agrees with the finding of Boesten & Stroosnijder (1986). They showed that Ritchie's α-value is volatile over varying atmospheric demand and proposed a more stable Beta value for prediction of the second stage evaporation.

5.3.1.4. Sensitivity analysis for slope change

Table 5.1 shows the range of values the slope can assume under a given size variation and a drying condition. To appreciate the statistical differences observed, sensitivity analysis was done within the range of slope variation observed for the Kenilworth/Bainsvlei ecotope. Such analysis was done for the variation observed during the first drying cycle of the standard 1:2 plot in the Kenilworth/Bainsvlei ecotope. The result of this sensitivity analysis is presented in Table 5.5. This table shows the cumulative evaporation calculated by the empirical linear relationship between cumulative evaporation and square root of

time. The scenarios considered were: a single slope was adopted for the whole plot and a slope being computed for each section separately. The result showed that when a single slope value was adopted for the whole plot, the cumulative evaporation would be comparable to the one observed for the ridge, only bringing a 5% difference. This slope would under predict the evaporation from the furrow by 100%. On the contrary it would over predict the evaporation from the runoff area at least by 40%.

Table 5.5 Sensitivity analysis of slope variation across different sections of the micro-landscape.

	Whole plot	1:2Ridge	1:2Furrow	1:2RO1	1:2RO2
slope	0.93	1.07	1.80	0.54	0.33
y-intercept	0.56	0.35	1.27	0.35	0.25
Cumulative evaporation values predicted for six days	1.49	1.42	3.06	0.89	0.58
	1.88	1.87	3.81	1.11	0.72
	2.17	2.21	4.38	1.28	0.82
	2.42	2.49	4.86	1.42	0.91
	2.64	2.75	5.28	1.55	0.99
	2.84	2.97	5.66	1.66	1.06
percentage difference		5%	99%	-41%	-63%

From the above result of sensitivity analysis, it is obvious that the heterogeneous nature of the IRWH micro-landscape does not lend itself to homogenous treatment of the surface in predicting evaporation. This would have an implication for the homogenous model use over the whole field. For instance, the use of single alpha-value in characterizing an ecotope (Hensley *et al*., 2000; Botha *et al*., 2003) can be representative only for the surface conditions of the same nature. The flat surface from which the evaporation curve was determined might represent the flat surface strip of the IRWH but for better prediction, field determined slope values are required. For evaporation characteristics to be representative of a given system it should be determined under the same tillage condition (Boesten & Stroosnijder, 1986).

5.3.2. Effects of different basin to runoff strip length ratios on evaporation

Spatially averaged cumulative evaporation observed on different basin to RSL ratios are presented in Table 5.6. The cumulative evaporation amounts were collated from the evaporation observed over different sections of the micro-landscape of IRWH. The analysis of variance done on these value showed that there was no significant difference ($\alpha = 0.05$) between the evaporation observed on different basin to runoff ratios.

Table 5.6 Five day cumulative evaporation on different basin to RSL ratio.

Ecotope	Drying cycle	Basin to RSL ratio		
		1:1	1:2	1:3
Paradys/Tukulu	1	9.9	8.0	6.7
	2	8.3	8.4	8.8
	3	8.3	4. 4	6.6
Kenilworth/ Bainsvlei	1	1.9	2.2	1.7
	2	4.6	4.0	4.1
	3	5.0	5.3	4.1

The statistical non-significance found for the different ratios defies the hypothesis that there would be difference in the evaporation observed with the addition or subtraction of 1 meter of the runoff strip to the standard 1:2 ratio. This could be due to the fact that the major contributor to evaporation was the basin strip (ridge and the furrow) and this remains to be the same for all ratios. This finding is applicable only to a fallow period when the soil surface is kept free from plants to conserve soil water. There is a research need for accurate quantification of evaporation difference on different basin to RSL ratios during growing period. Studies done on the influence of row spacing on evaporation indicate that the wider the spacing the greater the evaporative loss (Daamen *et al.*, 1995; Sharrat & McWilliams, 2005). Yunusa *et al*. (1994), however, show that row spacing failed to bring change on evaporation for spring wheat grown on a Mediterranean environment. This accentuates the need for further research to determine the influence on any given ecotope.

5.4. Conclusions and recommendations

IRWH micro-landscape does create a significant variation in the evaporation observed from the field and thus the whole field cannot be taken as uniform piece of land. This will have an implication in modelling evaporation over an IRWH field, in which separate models need to be adopted for the different sections of the micro-landscape. Despite the significant difference observed among the different sections of the micro-landscape, there was no difference on the spatially averaged evaporation in the different basin to RSL ratios. It is recommended that comparison of evaporation from different ratios be conducted during growing period, when the presence of plants would create different micro-climate.

References

Bennie, A.T.P., Strydom, M.G. & Vrey, H.S., 1998. The application of computer models for agricultural water management on ecotope level [Afr.]. Water Research Commission report No. 625/1/98, Pretoria, South Africa.

Boesten, J.J.T.I. & Stroosnijder, L., 1986. Simple model for daily evaporation from fallow tilled soil under spring conditions in a temperate climate. *Neth. J. Agr. Sci.* **34**:75–90.

Bonsu, M., 1997. Soil water management implication during the constant rate and the falling rate stages of soil evaporation. *Agric. Water Manage.* **33**:87–97.

Botha, J.J., van Rensburg, L.D., Anderson, J.J., Hensley, M., Macheli, M.S., van Staden, P.P., Kundhlande, G., Groenewald, D.C. & Baiphethi, M.N., 2003. Water conservation techniques on small plots in semi-arid areas to enhance rainfall use efficiency, food security, and sustainable crop production. Water Research Commission report No. 1176/1/03, Pretoria, South Africa.

Bothma, C.B., 2009. In-field runoff and soil water storage on duplex soils at Paradys Experimental Farm. M.Sc. thesis University of the Free State, Bloemfontein, South Africa.

Bresler, E., Kemper, W.D. & Hanks, R.J., 1969. Infiltration, redistribution, and subsequent evaporation of water from soil as affected by wetting rate and hysteresis. *Soil Sci. Soc. Am. J.* **33**:832–840.

Daamen, C.C., Simmonds, L.P. & Sivakumar, M.V.K., 1995. The impact of sparse millet crops on evaporation from soil in semi-arid Niger. *Agric. Water Manage.* **27**:225–242.

GraphPad Software Inc., 2007. *Prism 5 statistics guide*. Graphpad Software Inc., San Diego CA, www.graphpad.Com.

Hanks, R.J., Bowers, S.A. & Bark, L.D., 1961. Influence of soil surface conditions on net radiation, soil temperature and evaporation. *Soil Sci*. **91**(4):233–238.

Hensley, M., Botha, J.J., Anderson, J.J., van Staden, P.P. & du Toit, A., 2000. Optimizing rainfall use efficiency for developing farmers with limited access to irrigation water. Water Research Commission report No. 878/1/00, Pretoria, South Africa.

Hillel, D., 1982. *Introduction to Soil Physics*. Academic press, New York.

Hoffman, J.E., 1997. Quantifying and prediction of evaporation from the soil surface under dryland crop production [Afr.]. Ph.D. thesis University of the Free State, Bloemfontein, South Africa.

Kerridge, B., Hornbuckle, J.W., Christen, E.W. & Faulkner, R.D., 2008. Soil spatial variability effects on irrigation efficiency. Irrigation Australia Conference. 20 - 22 May 2008.

Mavimbela, S.S., 2012. The Merging of micro-flood irrigation with in-field rainwater harvesting. Ph.D. thesis University of the Free State, Bloemfontein, South Africa.

Mzezewa, J. & van Rensburg, L.D., 2011. Effects of tillage on runoff from a bare clayey soil on a semi-arid ecotope in the Limpopo Province of South Africa. *Water SA* **37**:165–172.

Ritchie, J.T., 1972. Model for predicting evaporation from a row crop with incomplete cover. *Water Resour. Res.* **8**(5):1204-1211.

SAS Institute Inc., 2006. *Administering SAS® Enterprise Guide® 4.1*. Cary, NC: SAS Institute Inc.

Sharratt, B.S. & McWilliams, D.A., 2005. Microclimatic and rooting characteristics of narrow-row versus conventional-row corn. *Agron. J.* **97**:1129–1135.

Suleiman, A.A. & Ritchie, J.T., 2003. Modeling soil water redistribution during second-stage evaporation. *Soil Sci. Soc. Am. J.* **67**:377–386.

Tesfuhuney, W.A., 2012. Optimizing runoff to basin area ratios for maize production with in-field rainwater harvesting. Ph.D. thesis University of the Free State, Bloemfontein, South Africa.

Van Rensburg, L.D., Bothma, C.B., Fraenkel, C.H., Le Roux, P.A.L. & Hensley, M., 2012. In-field rainwater harvesting: mechanical tillage implements and scope for up-scaling. *Irrig. and Drain.* 61(S2):138-147.

Yunusa, I.A.M., Belford, R.K., Tennant, D. & Sedgley, R.H., 1994. Row spacing fails to modify soil evaporation and grain yield in spring wheat in a dry Mediterranean environment. *Aust. J. Agr. Res.* **44**(4):661–676.

Zar, J.H., 1984. *Biostatistical analysis*. (Second edition) Englewood Cliffs, NJ: Prentice-Hall.

6. Modelling in-field runoff for different basin to runoff strip length ratios under in-field rainwater harvesting system

Abstract

In-field rainwater harvesting plays a pivotal role in crop production in semi-arid zones. The quantification of the in-field runoff parameter determines what proportion of the received rainfall could be harvested as run-on into the basins. The objectives of this study were: (i) to develop an empirical model and calibrate the Morin and Cluff (MC) runoff model for the Kenilworth/Bainsvlei and Paradys/Tukulu ecotopes (ii) to validate these models and compare the performance of the models. Runoff measured from the runoff strips of different basin to runoff strip length (RSL) ratios were used to calibrate and validate the models. Statistical performance evaluation parameters: RMSE, MAE, D-index and R^2 were used to measure the performance of the two models. For the Kenilworth/Bainsvlei ecotope the RMSE average of the three basin to RSL ratios were 5.7 and 6.8 mm for empirical runoff model and the MC model, respectively. These values were 4.4 and 7.8 mm for the Paradys/Tukulu ecotope with the empirical and MC runoff models, respectively. The comparison of the two models of in-field runoff prediction revealed that the empirical runoff model gave better prediction on both ecotopes.

Key words: runoff, runoff strip length, modelling, IRWH

6.1. Introduction

Comparison of crop yields under semi-arid environments indicated that the in-field rainwater harvesting (IRWH) is better than conventional practices (Hensley *et al*., 2000; Botha, 2006). These yield improvements range from 30% to 50% (Anderson, 2007). The observed yield increment is partly attributed to the extra water made available by harvesting the runoff. These attractive improvement results were obtained from experimental plots. The natural response to such success stories is wider implementation. Botha *et al*. (2007) reports the adoption of IRWH practice on homestead garden, in rural villages around Taba Nchu, South Africa. Such adoption is based on experiments and demonstrations conducted in these areas. In taking this adoption process to the next level, obviously there is a need for up-scaling, i.e. the transfer of IRWH practice from experimental plots and homestead gardens to crop fields. To achieve this, field level experiments need to be conducted. Conducting field experiments can be costly, time and energy consuming. Modelling can help to alleviate the difficulty incurred in conducting field experiments. Although there are many surface features that differentiate the IRWH system from conventional system, the major differentiating factor is the additional water harvested. Thus, water balance based modelling can capture the uniqueness of the system.

Modelling soil water balance is central in planning and developing optimized agricultural systems (Hensley *et al*., 1993; Zere *et al*., 2005). This importance is amplified more in arid and semi-arid areas where water availability is the limiting factor. Under dryland farming in arid and semi-arid areas, the little rainwater available must be directed to the beneficial use of plant production. To develop an optimized plant production system, the components of the water balance equation need to be quantified accurately. Direct measurement is a good way of collecting quantitative data. However, conditions exist in which direct measurement of the soil water balance components is costly and/or difficult. Under such conditions, application of models to get the best estimate of the components is the viable option (Meng & Quiring, 2008). The application of models enables us to get good estimates of the components of the water balance like drainage, evaporation and runoff instead of measuring them directly (Jalota *et al*., 2000). For an IRWH system

during a fallow season, runoff and especially evaporation are the paramount processes regulating the water that can be stored in the profile.

Modelling rainfall-runoff has been widely practiced to simulate the effect and fate of rainfall. Such simulations are important for predicting the runoff volumes and peak runoff rates, which are basic requirements in planning conservation measures (Onyando & Sharma, 1995). Modelling runoff in designing rainwater harvesting being a requisite, Young *et al.* (2002) provides a list of researches done to simulate runoff from the runoff producing area (RPA). Such simulations help to predict the amount of water that can be collected in the runoff receiving area (RRA).

Locally, studies conducted in the semi-arid areas of central South Africa have identified models for use in predicting runoff for IRWH (Hensely *et al*., 2000; Botha *et al.*, 2003; Anderson, 2007). Anderson (2007) has compared the performance of different models for runoff prediction, and reported the model and condition in which runoff was predicted with acceptable level of accuracy. The Morin & Cluff (1980) [referred to as MC here after] runoff model was identified as the best model that performed well under different treatments of IRWH. Anderson (2007) has discussed further the performance of this model by taking instances where the model predicted well and instances where it failed to do so. This model was also used by Zere *et al*. (2005) and Welderufael (2006) to predict runoff and investigate a scenario of IRWH application. The MC runoff model is built on the Morin & Benyamini (1977) infiltration equation. This equation is a Horton (1936) type equation but it adds intensity and surface particle strength as important role players. Morin & Benyamini (1977) assert that reduction in infiltration is affected more by surface crusting than it does by water regime change. The inclusion of a parameter representing the soil surface particle strength, gives this model an edge for use under IRWH where surface crusting is the prevalent feature of the runoff strip.

The objective of this chapter is to:

i. Develop an empirical runoff prediction model for the Kenilworth/Bainsvlei and Paradys/Tukulu ecotopes.
ii. Calibrate the MC runoff model for the Kenilworth/Bainsvlei and Paradys/Tukulu

ecotopes.

iii. Validate the developed and calibrated models; and compare the performance of the models.

6.2. Materials and methods

The modelling exercise was done for two ecotopes: the Kenilworth/Bainsvlei and the Paradys/Tukulu ecotopes. The details of the climate and soil information pertaining to both ecotopes are provided in Chapter 1. The methods employed in collecting data and the modelling exercises are described below.

6.2.1. Measurement of runoff

The measured runoff amounts were of two types (Table 6.1). The first set was runoff amounts measured from simulated rain events. A Hofrey rainfall simulator was used to generate the designed rainfall events. The Hofrey rainfall simulator setup is described in Figure 3.1. The detail of runoff measurements from the simulated rainfall events is discussed in Section 3.2.2. The runoff amount measured in this setup represented an area of 1 m by 1 m. The use of these data with regard to the different runoff strip length (RSL) is discussed in the next section.

The second set of runoff data collected were from natural rainfall events. Runoff plots were prepared within the IRWH plots. These runoff plots were constructed by erecting galvanized iron sheets (Figure 6.1). These sheets were inserted into the soil 200 mm deep giving it anchorage and another 200 mm stood out forming the border of the runoff plots. The runoff plots had a width of 1700 mm and varying length depending on the basin to RSL ratio of the plots. Thus there were three lengths of 1000, 2000 and 3000 mm, representing 1:1, 1:2 and 1:3 basin to RSL ratios, respectively. At the down-slope end of these plots gutters were fitted to channel runoff into drums from which measurements were taken after rainfall events. Similar to the data from simulated rainfall events the runoff volume was converted to depth by dividing it by the surface areas of the plots.

Table 6.1 Rainfall event amounts and the generated runoff amounts for the Kenilworth/Bainsvlei and Paradys/Tukulu ecotopes.

Ecotope	Date	Rainfall (mm)	Runoff (mm)			Rainfall type
			1:1	**1:2**	**1:3**	
Kenilworth/Bainsvlei	Jun-09	30.9*	14.8	12.1	10.4	simulated
	Jun-09	30.9*	17.0	13.8	11.8	simulated
	Jun-09	30.9*	16.7	13.6	11.6	simulated
	2-Nov-09	10.0**	1.8	2.2	1.0	natural
	6-Nov-09	18.0**	3.6	7.8	12.8	natural
	9-Nov-09	12.0**	7.0	5.8	11.3	natural
	19-Nov-09	24.0**	10.3	11.7	22.2	natural
	10-Dec-09	13.7**	11.3	8.3	10.7	natural
	4-Jan-10	19.9**	0.7	1.2	1.6	natural
	20-Jan-10	10.6*	3.4	3.4	0.1	natural
	23-Jan-10	16.6*	12.7	7.4	8.4	natural
	24-Feb-10	61.9**	47.2	37.8	30.4	natural
	2-Mar-10	9.0*	1.4	1.2	1.3	natural
	20-Mar-10	18.8*	13.9	14.1	9.4	natural
	4-May-10	13.0*	3.4	3.4	0.1	natural
	13- May-10	14.3**	7.5	8.3	2.2	natural
Paradys/Tukulu	Oct-08	49.5*	14.0	15.6	17.0	simulated
	Oct-08	88.5*	46.0	54.4	61.7	simulated
	Oct-08	183.0*	119.0	142.9	163.7	simulated
	May-09	30.9*	17.9	20.3	22.4	simulated
	May-09	30.9*	15.0	16.9	18.4	simulated
	May-09	30.9*	19.4	22.1	24.5	simulated
	May-09	15.5*	5.4	5.2	5.0	simulated
	4-May-09	14.8**	3.8	3.4	2.5	natural
	5-May-09	15.0**	4.0	6.9	7.1	natural
	5-Nov-09	15.0**	2.2	1.1	0.6	natural
	19-Nov-09	50.0**	26.4	35.5	28.7	natural
	21-Dec-09	60.0**	28.0	36.0	38.6	natural
	1-Jan-10	20.0**	15.7	10.6	12.7	natural
	7-Jan-10	24.0**	11.8	12.2	14.9	natural
	8-Jan-10	27.0**	15.7	17.3	21.2	natural
	16-Feb-10	18.0**	6.7	9.9	12.7	natural
	18-Feb-10	8.0**	3.0	1.8	2.1	natural

* data used for calibration ** data used for validation

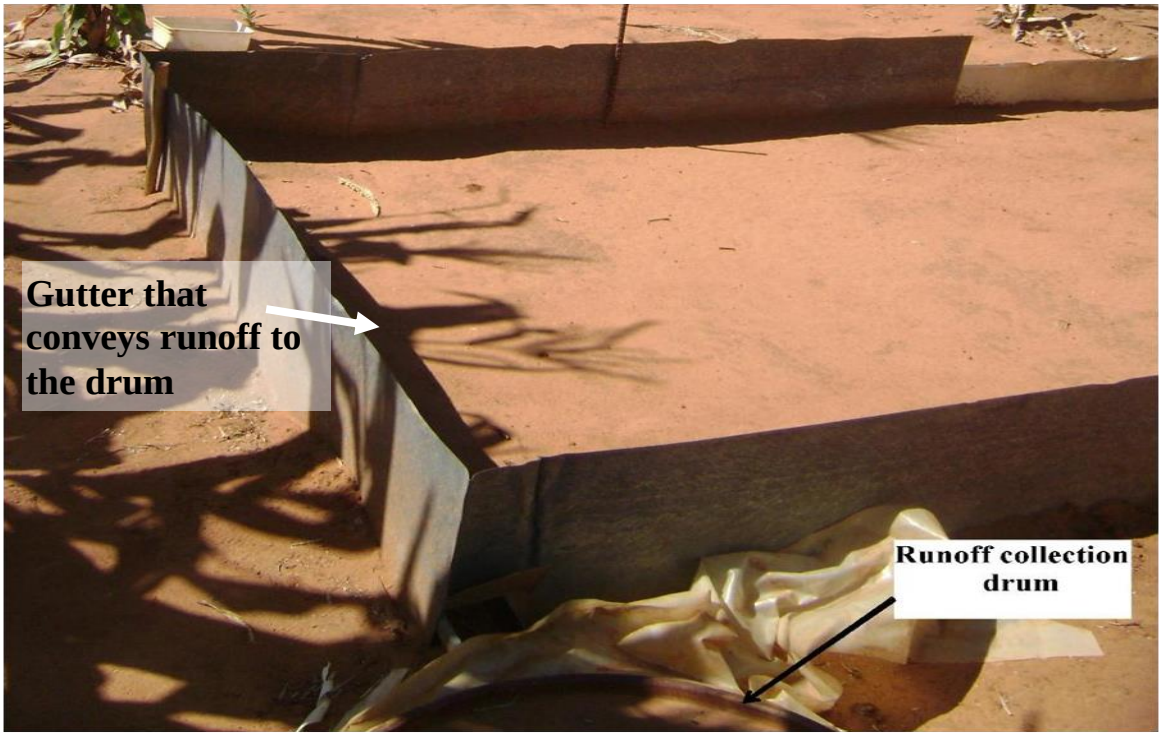

Figure 6.1 Illustration of the layout of a typical runoff plot in the field under IRWH.

6.2.2. Data selection for modelling

6.2.2.1. Paradys/Tukulu ecotope

For the Paradys/Tukulu ecotope, the collected runoff data was split into two sets. The first set was made up from 7 runoff events collected from simulated rainfall. The simulated rainfall events were of different amount and varying intensity patterns. Three simulations were taken from Bothma (2009) conducted on the same site. The simulations had 3 constant intensities, *viz*. 33, 59 and 120 mm hr^{-1}, which lasted for 90 minutes. These simulations were the result of 9 replications. Another 4 rainfall simulations conducted during 2009 were also used. These rainfall simulations had varying rainfall intensities, imitating a natural rainfall. These simulations were: the first set with high intensity arriving early during the rain events; the second set with the intensities displaying a normal distribution during the rain events; and the third set with constant intensity as in the case of Bothma (2009). These 3 simulations had a rainfall amount of 30.8 mm and duration of 70 minutes, collated from three replications. The fourth rainfall simulation was done with a varying intensity lasting for 1 hour and an amount of 15 mm.

The intensity variation was done every five minutes and the runoff amount was also recorded for the same 5 minute duration. There was an advantage with these artificial rain simulations, not only in that there was deliberate control of the application intensity but also that they enabled good record of infiltration rate with time.

The second set of data was made of 10 runoff events collected from natural rainfall events. This data was used for validation of the models which were calibrated by the first set. The rainfall events were received between May 2009 and February 2010. The amount of the rainfall events ranged from 8 to 60 mm.

6.2.2.2. Kenilworth/Bainsvlei ecotope

Similarly on the Kenilworth/Bainsvlei ecotope, runoff data collected from both simulated and natural rainfall events was used. Unlike the condition described above, the first set of data used for the calibration was made of runoff data collected from simulated and natural rainfall events. Three simulated rainfall events with amount of 30.8 mm, duration of 70 minutes and varying intensity patterns were used. In addition to these, 5 randomly selected runoff data sets collected from natural rainfall events were used for calibration. The second set was all made up from 8 runoff data sets collected from natural rainfall events. This set was used to validate the calibrated models. The rainfall events from which the runoff was collected ranged from 9 mm to 61.9 mm.

6.2.3. Runoff amount relation among the different basin to RSL ratios

The runoff amounts collected for each basin to RSL ratio were related by linear regression between each other to determine runoff amounts related for each RSL. This relation helped to replace data loss in cases of breakage of one runoff plot while the others were intact. Another instance this relationship was used was to convert the simulated runoff amounts, which were collected from a 1 m length, into the 2 and 3 m lengths.

6.2.4. Simulation of runoff

Simulation of runoff was done by considering two models. The first model was the development of an empirical model relating the rainfall and measured runoff amounts. This was done by fitting linear regression equations. The second model used was the MC model.

6.2.4.1. Calibration of MC model

To explain the parameters required during calibration, a brief description of the MC model is required. This model was developed based on the Morin & Benyamini (1977) infiltration equation. They divided storm duration into smaller time segments in a way that addresses the change of intensity over the storm duration. By applying the Morin & Benyamini (1977) infiltration equation for a given segment they came up with this equation:

$$F_i = I_F \Delta t_i + [(I_I - I_F)/(-\gamma P_i)]\,[exp(-\gamma D_i) - exp(-\gamma D_{i-1}) \quad (6.1)$$

Where:

F_i = rainwater amount infiltrated during time segment *i* (mm)

I_F = final infiltration rate of the soil (mm hr^{-1})

Δt_i = length of time segment *i* (hr)

I_I = initial infiltration rate of the soil (mm hr^{-1})

γ = soil surface particle strength

P = rainfall intensity (mm hr^{-1})

D_i & D_{i-1} = amount of rain (mm) received during time segment *i* and *i*-1 respectively

The runoff (R_i) for the time segment *i* is then given by:

$$R_i = D_i + SD_{i-1} - F_i - SD_{max} \quad (6.2)$$

Where:

SD_{i-1} = surface storage and detention (mm) sustained over segment *i*-1

SD_{max} = maximum surface storage and detention (mm)

The runoff for a rain storm is then given by integration of Equation 6.2 over the time segments. From the parameters that are given on Equations 6.1 and 6.2, the parameters γ and SD_{max} are determined in the process of calibration, while the remaining parameters are measured values.

6.2.4.2. Infiltration input parameters for the MC model

The first sets of rainfall events (type indicated on the last column of Table 6.1) were collected from simulated rain events and this provided a good picture on how infiltration and runoff fared with rainfall intensity and time. From the 5-minute runoff records obtained during rain event simulation, two important parameters of infiltration were obtained. Using these data the cumulative infiltration amount versus time was plotted (Figure 6.2). The power regression trend lines (Figure 6.2) provided the constants which are the parameters *a* and *b* of Kostiakov's infiltration model given below.

$$I_c = a*(t)^b \qquad (6.3)$$

Where

I_c = cumulative infiltration (mm)
t = time (minute)
a and b = empirical constants

The Kostiakov's infiltration rate is given by the following equation using the same constants.

$$I = a * b * (t)^{b-1} \qquad (6.4)$$

Where

I = infiltration rate (mm hr^{-1})

The parameters I_F and I_I are determined from the infiltration observed during rainfall simulation. By applying Equation 6.4, the I_I is determined as the rate for minute 1 and I_F as the rate for which rate difference between consecutive minutes become less than 0.1 (Welderufael, 2006). The infiltration equation developed following the above procedure for both ecotopes are given Figure 6.2. The infiltration rates (Table 6.2) were used in the calibration of the MC model.

Table 6.2 Initial and final infiltration values for the Kenilworth/Bainsvlei and Paradys/Tukulu ecotopes.

Infiltration parameter	Kenilworth/Bainsvlei		Paradys/Tukulu	
	Time	Value (mm hr^{-1})	Time	Value (mm hr^{-1})
initial	1 minute	42.4	1 minute	44.2
final	40 minute	9.1	37 minute	6.9

With the above input parameters (Table 6.2), the PutuRun software (Walker & Tsubo, 2003) which uses the MC runoff model was used to determine the runoff amounts for different scenarios of γ and SD_{max} values. The calibration is conducted to obtain best performance of the model as judged based on the criteria given by Wilmott (1981).

Both the empirical and the MC models were validated on independent data sets.

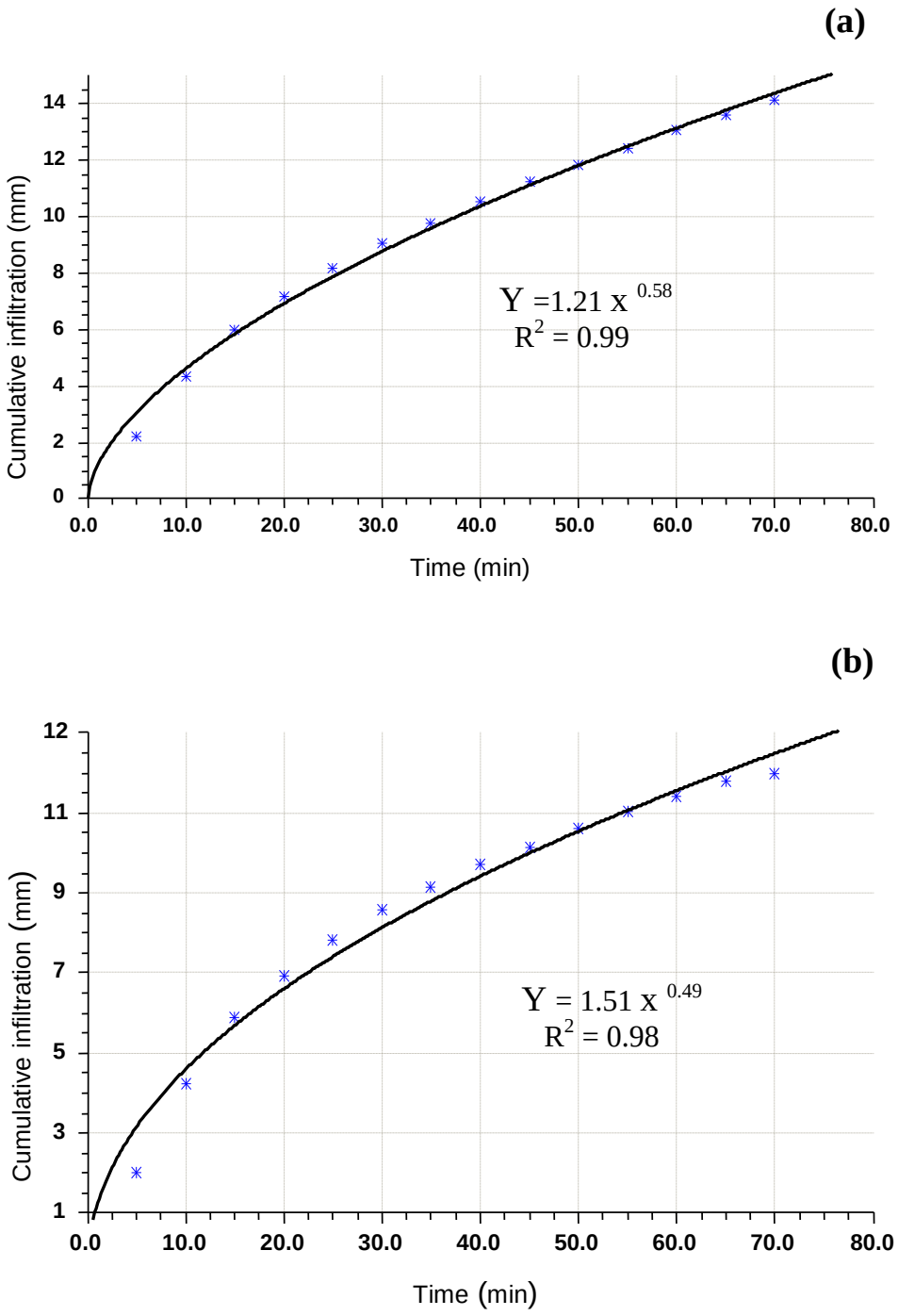

Figure 6.2 Cumulative infiltration plotted versus time with power regression line fitted (a) Kenilworth/Bainsvlei and (b) Paradys/Tukulu ecotopes.

6.3. Results and discussion

6.3.1. Development of empirical runoff model

The developed empirical relationships between the amount of rainfall and runoff generated for the Kenilworth/Bainsvlei ecotope are presented in Figure 6.3. The modelled linear equations are provided on the graphs. The coefficient of determination (R^2) presented along with the equations showed the goodness of fit. The R^2 for the three basin to RSL ratios were comparable which ranged from 0.76 to 0.81. Similar information is presented in Figure 6.4 for the Paradys/Tukulu ecotope. The linear models for this ecotope had an excellent goodness of fit (R^2 = 0.97). This was the same for the three basin to RSL ratios. The information provided on those graphs indicated only how the resulting models were representative of the data used to develop them. The statistical performance of the developed empirical models is given in Table 6.3. The parameters provided in Table 6.3 show the performance of the models on calibration data.

From Table 6.3 it can be seen that empirical models had good performance on the calibration data. The statistical parameters obtained for the Kenilworth/Bainsvlei ecotope showed there was good model performance on the calibration data. The mean error involved as indicated by the RMSE values ranged between 2.2 and 2.6 mm. The close to 1 values of D-index obtained also attested that there was good agreement between the measured and predicted for the three ratios. The small y-intercept values and the close to 1 values of the slope indicate that the prediction line lied close to the 1:1 line. The small RMSEs/RMSE ratios show that the systematic error introduced was small. The statistical parameters for the Paradys/Tukulu ecotope showed that mean error involved from the use of the models was relatively higher. The RMSE values ranged between 6 and 8.5 mm. This does not contradict the excellent goodness of fit described above from the graphs relating rainfall and runoff amounts. The RMSE was a bit exaggerated because of the exceptionally high rainfall event-amount used in the calibration data (data taken from Bothma, 2009). Nevertheless, the other parameters testified to the goodness of the performance. The D-index was 1 indicating good agreement. The close to 1 slope and close to zero values of y-intercept showed that the prediction lines run close to the 1:1 line [a line that shows perfect agreement between predicted and measured values].

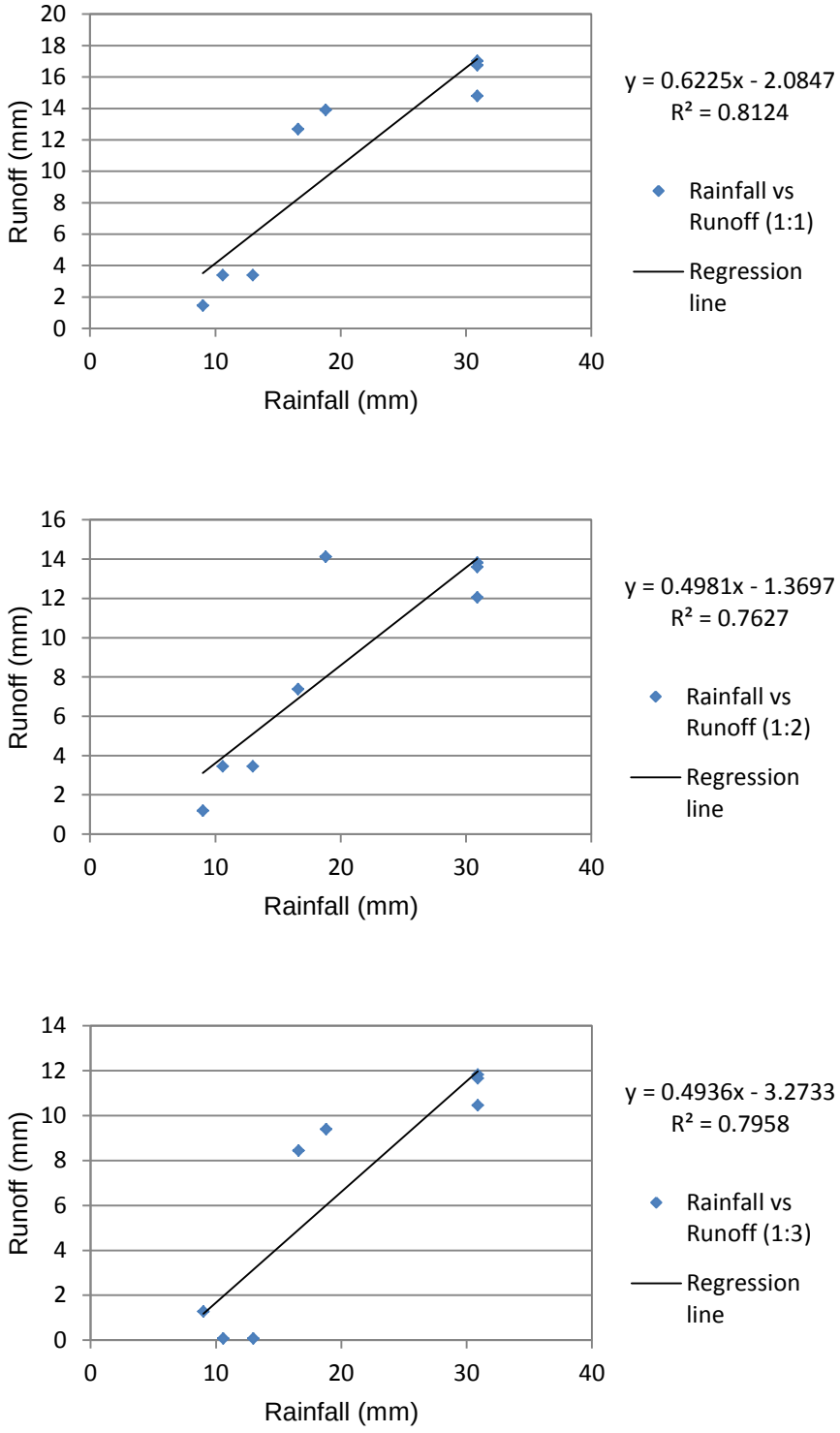

Figure 6.3 Relationship between rainfall and runoff amounts on the Kenilworth/Bainsvlei ecotope.

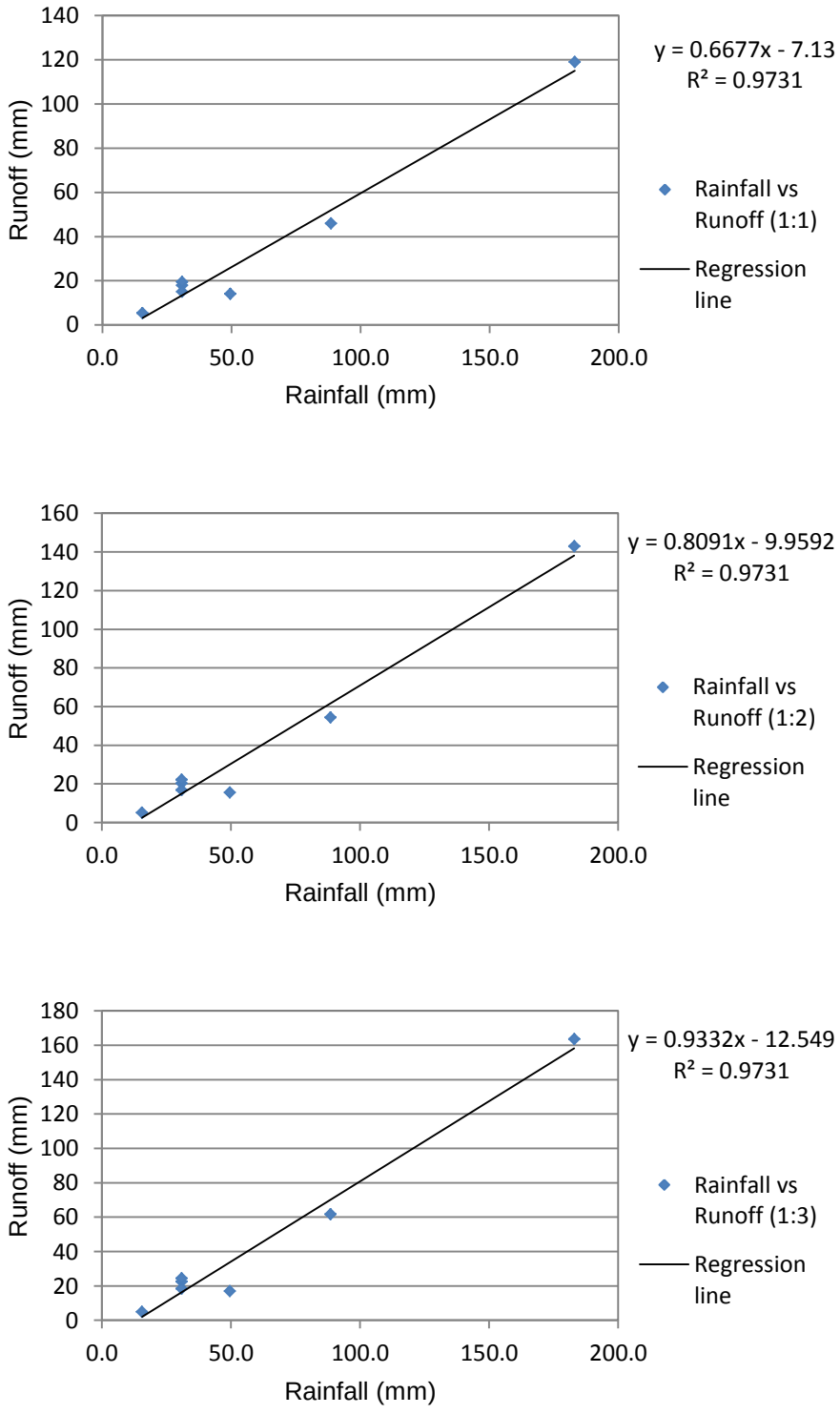

Figure 6.4 Relationship between rainfall and runoff amounts on the Paradys/Tukulu ecotope.

Table 6.3 Statistical performance of the empirical runoff models on the calibration data.

Statistical parameter	Kenilworth/Bainsvlei ecotope			Paradys/Tukulu ecotope		
	1:1	1:2	1:3	1:1	1:2	1:3
RMSE	2.650	2.461	2.215	6.021	7.296	8.415
RMSEs	1.149	1.199	1.001	0.989	1.200	1.381
RMSEu	2.388	2.149	1.976	5.939	7.197	8.301
MAE	2.178	1.653	1.748	5.110	6.193	7.142
R^2	0.812	0.763	0.796	0.973	0.973	0.973
D-index	0.947	0.929	0.941	0.993	0.993	0.993
slope (b)	0.812	0.763	0.796	0.973	0.973	0.973
Y-intercept (a)	1.955	2.050	1.356	0.911	1.068	1.203
RMSEs/RMSE	0.434	0.487	0.452	0.164	0.164	0.164

6.3.2. Calibration of MC

The MC model was calibrated for the Kenilworth/Bainsvlei and Paradys/Tukulu ecotopes using half of the data presented in Table 6.1 (indicated with single asterisk). The initial and final infiltration rate values presented in Table 6.2 were used as input for the model. The model was run with different combinations of soil surface particle strength (γ) and surface storage and detention values (*SD)*. For the Kenilworth/Bainsvlei ecotope the following γ values of 0.6, 0.6 and 0.7 mm^{-1} were found to give the best prediction for the 1:1, 1:2 and 1:3, respectively. The *SD* value of 1 mm gave best prediction for all three basin to RSL ratios. For Paradys/Tukulu the following surface particle strength (γ) values of 0.5 mm^{-1} for the 1:1 plot and 0.3 mm^{-1} for the 1:2 and 1:3 plots were found to give best prediction of runoff. The *SD* values of 5 mm for the 1:1 and 1:2 plots; and 6 mm for the 1:3 plot gave best predictions. The differences observed in the calibration variables (*SD* and γ) for the different plots were not very big so as to lose their physical meaning. The plots were considered homogenous except for the RSL difference. The fact that the observed difference was small was an assertion that plots were homogenous in terms of surface conditions and the physical meaning of the variable holds true for those plots. The statistical performance of the calibrated MC model is given in Table 6.4 for both ecotopes.

Table 6.4 Statistical performance of the MC runoff model on the calibration data sets for the Kenilworth/Bainsvlei and Paradys/Tukulu ecotopes.

Statistical parameter	Kenilworth/Bainsvlei ecotope			Paradys/Tukulu ecotope		
	1:1	1:2	1:3	1:1	1:2	1:3
RMSE	5.960	5.869	6.258	22.247	13.395	7.915
RMSEs	2.163	1.956	2.834	20.895	11.028	2.162
RMSEu	5.554	5.533	5.580	7.637	7.604	7.614
MAE	4.640	5.122	5.187	14.495	9.803	6.070
R^2	0.612	0.615	0.614	0.979	0.979	0.979
D-index	0.843	0.814	0.787	0.939	0.981	0.994
slope (b)	1.141	1.385	1.435	1.422	1.175	1.019
Y-intercept (a)	-3.453	-3.524	-1.025	-0.264	0.860	1.082
RMSEs/RMSE	0.363	0.333	0.453	0.939	0.823	0.273

The performance results (Table 6.4) showed that the MC model provided good runoff prediction with acceptable R-squared and D-index values. The RMSE values indicate the error associated with the predication. In the case of the Kenilworth/Bainsvlei ecotope all three plots had comparable RMSE values of around 6 mm. Conversely, on the Paradys/Tukulu ecotope relatively higher errors were observed. Bahat *et al*. (2009) reason out that the presence of extreme values resulted in high RMSE values. The higher RMSE observed were due to one set of data that had extreme values, as explained above for the calibration of the empirical model. The same data was used for the calibration of this model. The RMSEs/RMSE reported for the 1:1 and 1:2 were higher. This is because in those two cases the model tends to over-predict the runoff amount generated. This can be explained by examining the data used for calibration. Within the dataset used for calibration of the Paradys/Tukulu ecotope, the ones taken from Bothma (2009) were systematically over estimated. Since these rainfall events were of heavy and extreme categories, the error associated was also exaggerated.

6.3.3. Validation of the runoff models

The validation results for both models and ecotopes are shown in Figures 6.5 and 6.6. The graphs show the relationship of the measured runoff values with the simulated values. How far a regression line of the measured versus the simulated deviates from the

1:1 line is an indication of the performance of the model. In such graphical analysis, the slope and the y-intercept of the regression line provide good information. In Figures 6.5 and 6.6, the linear equations containing the slope and the y-intercept are provided next to each regression line. In relative terms, it can be seen that both models had better slope values for the Paradys/Tukulu ecotope than the Kenilworth/Bainsvlei ecotope. The statistical performance results for the validation data is shown in Table 6.5. The performance in comparison to the calibration performance is discussed below, while comparison between the two models is discussed in the next section.

The statistical performance test results presented in Table 6.5 showed that the models perform equally well as with the calibration results. On the Kenilworth/Bainsvlei ecotope both models had comparable RMSE values. The difference in RMSE values observed was more for the empirical model as compared to that of the MC model. Contrary to this, the RMSE values observed on the validation data for both models improved in the case of the Paradys/Tukulu ecotope. The observed improvement in RMSE values was bigger for the MC model compared to the empirical model. For instance the improvement observed for the MC model for the 1:1 and 1:2 plots was 15 and 6 mm. This result confirms the claim made above that higher RMSE values observed for the calibration results were mainly introduced by the extreme values of data taken from Bothma (2009).

6.3.3.1. Empirical model

Generally, on the Kenilworth/Bainsvlei ecotope the empirical model had a regression line close to 1:1 line. However, the closeness as measured by the slope of the regression lines was relatively lower. The slope values were different for each basin to RSL ratios. The slope values were 0.66, 0.69 and 0.64 for the 1:1, 1:2 and 1:3, respectively. In those three instances the y-intercept was close to zero, which made it to be closer to the 1:1 line at lower runoff values. In all instances, there was a tendency of under-predicting the runoff amount for higher runoff observations.

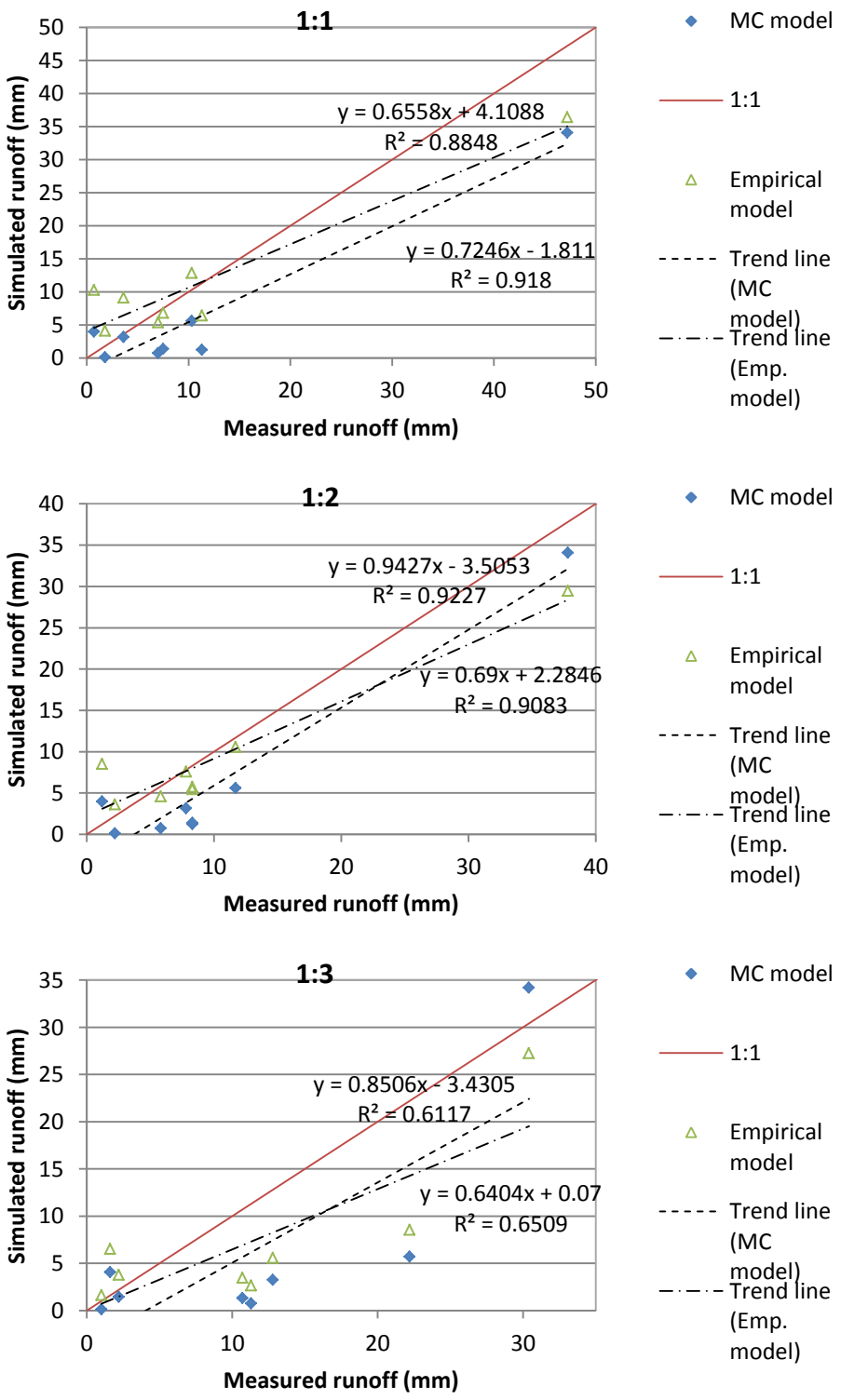

Figure 6.5 Validation results for the MC and empirical runoff models on the Kenilworth/Bainsvlei ecotope.

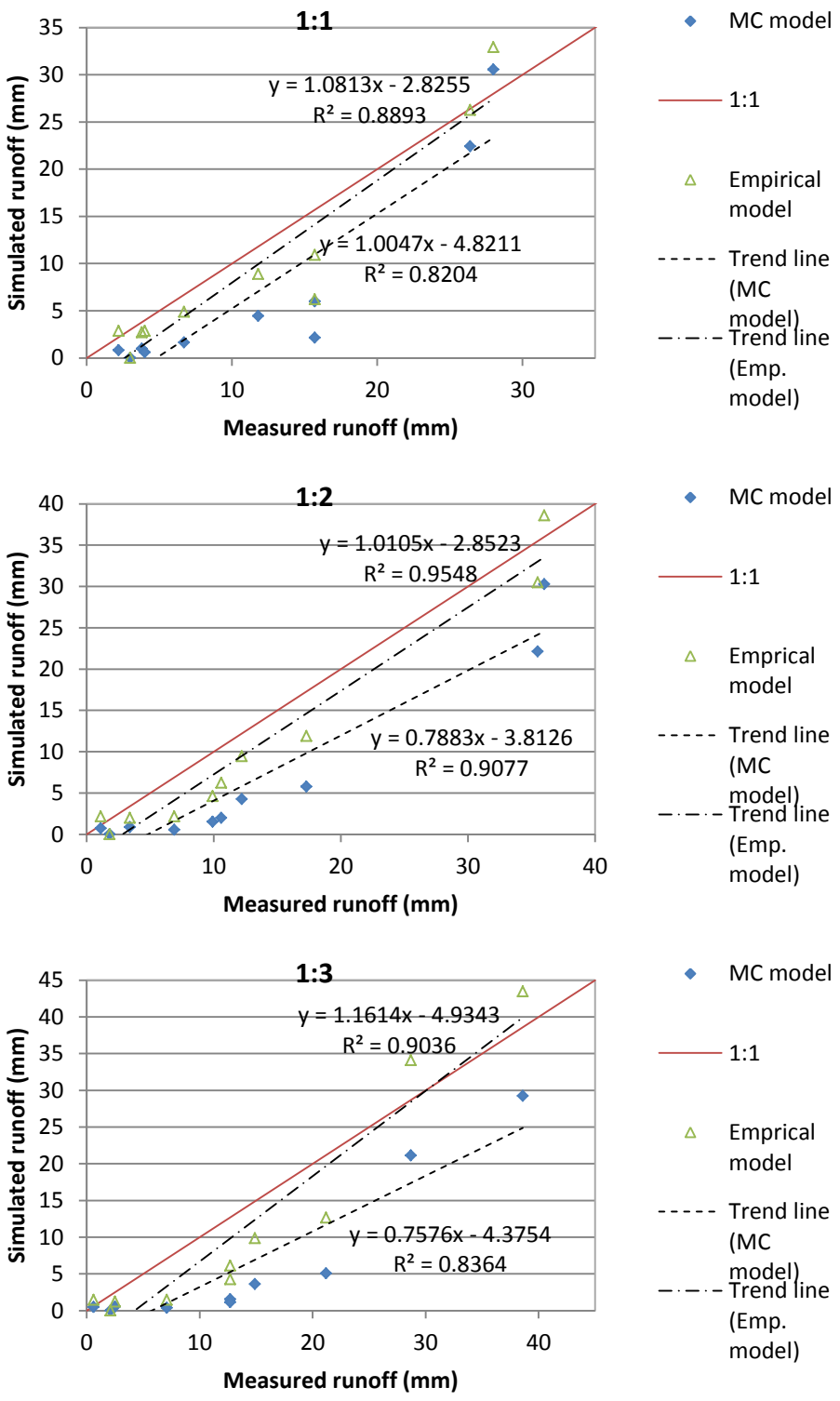

Figure 6.6 Validation results for the MC and empirical runoff models on the Paradys/Tukulu ecotope.

The validation results for the Paradys/Tukulu ecotope showed that the empirical model had very close regression lines to the 1:1 line. For all basin to RSL ratios, the slope values computed were very close to 1. The slope values were 1.1, 1 and 1.2 for the 1:1, 1:2 and 1:3, respectively. The y-intercept values were smaller negative values. This means for smaller values of observed runoff the model predicted zero runoff values. However, for the higher values of runoff observed this model gave comparable amounts.

Table 6.5 Statistical performance of the MC and empirical models on the validation data for the Kenilworth/Bainsvlei and Paradys/Tukulu ecotopes.

Ecotope	Statistical parameter	Empirical model			MC model		
		1:1	1:2	1:3	1:1	1:2	1:3
Kenilworth/Bainsvlei	RMSE	5.890	4.230	7.077	6.943	5.096	8.534
	RMSEs	4.853	3.497	5.378	6.238	4.148	5.357
	RMSEu	3.338	2.380	4.600	3.049	2.960	6.644
	MAE	4.756	3.135	5.860	5.706	4.794	6.723
	R^2	0.884	0.908	0.651	0.918	0.923	0.612
	D-index	0.938	0.948	0.841	0.923	0.945	0.833
	slope (b)	0.656	0.690	0.641	0.725	0.943	0.851
	Y-intercept (a)	4.110	2.280	0.060	-1.811	-3.505	-3.430
	RMSEs/RMSE	0.824	0.827	0.760	0.898	0.814	0.628
Paradys/Tukulu	RMSE	4.002	3.803	5.532	6.401	7.760	9.184
	RMSEs	2.015	2.712	3.267	4.766	7.140	8.300
	RMSEu	3.458	2.666	4.464	4.273	3.041	3.933
	MAE	2.986	3.445	4.883	5.278	6.664	7.796
	R^2	0.890	0.955	0.903	0.820	0.908	0.836
	D-index	0.958	0.976	0.955	0.897	0.887	0.841
	slope (b)	1.082	1.009	1.160	1.005	0.788	0.758
	Y-intercept (a)	-2.831	-2.830	-4.934	-4.821	-3.813	-4.375
	RMSEs/RMSE	0.503	0.713	0.591	0.745	0.920	0.904

6.3.3.2. MC model

The MC model performed well on the validation data of the Kenilworth/Bainsvlei ecotope, giving closer regression lines to the 1:1 line. The slope values observed for the different basin to RSL ratios were: 0.72, 0.94 and 0.85 for the 1:1, 1:2 and 1:3, respectively. The y-intercept values were close to zero. Nevertheless, in all instances the model under-predicted observed runoff amounts.

The validation results for the Paradys/Tukulu ecotope showed that the MC model had good prediction performance. This performance varied for the three basin to RSL ratios. For the 1:1 basin to RSL ratio, the slope was 1, yet it ran parallel to the 1:1 line. This means the line deviates from the 1:1 line by a magnitude of the y-intercept. The 1:2 basin to RSL ratio was next in rank with a slope value of 0.78 and y-intercept of -3.8. The 1:3 basin to RSL ratio came last in the rank with a slope value of 0.75. This line had a regression line that deviated wider at higher values of observed runoff.

6.3.4. Comparison of the two models

From the graphical presentation in Figures 6.5 and 6.6, the closeness to the 1:1 line of one model over the other clearly shows better performance. Further statistical performance test was vital to show the margin with which one outperforms the other. The performance test results presented in Table 6.5 helped to assess the model performance on its own and also to compare it with another for the same conditions.

Comparing the MC model with the empirical model for the Kenilworth/Bainsvlei ecotope had a comparable performance as shown by the statistical parameters in Table 6.5. The D-index for both models was similar. The observed slope values were better for the MC model while the y-intercept values were better for the empirical model. The ratio between RMSEs/RMSE was higher for both models indicating there was systematic under-prediction as shown in Figure 6.5. As revealed by the y-intercept values, the under-prediction starts from small value for the MC model while in the case of the empirical model on average gave good prediction for small values of runoff amounts. Thus, to determine the best model for use, the RMSE was consulted and the empirical model performed better by scoring about 1 mm less error.

The comparison between the MC and the empirical models was easier for the Paradys/Tukulu ecotope. The statistical model performance evaluation parameters presented in Table 6.5 showed clearly the edge one model had over the other. The empirical model performed better than the MC model in all accounts for all three basin to RSL ratios. The D-index values observed were comparable, but the slope, y-intercept, the

R^2 and RMSE values were better for the empirical model. The least RMSE advantage observed for the empirical model over the MC model was 2 mm.

The statistical performance parameters presented in Table 6.5 compared well with other studies done for runoff prediction in other ecotopes (Welderufael, 2006; Anderson 2007). Anderson (2007) reported RMSE values for the bare treatment on the Glen/Bonheim ecotope ranging from 5.1 to 7.02. Most of the values presented in the above tables compare well with the exception of the 1:3 basin to RSL ratio. The highest RMSE reported by Welderufael (2006) is 4.08 mm, a value found in the Mieso Hypo Calcic Vertisol ecotope. The RMSE values obtained for the empirical model were less than all the empirical models reported by Anderson (2007), the exception here again was the 1:3 basin to RSL ratio. One thing that must be noted here is that both in the case of Welderufael (2006) and Anderson (2007) the runoff plots used were of 2 m RSL. The D-index and slope values obtained for this study also were comparable to those obtained by Welderufael (2006) and Anderson (2007).

Model performance for the MC model and empirical models are reported by Anderson (2007). He treated those models as separate groups and comparison was done within each group. He chose the MC model as the best model for runoff prediction based on the physical explanation it can give with regard to rainfall intensity and soil surface particle strength. Nevertheless, Anderson (2007) own empirical model reported performed better than MC model. This agrees well with the findings above. Even if both models reported in this study gave good predictions results, the empirical models showed better prediction performance. The empirical models, although they are black-box models which might not provide explicit explanation on the physical process, they can provide good prediction for the locality it was developed for. This might be due to the information carried by the parameters collected specifically from the area of study. This finding supports the finding in Chapter two, that about 83% of the information needed to determine runoff amount is carried in the rainfall amount. This might not be a general truth, but with the type of rainfall amount prevailing in the area generally being of high intensity, it remains to be applicable. The linear nature of the empirical model also is helpful in determining threshold rainfall amount for which runoff can be harvested. By putting the value for Y

(representing runoff) in the equation to be equal to zero and solving for X, enables to determine the least rainfall required for measurable runoff to start.

6.4. Conclusion

In-field runoff prediction was acceptably modelled both with empirical and MC models. Based on the good correlations rainfall amount has on determining runoff amount, it was possible to develop an empirical runoff prediction model. The developed empirical model did capture the relationship well, and provided good prediction of runoff amount for both ecotopes. The calibrated MC runoff model provided good performance. After acceptable validation of the models, comparison for best prediction model was done. The empirical runoff prediction model provided the best prediction for both ecotopes.

References

Anderson, J.J., 2007. Rainfall-runoff relationships and yield responses of maize and dry beans on the Glen/Bonheim ecotope using conventional tillage and in-field rainwater harvesting. Ph.D. thesis University of the Free State, Bloemfontein, South Africa.

Bahat, Y., Grodek T., Lekach J. & Morin E., 2009. Rainfall-runoff modeling in a small hyper-arid catchment. *J. Hydrol.* **373**:204–217.

Botha, J.J., Anderson, J.J., Groenewald, D.C., Nhlabatsi, N.N., Zere, T.B., Mdibe, N. & Baiphethi, M.N., 2007. On-farm application of in-field rainwater harvesting techniques on small plots in the central region of South Africa. Volume 1. Water Research Commission report No. TT 313/07, Pretoria, South Africa.

Botha, J.J., van Rensburg, L.D., Anderson, J.J., Hensley, M., Macheli, M.S., van Staden P.P., Kundhlande, G., Groenewald, D.C. & Baiphethi, M.N., 2003. Water conservation techniques on small plots in semi-arid areas to enhance rainfall use efficiency, food security, and sustainable crop production. Water Research Commission report No. 1176/1/03, Pretoria, South Africa.

Botha, J.J., 2006. Evaluation of maize and sunflower production in semi-arid area using in-field rainwater harvesting. Ph.D. thesis University of the Free State, Bloemfontein, South Africa.

Bothma, C.B., 2009. In-field runoff and soil water storage on duplex soils at Paradys Experimental Farm. M.Sc. thesis University of the Free State, Bloemfontein, South Africa.

Hensley, M., Botha, J.J., Anderson, J.J., van Staden, P.P. & du Toit, A., 2000. Optimizing rainfall use efficiency for developing farmers with limited access to irrigation water. Water Research Commission report No. 878/1/00, Pretoria, South Africa.

Hensley, M., Hattingh, H.W. & Bennie, A.T.P., 1993. A water balance modelling problem and a proposed solution. 4th Annual Conference of the SADC-Land and Water Management Research Program, Windhoek, Namibia.

Horton, R.A., 1936. Hydrologic interrelations of water and soils. *Soil Sci. Soc. Am. Proc.* **1**:401–429.

Jalota, S.K., Arora, V.K. & Singh, O., 2000. Development and evaluation of a soil water evaporation model to assess the effects of soil texture, tillage and crop residue management under field conditions. *Soil Use Manage.* **16**:194-199.

Meng, L. & Quiring S.M., 2008. A comparison of soil moisture models using soil climate analysis network observations. *J. Hydrometeor.* **9**:641–659.

Morin, J. & Benyamini, Y., 1977. Rainfall infiltration into bare soils. *Water Resour. Res.* **3**(5):813-817.

Morin, J. & Cluff, C.B., 1980. Runoff calculation on semi-arid watersheds using a rotadisk rainulater. *Water Resour. Res.* **16**(6):1085-1093.

Onyando, J.O. & Sharma, T.C., 1995. Simulation of direct runoff volumes and peak rates for rural catchments in Kenya, East Africa. *Hydrol. Sci. J.* **40**(3):367-380.

Walker, S. & Tsubo, M., 2003. Estimation of rainfall intensity for potential crop production on clay soil with in-field water harvesting practices in a semi-arid area. Water Research Commission report No. 1049/ 1/02, Pretoria, South Africa.

Welderufael, W.A., 2006. Quantifying rainfall-runoff relationships on selected benchmark ecotopes in Ethiopia: a primary step in water harvesting research. Ph.D. thesis University of the Free State, Bloemfontein, South Africa.

Willmott, C.J., 1981. On the validation of models. *Phys. Geogr.* **2**:184-194.

Young, M.D.B., Gowing, J.W., Wyseure, G.C.L. & Hatibu, N., 2002. Parched-Thirst: development and validation of a process-based model of rainwater harvesting. *Agric. Water Manage.* **55**:121-140.

Zere, T.B., van Huyssteen, C.W. & Hensley, M., 2005. Estimation of runoff at Glen in the Free State Province of South Africa. *Water SA* **31**(1):17-22.

7. Modelling soil water evaporation for different basin to runoff strip length ratios under in-field rainwater harvesting system

Abstract

In-field rainwater harvesting is mainly developed to stop ex-field runoff. The fact that it stores the harvested water deeper in the soil profile, however, helps the system to reduce soil water evaporation. Yet, soil water evaporation remains to be major mechanism of water loss under in-field rainwater harvesting. Thus, there is need to quantify and model this parameter. The objectives of this study were: (i) to develop an empirical model and calibrate the Ritchie evaporation prediction (REP) model for the Kenilworth/Bainsvlei and Paradys/Tukulu ecotopes (ii) to validate these models and compare the performance of the models. Evaporation data measured by DFM capacitance probes were used to calibrate (develop) and validate the models. Statistical performance evaluation parameters: RMSE, MAE, D-index and R^2 were used to measure the performance of the two models. For the Kenilworth/Bainsvlei ecotope the RMSE average of the three basin to RSL ratios was 2.3 mm for both models. This value was 2.3 and 2 mm for the Paradys/Tukulu ecotope with the empirical and REP models, respectively. From the detail comparison of the two models, it was concluded that the empirical evaporation model performed better on the Kenilworth/Bainsvlei ecotope. The REP model, on the other hand, performed better on the Paradys/Tukulu ecotope.

Key words: evaporation, runoff strip length, modelling, IRWH

7.1. Introduction

The practice of in-field rainwater harvesting (IRWH), although mainly designed for maximizing rainwater productivity by harvesting runoff, it does make some contributions in reducing soil water evaporation (Es). Es values under IRWH during fallow and growing seasons were 17% and 15% less than conventional tillage system (Botha, 2006). Botha *et al*. (2003) found that it requires at least 22 mm of rain to effect infiltration beyond the active evaporation zone (100 mm) on the runoff strip, while in the basins it only requires 9 mm. This magnifies the role IRWH plays in concentrating water into the basins and effect deeper storage, thus reducing water available for evaporation. Despite this reduction, evaporation loss remains to be high. During a growing season Botha *et al*. (2003) found Es accounted for 69% and 75% of the annual rainfall for sunflower and maize respectively. Botha *et al.* (2003) also developed empirical relationship between Es and rainfall received. From this relationship, it was estimated that 46% and 88% of the received rainfall evaporates under low and high rainfall, respectively during a fallow season. This shows that not only the Es during fallow will be different from that of growing season, but also it shows that Es is a function of the amount of rainfall.

Evaporation estimation has been a subject of modelling for long. Johnson & Ritchie (1990) generally classified the models developed as mechanistic and functional. The mechanistic ones are based on known principles of physical process (Lascano, 1991) which makes them a bit complicated and require parameters which might not be readily available. The functional ones, on the other hand, are relatively simpler and require parameters that are easier to measure and thus command a wider use. Suleiman & Ritchie (2003) provide list of literatures reviewing the mechanistic models and they noted there is relatively fewer for the functional ones despite the wider use. Nevertheless, there is continued endeavor to develop a better or more refined functional evaporation model. The most widely used models are Ritchie (1972) and Boesten & Stroosnijder (1986) models. Jalota *et al*. (1988) modified the square root of time and cumulative evaporation relationship by introducing a way to determine the cutoff time between first and second stages and cumulative evaporation being calculated as a function of potential evaporation. Malik *et al*. (1992) also modeled evaporation as a function of potential evaporation and

the actual rate varies according to the depth of the advancing drying front. Aydin (2008) describes a model of estimating evaporation as a function of potential evaporation and soil water potential. There is a major similarity with all these models in that evaporation is determined as a function of the driving atmospheric force and the restricting or limiting soil condition.

In South Africa the evaporation studies undertaken applied different models. Hattingh (1993) measured evaporation on the Glen/Hutton ecotope and applied the Boesten & Stroosnijder (1986) model and Ritchie (1972). He observed that although the Boesten & Stroosnijder (1986) model made a reliable prediction, yet the Ritchie (1972) model performed better under the prevailing conditions. Hoffman (1997) fitted the cumulative evaporation data with the Rose (1968), Ritchie (1972), Kijne (1973) and Al-Khafaf *et al*. (1989) models and also developed an empirical equation based on change in water content and time. He found that the Ritchie (1972) model predicted evaporation better than the other models. Bennie *et al.* (1998) used the Ritchie (1972) and Rose (1968) models and concluded that the former predicted evaporation better. These findings compare well with what Yunusa *et al*. (1994) found elsewhere. Botha (2006) used the Ritchie (1972) model and noted the volatility of α-value which differed over summer and winter seasons. Nhlabatsi (2010) compared five models of predicting Es: field hydraulic conductivity, Darcy-equation, Hydraulic diffusivity, Ritchie (1972) and Rose (1968) models. The former model gave the best prediction of Es.

The objective of this chapter is to model soil water evaporation in the basin strip of the IRWH system, under different basin to runoff strip length (RSL) ratios. The following sub-objectives were developed to structure the work:

i. Develop a functional model for predicting soil water evaporation after rainfall events for the Paradys/Tukulu and Kenilworth/Bainsvlei ecotopes.
ii. Calibrate the Ritchie (1972) evaporation prediction (REP) models for the Paradys/Tukulu and Kenilworth/Bainsvlei ecotopes
iii. Validate the developed and calibrated models; and compare the performance of the models

7.2. Materials and Methods

The modelling exercise was done for two ecotopes: the Kenilworth/Bainsvlei and the Paradys/Tukulu ecotopes. The details of the climate and soil information pertaining to both ecotopes are provided in Chapter 1. The methods employed in collecting data and the modelling exercises are described below.

7.2.1. Measurement of evaporation

On the experimental plots of Paradys/Tukulu ecotope, 0.8 m long capacitance (DFM) probes (Figure 7.1) were used to measure the soil water content. The detail description of DFM probes is provided in Section 5.2.3. The probes were installed on 08 November 2009 and stayed in place until 27 May 2010. From the soil water record of the season, two drying cycles of rain free days and when the surface was weed-free were selected. The selected drying cycles elapsed between 19 - 27 November, 2009 and 06 - 14 April, 2010 for the first and second cycles respectively. Evaporation was determined by considering the change of water content on the upper 300 mm depth. The change in water content is measured by three sensors each representing 100 mm.

In the Kenilworth/Bainsvlei ecotope, the same kind of capacitance probes were used to measure soil water content but since this soil was deeper the 1.2 m long probes were installed. The description about the position of the sensors is given in Section 5.2.3. The water content measurement was done between 05 November 2009 and 08 June 2010. The drying cycles selected were the days spanning between 17 February to 23 February and 25 February to 2 March, respectively for the first and second drying cycles. Evaporation during the drying cycles was computed by monitoring change of soil water content on the top 300 mm. This depth was represented by the first top sensor.

Evaporation values measured for the selected drying cycles of the two ecotopes are presented in Table 7.1. Since the drying cycles were chosen to be rain free days, the length of the drying cycles were dependent on the incident of a rain event. Depending on the available water for evaporation and prevailing atmospheric conditions the amount of daily evaporation varied between the different cycles.

Table 7.1 Cumulative evaporation (mm) for both ecotopes in the basins of in-field rainwater harvesting system [1 and 2 represent the two drying cycles used for calibration (development) and validation of models].

Days after rain	Kenilworth/Bainsvlei ecotope						Paradys/Tukulu ecotope					
	1:1		1:2		1:3		1:1		1:2		1:3	
	1	2	1	2	1	2	1	2	1	2	1	2
1	1.4	4.4	3.0	3.4	1.6	4.7	1.5	4.3	3.5	5.3	3.1	4.9
2	1.9	5.0	3.8	4.3	2.1	5.4	2.9	6.0	6.2	8.0	6.7	7.0
3	2.1	5.5	4.6	5.0	2.4	5.8	5.6	6.2	9.5	9.3	9.5	8.1
4	2.4	5.8	4.9	5.5	2.7	6.2	6.6	6.6	11.0	10.1	11.3	8.8
5	2.5	6.1	5.3	5.9	2.9	6.4	7.3	7.7	12.2	10.7	12.8	9.9
6	2.7		5.5		3.1		7.9	8.8	13.2	11.0	14.5	10.2
7							8.5	9.8	14.1	11.7	15.9	11.4
8							9.0	10.4	14.8	12.3	17.1	12.1
9							9.4	11.0	15.5	12.9	18.2	12.8

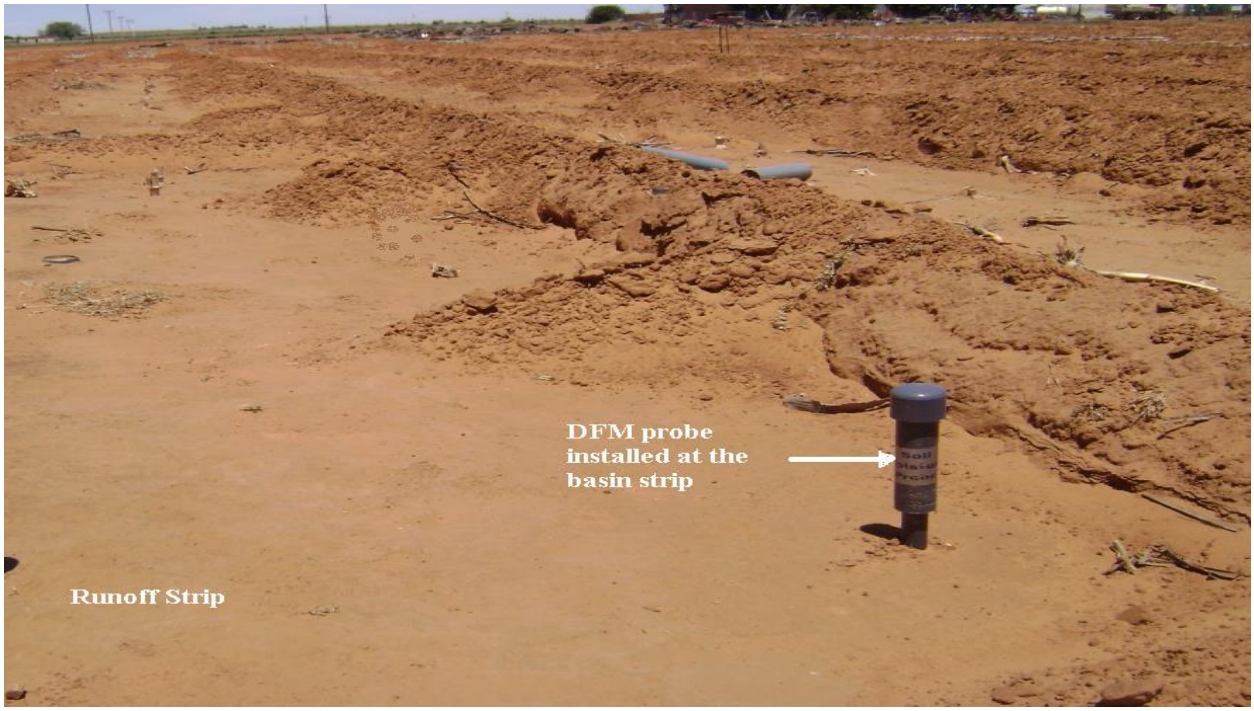

Figure 7.1 One of the water content measuring DFM probes installed on different sections of IRWH micro-landscape.

7.2.2. Simulation of evaporation

Simulation of cumulative evaporation lost from the basins was done using two methods. The two methods used were an empirical model developed for a specific ecotope and the

REP model. The first stage of evaporation during summer lasts only for few hours and it can be omitted without bringing much deviation in the prediction of evaporation (Hoffman, 1997; Bennie *et al*., 1998). Thus, the simulations conducted in this study, the computation of cumulative evaporation was done considering only second stage evaporation.

7.2.2.1. Empirical model

The empirical model was developed by taking data collected from one drying cycle. The parameters considered were cumulative potential evaporation and the square root of days after rain. Multiple linear regression was used to relate these parameters with the cumulative evaporation. Coefficient of determination (R^2) is reported for each regression equation developed, as a measure of goodness of fit.

7.2.2.2. REP model

The data used for the development of the empirical model was used to calibrate the REP model for each basin to RSL ratio. The calibration of REP model only needed the determination of the α-value from the drying cycle considered. The α-value was determined as the slope of the linear relationship between cumulative evaporation and the square-root of time. The coefficient of determination (R^2) is reported as measure of goodness of fit.

7.2.2.3. Validation of the models

Both models were validated on an independent set of data from the second drying cycle. The models were run on the inputs of the second drying cycle and the values predicted by the models were compared to the measured amounts of cumulative soil water evaporation. The performance of the models was evaluated as described in the next section.

7.2.3. Statistical analysis

Statistical model evaluation during both calibration and validation run of the models were done by using the model performance parameters suggested by Willmott (1981). These

parameters include the index of agreement (D-index), mean absolute error (MAE), root mean square error (RMSE) with its systematic ($RMSE_s$) and unsystematic ($RMSE_u$) components, and the coefficient of determination (R^2).

7.3. Results and discussion

7.3.1. Development of functional evaporation model

Empirical relationship between observed cumulative evaporation, the square root of time and reference evapotranspiration (ET_o) was developed. This relationship was captured in the Equations 7.1 – 7.6. This relationship in essence combines the relationships depicted by REP model and Boesten & Stroosnijder (1986) model. This can provide more relevant information about the prevailing local conditions because of the extra atmospheric parameter included. The contribution each parameter makes towards predicting evaporation can be observed from the coefficients (weights) accorded. As can be seen from the Equations of 7.1 to 7.6, in all instances of both ecotopes more weight was given to the time variable. This could be a good indication to the physical meaning these variables have. Since the observed values represented the second stage of evaporation, the evaporative demand play little role in determining the amount of evaporation observed. The same observation could be done by making stepwise regression (not reported here). In such exercise the parameter which received more weight in the equations below account for more than 90% of the coefficient of determination (R^2).

Kenilworth/Bainsvlei ecotope

1:1

$$\sum \mathrm{E}\,(\mathrm{t}) = 2.373\sqrt{t} - 0.446\sqrt{\sum \mathrm{ET_o}} + 2.674 \qquad R^2 = 0.999 \qquad (7.1)$$

1:2

$$\sum \mathrm{E}\,(\mathrm{t}) = 3.543\sqrt{t} - 0.677\sqrt{\sum \mathrm{ET_o}} + 0.839 \qquad R^2 = 1 \qquad (7.1)$$

1:3

$$\sum \mathrm{E}\,(\mathrm{t}) = 3.205\sqrt{t} - 0.818\sqrt{\sum \mathrm{ET_o}} + 2.693 \qquad R^2 = 0.998 \qquad (7.3)$$

Paradys/Tukulu ecotope

1:1

$$\sum \mathrm{E}\,(\mathrm{t}) = 8.66\sqrt{t} - 1.937\sqrt{\sum \mathrm{ET_o}} - \ 3.267 \qquad R^2 = 0.987 \qquad (7.4)$$

1:2

$$\sum \mathrm{E}\,(\mathrm{t}) \ = 3.080\sqrt{t} \ + 0.204\sqrt{\sum \mathrm{ET_o}} \ + \ 2.726 \qquad R^2 = 0.963 \qquad (7.5)$$

1:3

$$\sum \mathrm{E}\,(\mathrm{t}) = 10.428\sqrt{t} - 1.227\sqrt{\sum \mathrm{ET_o}} - \ 4.685 \qquad R^2 = 1 \qquad (7.6)$$

Where:

$\sum E(t)$ = cumulative evaporation at time t (days)

$\sum ET_o$ = cumulative reference evapotranspiration (mm)

The empirical models (Equations 7.1 - 7.6) had shown acceptable prediction performance. The statistical performance evaluation results are presented in Table 7.2. The performance results reported in Table 7.2 showed exceptionally good performance on the calibrations data. The empirical model had less than 0.1 mm errors observed for the Kenilworth/Bainsvlei ecotope. The D-index and slope values were 1 showing perfect agreement. The y-intercept values were zero if considered to a 1 decimal point. Thus indicating the regression line was more or less similar to the 1:1 line. The small values of RMSEs/RMSE indicate the very little error that was observed was arbitrary and there was no systematic error.

Similarly the same good performance was observed with the Paradys/Tukulu ecotope. The RMSE values reported were all less than 0.4 mm. The R^2, D-index and slope values observed were very close to 1. The observed y-intercept values were very small which were less than 0.4. This testified that the regression line of measured and predicted values for the calibration data run very close to the 1:1 line. The RMSEs/RMSE ratio was very small indicating that the errors observed were more of unsystematic errors.

Table 7.2 Statistical model performance parameters of the empirical model on the calibration data.

Statistical parameter	Kenilworth/Bainsvlei ecotope			Paradys/Tukulu ecotope		
	1:1	1:2	1:3	1:1	1:2	1:3
RMSE	0.019	0.015	0.025	0.298	0.432	0.049
RMSEs	0.001	0.000	0.001	0.035	0.083	0.001
RMSEu	0.019	0.015	0.025	0.296	0.424	0.049
MAE	0.015	0.014	0.021	0.210	0.368	0.041
R^2	0.999	1.000	0.998	0.987	0.963	1.000
D-index	1.000	1.000	1.000	0.997	0.990	1.000
slope (b)	0.999	1.000	0.998	0.987	0.963	1.000
Y-intercept (a)	0.005	0.001	0.010	0.088	0.376	0.001
RMSEs/RMSE	0.031	0.017	0.042	0.116	0.192	0.010

7.3.2. Calibration of REP model

As indicated in the methodology, the evaporation prediction involved only the second stage of evaporation. This means for the REP model only the parameter α need to be determined. The relationship between the cumulative evaporation value and square root of time is illustrated in Figure 7.2. From this relationship, the α-values were determined empirically. In the Kenilworth/Bainsvlei ecotope the α-values were found to be 3.09, 2.82 and 3.28 mm day $^{-0.5}$ for the 1:1, 1:2 and 1:3 basin to RSL ratios, respectively. In the Paradys/Tukulu ecotope α-values of 3.12, 4.63 and 5.80 mm day $^{-0.5}$ were found for the 1:1, 1:2 and 1:3 basin to RSL ratios, respectively. It is a known fact that the α-values differ with soil types as well as atmospheric evaporative conditions. Here the observed difference was with in the soil types and same evaporative conditions. This difference was proved in the Chapter 5 where evaporation difference over different sections of the IRWH micro-landscape was investigated. Despite the observed difference of Es on different sections of the micro-landscape, the spatially averaged Es difference for different basin to RSL ratio was not statistically significant. Nevertheless, since this chapter deals with Es from the basin strip only each basin to RSL ratio is treated separately.

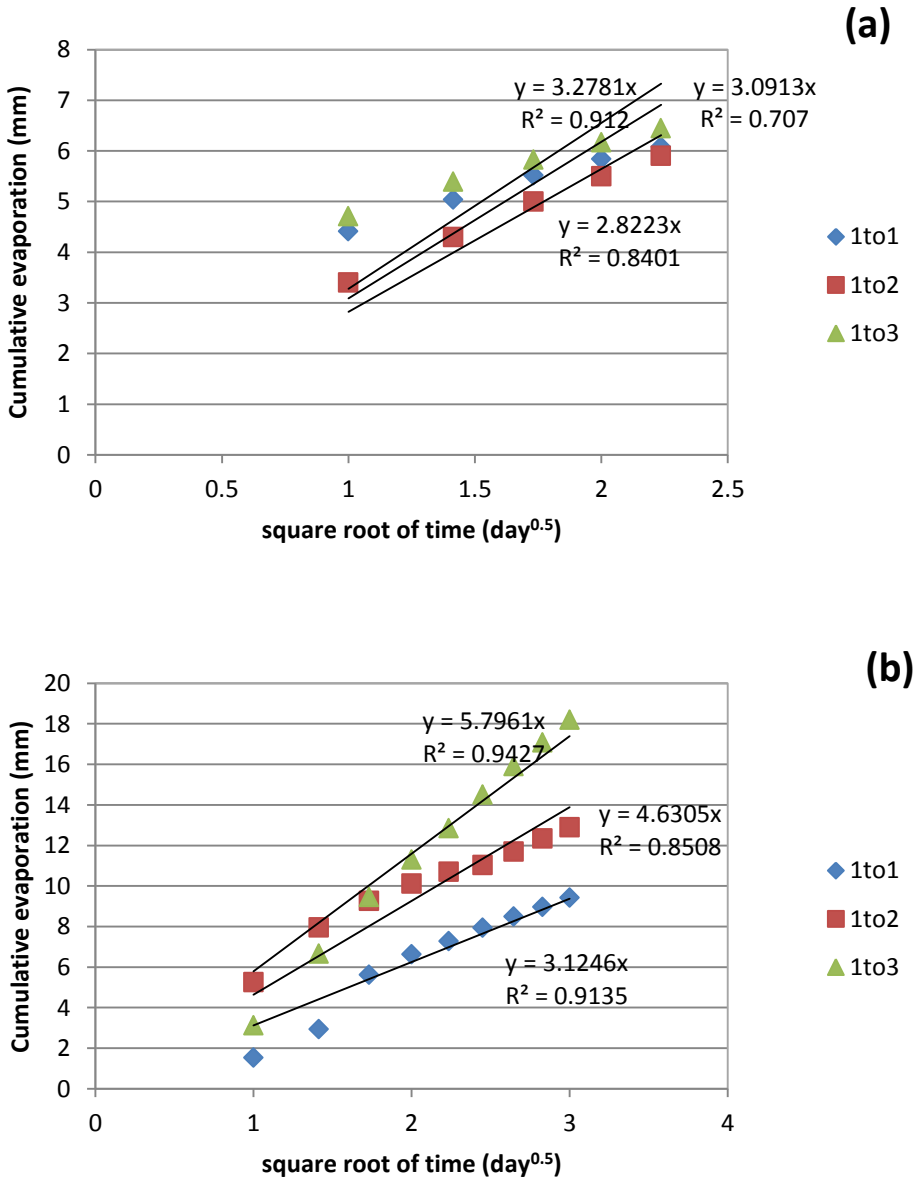

Figure 7.2 Relationship between cumulative evaporation and square root of time for (a) the Kenilworth/Bainsvlei ecotope and (b) the Paradys/Tukulu ecotope.

The variation in α-values with differing soil texture observed for the two ecotopes is in keeping with the values presented in Ritchie (1972). He showed that α-value increased from sand to clay loam and indicated that it is approximately proportional to the hydraulic conductivity of the soil. Bennie *et al.* (1998) developed an empirical relationship between the desortptivity and the α value of the soil. Using this empirical relationship the α-values 5.6 and 6.4 mm day$^{-0.5}$ were found for Kenilworth/Bainsvlei and

Paradys/Tukulu ecotopes, respectively. This wide overestimation could be due to surface condition differences between the IRWH and conventionally cultivated land. Nevertheless, the α-values [6.57 and 2.75 mm day$^{-0.5}$] obtained by Hensley *et al.* (2000) are comparable with values observed in this study. The α-values obtained by Botha (2006) under IRWH system fall within the range of values obtained in this study.

The model performance results for the calibration of REP model are presented in Table 7.3. The RMSE results obtained showed that the errors of prediction were low, not more than 1 mm, except in the case of 1:3 (RMSE = 1.13) basin to RSL ratio. The D-index showed very good agreement and the slopes obtained for both ecotopes were close to 1. The y-index obtained shows a slight deviation from zero. This deviation was bigger for the 1:1 and 1:3 bastin to RSL ratios of the Kenilworth/Bainsvlei ecotope. This deviation indicated that in the early days of the drying cycle, there was a tendency of under-predicting the evaporation values. The ratio of RMSEs/RMSE also showed that there was systematic error introduced. This systematic error had to do with the under-prediction on the early days, while over predicting evaporation on the latter days.

Table 7.3 Statistical model performance parameters of the REP model on the calibration data.

Statistical parameter	Kenilworth/Bainsvlei ecotope			Paradys/Tukulu ecotope		
	1:1	1:2	1:3	1:1	1:2	1:3
RMSE	0.766	0.355	0.850	0.756	0.867	1.130
RMSEs	0.762	0.350	0.839	0.655	0.660	1.113
RMSEu	0.076	0.063	0.136	0.378	0.563	0.196
MAE	0.656	0.311	0.719	0.519	0.790	0.842
R^2	0.997	0.997	0.991	0.963	0.963	0.997
D-index	0.846	0.972	0.827	0.972	0.972	0.982
slope (b)	2.232	1.381	2.341	0.753	1.278	0.774
Y-intercept (a)	-6.779	-1.923	-7.850	1.776	-3.035	3.055
RMSEs/RMSE	0.995	0.984	0.987	0.866	0.761	0.985

7.3.3. Validation of the two evaporation models

The validation results for the two models are presented in Figures 7.3 and 7.4. The performance observed was variable on the two ecotopes. Even on a same ecotope the performance was different for different basin to RSL ratios. Generally both models

performed better on the Paradys/Tukulu ecotope as compared to the Kenilworth/Bainsvlei ecotope. The detail of the performance in each model is discussed below.

7.3.3.1. Empirical model

This model performed acceptably well in most of the instances. Nevertheless, there were some instances also that it had shown a bit of deviation from the 1:1 line. For instance, the prediction for both ecotope on the 1:3 basin to RSL ratio had the biggest deviations. The slope and the y-intercept values observed for these instances were reflective of the deviation. Slope value of 2.1 and y-intercept of -6.8 showed that the prediction digressed for the 1:3 basin to RSL ratio in the Paradys/Tukulu ecotope. In the Kenilworth/Bainsvlei ecotope, although the slope was not as big as that of the Paradys/Tukulu ecotope the deviation was shown by the magnitude of the y-intercept (-7.9). In other basin to RSL ratios, the performance was acceptable although it had decreased from the performance observed on the calibration data. The slope values were not much far deviated from 1 and the y-intercept values were comparably better.

7.3.3.2. REP model

The REP model had good performance with the validation results of the Paradys/Tukulu ecotope. The observed slope did not vary much from that of the 1:1 line. The y-intercept values were close to zero providing it good elevation on the y axis. Conversely, the performance on the Kenilworth/Bainsvlei ecotope showed a bit of deviation. In the 1:1 and 1:3 basin to RSL ratios the deviation was evidenced by the higher values of the slope (2.4 and 2.5, respectively). The y-intercept values were equally deviant from that of the 1:1 line. In the case of the 1:2 basin to RSL ratio, the slope observed was not much different from the that of the 1:1 line but the y-intercept differed a bit from zero (- 4.2). This negative y-intercept gave it a lower elevation from the 1:1 line and thus consistently under-predicting the observed evaporation values.

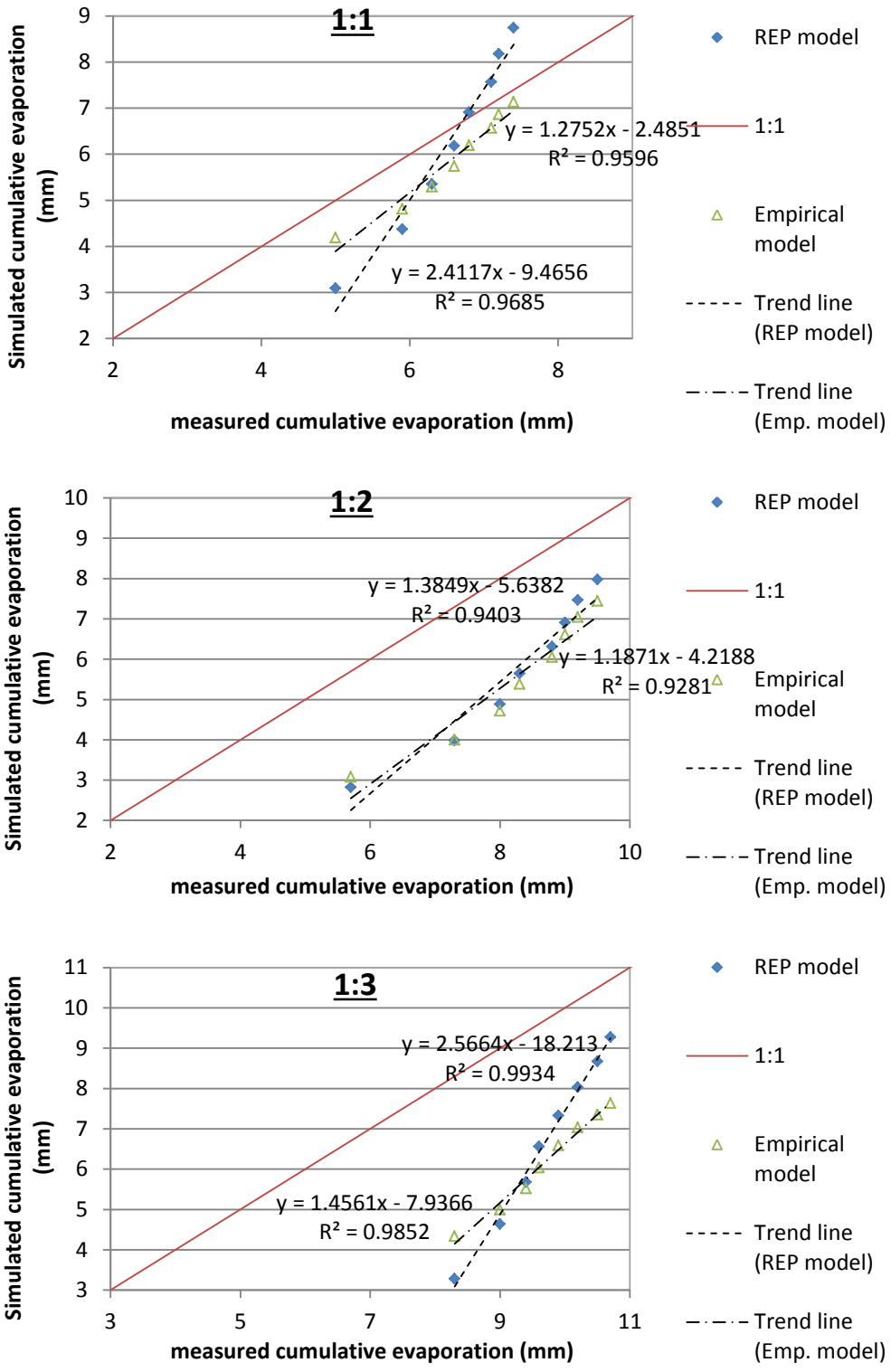

Figure 7.3 Validation results for the empirical and REP models for Kenilworth/Bainsvlei ecotope.

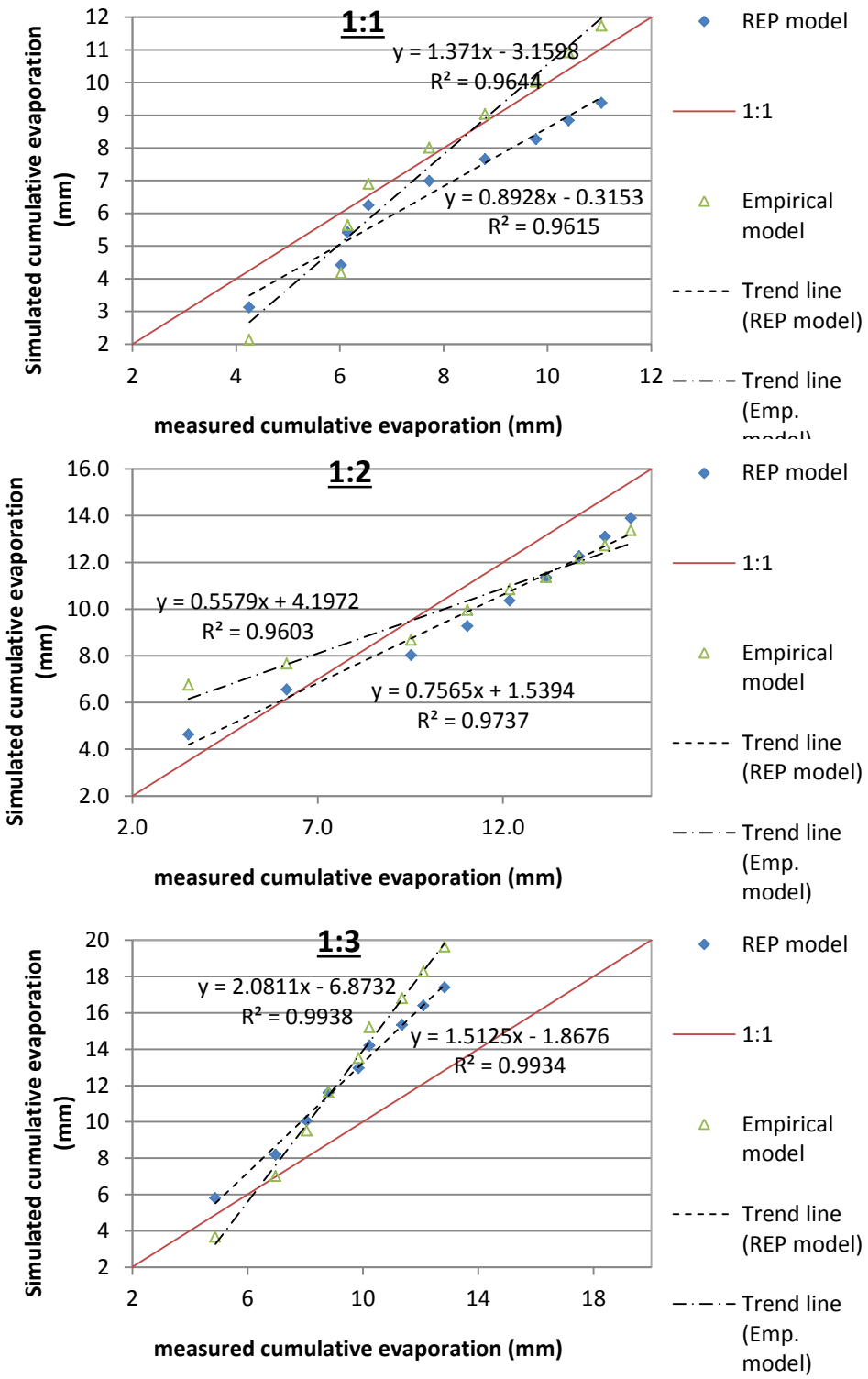

Figure 7.4 Validation results for the empirical and REP models for Paradys/Tukulu ecotope.

For better evaluation of the two models, the statistical performance results on the validation data is presented in Tables 7.4 and 7.5. The RMSE values ranged from 0.7 – 4.3 and 1.1 – 3.2 mm for the empirical and REP models, respectively. The D-index values were comparable for the two models. In all instances the RMSEs/RMSE ratio was close 1, which indicated that there was more systematic error involved. This was the indication for the systematic pattern of over and under predictions observed in Figures 7.3 and 7.4. The comparison between the two models is discussed in the next section.

7.3.4. Comparison between the two evaporation models

Along with the validation results depicted on Figures 7.3 and 7.4, the statistical results for model performance presented in Tables 7.4 and 7.5 enabled to clearly determine the better model for each case. On the Kenilworth/Bainsvlei ecotope, both models had comparable performance for the 1:2 basin to RSL ratio. In this basin to RSL ratio the REP model was better by slight margin of lesser error. Conversely, in the 1:1 and 1:3 basin to RSL ratios the empirical method was the better model. The deviant slope and y-intercept values for REP model showed that there was no equality correspondence between measured and simulated values.

Table 7.4 Statistical performance results for the validation data for the Kenilworth/Bainsvlei ecotope.

Statistical parameter	Empirical			REP		
	1:1	1:2	1:3	1:1	1:2	1:3
RMSE	0.742	2.716	3.532	1.121	2.545	3.242
RMSEs	0.716	2.688	3.529	1.073	2.513	3.238
RMSEu	0.194	0.384	0.134	0.322	0.405	0.157
MAE	0.686	2.680	3.513	0.963	2.472	3.018
R^2	0.960	0.928	0.985	0.969	0.940	0.993
D-index	0.839	0.545	0.332	0.809	0.586	0.401
slope (b)	1.275	1.187	1.456	2.412	1.385	2.566
Y-intercept (a)	-2.485	-4.219	-7.937	-9.466	-5.638	-18.213
RMSEs/RMSE	0.965	0.990	0.999	0.958	0.987	0.999

For the Paradys/Tukulu ecotope, the comparison between the two models can be easily judged. The performance results of both models for this ecotope are presented in Table 7.5. The lesser RMSE, closer to 1 slope and smaller y-intercept values reported for the

REP model in the 1:2 and 1:3 basin to RSL ratios made it clear that REP model performed better. In the case of the 1:1 basin to RSL ratio the RMSE values were comparable for both models. The difference observed for the slope and y-intercept values, however, showed that the REP model was better. With the slope values close to 1, the magnitude of the y-intercept is very critical. The importance of the y-intercept is also crucial in the prediction of evaporation for which the major amount is accounted in the early days of the evaporation process. Thus REP model had better overall performance on this ecotope.

Table 7.5 Statistical performance results for the validation data for the Paradys/Tukulu ecotope.

Statistical parameter	Empirical			REP		
	1:1	1:2	1:3	1:1	1:2	1:3
RMSE	1.015	1.844	4.262	1.243	1.577	3.238
RMSEs	0.840	1.800	4.244	1.181	1.509	3.224
RMSEu	0.571	0.402	0.397	0.387	0.458	0.298
MAE	0.756	1.771	3.617	1.158	1.507	2.978
R^2	0.964	0.968	0.994	0.961	0.975	0.993
D-index	0.961	0.902	0.730	0.916	0.948	0.775
slope (b)	1.371	0.582	2.081	0.893	0.754	1.512
Y-intercept (a)	-3.160	3.801	-6.873	-0.315	1.557	-1.868
RMSEs/RMSE	0.827	0.976	0.996	0.950	0.957	0.996

The results reported for this study as discussed above gave acceptable prediction and it was imperative to see how they compared with other studies. To do such comparison there is one hurdle of finding studies that had reported comparable parameters. For instance, Hoffman (1997) reported only the slope and R^2 of the models used. According to Willmott (1981) these are not enough parameters to test model performance. Bennie *et al*. (1998) reported only by how much percentage the prediction line deviated from that of the 1:1 line. A study done by Yunusa *et al*. (1994) reported sum of squared deviations (SSD). In order to make the comparison, the RMSE reported above were converted to SSD. Yunusa *et al*. (1994) reported SSD values ranging from 27 to 42 mm^2. The RMSE of the selected models (REP for Paradys, empirical for Kenilworth) had an SSD lower than this range for the 1:1 and 1:2 basin to RSL ratios. The 1:3 basin to RSL ratio had higher SSD than the range reported by Yunusa *et al.* (1994). Jalota *et al.* (2000) found

RMSE values of water loss (evaporation + drainage) 8.2, 20.4, 23.1 and 17.4 mm for untreated, residue-mulch, tillage and residue-incorporated treatments, respectively. Direct comparison with this result is not appropriate because these values included the drainage losses, yet such higher RMSE indicates the values obtained for this study (Tables 7.4 and 7.5) were acceptable. Ventura *et al.* (2006) used energy balance model and continuous soil water measurement to calculate evaporation, and found an RMSE between 0.6 – 1.3 mm day^{-1}. This range of RMSE was not comparable directly because it was rated per day, but if considered in cumulative terms, the RMSE would be compounded. Thus the RMSE observed for this study would be comparable to the envisaged cumulative value.

Bennie *et al.* (1998) although they did not report the parameters like RMSE, the chapter on refinement of the prediction provide good contribution which might be useful for this study. They show that the prediction by Ritchie (1972) systematically underestimate measured evaporation while the Rose (1968) model systematically overestimated it. To correct the under prediction of the model they proposed that the constants for the prediction equation be adjusted by the percentage of under prediction. This is one good method of removing or alleviating the systematic errors reported in Tables 7.4 and 7.5. For instance, in the cases where the model prediction runs parallel to the 1:1 line and consistently under-predicting it, correcting by the amount of the y-intercept would produce good results. Adjusting the prediction equations accordingly, thus can refine the prediction to a better level and lessen the systematic error.

7.4. Conclusion and recommendation

A combination of the cumulative reference evapotranspiration and square-root of time has good correlation with the cumulative soil water evaporation. From this correlation, it was possible to develop an empirical prediction models. The developed empirical models did capture the relationship well and provided good prediction performance of cumulative evaporation for both ecotopes. The same good performance was obtained for the REP model. Thus, both the empirical and REP models can be used to predict cumulative evaporation from the basins of IRWH system. The evaporation prediction model performance varied for the two ecotopes. The empirical evaporation prediction model

performed better on the Kenilworth/Bainsvlei ecotope. Conversely the REP model gave best prediction for Paradys/Tukulu ecotope. Hence, the use of a model according to the best performance for each ecotope is recommended

References

Al-Khafaf, S., Sharnan, F.A., Wierenga, P.J. & Iyada, A.D., 1989. Some empirical relations for the prediction of soil evaporation, transpiration and root water uptake under field conditions. *Agric. Water Manage.* **16**:323-335.

Aydin, M., 2008. A model for Evaporation and Drainage investigations at Ground of Ordinary Rainfed-areas. *Ecol. Modell.* **217**:148–156.

Bennie, A.T.P., Strydom, M.G. & Vrey, H.S., 1998. The application of computer models for agricultural water management on ecotope level [Afr.]. Water Research Commission report No. 625/1/98, Pretoria, South Africa.

Boesten, J.J.T.I. & Stroosnijder, L., 1986. Simple model for daily evaporation from fallow tilled soil under spring conditions in a temperate climate. *Neth. J. Agr. Sci.* **34**:75–90.

Botha, J.J., van Rensburg, L.D., Anderson, J.J., Hensley, M., Macheli, M.S., van Staden, P.P., Kundhlande, G., Groenewald, D.C. & Baiphethi, M.N., 2003. Water conservation techniques on small plots in semi-arid areas to enhance rainfall use efficiency, food security, and sustainable crop production. Water Research Commission report No. 1176/1/03, Pretoria, South Africa.

Botha, J.J., 2006. Evaluation of maize and sunflower production in semi-arid area using in-field rainwater harvesting. Ph.D. thesis University of the Free State, Bloemfontein, South Africa.

Hattingh, H.W., 1993. The estimation of evaporation from the soil surface under dryland wheat and maize production [Afr.]. M.Sc. thesis University of the Free State, Bloemfontein, South Africa.

Hensley, M., Botha, J.J., Anderson, J.J., van Staden, P.P. & du Toit, A., 2000. Optimizing rainfall use efficiency for developing farmers with limited access to irrigation water. Water Research Commission report No. 878/1/00, Pretoria, South Africa.

Hoffman, J.E., 1997. Quantifying and prediction of evaporation from the soil surface under dryland crop production [Afr.]. Ph.D. thesis University of the Free State, Bloemfontein, South Africa.

Jalota, S.K., Arora, V.K. & Singh, O., 2000. Development and evaluation of a soil water evaporation model to assess the effects of soil texture, tillage and crop residue management under field conditions. *Soil Use Manage.* **16**:194-199.

Jalota, S.K., Prihar, S.S. & Gill, K.S., 1988. Modified square root of time relation to predict evaporation trends from bare soil. *Aust. J. Soil Res.* **26**:281-289.

Johnson, B.S. & Ritchie, J.T., 1990. Soil and plant factors affecting evaporation. *Irri. of Agric. Crops* - Agronomy Monograph no. **30**:363-388.

Kijne, J.W., 1973. Evaporation from bare soils. In: Ecological studies: physical aspects of soil and salts in ecosystems. Hadas, A., Swartzendruber, D., Rijtema, P.E., Fuchs, M. & Yarton, B., (Ed's). Chapman and Hall, London. pp. 221-226.

Lascano, R.J., 1991. Review of models for predicting soil water balance. Soil water balance in the Sudano-Sahelian zone (Proceedings of the Niamey Workshop, February 1991). IAHS Publ. no. 199.

Malik, R.S., Anlauf, R. & Richter, J., 1992. A simple model for predicting evaporation from bare soils. *J. Plant Nutr. Soil Sci.* **155**(4):293-299.

Nhlabatsi, N.N., 2010. Soil surface evaporation studies on the Glen/Bonheim ecotope. Ph.D. thesis University of the Free State, Bloemfontein, South Africa.

Ritchie, J.T., 1972. Model for predicting evaporation from a row crop with incomplete cover. *Water Resour. Res.* **8**(5):1204-1211.

Rose, D.A., 1968. Water movement in porous materials. III. Evaporation of water from a soil. *Brit. J. Appl. Phys.* **2**(1):1779-1791.

Suleiman, A.A. & Ritchie, J.T., 2003. Modeling soil water redistribution during second-stage evaporation. *Soil Sci. Soc. Am. J.* **67**:377–386.

Ventura, F., Snyder, R.L. & Bali, K.M., 2006. Estimating evaporation from bare soil using soil moisture data. *J Irrig. Drain. E-ASCE.* **132**(2):153-158.

Willmott, C.J., 1981. On the validation of models. *Phys. Geogr.* **2**:184-194.

Yunusa, I.A.M., Sedgley, R.H. & Tennant, D., 1994. Evaporation from bare soil in South-Western Australia: a test of two models using lysimetry. *Aust. J. Soil Res.* **32**:437-46.

8. Soil water balance under in-field rainwater harvesting: Integration of the models of the water balance components

Abstract

Fallowing under in-field rainwater harvesting system can create an opportunity for increasing the amount of water stored in the profile. Water storage is the result of conserving the gains and minimizing the losses of water. This can fairly be represented by using well calibrated and validated models of the components of soil water balance. The objective of this study was to evaluate the storage gains achieved by different basin to runoff strip length (RSL) ratios during fallow period. To characterise the water balance of the IRWH system, models of the components of the water balance were integrated. Validated runoff and evaporation models, drainage curve and daily rainfall data were used to observe the daily soil water change. The plot level rainwater storage efficiency (RSE) values on the Kenilworth/Bainsvlei ecotope ranged from 8 to 33% and 29 to 58% for the long and short fallows, respectively. These ranges for the Paradys/Tukulu were 7 to 24% and 23 to 56% for the long and short fallows, respectively. The simulation revealed that for different scenarios of the long fallow, the 1:1, 1:2 and 1:3 basin to RSL ratios did not show much variation in the storage achieved. For short fallow, however, the amount of water stored increased with increasing RSL.

Key words: soil water balance, fallow, runoff strip length, soil water storage, IRWH

8.1. Introduction

The potential root zone within the in-field rainwater harvesting (IRWH) system is very important as it determines the water storage capacity. Storage of runoff water within the soil profile is one of the main aims of in-field rainwater harvesting. This practice increases the productivity of rainwater by reducing the major unproductive losses, namely runoff and evaporation from the soil surface. Water storage within the soil profile is central for many forms of *in-situ* rainwater harvesting like micro-catchments, contour bunds, semi-circular bunds and contour ridges (Critchley & Siegert, 1991). Such rainwater storage in the soil profile has provided IRWH a water conservation advantage both during the fallow and growing periods compared to the conventional tillage system (Botha *et al*., 2003). The storage of rainwater with IRWH during the fallow period provides the crop with a pre-plant water advantage during the establishment of the crops. Furthermore, the storage of runoff water during the fallow periods can reduce the risk of crop failure during dry (below-average) years. Hensley *et al*. (2000) reported that during the extremely dry 98/99 growing season only the IRWH plots, with a long fallow period, had produced a yield.

Since the end goal of rainwater harvesting practices is the provision of water for crop production, quantifying the storage gains available for use by crops is pivotal. Soil water storage is a function of local interaction of the supply of water entering the profile and the demand for water out of the profile (Milly, 1994). This is basically the water balance of the soil, which can be described by the following simple equation (Hillel, 1980):

Change in soil water content = Water gains – Water loses (8.1)

Under field conditions, the simple variables given in Equation 8.1 are not easily quantified. This is particularly true for the "water loses" variable. This term can have sub-components like: runoff, evaporation and deep drainage depending on the condition of application, which are difficult to measure. To deal with such challenges models of sub-components are used in the water balance (Jalota *et al*., 2000). Milly (1993) affirms that the build-up of water in the soil profile from precipitation and the subsequent depletion by the losses can be adequately described by models.

Accounting for the water in the soil profile with the water balance equation is very essential to asses the performance of a rainwater harvesting system. This accounting is done by either measuring the water balance components or modelling them. Most of the time the component which is more difficult to measure is left out to be quantified by the water balance. Oweis & Taimeh (1996) evaluated a rainwater harvesting system by analysing the water balance components. They measured all the water balance components except evaporation which is determined from the water balance equation. Hensley *et al.* (2000) and Botha *et al.* (2003) used the water balance components of the growing season to explain the yield difference observed between the IRWH and the conventional tillage treatments. In those studies they modelled the water balance components like runoff, evaporation and deep drainage. Mugabe (2004) has shown the benefits of infiltration pits in increasing water stored in the soil. He quantified the water storage by measuring only the soil water content at different times and did not quantify or model the other components of the water balance equation. Wang *et al*. (2007) also evaluated the water-use efficiency of ridge and furrow micro-water harvesting by measuring only the runoff.

Accounting of water during fallow season in an IRWH system must be geared towards determining the storage achieved. Botha *et al*. (2003) had shown that the standard 1:2 basin to runoff strip length (RSL) ratio IRWH creates better opportunity to store water compared to conventional tillage. The recent advances that enabled the mechanized preparation of any desired basin to RSL ratio (van Rensburg *et al*., 2012), necessitates the investigation of effect of different RSL from the standard 2 m runoff area. Generally, the amount of runoff that can be harvested is expected to increase with increasing RSL. However, depending on the rainfall characteristics and soil conditions different results can be obtained. For instance, the runoff amount measured from a 20 m runoff strip was less than that of a 2 m runoff strip (Botha, 2006). Based on this, it was hypothesised that different basin to RSL ratios will achieve different soil water storage during the fallow period. Thus, the objectives of this study were (i) to characterize the water balance under IRWH plots by integrating models of the water balance components; (ii) to evaluate the storage gains achieved by different basin to RSL ratio during the fallow period.

8.2. Materials and methods

8.2.1. Description of the experiment

This study targeted the simulation of the dynamics of water storage in the soil profile. The simulations were done for the Kenilworth/Bainsvlei and Paradys/Tukulu ecotopes. The detail soil and climatic properties of the two ecotopes are provided in Chapter 1. The principal characteristics among other important physical characteristics, which determine the storage of water in the profile is the depth of the soil. The two ecotopes considered here were different in this regard. The Kenilworth/Bainsvlei ecotope had a deep soil and the simulation was done for the top 1800 mm. The Paradys/Tukulu ecotope had shallow soil and the simulation was done for the depth of 900 mm. The storage in the soil profile then refers to the water held on these depths of the two soils. The methods and models of simulating the water balance components are described in the following sections.

The experiment was conducted in three variation of basin to RSL ratios. The three basin to runoff strip length variations were: 1:1, 1:2 and 1:3. The water balance components which varied for the three sets were the runoff collected and the soil water evaporation. Thus different models were used to simulate these components in each ratio variation.

8.2.2. Simulation of the water balance components

The simulation of the water balance for the two ecotopes was done in a Microsoft Excel spreadsheet to determine the water storage achieved with the IRWH system. Since the practice of rainwater harvesting directs the water into the profile under the basin, the study mainly focused on the water balance under the basins. For the purpose of providing the full picture of water dynamics under IRWH system, the water balance was also done for every 1 m of the runoff strip and the combined result of the basin and runoff strip is presented. The water balance exercise for the two strips of IRWH, as presented in Equation 8.2, varies in terms of the runoff (IR_{off}) factor. It becomes positive for the basin strip and negative for the runoff strip.

$$\Delta W = R \pm IR_{off} - Es - D \quad (8.2)$$

Where:

ΔW	=	change in soil water content (mm)
R	=	rainfall (mm)
IR_{off}	=	in-field runoff: positive for basin & negative for runoff strip (mm)
Es	=	evaporation from the soil (mm)
D	=	deep drainage (mm)

The simulation with Equation 8.2 was programmed to determining the daily change in soil water content. The ΔW in Equation 8.2 would be expressed as the difference of soil water content of two consecutive days (Equation 8.3). Thus the equation can be expressed as:

$$W_{i+1} - W_i = R \pm IR_{off} - E_s - D \quad (8.3)$$

$$W_{i+1} = R \pm IR_{off} - E_s - D + W_i \quad (8.4)$$

Where:

W_i	=	initial soil water content (mm)
W_{i+1}	=	soil water content for the next day (mm)

Having the initial soil water content and the input for the components of the water balance, the soil water content in a daily time step was computed. The procedure in determining each component of the water balance is discussed below.

8.2.2.1. Weather data

Daily weather data for the two stations representing the two ecotopes were obtained from the ARC-ICW Weather Data Bank. The weather station for the Kenilworth/Bainsvlei ecotope was located within the experimental field. The weather station at the Paradys/Tukulu ecotope was vandalized and another station closer to it (Wegsluit weather station) was used. The daily rainfall data was used directly as an input for the water balance described in Equation 8.4. Another important weather parameter needed was the daily reference evapotranspiration (ET_o) data. This was used as an input in the simulation of soil water evaporation (Es). The weather data from these two stations were

used to validate the model as well as to describe the simulation results for the year 2009-2010.

Another weather data set was used for setting up of different scenarios which are discussed in Section 8.2.4. This data set was long-term daily weather data from the period 1922 to 2007 for the Glen Agricultural Institute, which is representative of the climate in the Bloemfontein area. From this data set, the years that were representative of the selected scenario were used. The rainfall and ET_o from this data set were used as input for the models.

8.2.2.2. Runoff simulation

To determine the in-field runoff amount that was used as an input for Equation 8.4, empirical runoff models developed for each ecotope were used. The empirical models related rainfall amount to the runoff generated. The runoff models used were peculiar for a given runoff strip length. These models were developed in Chapter 6. The models used were of the forms given below and the coefficients for each model are given in Table 8.1.

$$IR_{off} = aR + b \tag{8.5}$$

Where:

IR_{off} = Runoff (mm)

R = Rainfall (mm)

a & b = Coefficients (values are provided in Table 8.1)

Table 8.1 Coefficients for Equation 8.5 under different basin to RSL ratios on the Kenilworth/Bainsvlei and Paradys/Tukulu ecotopes.

Coefficients	Kenilworth/Bainsvlei ecotope			Paradys/Tukulu ecotope		
	1:1	1:2	1:3	1:1	1:2	1:3
a	0.622	0.498	0.494	0.668	0.809	0.933
b	-2.080	-1.370	-3.270	-7.130	-9.960	-12.550

8.2.2.3. Evaporation simulation

The daily soil evaporation values used as an input for Equation 8.4 were determined by employing evaporation models. Two types of evaporation model were used; (i) Ritchie (1972) evaporation prediction (REP) model and (ii) empirical models developed for each basin to RSL ratio. The empirical models were used for the Kenilworth/Bainsvlei ecotope, while the REP model was used for the Paradys/Tukulu ecotope (Equation 8.7). The models used for the basin area were validated in Chapter 7 and the validation results for the models used on runoff areas are provided in Appendices B.1 – B.2. The empirical models used for the Kenilworth/Bainsvlei ecotope were of the form given in Equation 8.6. The coefficients for different sections are provided in Table 8.2.

$$\sum \mathrm{E(t)} = \mathrm{c}\sqrt{t} - \mathrm{d}\sqrt{\sum \mathrm{ET_o}} + \mathrm{f} \qquad (8.6)$$

Where:

$\sum$E(t)	=	Cumulative evaporation at time t (days)
$\sum ET_o$	=	Cumulative reference evapotranspiration
c, d and f	=	Coefficients (values are provided in Table 8.2)

$$\sum \mathrm{E\ (t)} = \alpha\sqrt{t} \qquad (8.7)$$

Where:

$\sum$E(t)	=	Cumulative evaporation at time t in days (mm)
$\sum ET_o$	=	Cumulative reference evapotranspiration (mm)
α	=	Parameter characterizing the Es process (mm $d^{-0.5}$); values for each section is provided in Table 8.2

Table 8.2 Coefficients for Equations 8.6 and 8.7 representing each meter of the different basin to RSL ratios.

Coefficients	1m basin area			1st 1 m RSL			2nd 1m RSL		3rd 1m RSL
	1:1	1:2	1:3	1:1	1:2	1:3	1:2	1:3	1:3
c	2.373	3.543	3.205	2.701	3.320	3.892	3.195	1.738	1.224
d	-0.446	-0.677	-0.818	-0.676	-1.101	-1.052	-0.864	-0.424	-0.192
f	2.670	0.839	2.690	0.190	0.235	1.153	0.133	0.456	0.775
α values	3.1	4.6	5.8	4.1	4.8	3.9	2.7	2.8	1.5

For the purpose of simulating soil water evaporation on a daily time step and to determine the effect of wetting from rain, a procedure adapted from Ritchie (1972) was used (Figure 8.1). Time *t* represented days after rain. The amount of rain that was enough to reset the time *t* to zero was determined by the algorithm given in Figure 8.1. In the algorithm two terms of evaporation are given: the cumulative evaporation (∑Es) and daily evaporation (Es). In the flow chart describing the algorithm the decision box just before the end is reached from four directions. In the three directions Es is directly determined, while in the one direction ∑Es is determined. In the case where ∑Es is given Es was determined by subtracting the ∑Es of consecutive days.

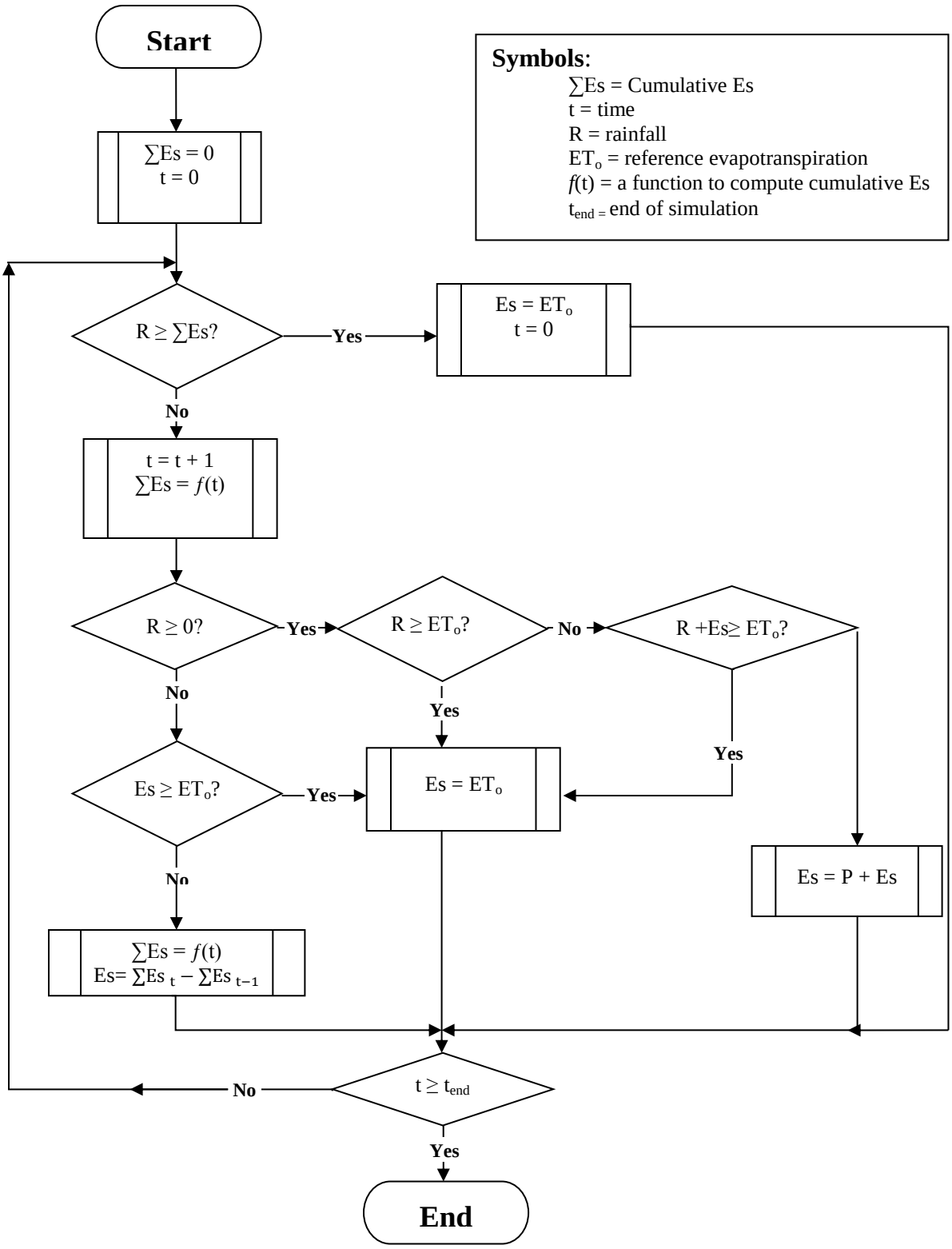

Figure 8.1 Flow chart for determining evaporation from the soil on a daily time step.

8.2.2.4. Drainage simulation

The deep drainage input for Equation 8.4 was determined by drainage curve equations (Equations 8.8 and 8.9). The drainage curves were constructed from data provided in Appendix C and G of Chimungu (2009). These data were water content of covered soil monolith taken at selected times after saturation of the soil. Chimungu (2009) determined the drained upper limit (DUL) of the two soils, which were 475 and 227 mm for the Kenilworth/Bainsvlei and Paradys/Tukulu ecotopes, respectively for the depths considered (root-zone). For values of soil water content less than the DUL the drainage values were assumed to be negligible and taken as zero (Ratliff *et al*., 1983). For values greater than the DUL, the relations between soil water content and daily drainage amount developed from the drainage curve were employed (Bennie *et al*., 1998). These relations for each ecotope are given below:

Kenilworth/Bainsvlei ecotope:

$$D = 8E - 15e^{0.068W} \quad (8.8)$$

Paradys/Tukulu ecotope:

$$D = 3E - 61e^{0.5582W} \quad (8.9)$$

Where:

D = Daily drainage amount (mm)

W = Soil water content (mm)

8.2.3. Validation of the integrated soil water balance model

To validate the integrated water balance model, the simulated daily soil water content was compared to the measured daily soil water content. The soil water content was measured by DFM capacitance probes. The details of soil water measurement of the probes are given in Section 5.2.3. The time selected for the validation of the integrated water balance model spanned between, March 24, 2010 and June 08, 2010 for the Kenilworth/Bainsvlei ecotope and March 01, 2010 and May 26, 2010 for the Paradys/Tukulu ecotope. These provided 76 and 87 test days for the

Kenilworth/Bainsvlei and Paradys/Tukulu ecotopes, respectively. The simulation depth was made to match to that of the soil water measurement. The model performance evaluation parameters described in Wilmott (1981) were used for model evaluation.

8.2.4. Comparison of scenarios of water storage

To create relevant scenarios different initial soil water content and climatic variation were considered. Long-term climatic data (84 years) was analysed to see the variation of rainfall over long and short fallow seasons (for details see Appendices A.1 – A.4). For long fallow of 18 months the average rainfall was 621 mm while for the short fallow it was 164 mm. Based on this information two variations of rainfall amount were considered: a near-average and a below-average. Two variations of initial soil water content were also considered. These variations were: half-full profile and empty profile. The water content for empty profile was assumed as the residual water content or the water content of the soil profile at 1500 KPa. The average value between this water content and DUL was then taken as the half-full profile water content.

Combinations of the above initial soil water and rainfall variations were used to setup four different scenarios. These scenarios were: near-average rainfall – empty soil profile (NAR-EP), near-average rainfall – half-full soil profile (NAR-HP), below-average rainfall – empty soil profile (BAR-EP) and below-average rainfall – half-full soil profile (BAR-HP). These scenarios were created for long-fallow and short-fallow. The long fallow spanned 18 months, while the short fallow spanned 6 months. In total there were 8 scenarios and each scenario was applied to simulate the soil water balance under the three basin to RSL ratios.

8.2.5. Rainwater storage efficiency

Rainwater storage efficiency was computed for each scenario by Equation 8.10. The storage achieved during the time of simulation was considered.

$$\mathrm{RSE} = \Delta W / R \times 100 \tag{8.10}$$

Where:

ΔW = Change in water content (mm)

R = Rainfall amount received (mm)

8.3. Results and discussion

8.3.1. Performance of the integrated water balance model on the basin strip

The simulated and the measured soil water content of the period selected for validation of the integrated soil water balance model are presented in Figures 8.2 (Kenilworth/Bainsvlei ecotope) and 8.3 (Paradys/Tukulu ecotope) for three basin to RSL ratio. From these figures it can be seen that the simulated daily soil water content followed the same trend as that of the measured. This is clearly seen in the case of Kenilworth/Bainsvlei ecotope in that every inflection point of the two lines for the simulated and measured were the same only varying in elevation. In the case of the Paradys/Tukulu ecotope, the simulated line generally followed the same pattern as that of the measured with minor differences. This is due to the weather data used for that ecotope. The data was not exactly from the same locality but from another station nearby which could have minor differences.

The depiction of the simulated and measured soil water content in Figures 8.2 and 8.3 enables only visual comparison between the two ecotopes. Table 8.3 takes this comparison further by providing quantitative evaluation of the integrated soil water balance model. From this table it can be seen that the integrated model gave good prediction with acceptable errors involved. The error involved is indicated by the RMSE values reported. This error is acceptable because this is the sum total of the three (evaporation, runoff and drainage) models of the components of the soil water balance. From Chapter 6 and 7, it can be seen that there was some level of error involved in applying the runoff and evaporation models, contributing to this total error.

From Table 8.3 it can be seen that the D-index value and the coefficients of determination (R^2) were fairly acceptable for Kenilworth/Bainsvlei ecotope. Comparable D-index values were also found for the Paradys/Tukulu ecotope. The R^2 values, however, were

poor. This has resulted from the disparity in weather data used for the Paradys/Tukulu ecotope. The RMSEs/RMSE ratio showed that there was a systematic bias, which is clearly indicated on Figures 8.2 and 8.3 by the over prediction of soil water content. The simulated soil water content tend to over-predict soil water content on average by the indicated mean absolute error (MAE).

Table 8.3 Statistical performance evaluation for the validation of the integrated soil water balance.

Statistical parameter	Kenilworth/Bainsvlei ecotope			Paradys/Tukulu ecotope		
	1:1	1:2	1:3	1:1	1:2	1:3
RMSE	28.06	26.59	24.79	16.11	14.40	13.86
RMSEs	27.70	26.12	23.94	15.55	12.88	12.35
RMSEu	4.45	4.98	6.40	4.22	6.44	6.29
MAE	27.29	25.25	22.93	12.61	13.07	12.56
R^2	0.61	0.76	0.60	0.19	0.29	0.42
D-index	0.45	0.61	0.60	0.49	0.58	0.58
RMSEs/RMSE	0.99	0.98	0.97	0.97	0.89	0.89

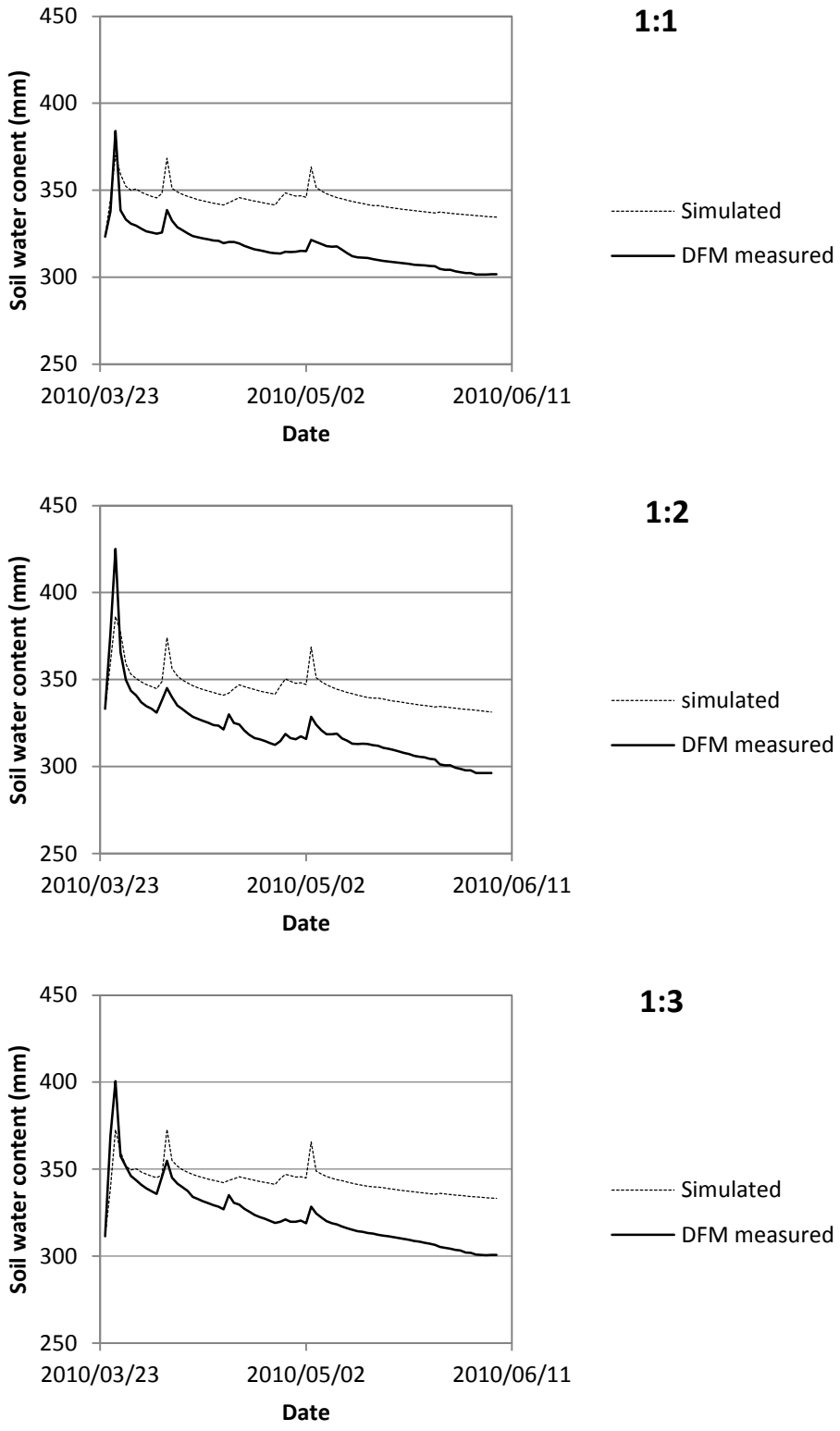

Figure 8.2 Measured and simulated soil water content for the basin strip as influenced by different RSL on the Kenilworth/Bainsvlei ecotope.

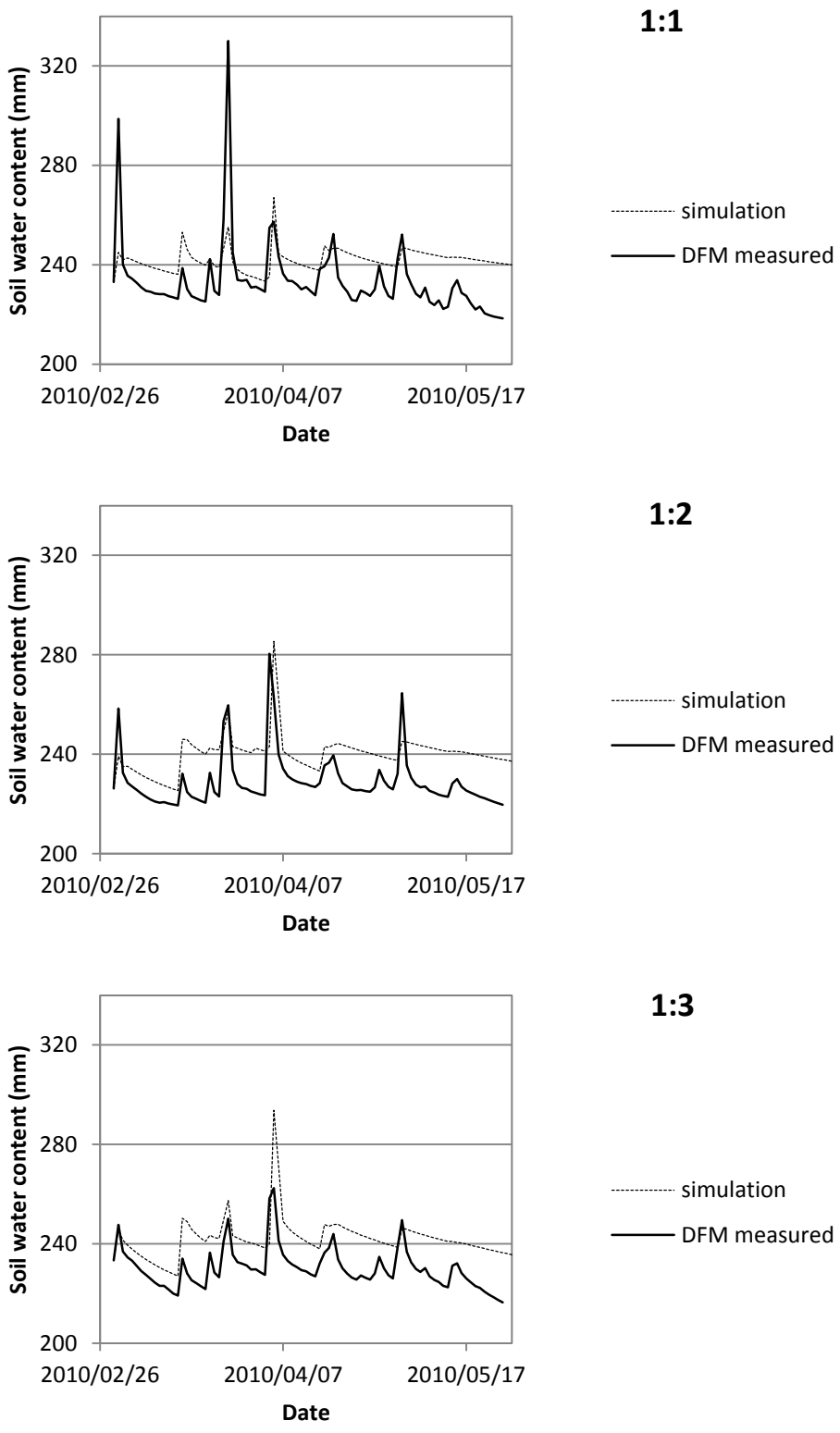

Figure 8.3 Measured and simulated soil water content for the basin strip as influenced by different RSL on the Paradys/Tukulu ecotope.

To justify the use of the integrated soil water balance model, the performance results (Table 8.3) need to be compared to other soil water balance studies. When comparing the RMSE values the fact that it is scale dependent should be taken into consideration (Ahlburg, 1992). For instance the casual comparison between the two ecotopes might give the impression that the results were better for Paradys/Tukulu ecotope. However, this need to be evaluated with respect to the soil depth considered for each ecotope. Since RMSE is scale dependent, with increasing depth the error increases accordingly. Zere (2005) for instance, reported RMSE values that ranged between 0.3 and 13.9 mm, yet this was done for layers that sub-divided the potential rooting depth to sub-layers of 300 mm. Pooling the RMSE values of the sub-layers gave values comparable to that of Kenilworth/Bainsvlei ecotope. Moret *et al*. (2007) reported an average of 0.03 m^3 m^{-3} of RMSE for a depth of 700 mm. This yields an RMSE of 21 mm for the depth considered. Abraha & Savage (2008) reported RMSE values of 7.1, 14.9 and 15.9 mm for rooting depth of 400, 400 and 700 mm, respectively. These RMSE value are comparable to that of Paradys/Tukulu ecotope, which was simulated for potential rooting depth of 900 mm. Abraha & Savage (2008) also reported the systematic and unsystematic RMSE values and the calculation of the RMSEs/RMSE yielded values ranging from 0.25 to 0.9, with most of the values greater than 0.8.

8.3.2. Sample fallow soil water balance simulation on the basin strip

The resulting soil water levels from transactions of water gain and loss for the soil depths considered are captured in the outcomes of the integrated soil water model. These results are presented in Figures 8.4 and 8.5. These figures showed that there was a sharp increase in the soil water content with the input of rain incidents, followed by gradual decline due to evaporation. In the earlier days of the fallow period, since the soil water content was low and the incidents of rain was high there was sharp increase until the soil water content reached the DUL values. Beyond the DUL values sharp increase in soil water content due to rain inputs were followed by decline due to drainage plus evaporation.

The dynamics of soil water accumulation varied depending on the initial soil water content and the basin to RSL ratio, till the time soil water reached the DUL value.

Beyond the DUL value the drainage process controls the soil water content, thus all the ratios are expected to behave more or less similarly. At the Kenilworth/Bainsvlei ecotope, the initial soil water contents were 384, 395 and 362 mm for the 1:1, 1:2 and 1:3 ratios, respectively. Since the 1:2 basin to RSL ratio had the highest initial soil water content, it reached the DUL value a week earlier than the other ratios. The 1:3 basin to RSL ratio reached the DUL at equal time with the 1:1 despite the initial soil water content of the former being 20 mm lower than the latter. The runoff harvested for the different ratios was different but the variation was not linear. The runoff amount ranking according to the rain conditions that prevailed in the year 2009-2010 was 1:2, 1:3 and 1:1 (the detail is given in Table 8.4). This ranking can be confusing since more runoff is expected with increased RSL. The difference can be explained by the models (section 8.2.2.2) representing the two basin to RSL ratios. The threshold rainfall amount needed for runoff generation in the 1:2 ratio was 4 mm less than that of the 1:3 ratio. This means if the majority of rain events received is of lower rainfall amount, more runoff is expected in the 1:2 ratio. Conversely, if considerable number of the rain events come as events of higher rainfall amounts, more runoff is expected from the 1:3 ratio compared to 1:2 ratio. In the case of the Paradys/Tukulu ecotope the initial soil water contents were comparable with 180, 185 and 186 mm for the 1:1, 1:2 and 1:3 basin to RSL ratios, respectively. Since the runoff generation for this ecotope was linearly related to the RSL, the time need for each ratio was according to the RSL. In both ecotopes the DUL was reached within two months of the rainy season. Under such condition where the storage capacity is limited and a relatively wet year is experienced the rainwater from subsequent events is bound to be lost in the form of evaporation and drainage.

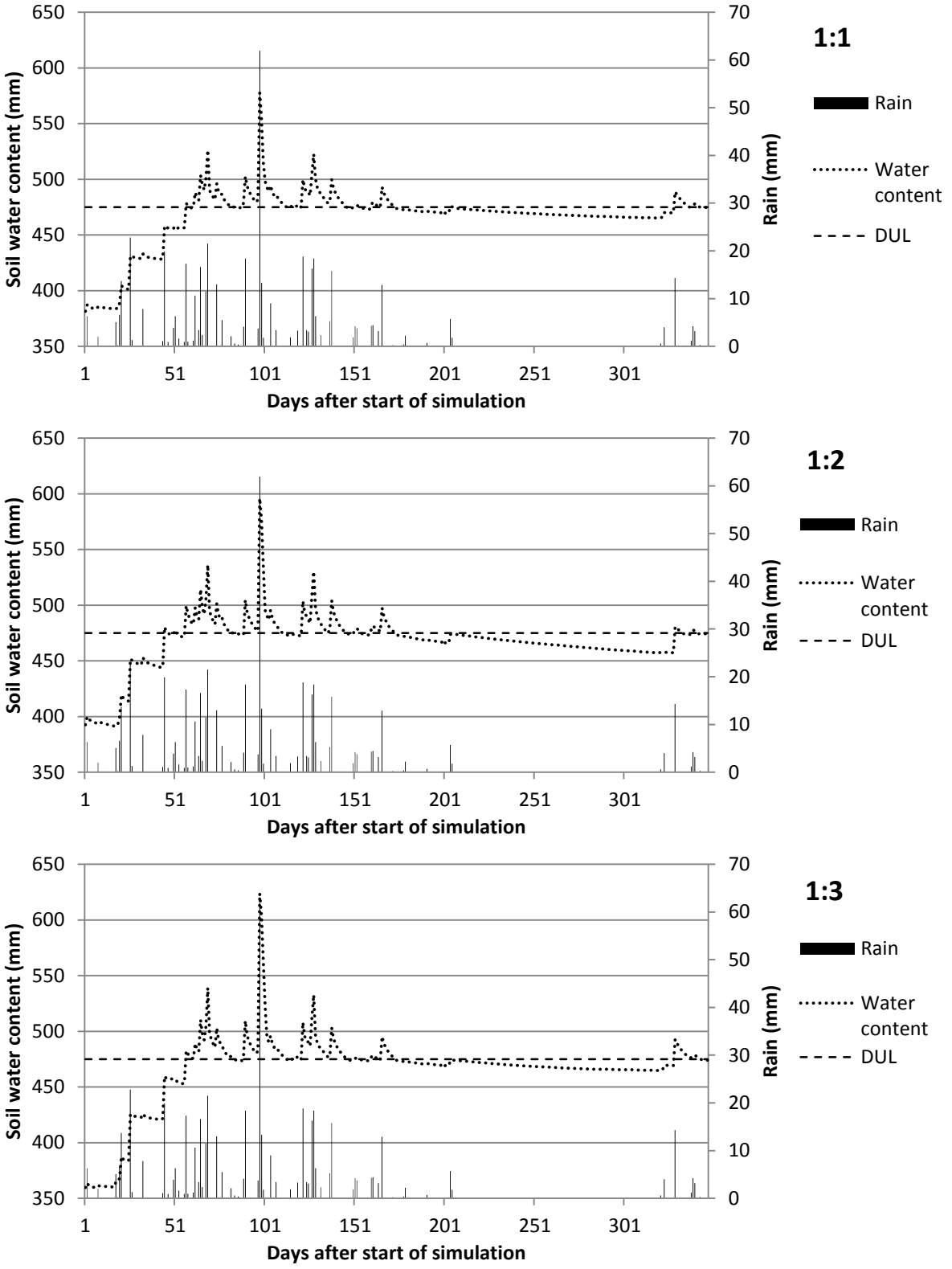

Figure 8.4 Soil water content during fallow soil water balance simulation on the basin strip of Kenilworth/Bainsvlei ecotope for different basin to RSL ratios.

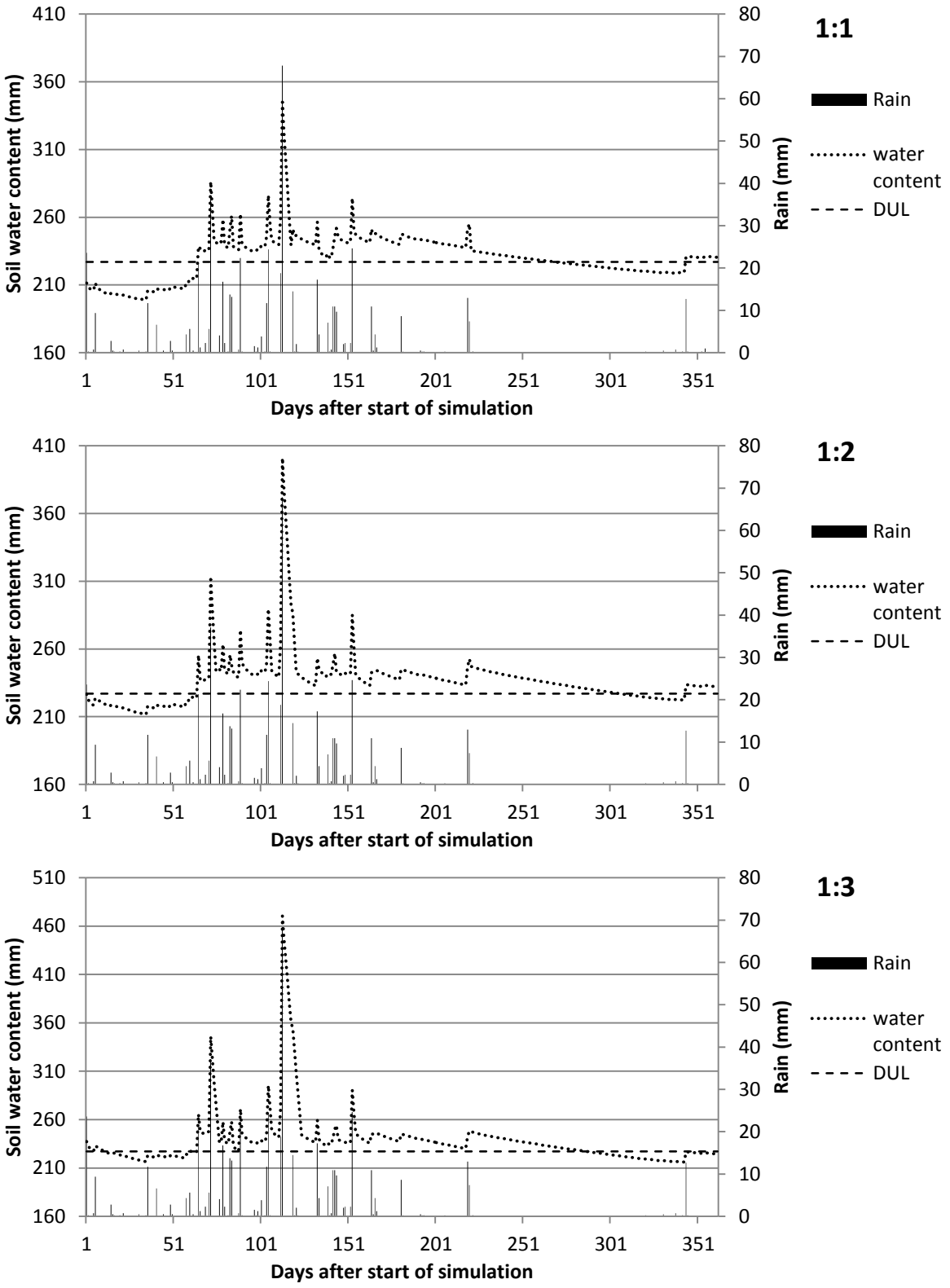

Figure 8.5 Soil water content during fallow soil water balance simulation on the basin strip of Paradys/Tukulu ecotope for different basin to RSL ratios.

Table 8.4 Water balance components for simulation done with measured initial soil water content during the fallow period on the Kenilworth/Bainsvlei and Paradys/Tukulu ecotopes (Nov 2009 – Nov 2010).

Ecotope	Water balance components	Basin to RSL ratios		
		1:1	1:2	1:3
Kenilworth/Bainsvlei	Rain (mm)	492.8	492.8	492.8
	Evaporation (mm)	216.2	313.4	225.1
	Runoff (mm)	195.3	338.2	327.5
	Drainage (mm)	381.6	438.8	483.7
	Change (mm)	90.3	78.8	111.5
Paradys/Tukulu	Rain (mm)	516.3	516.3	516.3
	Evaporation (mm)	262.0	289.3	337.7
	Runoff (mm)	122.6	253.2	394.4
	Drainage (mm)	326.6	434.0	534.5
	Change (mm)	50.3	46.2	38.1

8.3.3. Comparison of scenarios of fallow soil water storage under basin strip

8.3.3.1. Long fallow

Under long fallow conditions, there is ample time for enough rain to be intercepted and stored in the profile, because it covers the rainy season of the year. This can be deducted from the average rainfall value of 621 mm. Hence, the difference that can be observed for the different basin to RSL ratios would be dependent on the presence of enough storage volume (depth) to accommodate the rain intercepted. Thus, relatively the effect of basin to RSL ratio would be more perceptible in the Kenilworth/Bainsvlei ecotope compared to the Paradys/Tukulu ecotope.

On the Kenilworth/Bainsvlei ecotope the runoff generation observed for the different scenarios did not show direct linear relationship with RSL (Table 8.5). For the scenarios considered the 2 m RSL had higher runoff generation capacity than the other two. This happened because of rain events that were able to generate runoff in the 2 m did not generate runoff or was very little for the 3 m RSL. Evaporation was a major form of

water loss in the system. The evaporation proportion ranged from 36 – 58% of the water input (rainfall + runoff). Evaporation as a percentage of the water input had inverse linear relationship with RSL. This value was the highest for the 1 m and the least for 3 m RSL. Drainage proportion of the water input ranged from 0% under BAR-EP to 48% under NAR-HP. The relatively bigger storage capacity of this ecotope depending on the climatic conditions determined if drainage will be present or not.

The behaviour of water balance components for the Paradys/Tukulu ecotope was different from that of the Kenilworth/Bainsvlei ecotope. For the Paradys/Tukulu ecotope all the components of the water balance were directly related to RSL. Thus for all the scenarios each water balance component amounts linearly increased as the RSL increased from 1 m to 3 m. The major form of water loss for all the scenarios considered was evaporation and it accounted for at least 50% of the water input (rain + runoff) into the soil. Evaporation when seen in the form of percentage of the water input, it had inverse linear relationship as in the case of the Kenilworth/Bainsvlei ecotope. Drainage was also a major shareholder in which the proportion ranged from 12 to 41% depending on the amount of rain received and RSL.

8.3.3.1.1. Storage

Generally, the soil water storage during long fallow did not vary much across the different basin to RSL ratios considered. The three basin to RSL ratios achieved soil water storage equally well. This is mainly due to the fact that there was enough rainfall intercepted to fill up the available storage. The only exception was for the scenario of below-average rainfall (BAR-EP) in the Kenilworth/Bainsvlei ecotope where the three ratios had varying level of water stored at the end of the fallow season. Under such exceptional condition, having longer runoff strip is beneficial to achieve better soil water storage of the intercepted rainfall. For this scenario (BAR-EP) the rain received was enough to fill up the storage capacity of the Paradys/Tukulu ecotope. Thus the storage achieved was comparable among the different basin to RSL ratio.

Table 8.5 Cumulative values of the water balance components (mm) for the different scenarios under long fallow conditions on the Kenilworth/Bainsvlei and Paradys/Tukulu ecotopes.

Ecotope	Water balance components	NAR-EP			NAR-HP			BAR-EP			BAR-HP		
		1:1	1:2	1:3	1:1	1:2	1:3	1:1	1:2	1:3	1:1	1:2	1:3
Kenilworth/Bainsvlei	Rain	627.8	627.8	627.8	627.8	627.8	627.8	322.5	322.5	322.5	322.5	322.5	322.5
	Evaporation	385.5	450.8	379.1	394.6	462.3	388.8	242.6	291.2	246.3	260.1	314.1	264.5
	runoff	255.6	440.2	417.0	255.6	440.2	417.0	126.4	217.5	200.7	126.4	217.5	200.7
	Drainage	195.0	318.6	365.1	332.9	454.0	502.5	0.0	0.0	0.0	55.5	98.8	123.6
	Δw	303.0	298.7	300.5	156.0	151.7	153.5	206.4	248.7	276.9	133.3	127.0	135.1
Paradys/Tukulu	Rain	627.8	627.8	627.8	627.8	627.8	627.8	322.5	322.5	322.5	322.5	322.5	322.5
	Evaporation	439.5	455.1	494.4	453.5	474.0	517.2	253.6	253.3	286.1	285.2	293.4	325.7
	runoff	119.3	245.2	375.8	119.3	245.2	375.8	49.6	92.4	133.5	49.6	92.4	133.5
	Drainage	214.0	317.4	407.9	243.2	338.4	419.6	45.0	88.6	103.3	61.6	88.5	103.7
	Δw	93.6	100.6	101.3	50.4	60.7	66.8	73.5	73.0	66.6	25.3	33.0	26.6

Δw: Change in soil water content
NAR-EP: Near-average rainfall – empty soil profile
NAR-HP: Near-average rainfall – half-full soil profile
BAR-EP: Below-average rainfall – empty soil profile
BAR-HP: Below-average rainfall – half-full soil profile

Table 8.6 Cumulative values of the water balance components (mm) for the different scenarios under short fallow conditions on the Kenilworth/Bainsvlei and Paradys/Tukulu ecotopes.

Ecotope	Water balance components	NAR-EP			NAR-HP			BAR-EP			BAR-HP		
		1:1	1:2	1:3	1:1	1:2	1:3	1:1	1:2	1:3	1:1	1:2	1:3
Kenilworth/Bainsvlei	Rain	162.3	162.3	162.3	162.3	162.3	162.3	122.6	122.6	122.6	122.6	122.6	122.6
	Evaporation	85.4	107.4	71.1	90.6	114.6	78.6	70.7	78.5	72.5	84.1	97.2	86.8
	runoff	64.8	110.8	111.2	64.8	110.8	111.2	44.9	78.9	61.6	44.9	78.9	61.6
	Drainage	0.0	0.0	0.0	0.0	6.2	33.5	0.0	0.0	0.0	0.0	0.0	0.0
	Δw	141.7	165.7	202.4	136.5	152.3	161.4	96.7	123.0	111.7	83.3	104.2	97.4
Paradys/Tukulu	Rain	162.3	162.3	162.3	162.3	162.3	162.3	122.6	122.6	122.6	122.6	122.6	122.6
	Evaporation	91.6	106.7	112.4	103.6	123.2	133.7	52.9	56.9	60.1	81.1	97.0	100.0
	runoff	35.5	72.7	109.9	35.5	72.7	109.9	12.2	20.3	28.3	12.2	20.3	28.3
	Drainage	19.7	39.5	58.6	40.6	59.2	84.3	0.0	0.0	0.0	0.0	0.0	0.0
	Δw	86.4	88.9	101.2	53.7	52.7	54.3	81.9	86.0	90.8	53.7	46.0	50.9

Δw: Change in soil water content
NAR-EP: Near-average rainfall – empty soil profile
NAR-HP: Near-average rainfall – half-full soil profile
BAR-EP: Below-average rainfall – empty soil profile
BAR-HP: below-average rainfall – half-full soil profile

8.3.3.2. Short fallow

With the conditions prevailing during a short fallow period of between harvest time and the summer planting that follows, different outcomes of storage are observed for different basin to RSL ratios. The scenario variations of climate and soil water storage capacity had profound influence on the resulting storage. The average rainfall observed from the long-term climatic data was 164 mm. This rainfall amount was enough to fill up the storage capacity of the Paradys/Tukulu ecotope but not that of the Kenilworth/Bainsvlei ecotope. The effect of climate clearly dictated the water storage conditions when below-average rainfall scenarios were considered. For the below-average rainfall scenarios, both ecotopes failed to reach a full profile even with the half-full profile scenarios. Under these conditions the contribution of RSL difference in determining the amount of soil water storage could be clearly observed.

As described for the long-fallow, the water balance components' relationship with RSL was not direct for the Kenilworth/Bainsvlei ecotope (Table 8.6). For the near-average rainfall scenario, the runoff collected increased with RSL but the difference observed between the 2 m and 3 m RSLs was less than 1 mm. For the below-average rainfall, the runoff collected for the 2 m RSL was higher than that of the 3 m. The runoff generation capacity of the 3 m, as discussed above, becomes more if there were considerable big amount rainfall events during the season. For smaller events the 2 m will generate some runoff while the 3 m RSL does not. This explains the difference observed for the average and below-average rainfall scenarios. The evaporation amount observed for the 2 m RSL was consistently higher than 1 and 3 m RSLs. The observed evaporation as a proportion of the input water (rain + runoff) was comparable for the three RSLs on the below-average rainfall scenarios. This value on the near-average rainfall scenarios was comparable for the 1 and 2 m RSLs, while that of the 3 m was consistently lower. The drainage component did not exist except for the NAR-HP scenario. The observed drainage in this scenario was minimum and only occurred in the 2 and 3 m RSLs. This shows the impact of extra runoff harvested.

For the Paradys/Tukulu ecotope, the water balance components increased linearly with increasing RSL. This linear relationship was typical for the runoff and clearly showed the effect of an RSL increase. The evaporation amount observed in all scenarios followed this same pattern. However, the evaporation as a proportion of the water input (rain + runoff) was comparable among the RSLs considered, except in two scenarios: NAR-EP and BAR-HP. In the NAR-EP scenario the evaporation proportion for the 3 m RSL was lower than the other two. This is because of the relatively higher runoff value compared to the observed evaporation value. In the BAR-HP scenario the evaporation proportion observed for the 1m RSL was less than the other two. For this scenario, although there was linear increase in runoff about 8 mm for every 1 m RSL increase, the increase in evaporation from 1 m to 2m was double of the runoff. Drainage was observed only for the near-average rainfall scenarios. The drainage values increased with increasing RSL, which was the result of increased water input from the runoff harvested.

8.3.3.2.1. Storage

The impact of RSL difference on soil water storage is more visible during the short fallow period. For short fallow there is time limitation, the rain amount that can be received is also limited. With limited rain, the available storage capacity would not be filled and the ability of the system to convert the available rain into soil water storage would be clearly perceived. For the near-average rainfall scenarios of the Kenilworth/Bainsvlei ecotope, the storage linearly related with RSL. However, for the below-average rainfall scenarios there was a discrepancy. In this case, although there was increase in stored water with increased RSL, the storage was more for 2 m compared to that of 3 m. This is impact of the runoff as discussed above. For the Paradys/Tukulu ecotope the average rainfall received during short fallow was enough to fill up the storage space that the difference created by RSL would not be easily perceptible. Nevertheless, the NAR-EP scenario showed the linear increase of stored water with increasing RSL. For the below-average rainfall scenarios, there was a linear increase of 8 mm of runoff for every 1m RSL increase. This increase translated into about 4 mm difference of stored water for the BAR-EP scenario, while on the BAR-HP the storage was dictated by the amount of evaporation observed and thus there was discrepancy in the storage observed.

8.3.4. Plot level water balance simulation

8.3.4.1. Long fallow

The water balance components, spatially averaged to represent the whole plot, for the three basin to RSL ratios under different scenarios are presented in Table 8.7. When considering the water balance at a plot level of IRWH, the runoff term cancels out between the runoff strip and basin strip. This mathematically confirms that the ex-field runoff is zero. Thus the storage achieved under the IRWH system during the fallow period is a function of the two forms of loses: evaporation and drainage. From the evaporation values given in Table 8.7, the average values for the plot are less than the values given for the basins (Table 8.5). This shows that evaporation is higher on the basins and this is the result of the availability of more water in the basins as described in Chapter 5. The variation in evaporation amount observed for the different basin to RSL ratios did not have any definite pattern on the Kenilworth/Bainsvlei ecotope. The variation observed was more of random variation. At the Paradys/Tukulu ecotope, however, the evaporation appeared to increase with increasing RSL. This can be the super-imposing effect of the evaporation observed on the basin (Table 8.5). The evaporation for the basin increased linearly with increasing RSL in this ecotope, while the detail result of the runoff strip (Appendices C.1 – C.6) showed a mixed pattern.

Comparing the drainage for the whole plot to that of the basins only reveals that, that average value is reduced by more than 50%. Due to the rainwater harvesting design which concentrates the runoff water into the basins, once the DUL is exceed much drainage is expected in the basin strip. Generally, when considering the basin strip only the drainage increases with RSL increasing. The plot level drainage, however, decreases with increasing RSL. This is mainly due to the evening-out effect of the extra RSL which experience lower drainage compared to the basin strip. This pattern of drainage is clearly perceptible during wet years, while on the below-average rainfall scenarios the drainage observed between different basin to RSL ratios are comparable.

Table 8.7 Cumulative values of the water balance components (mm) for the different scenarios under long fallow conditions on the Kenilworth/Bainsvlei and Paradys/Tukulu ecotopes.

Ecotope	Water balance components	NAR-EP			NAR-HP			BAR-EP			BAR-HP		
		1:1	1:2	1:3	1:1	1:2	1:3	1:1	1:2	1:3	1:1	1:2	1:3
Kenilworth/Bainsvlei	Rain	627.8	627.8	627.8	627.8	627.8	627.8	322.5	322.5	322.5	322.5	322.5	322.5
	Evaporation	374.3	413.1	378.0	393.7	425.1	385.8	217.0	236.9	242.8	246.5	261.8	226.9
	runoff	0.0	0.0	0.0	0.0	0.0	0.0	0.0	0.0	0.0	0.0	0.0	0.0
	Drainage	97.5	106.2	91.3	166.5	151.3	125.6	0.0	0.0	0.0	27.8	32.9	30.9
	Δw	156.0	108.5	158.5	67.6	51.4	116.4	105.5	85.6	79.7	48.2	27.8	64.7
Paradys/Tukulu	Rain	627.8	627.8	627.8	627.8	627.8	627.8	322.5	322.5	322.5	322.5	322.5	322.5
	Evaporation	354.8	375.3	399.3	370.5	392.3	414.2	216.0	232.2	239.6	251.6	268.0	270.0
	runoff	0.0	0.0	0.0	0.0	0.0	0.0	0.0	0.0	0.0	0.0	0.0	0.0
	Drainage	180.3	159.1	134.3	206.2	176.6	153.4	28.1	32.9	30.4	36.7	32.8	30.9
	Δw	92.7	93.4	94.2	51.1	58.9	60.2	78.4	57.4	52.5	34.2	21.7	21.6

Δw: Change in soil water content
NAR-EP: Near-average rainfall – empty soil profile
NAR-HP: Near-average rainfall – half-full soil profile
BAR-EP: Below-average rainfall – empty soil profile
BAR-HP: Below-average rainfall – half-full soil profile

Table 8.8 Cumulative values of the water balance components (mm) for the different scenarios under short fallow conditions on the Kenilworth/Bainsvlei and Paradys/Tukulu ecotopes.

Ecotope	Water balance components	NAR-EP			NAR-HP			BAR-EP			BAR-HP		
		1:1	1:2	1:3	1:1	1:2	1:3	1:1	1:2	1:3	1:1	1:2	1:3
Kenilworth/Bainsvlei	Rain	162.3	162.3	162.3	162.3	162.3	162.3	122.6	122.6	122.6	122.6	122.6	122.6
	Evaporation	87.6	89.7	69.0	93.4	96.5	73.6	72.3	72.6	73.9	85.1	86.8	85.4
	runoff	0.0	0.0	0.0	0.0	0.0	0.0	0.0	0.0	0.0	0.0	0.0	0.0
	Drainage	0.0	0.0	0.0	0.0	2.1	8.4	0.0	0.0	0.0	0.0	0.0	0.0
	Δw	74.7	72.6	93.3	69.0	63.7	80.3	50.3	50.0	48.7	37.5	35.8	37.2
Paradys/Tukulu	Rain	162.3	162.3	162.3	162.3	162.3	162.3	122.6	122.6	122.6	122.6	122.6	122.6
	Evaporation	82.3	90.3	89.4	95.9	105.0	102.2	54.3	55.4	61.3	87.2	90.2	89.7
	runoff	0.0	0.0	0.0	0.0	0.0	0.0	0.0	0.0	0.0	0.0	0.0	0.0
	Drainage	9.9	13.2	14.7	20.3	19.7	21.1	0.0	0.0	0.0	0.0	0.0	0.0
	Δw	70.1	58.8	58.2	46.1	37.6	39.0	68.3	67.2	61.3	35.4	32.4	32.9

Δw: Change in soil water content
NAR-EP: Near-average rainfall – empty soil profile
NAR-HP: Near-average rainfall – half-full soil profile
BAR-EP: Below-average rainfall – empty soil profile
BAR-HP: Below-average rainfall – half-full soil profile

The storage achieved for the two different ecotopes was remarkably different. For the Kenilworth/Bainsvlei ecotope hardly notable storages were observed on the runoff strip and thus the spatially averaged storage value for the whole plot was about 50% less than that of the basins. Contrary to this, that of the Paradys/Tukulu ecotope was comparable for the basins and the whole plot. This is mainly the effect of the limited storage capacity for this ecotope which is about 60 mm.

8.3.4.2. Short fallow

The water balance components resulting from the simulation done for different scenarios during short fallow seasons are presented in Table 8.8. Since ex-field runoff does not exist, the runoff term is zero. With regard to drainage, the rainfall amount that could be intercepted in this short period is limited, no drainage or very little drainage is observed depending on the scenario. For the Kenilworth/Bainsvlei ecotope a very negligible amount of drainage was observed only for NAR-HP scenario. For the Paradys/Tukulu ecotope drainage amount of 10 - 21 mm was observed during the near-average rainfall scenarios. Besides these scenarios the drainage was zero. Thus, as can be observed from Table 8.8, the dominant process during the short fallow is the soil water evaporation. The evaporation observed for the whole plot was comparable to that of the basin for the Kenilworth/Bainsvlei ecotope. The only exception observed is the 1:2 basin to RSL ratio which had higher evaporation on the basins compared to the plot values. For the Paradys/Tukulu ecotope, evaporation values of the near-average rainfall scenarios were more on the basins compared to the whole plot. However, for the below-average rainfall scenarios evaporation values were comparable for basin and that of the whole plot. This strengthens the observation made in Chapter 5 that evaporation is more in the basin area which is the effect of harvested water being channelled into to this strip. This effect is super-imposingly remarkable during wet years (as observed for the long fallow and near-average rainfall of short fallow), but might not be perceptible for relatively drier scenarios (below-average rainfall).

Storage during short fallow therefore is a function of the evaporation. The storage achieved was mainly from that of the basins. This is especially true for the

Kenilworth/Bainsvlei ecotope, because the storage achieved was very little on the runoff strip. Thus, the comparison of the basin and plot storage shows that it decreased by 50% for the plot. In the case of the Paradys/Tukulu, in contrast to what was observed for the long fallow, there was a decrease in the evaporation value for the whole plot compared to that of the basin only. This comparison showed that the percentage decrease ranged between 14 and 42%. This difference observed is impact of over-capacity rain received for the long fallow compared to the short fallow average of 164 mm.

8.3.5. Rainwater storage efficiency

The rainwater storage efficiency (RSE) values computed according to Equation 8.10 for the basin strip and plot level are presented in Table 8.9. As can be deducted from Equation 8.10, RSE is dependent on the storage capacity of the soil considered and the amount of rain intercepted. The scenarios considered catered both for rainfall amount and storage capacity variation. Based on these variations, the RSE values of the basin strip ranged from 24 to 86% and 68 to 125% in the Kenilworth/Bainsvlei ecotope for the long and short fallows, respectively. These ranges for the Paradys/Tukulu ecotope were 8 to 23% and 32 to 74% for the long and short fallows, respectively. Under normal conditions 100% RSE is impossible because of the losses (evaporation and drainage) involved. In this study, despite the observed losses of evaporation, more than 100% RSE was obtained for some scenarios owing to the runoff harvested. The RSE values that can correspond to normal conditions are given for the plot level. The plot level RSE values ranged from 8 to 33% and 29 to 58% for the long and short fallows, respectively. These ranges for the Paradys/Tukulu were 7 to 24% and 23 to 56% for the long and short fallows, respectively. Botha *et al*. (2003) found fallow (7-8 months) RSE values ranging from 5 to 21% under IRWH system for an average rainfall of 298 mm. From the RSE values presented in Table 8.9, it can be seen that short fallow has higher efficiency compared to long fallow. This is in keeping with the findings of Moret *et al*. (2006).

8.3.5.1. Long fallow

From the simulation results of the long fallow, there was no big difference in the RSE values obtained for different basin to RSL ratios, when considering the basin strip only.

This is mainly the effect of enough rainfall being received to fill up the available storage capacity. The soil water holding capacity determines the highest possible water storage during fallow (Monzon *et al.*, 2006). Thus, once the water content has reached DUL, extra water harvested does not improve the RSE any further. The only exception observed for the long fallow is the BAR-EP scenario of the Kenilworth/Bainsvlei ecotope. In this scenario, the rainfall amount was low that can be accommodated by the storage capacity of that ecotope and thus linear increase of RSE with increasing RSL was observed. In the case of plot level RSE values, the Paradys/Tukulu ecotope showed more or less the same pattern as that of basin strip, in which all basin to RSL ratios had comparable RSE. This indicates that considerable amount of storage was achieved in the runoff strip besides the basin strip. On Kenilworth/Bainsvlei ecotope, the RSE observed did not show consistent pattern with RSL increase. The 1:2 basin to RSL ratio, however, had lower RSE value which was the result of higher evaporation observed for this ratio. The RSE values obtained for the plot level, for this ecotope, were less by at least 50% from that of the basin strip. This shows that the storage achieved on the runoff strip was considerably less.

8.3.5.2. Short fallow

Short fallow realized higher basin strip and plot level RSE values for both ecotopes. The basin strip RSE was higher from that of plot level owing to the harvested runoff. The following observation could be gleaned from the basin strip RSE values. For the Kenilworth/Bainsvlei ecotope the lower rainfall amount relative to the storage capacity enabled it to achieve very high RSE. The RSE obtained for different basin to RSL ratios had the expected difference for the scenarios of near-average rainfall. However, for the below-average rainfall scenarios the 2 m and 3 m RSLs had discrepancy which was the effect of the type of rainfall (high *vs*. low amount) that prevailed during the season. For the Paradys/Tukulu ecotope the limited storage capacity still played a major role, in that even with lower rainfall amounts (compared to long fallow) the soil water content reached DUL. Nevertheless, for the scenarios of empty-profile there was linear increase in RSE in relation to increasing RSL. For the scenarios of half-full profile there was no perceptible difference between different basin to RSL ratios.

Table 8.9 Rainwater storage efficiency (RSE) for the different scenarios on the Kenilworth/Bainsvlei and Paradys/Tukulu ecotopes.

Section of IRWH	Fallow type	Scenarios	Kenilworth/Bainsvlei ecotope			Paradys/Tukulu ecotope		
			1:1	1:2	1:3	1:1	1:2	1:3
Basin Strip	Long fallow	NAR-EP	48%	48%	48%	15%	16%	16%
		NAR-HP	25%	24%	24%	8%	10%	11%
		BAR-EP	64%	77%	86%	23%	23%	21%
		BAR-HP	41%	39%	42%	8%	10%	8%
	Short fallow	NAR-EP	87%	102%	125%	53%	55%	62%
		NAR-HP	84%	94%	99%	33%	32%	33%
		BAR-EP	79%	100%	91%	67%	70%	74%
		BAR-HP	68%	85%	79%	44%	38%	42%
Plot level (basin and runoff strips combined)	Long fallow	NAR-EP	25%	17%	25%	15%	15%	15%
		NAR-HP	11%	8%	19%	8%	9%	10%
		BAR-EP	33%	27%	25%	24%	18%	16%
		BAR-HP	15%	9%	20%	11%	7%	7%
	Short fallow	NAR-EP	46%	45%	58%	43%	36%	36%
		NAR-HP	42%	39%	50%	28%	23%	24%
		BAR-EP	41%	41%	40%	56%	55%	50%
		BAR-HP	31%	29%	30%	29%	26%	27%

The plot level RSE values, in the case of Kenilworth/Bainsvlei ecotope, were more of a function of the evaporation observed. In the below-average rainfall scenarios the evaporation observed for different basin to RSL ratios was comparable and the RSE values were also comparable. For the near-average rainfall scenarios there was an increase in RSE with RSL increasing from 1 m to 3 m, but the 2 m was an exception. The 1:2 basin to RSL ration consistently showed higher evaporation and consequently had lower RSE. The plot level RSE values observed for the Paradys/Tukulu ecotope were comparable for the 1:2 and 1:3 basin to RSL ratios, but were higher for 1:1 ratio. From the basin strip RSE values it can be seen the three ratios had comparable values. The difference observed on the plot level is the averaging effect of lower storage observed for the runoff strip. The reduction observed for the 1:1 ratio was less while for the 1:2 and 1:3 ratios the weighting factor increased with increasing RSL.

8.4. Conclusions and recommendations

The water balance simulation by the integrated soil water balance model revealed that the IRWH system makes good provision for rainwater storage during the fallow period. From the different scenarios considered for long fallow it can be concluded that the different basin to RSL ratios considered do not have differences in the amount of water stored. For short fallow, however, the amount of water stored increased with increasing RSL. Due to the amount of rain received and limited storage, long fallow, was not efficient in that much of the harvested water is lost through drainage. The short fallow, however, had better RSE and could enhance the productivity of IRWH. The rainwater storage efficiency of an IRWH system increases if the fallow period started with low soil water content. From the different scenarios of amount of rainfall, it is recommended that ecotopes experiencing wetter climate need to use the 1 m RSL because it can achieve the same storage compared to 2 m and 3 m RSLs.

References

Abraha, M.G. & Savage, M.J., 2008. The soil water balance of rainfed and irrigated oats, Italian rye grass and rye using the CropSyst model. *Irrigation Science* **26**:203–212.

Ahlburg, D.A., 1992. A commentary on error measures: error measures and the choice of a forecast method. *International Journal of Forecasting* **8**:99-100.

Bennie, A.T.P., Strydom, M.G. & Vrey, H.S., 1998. The application of computer models for agricultural water management on ecotope level [Afr.]. Water Research Commission report No. 625/1/98, Pretoria, South Africa.

Botha, J.J., van Rensburg, L.D., Anderson, J.J., Hensley, M., Macheli, M.S., van Staden, P.P., Kundhlande, G., Groenewald, D.C. & Baiphethi, M.N., 2003. Water conservation techniques on small plots in semi-arid areas to enhance rainfall use efficiency, food security, and sustainable crop production. Water Research Commission report No. 1176/1/03, Pretoria, South Africa.

Botha, J.J., 2006. Evaluation of maize and sunflower production in semi-arid area using in-field rainwater harvesting. Ph.D. thesis University of the Free State, Bloemfontein, South Africa.

Chimungu, J.G., 2009. Comparison of field and laboratory measured hydraulic properties of selected diagnostic soil horizons. M.Sc. thesis University of the Free State, Bloemfontein, South Africa.

Critchley, W. & Siegert, K., 1991. Water harvesting. A manual for the design and construction of water harvesting schemes for plant production. FAO Paper No. AGL/misc. /17/91, FAO, Rome.

Hensley, M., Botha, J.J., Anderson, J.J., van Staden, P.P. & du Toit, A., 2000. Optimizing rainfall use efficiency for developing farmers with limited access to irrigation water. Water Research Commission report No. 878/1/00, Pretoria, South Africa.

Hillel, D., 1980. *Applications of soil physics*. Academic press. New York.

Jalota, S.K., Arora, V.K. & Singh, O., 2000. Development and evaluation of a soil water evaporation model to assess the effects of soil texture, tillage and crop residue

management under field conditions. *Soil Use Manage.* **16**:194-199.

Milly, P.C.D., 1993. An analytic solution of the stochastic storage problem applicable to soil water. *Water Resour. Res.* **29**(11):3755–3758.

Milly, P.C.D., 1994. Climate, soil water storage, and the average annual water balance. *Water Resour. Res.* **30**(7):2143–2156.

Monzon, J.P., Sadras, V.O. & Andrade, F.H., 2006. Fallow soil evaporation and water storage as affected by stubble in sub-humid (Argentina) and semi-arid (Australia) environments. *Field Crops Research* **98**:83–90.

Moret, D., Arru´e, J.L., Lo´pez, M.V. & Gracia, R., 2006. Influence of fallowing practices on soil water and precipitation storage efficiency in semiarid Aragon (NE Spain). *Agric. Water Manage.* **82**:161-176.

Moret, D., Braud, I. & Arru´e, J.L., 2007. Water balance simulation of a dryland soil during fallow under conventional and conservation tillage in semiarid Aragon, Northeast Spain. *Soil & Tillage Research* **92**:251-263.

Mugabe, F.T., 2004. Evaluation of the benefits of infiltration pits on soil moisture in semi-arid Zimbabwe. *Journal of Agronomy* **3**(3):188-190.

Oweis, T.Y. & Taimeh, A.Y., 1996. Evaluation of a small basin water-harvesting system in the arid region of Jordan. *Water Resour. Manage.* **10**:21-34.

Ratliff, L.F., Ritchie, J.T. & Cassel, D.K., 1983. Field-measured limits of soil water availability as related to laboratory-measured properties. *Soil Sci. Soc. Amer. J.* **47**:770-775.

Ritchie, J.T., 1972. Model for predicting evaporation from a row crop with incomplete cover. *Water Resour. Res.* **8**(5):1204-1211.

Van Rensburg, L.D., Bothma, C.B., Fraenkel, C.H., Le Roux, P.A.L. & Hensley, M., 2012. In-field rainwater harvesting: mechanical tillage implements and scope for up-scaling. *Irrig. and Drain.* 61(S2):138-147.

Wang, Q., Zhang, E., Li, F. & Li, F., 2007. Runoff efficiency and the technique of micro-water harvesting with ridges and furrows, for potato production in semi-arid areas.

Water Resour. Manage. **22**:1431–1443.

Willmott, C.J., 1981. On the validation of models. *Phys. Geogr.* **2**:184-194.

Zere, T.B., 2005. The hydropedology of selected soils in the Weatherley catchment in the Eastern Cape Province of South Africa. Ph.D. thesis University of the Free State, Bloemfontein, South Africa.

9. Summary and recommendations

9.1. Summary

The main objective of this study was the integration of rainfall-runoff and evaporation models in order to determine the storage gains of a fallow practice under in-field rainwater harvesting (IRWH). The study was conducted on the Kenilworth/Bainsvlei and Paradys/Tukulu ecotopes. These ecotopes share the same semi-arid climatic conditions. The major proportion of the rainfall is received during summer and the long-term annual average rainfall is 543 mm. The fact that these ecotopes experience a summer rainy season when the evaporative demand is at its highest reveals the importance of the evaporation process. The ecotopes varied in terms of soil types. The Kenilworth/Bainsvlei ecotope has a sandy loam orthic A-horizon, overlying a fairly homogenous apedal B-horizon. The soil has an effective rooting depth of 2100 mm. The Paradys/Tukulu ecotope has a sandy clay loam orthic A-horizon underlain by a sandy clay B-horizon. This ecotope had a shallow soil depth of 900 mm. These two ecotopes provide a range that covers the dominant agricultural soils in the region in terms of soil texture and depth. These physical soil properties are important with regard to runoff generation and storage of water deeper in the soils under the IRWH structures.

IRWH increases the productivity of the received rainwater and reduces the risk of crop failure by channelling harvested runoff water into basins to store it in the profile under the basins. This storage provides a good reserve of water supply for crops during dry spells that can occur between rainfall events as a pre-plant water supply for the growing season. This reserve can be boosted by applying a fallow practice. Fallowing, as a means of water conservation, involves keeping the land free from plants and controlling weeds by spraying herbicides. The absence of plants during the fallow period leaves soil water evaporation and runoff to be the major role players in the system. Since IRWH is a runoff farming system, runoff is a central process. Soil water evaporation, on the other hand, plays a major role by determining how much of the harvested rainwater remains in the soil. Thus it was hypothesised that by integrating rainfall-runoff and evaporation models, it would be possible to characterize the water balance under the IRWH system; and to

estimate water storage during the fallow period that would be available for the next crop. With the overall objective of selecting and evaluating rainfall-runoff and soil water evaporation models, sub-objectives dealing with rainfall-runoff and soil water evaporation were addressed in different chapters.

Runoff that can be harvested in an IRWH system is a function of soil surface conditions and rainfall characteristics. Hence, rainfall event characteristics need to be analysed in order to identify parameters that are of particular significance in determining runoff generation. For this purpose, pluviographic data for the period 1992 to 2007 were analysed (Chapter 2). An algorithm of identifying rainfall events from pluviographic data was developed before the events were statistically analysed. The analyses showed that based on a threshold value for runoff generation, about 33% of the rainfall events received did not make any contribution to rainwater harvesting. The rainfall events of importance for IRWH were found to be 30 minutes and longer. Among the rainfall event characteristics considered rainfall amount and intensity were significant in determining the amount of runoff generated. The analysis further provided classes of the rainfall event characteristics with the corresponding representation from the long-term data. This serves as a guideline for producing relevant simulations, when rainfall simulation studies are intended.

Rainfall simulation can provide a practical way of mimicking natural rainfall events and observing the resulting infiltration/runoff split of the received rain. A Hofrey, mobile rainfall simulator, was used to generate rainfall events of variable intensity patterns and to observe the resulting infiltration and runoff under the IRWH setting (Chapter 3). Intensity patterns had a significant effect on the amount of runoff on the Paradys/Tukulu ecotope, but not for the Kenilworth/Bainsvlei ecotope. The monitoring of the infiltration front progress showed that it only affected the top 200 mm on both ecotopes which have varying clay contents. For the amount of rainfall events received in these ecotopes, the result shows that the amount of infiltration or runoff is mainly controlled by the top horizon of the soil. Thus, the infiltration progress during a rainfall event, for an IRWH system, can be grossly categorized according the top horizon considered. In the South

African soil classification system, this grouping could be simple in that there are only 5 diagnostic surface horizons.

In addition to runoff, as pointed above, soil water evaporation plays a significant role in the IRWH system. Before the modelling of soil water evaporation can be dealt with, issues of accurately measuring this component and its variation in the IRWH system need to be addressed. A comparison of the neutron water meter and DFM capacitance probe in measuring soil water evaporation from the top 300 mm of the soil was conducted (Chapter 4). The soil water evaporation values measured by these two instruments were compared to a control measured by a micro-lysimeter. The statistical comparison results indicated that the capacitance probes measured evaporation values were not significantly different while that of the neutron water meter was significantly different. This justified the use of capacitance probes to measure across the micro-landscape created by the IRWH system.

Comparison of soil water evaporation across different sections of the micro-landscape induced by IRWH was conducted (Chapter 5). The sections of micro-landscape of IRWH considered here were the ridge, furrow and every one meter of the crusted flat surface of the runoff strip. The comparison revealed that there were significant differences between these sections. Thus, the model that deals with soil water evaporation from an IRWH field need to treat the sections separately. The evaporation values observed for the different sections were spatially averaged to obtain plot level evaporation. The plot level soil water evaporation was compared between three basin to runoff strip length (RSL) ratios. This comparison revealed that there were no significant differences between the basin to RSL ratios considered.

Models of both rainfall-runoff and soil water evaporation were calibrated and validated for each ecotope. The rainfall-runoff models were used to predict the in-field runoff induced from the runoff strip of the IRWH system (Chapter 6). The models considered were: Morin and Cluff (1980) (MC) and locally developed empirical runoff models. The empirical runoff model related runoff amount with the amount of rainfall received. Both models gave good prediction of in-field runoff for different basin to RSL ratios. The

different coefficients obtained for different basin to RSL ratios revealed the effect of RSL on runoff generation. Statistical model performance evaluation parameters were used to compare the performance of the two models. The result showed that for both ecotopes the locally developed empirical runoff models performed better.

Soil water evaporation modelling was done on evaporation data of selected rain-free drying cycles (Chapter 7). To address the finding of Chapter 5, evaporation modelling of different sections was done separately. Two models of soil water evaporation: Ritchie (1972) evaporation prediction (REP) model and locally developed empirical model were considered. The empirical model used two parameters: square-root of time and square-root of cumulative reference evaporation to predict soil water evaporation. Both models showed acceptable performance, but the performance varied for the two ecotopes. The empirical evaporation prediction model performed better on the Kenilworth/Bainsvlei ecotope, while the REP model gave the best prediction for the Paradys/Tukulu ecotope. Hence, the use of a model according to the best performance for each ecotope was recommended.

Integration of the water balance component models was done to simulate the water storage achieved during the fallow season under different basin to RSL ratios of the IRWH system. The rainfall-runoff and evaporation models that showed the best performance for each ecotope were used to predict in-field runoff and evaporation, respectively. The in-field runoff and evaporation were the major players in determining the storage achieved in the soil profile of the basins. When soil water content was more than the drained upper limit (DUL) a drainage model was used. This water balance simulation was done for a short fallow (6 months) and long fallow (18 months) period. The simulations revealed that, for the long fallow, the basin to RSL ratio did not have a significant effect on the amount of soil water storage achieved. For the short fallow, on the other hand, the amount of water storage achieved increased with increasing RSL. Thus, it is recommended that ecotopes experiencing wetter climate need to use shorter RSL. Short RSL could achieve equal storage compared to the longer ones when the intercepted rain is enough to fill-up the profile.

9.1.1. Insights gained from the study

From the analyses of rainfall events the runoff producing potential of the received rain could be determined. Such analyses reveal that certain percentage (67% for this study) of the rainfall received has runoff production potential. This is helpful in focusing the planning of IRWH system. Furthermore, among the rainfall event characteristics considered rainfall event amount and intensity had significant effect on runoff amount produced.

Different parameters of rainfall intensity, such as average intensity, peak intensity, intensity pattern; can be considered with regard to their effect in runoff production. The rainfall intensity pattern does have a potential to influence the runoff amount generated. The expected influence is that higher intensity early during rainfall event produces less runoff, but this influence could vary on different soils.

Evaporation observation done on different sections of an IRWH micro-landscape indicated that it varied over different sections. An important lesson learned is that micro-landscape created by the IRWH practice has an influence on the soil water evaporation in the system. Thus, modelling of the system should take into account this variation into consideration.

The modelling of the two major losses of rainwater namely, soil water evaporation and runoff, could be done providing fair representation of the water dynamics of the IRWH system. By integrating the different components of the soil water balance the storage gains achieved can be clearly assessed. From such exercises it could be seen that the coupling of fallowing with the IRWH provides good opportunity to provide pre-plant water advantage by storing water in the soil. This practice is efficient only for short-fallow.

9.2. Recommendations

Fallowing under an IRWH system makes good provision for water storage. This storage can be gauged by employing rainfall-runoff and soil water evaporation models. The efficiency of fallowing for water storage in agricultural land has been a controversial

issue. This study has shown that the rainwater storage efficiency greatly varied depending on the scenarios. The efficiency is greatly affected by the received rainfall and the available storage capacity. The long fallow, for instance, was not very efficient in terms of water storage. The short fallow would be the best practice to couple with IRWH. This is particularly important because there is no opportunity cost involved since it does not cover the growing period.

This study addressed the practical representation of the IRWH water dynamics during the fallow period using water balance component models. Considerable work has also been done with regard to the growing period. Besides the work that have been done on the 2 m standard IRWH practice, studies involving different basin to RSL ratios have been done. These studies made valuable knowledge additions for the dryland (Tesfuhuney, 2012) and supplementary micro-flood irrigation (Mavimbela, 2012) IRWH system. Thus, there is a need to construct a practical model representation of the IRWH system by incorporating the works that have been done so far. This is a formidable task as it must address the applicability of the model in ecotopes beyond where the IRWH has been in practice so far.

Appendices

Appendix A.1 Rainfall amount recorded between 1June and 30 November of the same year, over the years 1923 to 2006

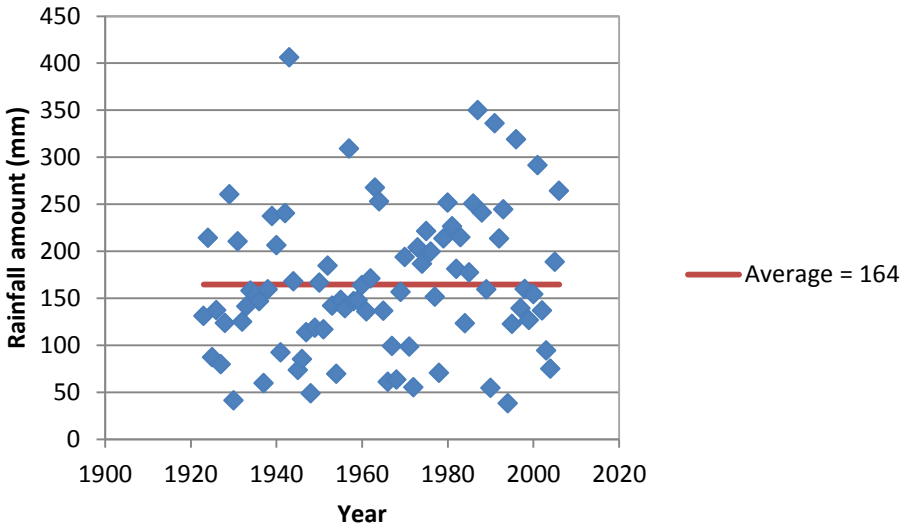

Appendix A.2 A histogram showing the frequency distribution of seasonal [1June - 30 November (6 months)] rainfall amount

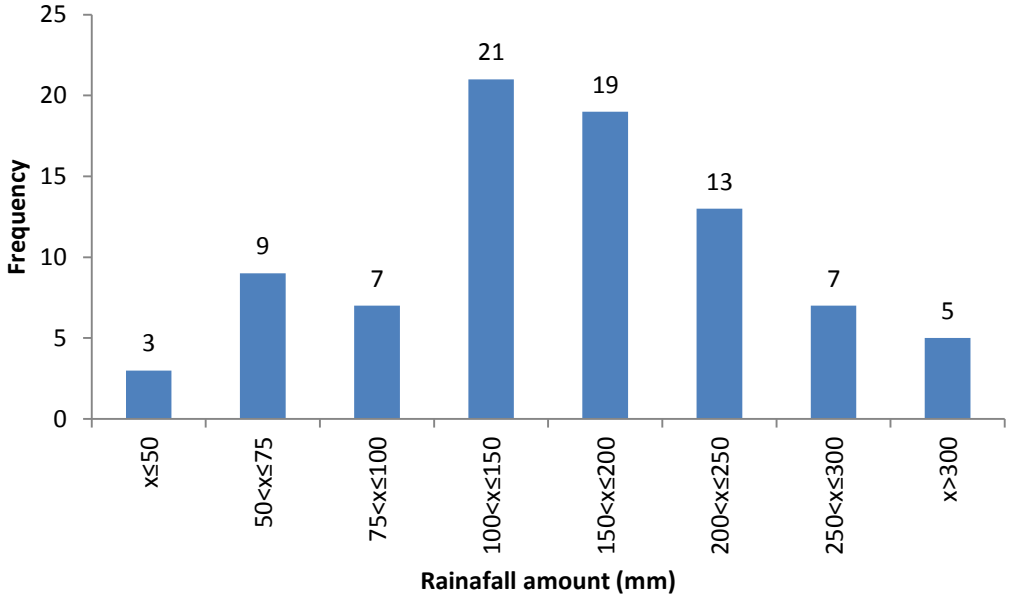

Appendix A.3 Rainfall amount recorded between 1 June and 30 November of the next year, over the years 1923 to 2006

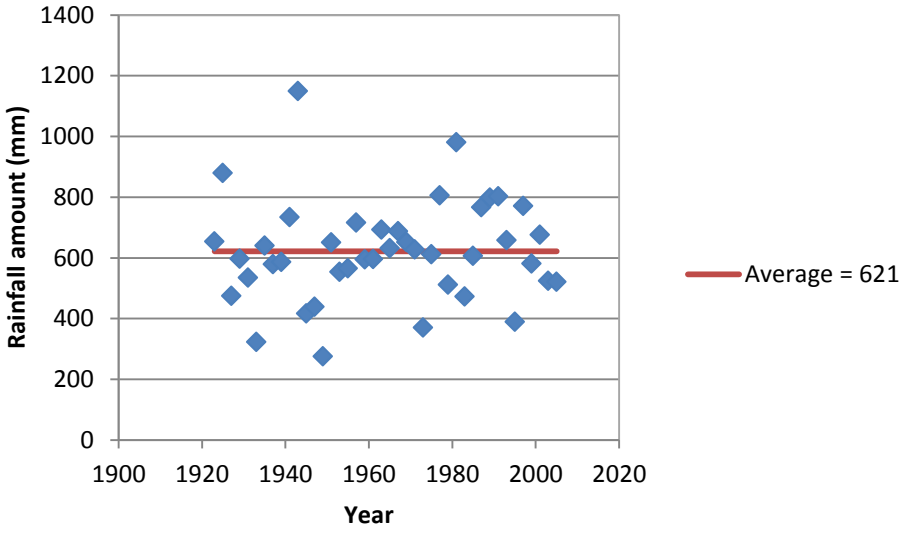

Appendix A.4 A histogram showing the frequency distribution of seasonal [1June - 30 November (18 months)] rainfall amount

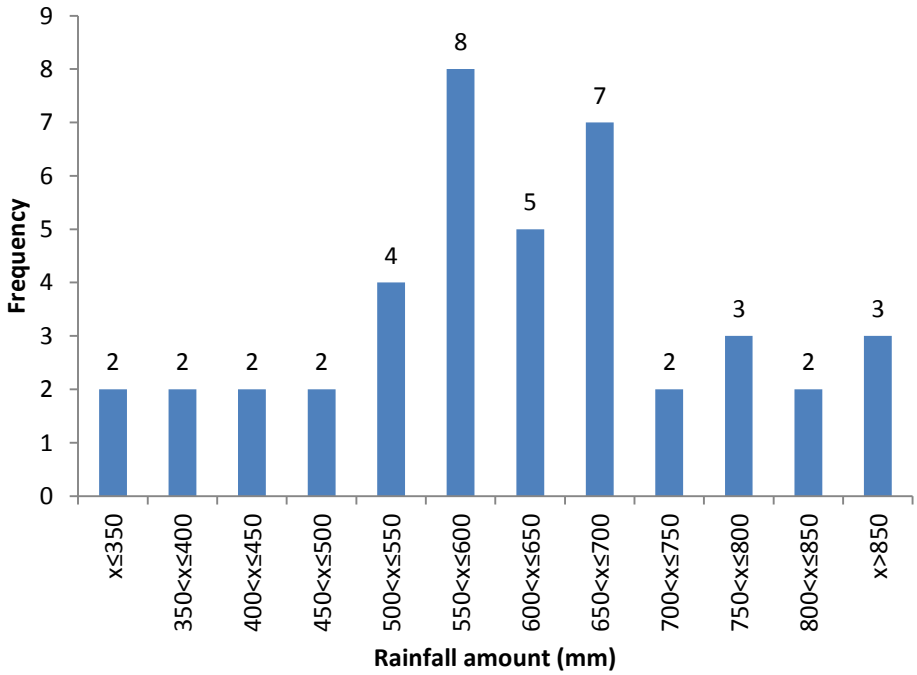

Appendix B.1 Empirical evaporation model performance evaluation on the runoff strip of IRWH system for Kenilworth/Bainsvlei ecotope.

	Calibration performance						Validation performance					
Length ratio	1:1	1:2		1:3			1:1	1:2		1:3		
Section	RO1	RO1	RO2	RO1	RO2	RO3	RO1	RO1	RO2	RO1	RO2	RO3
RMSE	0.015	0.029	0.011	0.015	0.008	0.011	0.955	1.586	0.627	0.854	0.282	1.176
RMSEs	0.000	0.002	0.000	0.000	0.000	0.000	0.947	1.569	0.585	0.782	0.265	1.174
RMSEu	0.015	0.029	0.011	0.015	0.008	0.011	0.122	0.233	0.224	0.343	0.096	0.060
MAE	0.011	0.023	0.009	0.013	0.007	0.009	0.890	1.531	0.502	0.746	0.241	1.150
r^2	0.999	0.995	1.000	1.000	0.999	0.999	0.983	0.932	0.954	0.928	0.975	0.987
D-index	1.000	0.999	1.000	1.000	1.000	1.000	0.721	0.483	0.866	0.773	0.917	0.381
slope (b)	0.999	0.995	1.000	1.000	0.999	0.999	1.536	1.662	1.663	2.435	1.674	1.805
intercept (a)	0.002	0.014	0.001	0.002	0.001	0.002	-3.071	-4.473	-2.976	-6.718	-1.805	0.019
RMSEs/RMSE	0.028	0.074	0.020	0.022	0.024	0.032	0.992	0.989	0.934	0.916	0.940	0.999

RO1: 1st 1 m section of the runoff strip
RO2: 2nd 1 m section of the runoff strip
RO3: 3rd 1 m section of the runoff strip

Appendix B**.2** Ritchie evaporation model performance evaluation on the runoff strip of IRWH system for Paradys/Tukulu ecotope

	Calibration performance						Validation performance					
Length ratio	1:1	1:2		1:3			1:1	1:2		1:3		
Section	RO1	RO1	RO2	RO1	RO2	RO3	RO1*	RO1	RO2	RO1	RO2	RO3
RMSE	1.466	0.614	0.988	1.373	2.108	1.048		0.559	2.316	2.925	0.692	1.742
RMSEs	1.401	0.489	0.961	1.246	2.082	1.031		0.351	2.315	2.918	0.654	1.737
RMSEu	0.431	0.371	0.231	0.577	0.334	0.192		0.434	0.053	0.198	0.227	0.130
MAE	1.034	0.551	0.808	0.985	1.856	0.928		0.481	2.013	2.607	0.652	1.683
r^2	0.972	0.985	0.982	0.945	0.964	0.959		0.979	0.999	0.994	0.984	0.981
D-index	0.948	0.991	0.948	0.948	0.854	0.868		0.991	0.811	0.835	0.970	0.697
slope (b)	0.659	0.860	0.646	0.665	0.465	0.479		1.010	0.543	0.590	0.805	0.686
intercept (a)	3.307	1.451	2.216	3.012	3.483	1.778		-0.455	1.657	2.033	0.768	-0.145
RMSEs/RMSE	0.956	0.797	0.972	0.907	0.987	0.983		0.629	1.000	0.998	0.945	0.997

RO1: 1st 1 m section of the runoff strip
RO2: 2nd 1 m section of the runoff strip
RO3: 3rd 1 m section of the runoff strip
* Data needed for validation was not available due to probe breakage

Appendix C.1 Cumulative values of the water balance components for the different scenarios under long fallow conditions for the first 1 m section of the runoff strip.

Ecotope	Water balance components	NAR-EP			NAR-HP			BAR-EP			BAR-HP		
		1:1	1:2	1:3	1:1	1:2	1:3	1:1	1:2	1:3	1:1	1:2	1:3
Kenilworth/Bainsvlei	Rain	627.8	627.8	627.8	627.8	627.8	627.8	322.5	322.5	322.5	322.5	322.5	322.5
	Evaporation	363	401.3	379.4	392.7	408.2	389.9	191.3	210.4	239.4	232.9	240.2	190.9
	runoff	255.6	220.1	139	255.6	220.1	139	126.4	108.7	66.9	126.4	108.7	66.9
	Drainage	0	0	0	0	0	0	0	0	0	0	0	0
	Δw	9.2	6.4	109.4	-20.5	-0.5	98.9	4.8	3.4	16.2	-36.8	-26.5	64.7
Paradys/Tukulu	Rain	627.8	627.8	627.8	627.8	627.8	627.8	322.5	322.5	322.5	322.5	322.5	322.5
	Evaporation	270.1	250.4	274.9	287.4	270	291.6	178.4	186.2	176	218	226.2	214.4
	runoff	119.3	122.6	125.3	119.3	122.6	125.3	49.6	46.2	44.5	49.6	46.2	44.5
	Drainage	146.5	159.8	128.2	169.2	180.2	151.5	11.2	10	18.1	11.7	9.9	19.7
	Δw	91.9	95	99.4	51.9	55	59.4	83.2	80.1	84	43.2	40.1	44

Δw: Change in soil water content
NAR-EP: Near-average rainfall – empty soil profile
NAR-HP: Near-average rainfall – half-full soil profile
BAR-EP: Below-average rainfall – empty soil profile
BAR-HP: Below-average rainfall – half-full soil profile

Appendix C.2 Cumulative values of the water balance components for the different scenarios under long fallow conditions for the second 1 m section of the runoff strip.

Ecotope	Water balance components	NAR-EP			NAR-HP			BAR-EP			BAR-HP		
		1:1	1:2	1:3	1:1	1:2	1:3	1:1	1:2	1:3	1:1	1:2	1:3
Kenilworth/Bainsvlei	Rain		627.8	627.8		627.8	627.8		322.5	322.5		322.5	322.5
	Evaporation		387.2	383.3		404.9	388.8		209.2	250.3		231	225
	runoff		220.1	139		220.1	139		108.7	66.9		108.7	66.9
	Drainage		0	0		0	0		0	0		0	0
	Δw		20.5	105.5		2.8	100		4.6	5.3		-17.3	30.6
Paradys/Tukulu	Rain		627.8	627.8		627.8	627.8		322.5	322.5		322.5	322.5
	Evaporation		420.5	419.7		432.9	432.5		257.1	225.3		284.5	253.6
	runoff		122.6	125.3		122.6	125.3		46.2	44.5		46.2	44.5
	Drainage		0	0		11.2	8.9		0	0		0	0
	Δw		84.7	82.9		61.1	61.1		19.1	52.7		-8.2	24.4

Δw: Change in soil water content
NAR-EP: Near-average rainfall – empty soil profile
NAR-HP: Near-average rainfall – half-full soil profile
BAR-EP: Below-average rainfall – empty soil profile
BAR-HP: Below-average rainfall – half-full soil profile

Appendix C.3 Cumulative values of the water balance components for the different scenarios under long fallow conditions for the third 1 m section of the runoff strip.

Ecotope	Water balance components	NAR-EP			NAR-HP			BAR-EP			BAR-HP		
		1:1	1:2	1:3	1:1	1:2	1:3	1:1	1:2	1:3	1:1	1:2	1:3
Kenilworth/Bainsvlei	Rain			627.8			627.8			322.5			322.5
	Evaporation			370.1			375.6			235.3			227.1
	runoff			139			139			66.9			66.9
	Drainage			0			0			0			0
	Δw			118.7			113.2			20.3			28.5
Paradys/Tukulu	Rain			627.8			627.8			322.5			322.5
	Evaporation			408.2			415.5			271			286.3
	runoff			125.3			125.3			44.5			44.5
	Drainage			1			33.5			0			0
	Δw			93.4			53.6			7			-8.2

Δw: Change in soil water content
NAR-EP: Near-average rainfall – empty soil profile
NAR-HP: Near-average rainfall – half-full soil profile
BAR-EP: Below-average rainfall – empty soil profile
BAR-HP: Below-average rainfall – half-full soil profile

Appendix C.4 Cumulative values of the water balance components for the different scenarios under short fallow conditions for the first 1 m section of the runoff strip.

Ecotope	Water balance components	NAR-EP			NAR-HP			BAR-EP			BAR-HP		
		1:1	1:2	1:3	1:1	1:2	1:3	1:1	1:2	1:3	1:1	1:2	1:3
Kenilworth/Bainsvlei	Rain	162.3	162.3	162.3	162.3	162.3	162.3	122.6	122.6	122.6	122.6	122.6	122.6
	Evaporation	89.7	72.1	52.2	96.1	77.4	59.1	73.8	68.1	74.3	86	78.9	90.4
	runoff	64.8	55.4	37.1	64.8	55.4	37.1	44.9	39.4	20.5	44.9	39.4	20.5
	Drainage	0	0	0	0	0	0	0	0	0	0	0	0
	Δw	7.9	34.8	73	1.4	29.5	66.1	3.9	15.1	27.7	-8.3	4.3	11.7
Paradys/Tukulu	Rain	162.3	162.3	162.3	162.3	162.3	162.3	122.6	122.6	122.6	122.6	122.6	122.6
	Evaporation	72.9	79.4	72.1	88.1	96.4	85.8	55.6	57.4	54.9	93.3	97.3	90.9
	runoff	35.5	36.4	36.6	35.5	36.4	36.6	12.2	10.2	9.4	12.2	10.2	9.4
	Drainage	0	0	0	0	0	0	0	0	0	0	0	0
	Δw	54	46.5	53.6	38.7	29.5	39.9	54.7	55.1	58.2	17.1	15.1	22.3

Δw: Change in soil water content
NAR-EP: Near-average rainfall – empty soil profile
NAR-HP: Near-average rainfall – half-full soil profile
BAR-EP: Below-average rainfall – empty soil profile
BAR-HP: Below-average rainfall – half-full soil profile

Appendix C.5 Cumulative values of the water balance components for the different scenarios under short fallow conditions for the second 1 m section of the runoff strip.

Ecotope	Water balance components	NAR-EP			NAR-HP			BAR-EP			BAR-HP		
		1:1	1:2	1:3	1:1	1:2	1:3	1:1	1:2	1:3	1:1	1:2	1:3
Kenilworth/Bainsvlei	Rain		162.3	162.3		162.3	162.3		122.6	122.6		122.6	122.6
	Evaporation		89.5	83.6		97.5	85.6		71.1	73.4		84.4	81.6
	runoff		55.4	37.1		55.4	37.1		39.4	20.5		39.4	20.5
	Drainage		0	0		0	0		0	0		0	0
	Δw		17.4	41.6		9.4	39.6		12.1	28.6		-1.2	20.5
Paradys/Tukulu	Rain		162.3	162.3		162.3	162.3		122.6	122.6		122.6	122.6
	Evaporation		84.9	86.8		95.3	97.4		51.8	52		76.3	77.5
	runoff		36.4	36.6		36.4	36.6		10.2	9.4		10.2	9.4
	Drainage		0	0		0	0		0	0		0	0
	Δw		41	38.9		30.6	28.3		60.6	61.1		36.2	35.7

Δw: Change in soil water content
NAR-EP: Near-average rainfall – empty soil profile
NAR-HP: Near-average rainfall – half-full soil profile
BAR-EP: Below-average rainfall – empty soil profile
BAR-HP: Below-average rainfall – half-full soil profile

Appendix C.6 Cumulative values of the water balance components for the different scenarios under short fallow conditions for the third 1 m section of the runoff strip.

Ecotope	Water balance components	NAR-EP			NAR-HP			BAR-EP			BAR-HP		
		1:1	1:2	1:3	1:1	1:2	1:3	1:1	1:2	1:3	1:1	1:2	1:3
Kenilworth/Bainsvlei	Rain			162.3			162.3			122.6			122.6
	Evaporation			68.9			70.9			75.3			82.9
	runoff			37.1			37.1			20.5			20.5
	Drainage			0			0			0			0
	Δw			56.3			54.3			26.8			19.1
Paradys/Tukulu	Rain			162.3			162.3			122.6			122.6
	Evaporation			86.3			91.8			78.1			90.5
	runoff			36.6			36.6			9.4			9.4
	Drainage			0			0			0			0
	Δw			39.3			33.8			35.1			22.6

Δw: Change in soil water content
NAR-EP: Near-average rainfall – empty soil profile
NAR-HP: Near-average rainfall – half-full soil profile
BAR-EP: Below-average rainfall – empty soil profile
BAR-HP: Below-average rainfall – half-full soil profile

Appendix C.7 Daily rainfall and ET_o measurements for the Kenilworth/Bainsvlei and Paradys/Tukulu ecotopes.

Date	Kenilworth		Paradys	
	Rainfall	ET_o	Rainfall	ET_o
2009/11/04	-	-	23.6	1.0
2009/11/05	-	-	0.3	5.0
2009/11/06	-	-	0.0	6.1
2009/11/07	-	-	0.0	5.8
2009/11/08	-	-	0.8	5.9
2009/11/09	-	-	9.4	4.1
2009/11/10	-	-	0.0	5.1
2009/11/11	-	-	0.0	5.7
2009/11/12	-	-	0.0	6.1
2009/11/13	-	-	0.0	6.3
2009/11/14	-	-	0.0	6.4
2009/11/15	-	-	0.0	5.3
2009/11/16	-	-	0.0	5.8
2009/11/17	-	-	0.0	4.6
2009/11/18	-	-	2.8	1.7
2009/11/19	0.1	3.0	0.5	4.6
2009/11/20	6.3	2.4	0.3	3.2
2009/11/21	0.1	2.6	0.0	3.4
2009/11/22	0.0	4.9	0.0	5.6
2009/11/23	0.0	6.0	0.3	6.0
2009/11/24	0.0	5.0	0.0	5.7
2009/11/25	0.0	6.5	0.8	6.2
2009/11/26	2.0	5.7	0.0	6.9
2009/11/27	0.0	6.9	0.0	6.9
2009/11/28	0.0	6.5	0.0	6.6
2009/11/29	0.0	6.6	0.0	6.7
2009/11/30	0.0	7.1	0.0	7.4
2009/12/01	0.0	7.0	0.0	6.7
2009/12/02	0.0	7.5	0.0	7.9
2009/12/03	0.0	6.7	0.0	7.6
2009/12/04	0.0	7.9	0.5	7.2
2009/12/05	0.0	6.3	0.0	7.6
2009/12/06	5.1	6.0	0.0	5.3
2009/12/07	0.2	5.8	0.0	4.9
2009/12/08	6.6	3.7	0.3	4.4
2009/12/09	13.7	4.6	11.7	5.4
2009/12/10	0.0	6.3	0.0	7.0
2009/12/11	0.0	5.2	0.0	5.6
2009/12/12	0.0	5.3	0.0	6.3
2009/12/13	0.0	6.8	0.0	7.5
2009/12/14	22.8	4.8	6.6	4.3
2009/12/15	1.3	4.5	0.0	5.7
2009/12/16	0.0	7.0	0.0	7.2
2009/12/17	0.0	5.5	0.0	8.2
2009/12/18	0.0	7.5	0.5	8.2
2009/12/19	0.0	8.2	0.0	8.1
2009/12/20	0.0	6.8	0.0	7.3
2009/12/21	7.8	6.3	0.0	7.3
2009/12/22	0.0	6.2	2.8	6.8
2009/12/23	0.0	5.0	0.5	5.2
2009/12/24	0.0	7.1	0.0	7.9
2009/12/25	0.0	6.9	0.0	7.8
2009/12/26	0.0	6.9	0.0	8.5
2009/12/27	0.0	6.5	0.0	7.0
2009/12/28	0.0	6.2	0.0	8.6
2009/12/29	0.0	5.8	0.0	7.6
2009/12/30	0.1	7.1	0.0	7.9
2009/12/31	0.0	5.8	4.3	6.5
2010/01/01	1.1	4.3	0.0	4.5
2010/01/02	19.9	1.4	5.6	1.9
2010/01/03	0.0	4.7	0.0	4.9
2010/01/04	0.9	5.4	0.5	5.8
2010/01/05	0.0	5.7	0.0	5.7
2010/01/06	0.0	5.7	0.0	6.0
2010/01/07	3.9	4.0	21.3	4.2
2010/01/08	6.3	6.2	1.3	5.9
2010/01/09	0.0	4.1	0.0	4.5
2010/01/10	1.6	2.6	0.0	2.2
2010/01/11	0.1	4.2	2.3	4.4
2010/01/12	0.1	5.5	0.0	5.8
2010/01/13	0.9	5.2	5.6	4.7
2010/01/14	17.3	4.1	37.1	4.7
2010/01/15	1.0	6.1	0.0	6.0
2010/01/16	0.0	6.9	0.0	6.6
2010/01/17	0.0	6.5	0.0	6.4

Date	Kenilworth		Paradys	
	Rainfall	ET_o	Rainfall	ET_o
2010/01/18	1.2	6.1	0.0	6.0
2010/01/19	10.6	2.0	4.1	2.2
2010/01/20	0.0	4.0	0.0	5.5
2010/01/21	3.4	3.7	16.8	4.1
2010/01/22	16.6	1.2	2.3	1.7
2010/01/23	2.4	3.5	0.0	4.3
2010/01/24	0.0	5.0	0.3	5.4
2010/01/25	11.5	3.0	13.7	1.8
2010/01/26	21.5	1.4	13.2	2.5
2010/01/27	0.0	5.8	0.0	6.0
2010/01/28	0.0	6.5	0.0	6.3
2010/01/29	0.0	5.4	0.0	5.4
2010/01/30	0.0	5.0	0.8	5.2
2010/01/31	13.0	3.1	22.4	3.5
2010/02/01	0.1	5.9	0.3	5.9
2010/02/02	0.0	5.9	0.0	6.3
2010/02/03	5.5	4.5	0.0	5.5
2010/02/04	0.0	5.8	0.0	6.0
2010/02/05	0.0	6.1	0.0	6.3
2010/02/06	0.0	5.6	0.0	6.2
2010/02/07	0.0	5.7	0.0	5.3
2010/02/08	2.1	5.6	1.5	6.0
2010/02/09	0.0	5.8	0.3	6.1
2010/02/10	0.6	4.8	1.3	5.6
2010/02/11	0.0	4.6	0.0	4.9
2010/02/12	0.4	5.3	3.8	5.7
2010/02/13	0.0	6.3	0.0	6.2
2010/02/14	0.0	5.8	0.3	6.2
2010/02/15	4.1	5.5	11.7	5.5
2010/02/16	18.4	2.8	24.4	2.6
2010/02/17	0.0	5.3	0.3	5.3
2010/02/18	0.0	5.5	0.0	5.3
2010/02/19	0.0	4.9	0.0	5.7
2010/02/20	0.0	5.4	0.0	5.3
2010/02/21	0.0	5.0	0.0	5.3
2010/02/22	0.0	3.8	0.0	4.7
2010/02/23	3.7	4.6	18.8	4.4
2010/02/24	61.9	0.6	67.8	0.8
2010/02/25	13.3	4.6	0.0	3.8
2010/02/26	1.8	4.0	0.0	4.9
2010/02/27	0.0	4.3	0.0	4.6
2010/02/28	0.0	5.3	0.0	5.2
2010/03/01	0.0	5.1	0.0	5.0
2010/03/02	9.0	4.3	14.5	5.1
2010/03/03	0.1	4.7	0.3	4.3
2010/03/04	0.0	3.8	2.0	4.0
2010/03/05	3.4	4.3	0.3	4.4
2010/03/06	0.0	4.7	0.0	4.7
2010/03/07	0.0	4.7	0.0	4.9
2010/03/08	0.0	4.4	0.0	4.6
2010/03/09	0.0	4.6	0.0	4.7
2010/03/10	0.0	3.8	0.0	4.8
2010/03/11	0.0	4.8	0.0	5.1
2010/03/12	0.0	4.9	0.0	5.2
2010/03/13	1.9	4.0	0.0	4.9
2010/03/14	0.0	4.8	0.0	5.0
2010/03/15	0.0	3.6	0.0	3.6
2010/03/16	0.0	4.3	17.3	4.7
2010/03/17	3.3	4.0	4.3	4.3
2010/03/18	0.0	3.9	0.0	4.4
2010/03/19	0.0	4.2	0.0	4.6
2010/03/20	18.8	3.6	0.0	4.6
2010/03/21	0.0	3.7	0.0	4.4
2010/03/22	3.4	3.8	7.1	4.6
2010/03/23	3.1	3.8	0.3	4.2
2010/03/24	0.0	3.5	0.8	4.1
2010/03/25	16.3	3.0	10.9	3.5
2010/03/26	18.4	2.1	10.9	2.1
2010/03/27	6.3	3.7	9.7	4.1
2010/03/28	0.0	3.8	0.0	4.1
2010/03/29	0.0	3.7	0.0	4.1
2010/03/30	2.3	3.0	0.0	3.5
2010/03/31	0.0	1.9	2.0	2.4
2010/04/01	0.0	2.4	2.3	2.9
2010/04/02	0.0	3.4	0.0	3.6
2010/04/03	0.0	3.6	0.0	3.9
2010/04/04	5.3	3.4	2.3	3.4
2010/04/05	15.8	2.6	24.6	2.1
2010/04/06	0.0	2.5	0.0	2.8
2010/04/07	0.0	3.1	0.0	3.8

Date	Kenilworth		Paradys	
	Rainfall	ET_o	Rainfall	ET_o
2010/04/08	0.0	3.6	0.0	4.0
2010/04/09	0.0	3.4	0.0	4.1
2010/04/10	0.0	3.4	0.0	3.6
2010/04/11	0.0	3.3	0.0	3.7
2010/04/12	0.0	3.3	0.0	3.6
2010/04/13	0.0	3.4	0.0	3.8
2010/04/14	0.0	3.4	0.0	3.9
2010/04/15	0.0	3.2	0.0	3.5
2010/04/16	0.0	1.8	10.9	1.1
2010/04/17	1.9	2.5	0.5	2.1
2010/04/18	4.2	2.9	4.3	3.4
2010/04/19	3.8	2.1	1.3	2.4
2010/04/20	0.0	3.0	0.0	2.9
2010/04/21	0.0	2.8	0.0	3.0
2010/04/22	0.0	3.1	0.0	3.5
2010/04/23	0.0	2.8	0.0	2.9
2010/04/24	0.0	1.7	0.0	2.1
2010/04/25	0.0	2.1	0.0	2.3
2010/04/26	0.0	1.6	0.0	2.4
2010/04/27	4.3	0.8	0.0	1.1
2010/04/28	4.4	1.5	0.0	1.6
2010/04/29	0.1	2.3	0.0	2.8
2010/04/30	0.0	2.7	0.0	2.9
2010/05/01	3.2	2.5	0.0	2.8
2010/05/02	0.0	2.2	0.0	2.6
2010/05/03	12.9	0.9	8.6	0.9
2010/05/04	0.1	2.4	0.3	2.6
2010/05/05	0.1	2.3	0.0	2.7
2010/05/06	0.0	2.4	0.0	3.0
2010/05/07	0.0	2.6	0.0	2.9
2010/05/08	0.0	3.0	0.0	3.1
2010/05/09	0.2	3.0	0.0	3.3
2010/05/10	0.0	2.3	0.0	2.5
2010/05/11	0.0	2.2	0.0	2.5
2010/05/12	0.0	2.1	0.0	2.4
2010/05/13	0.0	3.0	0.0	3.1
2010/05/14	0.0	2.1	0.5	2.0
2010/05/15	0.4	0.6	0.3	0.7
2010/05/16	2.2	2.0	0.3	2.3
2010/05/17	0.0	2.2	0.0	2.4
2010/05/18	0.0	2.1	0.0	2.4
2010/05/19	0.0	2.4	0.0	2.4
2010/05/20	0.0	2.4	0.0	2.5
2010/05/21	0.0	2.4	0.0	2.6
2010/05/22	0.0	2.2	0.0	2.5
2010/05/23	0.0	2.3	0.0	2.5
2010/05/24	0.0	2.3	0.0	2.5
2010/05/25	0.0	2.5	0.0	2.5
2010/05/26	0.0	2.6	0.0	2.7
2010/05/27	0.0	2.5	0.0	2.6
2010/05/28	0.7	2.1	0.3	1.9
2010/05/29	0.0	2.2	0.0	2.1
2010/05/30	0.0	2.3	0.0	2.3
2010/05/31	0.0	1.4	0.0	1.6
2010/06/01	0.0	2.2	0.0	2.1
2010/06/02	0.0	2.4	0.0	2.2
2010/06/03	0.0	2.2	0.0	2.0
2010/06/04	0.0	2.6	0.0	2.6
2010/06/05	0.0	2.4	0.0	2.1
2010/06/06	0.0	2.5	0.0	2.4
2010/06/07	0.0	3.0	0.0	2.7
2010/06/08	0.0	2.5	0.0	2.4
2010/06/09	0.0	2.2	0.0	2.0
2010/06/10	5.7	0.7	13.0	0.7
2010/06/11	1.8	1.4	7.4	1.1
2010/06/12	0.0	1.9	0.0	1.5
2010/06/13	0.1	2.2	0.3	2.1
2010/06/14	0.0	2.4	0.0	2.2
2010/06/15	0.0	1.5	0.0	1.5
2010/06/16	0.0	1.5	0.0	1.3
2010/06/17	0.0	1.8	0.0	1.8
2010/06/18	0.0	2.1	0.0	1.9
2010/06/19	0.0	2.2	0.0	2.0
2010/06/20	0.0	2.1	0.0	2.0
2010/06/21	0.0	2.3	0.0	2.1
2010/06/22	0.0	2.6	0.0	2.4
2010/06/23	0.0	1.6	0.0	1.4
2010/06/24	0.0	2.0	0.0	1.9
2010/06/25	0.0	2.2	0.0	2.1
2010/06/26	0.0	2.3	0.0	2.3

Date	Kenilworth		Paradys	
	Rainfall	ET_o	Rainfall	ET_o
2010/06/27	0.0	2.8	0.0	2.4
2010/06/28	0.0	2.2	0.0	2.1
2010/06/29	0.0	2.2	0.0	2.2
2010/06/30	0.0	2.1	0.0	2.2
2010/07/01	0.0	2.3	0.0	2.1
2010/07/02	0.0	1.8	0.0	1.9
2010/07/03	0.0	1.8	0.0	1.7
2010/07/04	0.0	2.0	0.0	2.0
2010/07/05	0.0	1.6	0.0	1.4
2010/07/06	0.0	2.2	0.0	1.9
2010/07/07	0.0	2.4	0.0	2.2
2010/07/08	0.0	2.2	0.0	2.1
2010/07/09	0.0	1.6	0.0	1.4
2010/07/10	0.0	2.5	0.0	2.2
2010/07/11	0.0	1.7	0.0	1.8
2010/07/12	0.0	1.8	0.0	1.8
2010/07/13	0.0	2.3	0.0	2.2
2010/07/14	0.0	2.4	0.0	2.2
2010/07/15	0.0	2.1	0.0	2.0
2010/07/16	0.0	1.9	0.0	1.9
2010/07/17	0.0	2.2	0.0	2.1
2010/07/18	0.0	3.1	0.0	2.7
2010/07/19	0.0	2.5	0.0	2.4
2010/07/20	0.0	2.8	0.0	2.5
2010/07/21	0.0	3.3	0.0	2.6
2010/07/22	0.0	2.8	0.0	2.6
2010/07/23	0.0	2.7	0.0	2.6
2010/07/24	0.0	3.0	0.0	2.6
2010/07/25	0.0	2.7	0.0	2.6
2010/07/26	0.0	2.8	0.0	2.7
2010/07/27	0.0	2.9	0.0	2.7
2010/07/28	0.0	3.0	0.0	2.8
2010/07/29	0.0	3.2	0.0	2.9
2010/07/30	0.0	2.4	0.0	2.4
2010/07/31	0.0	2.4	0.0	2.5
2010/08/01	0.0	2.6	0.0	2.6
2010/08/02	0.0	2.9	0.0	2.8
2010/08/03	0.0	3.0	0.0	2.7
2010/08/04	0.0	3.6	0.0	3.1
2010/08/05	0.0	3.1	0.0	2.9

Date	Kenilworth		Paradys	
	Rainfall	ET_o	Rainfall	ET_o
2010/08/06	0.0	3.5	0.0	3.0
2010/08/07	0.0	3.2	0.0	2.9
2010/08/08	0.0	3.8	0.0	3.4
2010/08/09	0.0	2.6	0.0	2.4
2010/08/10	0.0	2.9	0.0	2.7
2010/08/11	0.0	2.9	0.0	2.7
2010/08/12	0.0	2.6	0.0	2.6
2010/08/13	0.0	2.9	0.0	2.9
2010/08/14	0.0	3.3	0.0	3.2
2010/08/15	0.0	3.7	0.0	3.7
2010/08/16	0.0	3.4	0.0	3.1
2010/08/17	0.0	3.5	0.0	3.3
2010/08/18	0.0	3.8	0.0	3.7
2010/08/19	0.0	3.5	0.0	3.2
2010/08/20	0.0	3.3	0.0	3.0
2010/08/21	0.0	3.4	0.0	3.2
2010/08/22	0.0	3.4	0.0	3.2
2010/08/23	0.0	2.9	0.0	2.8
2010/08/24	0.0	3.4	0.0	3.2
2010/08/25	0.0	3.4	0.0	3.2
2010/08/26	0.0	3.5	0.0	3.4
2010/08/27	0.0	3.3	0.0	3.2
2010/08/28	0.0	4.6	0.0	4.3
2010/08/29	0.0	4.5	0.0	4.0
2010/08/30	0.0	4.6	0.0	4.0
2010/08/31	0.0	4.7	0.0	4.2
2010/09/01	0.0	5.0	0.0	4.6
2010/09/02	0.0	4.7	0.0	4.7
2010/09/03	0.0	14.8	0.0	3.7
2010/09/04	0.0	4.5	0.0	4.5
2010/09/05	0.0	4.9	0.0	4.7
2010/09/06	0.0	4.8	0.0	5.0
2010/09/07	0.0	3.8	0.0	3.8
2010/09/08	0.0	4.2	0.0	3.5
2010/09/09	0.0	1.7	0.0	1.9
2010/09/10	0.0	4.6	0.0	4.2
2010/09/11	0.0	4.0	0.0	3.8
2010/09/12	0.0	4.5	0.0	4.5
2010/09/13	0.0	5.1	0.0	4.8
2010/09/14	0.0	5.7	0.0	5.3

Date	Kenilworth		Paradys	
	Rainfall	ET_o	Rainfall	ET_o
2010/09/15	0.0	6.3	0.0	5.8
2010/09/16	0.0	4.7	0.0	4.4
2010/09/17	0.0	4.4	0.0	3.1
2010/09/18	0.0	3.7	0.0	3.3
2010/09/19	0.1	4.0	0.0	2.4
2010/09/20	0.0	2.8	0.3	3.1
2010/09/21	0.0	2.1	0.0	1.9
2010/09/22	0.0	4.0	0.0	3.7
2010/09/23	0.0	5.6	0.0	4.8
2010/09/24	0.0	5.7	0.0	5.3
2010/09/25	0.0	6.3	0.0	4.9
2010/09/26	0.0	5.4	0.0	3.8
2010/09/27	0.0	5.2	0.0	4.6
2010/09/28	0.0	4.7	0.0	4.2
2010/09/29	0.0	4.5	0.0	4.2
2010/09/30	0.0	5.1	0.5	4.8
2010/10/01	0.0	5.8	0.0	5.0
2010/10/02	0.0	5.6	0.0	5.0
2010/10/03	0.0	6.4	0.0	6.1
2010/10/04	0.0	5.7	0.0	5.1
2010/10/05	0.6	4.7	0.0	4.4
2010/10/06	0.0	6.7	0.0	6.0
2010/10/07	4.0	4.9	0.8	4.3
2010/10/08	0.0	5.7	0.0	5.9

Date	Kenilworth		Paradys	
	Rainfall	ET_o	Rainfall	ET_o
2010/10/09	0.0	5.7	0.0	5.7
2010/10/10	0.0	6.8	0.0	6.5
2010/10/11	0.0	5.6	0.3	5.8
2010/10/12	0.0	4.8	0.0	4.9
2010/10/13	14.3	2.2	12.7	2.2
2010/10/14	0.0	4.2	0.3	4.4
2010/10/15	0.1	3.7	0.0	4.0
2010/10/16	0.0	4.4	0.0	4.1
2010/10/17	0.0	4.9	0.0	5.1
2010/10/18	0.0	5.7	0.0	5.6
2010/10/19	0.0	6.3	0.0	6.5
2010/10/20	0.0	6.8	0.0	6.4
2010/10/21	0.0	6.3	0.0	6.3
2010/10/22	1.2	2.7	0.3	3.1
2010/10/23	4.2	2.7	0.0	3.2
2010/10/24	3.2	3.3	1.0	4.3
2010/10/25	0.0	5.0	0.0	5.1
2010/10/26	0.0	5.4	0.0	5.5
2010/10/27	0.3	5.0	0.0	5.7
2010/10/28	0.0	5.6	0.0	5.4
2010/10/29	0.0	5.5	0.0	6.0
2010/10/30	0.0	6.9	0.0	6.5
2010/10/31	0.0	6.5	0.0	6.7